

**INVESTIGATIONS ON ANATASE TO RUTILE  
TRANSFORMATION IN PRESENCE OF DIFFERENT  
METAL OXIDES AND ATMOSPHERES**

**THESIS SUBMITTED  
TO  
UNIVERSITY OF KERALA  
IN FULFILMENT OF THE REQUIREMENTS  
FOR THE DEGREE OF  
DOCTOR OF PHILOSOPHY  
IN  
CHEMISTRY**

**UNDER FACULTY OF SCIENCE**

**BY**

**RIYAS.S**

**BEACH SAND MINERALS DIVISION  
REGIONAL RESEARCH LABORATORY (CSIR)  
TRIVANDRUM – 695 019  
KERALA, INDIA.**

**OCTOBER 2004**

## DECLARATION

I hereby declare that, the thesis entitled "*INVESTIGATIONS ON ANATASE TO RUTILE TRANSFORMATION IN PRESENCE OF DIFFERENT METAL OXIDES AND ATMOSPHERES*" embodies the results of the investigations carried out by me under the joint supervision of **Dr. P.N. Mohan Das** and **Dr. G. Krishnan** and the same has not been submitted elsewhere for any degree.

A handwritten signature in black ink, appearing to read 'S. Riyas', with the date '6/10/04' written to its right.

OCTOBER 2004

S. RIYAS



**Dr. P. N. MOHAN DAS M.Sc., Ph.D.**  
DEPUTY DIRECTOR  
HEAD, BSMD

REGIONAL RESEARCH LABORATORY (CSIR)  
TRIVANDRUM - 695019, INDIA

Phone : (0471) 2515250  
Fax : (0471) 2491712, 2490186  
E-mail : pnmd@rrlt.csir.res.in  
daspm@rediffmail.com

Residence : Steinberg  
: Trivandrum - 695019  
: Phone : (0471) 2490720

6<sup>th</sup> October 2004

## CERTIFICATE

This is to certify that the work embodied in the thesis entitled  
***“INVESTIGATIONS ON ANATASE TO RUTILE TRANSFORMATION IN  
PRESENCE OF DIFFERENT METAL OXIDES AND ATMOSPHERES”***  
is an authentic record of the research work carried out by **Mr. S. RIYAS** under  
my supervision in fulfillment of the requirements for the degree of **Doctor of  
Philosophy** in Chemistry of Kerala University, Thiruvananthapuram and  
further that no part there of has been presented before for any other degree.

(P.N. Mohan Das)

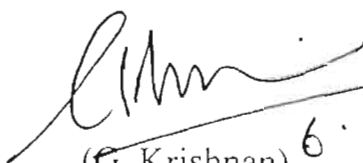
**University College, Thiruvananthapuram**  
**Department of Chemistry**

6<sup>th</sup> October 2004

Dr. G. Krishnan  
Reader and Head

**CERTIFICATE**

This is to certify that the work embodied in the thesis entitled *“INVESTIGATIONS ON ANATASE TO RUTILE TRANSFORMATION IN PRESENCE OF DIFFERENT METAL OXIDES AND ATMOSPHERES”* is an authentic record of the research work carried out by **Mr. S. RIYAS** under my co-supervision in fulfillment of the requirements for the degree of **Doctor of Philosophy** in Chemistry of Kerala University, Thiruvananthapuram and further that no part there of has been presented before for any other degree.

  
(G. Krishnan) 6.10.04

Dedicated to my beloved  
Parents and  
Teachers

## *Acknowledgements*

*I have indeed immense pleasure to express my deepest sense of gratitude and obligation to my Supervisor Dr. P.N. Mohan Das, Deputy Director, Regional Research Laboratory (CSIR), Trivandrum for the constant encouragement, invaluable advice, inspiration and excellent guidance.*

*I would like to extent my sincere thanks to Dr. G.Krishnan, Reader and Head, Dept. of Chemistry, University College, Trivandrum for co-guiding me to do the resrarch work in Regional Research Laboratory(CSIR).*

*I would like to extent my sincere thanks to Prof.T.K. Chandra shekar, Director, RRL (CSIR), Trivandrum for providing the necessary facilities to carry out my research.*

*I am grateful to Dr. G. Vijay Nair, former Director, RRL (CSIR), Trivandrum for having accorded permission to carryout my research work in RRL(CSIR), Trivandrum.*

*I record my heartfelt thanks to Dr.Suresh Das and to Mr. Robert Philip, Photochemistry research unit, RRL Trivandrum for rendering me all possible help in doing photo catalytic activity studies.*

*I express my deep gratitude to Dr. E.Jayakumari and to Dr. V. Ahamed Yasir for the invaluable helps during my research in RRL (CSIR) Trivandrum.*

*It is really a pleasure for me to extent my sincere thanks to all members of BSM Division, RRL, namely, Mr. K.H. Bhat, Mrs. M.E.K. Janaki, Mr.S. Velusami and Mr. S. Sasibhooshanan for their unstinted cooperation and I would like to thank Dr. Peter Koshy, Scientist, RRL for his help in carrying*

*out SEM analyses and Dr. Syama Prasad , Dr. Jose James, Mr. Gurusami and Mr. Oonnikrishnan for their help in XRD analyses.*

*I convey my thanks to all Research Scholars of RRL (CSIR) for their kind cooperation and timely help. All my friends and colleagues, who helped directly or indirectly, are also gratefully acknowledged.*

*Last but not least, I am most indebted to my parents, Sister and other members of my family for their encouragement and unwavering moral support, which were necessary to complete this work.*

*October 2004*

*S. RIYAS*

## CONTENTS

Declaration	
Certificate	
Acknowledgements	
Preface	
List of Publications	
CHAPTER 1 INTRODUCTION	1
1.1 General Introduction	1
1.2 Manufacturing Process of Titania	3
1.3 Industrial Applications of TiO <sub>2</sub>	4
1.4 Properties of Titania	10
1.5 Some Catalytic Reactions of Metal oxide Supported on Titania	21
1.5.1. Hydro de sulfurization (HDS)	21
1.5.2. Partial oxidation ( Selective Oxidation)	22
1.5.3. Carbon monoxide hydrogenation	24
1.5.4. Selective catalytic reduction of NO <sub>x</sub> (SCR)	25
1.5.5. Coal liquefaction	27
1.5.6. Ammonia synthesis	28
1.5.7. Isomerization	28
1.5.8. Carbon monoxide oxidation	29
1.5.9. Miscellaneous	30
1.6. Photo catalysis	31
1.7. Scope and Objective of the Present Investigation	35



CHAPTER 2	MATERIALS AND EXPERIMENTAL METHODS	37
2.1	Materials used	37
2.2	Experimental procedure	39
2.2.1.	Preparation of $\text{Fe}_2\text{O}_3/\text{TiO}_2$	39
2.2.1.1.	Co-precipitation	39
2.2.1.2.	Wet-impregnation	39
2.2.2.	Preparation of $\text{NiO}/\text{TiO}_2$	40
2.2.2.1.	Co-precipitation	40
2.2.2.2.	Wet-impregnation	40
2.2.3.	Preparation of $\text{Cr}_2\text{O}_3/\text{TiO}_2$	40
2.2.3.1.	Co-precipitation	41
2.2.3.2.	Wet-impregnation	41
2.2.4.	Preparation of $\text{MnO}_2/\text{TiO}_2$	41
2.2.4.1.	Co-precipitation	41
2.2.4.2.	Wet-impregnation	41
2.2.5.	Preparation of $\text{CuO}/\text{TiO}_2$	42
2.2.5.1.	Co-precipitation	42
2.2.5.2.	Wet-impregnation	42
2.3.	Photo Catalytic oxidation of Toluene to benzoic acid (Liquid phase)	42
2.4.	Crystallite size calculation	43
2.5.	Rutile percentage calculation	43
2.6.	Chemical analysis	43
2.6.1.	Estimation of $\text{TiO}_2$	43
2.6.2	Estimation of $\text{Fe}_2\text{O}_3$	45
2.6.3.	Estimation of $\text{NiO}$	45

2.6.4.	Estimation of Cr <sub>2</sub> O <sub>3</sub>	46
2.6.5.	Estimation of MnO <sub>2</sub>	47
2.6.6.	Estimation of CuO	47
2.7.	Instrumental methods employed	48
2.7.1.	Surface area analyzer	48
2.7.2.	Photo catalytic reactor	48
2.7.3.	Furnace and temperature programmer	48
2.7.4.	X - Ray Diffractometer	48
2.7.5.	Scanning Electron Microscope	48

## RESULTS AND DISCUSSION

CHAPTER 3	STUDIES ON Fe <sub>2</sub> O <sub>3</sub> DOPED TiO <sub>2</sub>	49
3.1	Chemical analysis	49
3.2	XRD studies	50
3.3.	Surface area studies	63
3.4.	Scanning Electron Microscopic studies.	65
3.5.	Transformation in Argon and Hydrogen atmospheres.	69
3.6.	Conclusions	78
CHAPTER 4	STUDIES ON NiO doped TiO <sub>2</sub>	80
4.1	Chemical analysis	81
4.2	XRD studies	81
4.3	Surface area studies	96
4.4	Scanning Electron Microscopic studies.	97
4.5	Transformation in Argon and Hydrogen atmospheres.	100
4.6.	Conclusions	109

CHAPTER 5	Studies on Cr <sub>2</sub> O <sub>3</sub> doped TiO <sub>2</sub>	110
5.1.	Chemical analysis	110
5.2.	XRD studies	111
5.3.	Surface area studies	124
5.4.	Scanning Electron Microscopic studies.	128
5.5	Transformation in Argon and Hydrogen atmospheres.	131
5.6.	Conclusions	140
CHAPTER 6	Studies on CuO doped TiO <sub>2</sub>	141
6.1	Chemical analysis	141
6.2	XRD studies	142
6.3.	Surface area studies	156
6.4.	Scanning Electron Microscopic studies.	157
6.5	Transformation in Argon and Hydrogen atmospheres.	160
6.6.	Conclusions	169
CHAPTER 7	Studies on MnO <sub>2</sub> doped TiO <sub>2</sub>	170
7.1	Chemical analysis	170
7.2	XRD studies	171
7.3.	Surface area studies	185
7.4.	Scanning Electron Microscopic studies.	186
7.5	Transformation in Argon and Hydrogen atmospheres.	189
7.6.	Conclusions	198

CHAPTER 8	STUDIES ON LIQUID PHASE PHOTO OXIDATION	199
	OF TOLUENE	
8.1.	Studies on undoped TiO <sub>2</sub> .	201
8.2.	Studies on Fe <sub>2</sub> O <sub>3</sub> /TiO <sub>2</sub> .	202
8.3.	Studies on Cr <sub>2</sub> O <sub>3</sub> /TiO <sub>2</sub> .	205
8.4.	Studies on NiO/TiO <sub>2</sub> .	207
8.5.	Studies on CuO/TiO <sub>2</sub> .	208
8.6.	Studies on MnO <sub>2</sub> /TiO <sub>2</sub> .	210
8.7.	Mechanism of Photochemical oxidation of Toluene.	213
8.8.	Conclusions	216
CHAPTER 9	SUMMARY AND CONCLUSIONS	218
REFERENCES		223

## PREFACE

Among the oxide based nano particles, titanium dioxide ( $\text{TiO}_2$ ) is a highly valuable material because of its optical and catalytic properties. Titania shows outstanding chemical stability, high refractive index, ultra-violet absorptivity and photo chemical activity which are expected to play a vital role in pigments, catalysts, ceramics etc: -

There are several industrially important reactions carried out using metal oxide doped titania as catalysts. Amorphous titania on heating transforms from metastable anatase to thermodynamically more stable rutile phase. This transformation is very important in selection of titania as a catalyst and as catalyst support. There is need for the study of kinetics of anatase-rutile transformation in doped titania. With this objective the project is selected for the Ph.D work. The Objectives of the research work are

- ❖ To prepare  $\text{TiO}_2$  doped with transition metal oxides such as  $\text{Fe}_2\text{O}_3$ ,  $\text{NiO}$ ,  $\text{Cr}_2\text{O}_3$ ,  $\text{MnO}_2$  and  $\text{CuO}$  in different weight percentages (5 & 15%) using two different methods namely co-precipitation using hydrazine hydrate and wet-impregnation.
- ❖ To study the kinetics of anatase-rutile transformation in doped titania as a function of temperature and time using powder XRD studies in air and to compare the transformation in air with that in argon (inert) and hydrogen atmosphere (reducing)
- ❖ To find the surface area and crystallite size variations in titania with rutilation.
- ❖ To investigate the surface morphological changes of doped titania samples with rutilation.

- ❖ To study the photo catalytic oxidation of toluene (in liquid phase) in presence of the prepared doped titania.

The lay out of the thesis is as follows.

Chapter I presents an introduction about the titania and metal oxide doped  $\text{TiO}_2$  catalysts and the detailed literature review on anatase-rutile transformation.

The experimental part of the work including the preparation of doped titania and its characterization is given in chapter II.

- Results and discussions are included in the Chapters III – VII.

Chapter VIII contains the results of toluene oxidation in photo catalytic path using the doped titania samples.

Chapter IX gives the summary and conclusions of the investigations. It is believed that the theoretical framework established in this work would contribute to the understandings of other important titania supported systems.

## List of Publications

1. Crystal structure transformation of  $\text{TiO}_2$  in presence of  $\text{Fe}_2\text{O}_3$  and NiO in air atmosphere.  
**S.Riyas**, V. Ahemed Yasir and P.N.Mohan Das, *Bull.Mater.Sci.*, 25, 4, **2002**, 267-273.
2. Studies on the effect of  $\text{Fe}_2\text{O}_3$  and  $\text{Cr}_2\text{O}_3$  on anatase-rutile transformation in  $\text{TiO}_2$ .  
**S.Riyas** and P.N.Mohan Das, *Br.Ceram.Trans*, 103, **2004**, 23-28.
3. Polymorphism in  $\text{TiO}_2$  under the influence of CuO and  $\text{MnO}_2$ .  
**S. Riyas**, G. Krishnan and P.N. Mohan Das  
*Acta Materialia* (Communicated)
4. Rutilation in nickel oxide doped titania prepared by different methods.  
**S. Riyas**, G. Krishnan and P.N. Mohan Das  
*Ceramics International* (Communicated)
5. Influence of Transition Metal oxides on Crystallographic Rearrangement in  $\text{TiO}_2$ .  
**S.Riyas**, Peter Koshy and P.N.Mohan Das  
(Presented in XXV Annual Conference of the Electron Microscopy and Allied Fields, 20<sup>th</sup> to 22<sup>nd</sup> February **2002** at IIT Bombay-India)
6. Surface Morphology of  $\text{Cr}_2\text{O}_3$  doped  $\text{TiO}_2$  with rutilation  
P.N.Mohan Das, **S.Riyas** and Peter Koshy  
(Presented in XXVI Annual Conference of the Electron Microscopy and Allied Fields, 16<sup>th</sup> to 18<sup>th</sup> April **2003** at CPRI Shimla- India)
7. Morphological changes of Nickel Oxide Supported on Titania with rutilation.  
**S.Riyas**, Peter Koshy and P.N.Mohan Das  
(Presented in XXVII Annual Conference of the Electron Microscopy and Allied Fields, April 1-3 **2004** at National Physical Laboratory, New Delhi - India)

---

---

*INTRODUCTION*

---

---



# CHAPTER 1

## INTRODUCTION

### 1.1 General Introduction

The element “Titanium” belonging to the group IV b of the modern periodic table was discovered by the Reverend William Gregor in 1790 [1]. In 1791 Gregor communicated to the journal de physique the description and chemical analysis of a black magnetic sand found in the parish of Menaccan, six miles south of Falmouth, in Corn Wall. The analysis showed almost 50 percent of a white metallic oxide, up to that time unknown to chemists [2]. The sand was given the name ‘Menaccanite’ from the locality, and the new metallic oxide recovered from it was ‘christened menaccine’ by Kirwan [3]. Berzelius [4], in his letters, mentioned Gregor several times in connection with his discovery, analysis and properties of mineral, and referred to him as a ‘celebrated mineralogist’. In 1795, Klaproth [5] noticed the close agreement between Gregor’s account of menaccine and the findings of his own investigations of the oxide extracted from “redschorl”( rutile) from Hungary. The identity of the two substances was soon established and Klaproth, acknowledging Gregor’s priority, applied the temporary name ‘Titanium’ to the new element [6].

The world titanium minerals-Reserves and Production are summarized in table

1.1

Table 1.1. Titanium minerals-Reserves and Production (1989) [7]

Country	Reserves ( $\times 10^6$ mt. $\text{TiO}_2$ )	Production ( $\times 10^3$ mt. ilmenite)
S.Africa	36.0	-----
Norway	32.0	930
India	31.0	150
China	30.0	150
Canada	27.0	-----
Australia	24.0	1692
USA	7.8	300
USSR	5.9	460
Sri Lanka	3.6	107
Brazil	1.6	144
Finland	1.4	----
Malaysia	1.0	520

Titanium is the ninth most abundant element in the earth's crust and is the fourth most abundant structural element [6]. Being highly reactive, it is always found combined with oxygen and other metal oxides and is never found in the metallic form in nature. Titanium is a persistent constituent of practically all crystalline rocks and of sediments derived from them. Of 800 igneous rocks analyzed in the laboratories of the United States geological survey, 784 contained the element. It is present in most minerals, and it makes up the principal metallic constituent in an important group, the most common of which are ilmenite, rutile, arizonite, perovskite, leucosene and sphene or

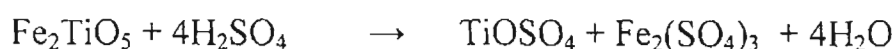
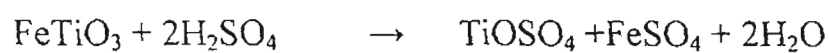
titanite. Titanium occurs as a minor constituent of most bauxities and all clays. Titanium has been found in a variety of sea creatures, animals, plants and human body. Plants contain a slightly higher proportion than animals. Titanium has been detected in hen's eggs, liver, brain, hair, nails and skin, nerve cells, kidney stones, silkworm tissues and embryos. [6]

It shows the characteristic valency of four, in addition to this di, tri and penta valent states are also reported in some compounds. Titanium forms oxides with all of the above mentioned valencies, or more specifically seven phases of its oxide exist with general formula  $TiO_{2n-1}$ . The value of 'n' ranges from 4 to 10. A wide range of possible compounds and structures exist in the Ti-O system, the dioxide is the most stable under ordinary conditions. Ilmenite is the most common mineral and its reserves are wide spread throughout the world including India. Indian ilmenite deposits are reported to be rich in  $TiO_2$  content[6]. Titanium dioxide is a ceramic material, commonly known as titania.

### **1.2 Manufacturing processes of titania**

Titanium dioxide pigments are manufactured by two processes[8] The sulphate process (extraction with sulfuric acid); and the Chloride process (extraction with chlorine).

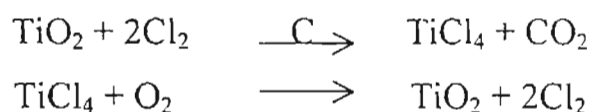
In the Sulphate process ilmenite is treated with sulphuric acid. This converts metaloxides in to soluble sulphates, primarily of titanium and iron.



After the resultant liquor has been allowed to settle to remove un reacted gangue minerals, a portion of the iron in solution is removed by cooling (crystallization)/centrifugation leaving a relatively clean titanium solution for

the hydrolysis stage. The product from this stage is a microcrystalline oxide of titanium (Pulp) which is converted in to the required crystalline state by calcinations. The process can be used for the production of both anatase and rutile grade pigments, although it is more suited for the production of anatase grade. Intense research was undertaken in the sulphate process technology to improve particle size, particle size distribution and other parameters. The most important problem with the process has been disposal of the waste products which leads to pollution. Various solutions have been developed to overcome these problems.

The chloride process seems relatively straight forward, ie. Extraction of titanium by chlorine from a titaniferrous ore, or rutile followed by oxidation of the titanium tetrachloride so produced to titaniumdioxide and chlorine.



The process is used mainly for rutile grade although some companies claim that the process could also be used to make anatase grade. The process was developed by Du-Pont, USA and the first commercial plant was installed in 1959. In the recent years particularly after 1960, all the new plants installed in USA have adopted chloride technology.

### 1.3 Industrial applications of TiO<sub>2</sub>

Titania is one of the top 20 inorganic chemicals of industrial importance. Although it is used in some non-pigmentary applications, the chemical and industrial interests on TiO<sub>2</sub> are almost solely derived from its pigmentary properties. It has been used as a pigment from the very beginning of 20<sup>th</sup> century.[8]

The important properties of a pigment are i) opacity - the ability to opacify the medium to which it is applied or the surface on which it is dispersed, ii) hiding power - the power to obscure a background of contrasting colours either by absorption or by scattering, iii) tinting strength – the ability to lighten a colourant, iv) gloss - surface finish, v) chalking resistance - the resistance to the disintegration of organic binders, which results in the formation of powdery chalk or free pigment particles on the surface, etc. Most of the above mentioned properties are in some way or other, related to refractive index, particle size, surface area, etc. Better pigmentary properties are observed in the oxides having higher refractive index and surface area. Since anatase is highly photoactive compared to rutile, the disintegration of organic binder occurs in anatase based pigments in presence of u.v radiations or radiations having wavelength less than 400 nm. The coated surface becomes powdery and moves away by wind or rain there by exposing the underlying section for further attack, which leads to the fading of colour. For the same reason, anatase is reported to be 'poor' in some of the pigmentary properties.[8] Hence, anatase is usually preferred in interior paints, while rutile is preferred in exterior ones including enamels and emulsions. Since, both anatase and rutile have different physical properties, they cannot be substituted by each other, but in some applications both can be used. In addition to the pigmentary uses of titania, about 100000 t a<sup>-1</sup> are sold for non-pigment applications.

In the manufacture of quality papers, anatase is preferentially used as a filler - to fill the crevices between the paper fiber and as opacifier and brightner, to improve smoothness and printability. Since it is a wide band gap semiconductor, it can absorb u.v light and emit radiations of higher

wavelength, which is the main requirement for optical brighteners.[8] Its lower density compared to that of rutile reduces the problems in handling of the paper at wet stage. It is less abrasive due to its lower hardness (compared to rutile), which results in lower consumption of cutting blades used in paper industry.[8]

The high refractive index and chemical inertness make  $\text{TiO}_2$  an ideal pigment for plastics. Even though some plastics are used in their natural colours, most of them are blended with pigment to obtain attractive colours, as well to opacify them. Addition of rutile confers resistance to u.v degradation. Anatase grade is used in textile industry for de-lustering of synthetic fibres.[8] Addition of  $\text{TiO}_2$  into ceramic materials improves their acid resistance and lowers the sintering temperature [9]. It also finds application in rubber, cosmetics, soap, pharmaceuticals, printing ink, roofing granules, floor coverings, etc.[8&9]

$\text{TiO}_2$  has found versatile applications in low as well as high temperature fields. Mesoporous  $\text{TiO}_2$  electrodes are used in photovoltaic applications.[10] The microstructure of  $\text{TiO}_2$  influences the photovoltaic response of the solar cell and thereby increases the overall efficiency of the system [10]. It is hence regarded as an important electrode material for extensive applications in low cost solar cells[11-13] and in electro chromics [14]. Photo excited  $\text{TiO}_2$  has a strong ability in killing of cancer cells in vitro and vivo, which suggests that the cell killing effect could be adopted as one of the possible anti-cancer modalities.[15] In recent years, much effort has been focused towards the development of renewable energy conversion and storage devices. For economically and environmentally viable devices, the right choice of material is of crucial importance. An important material in this

respect is  $\text{TiO}_2$ , whose combination of semi conducting as well as chemical stability makes it a suitable candidate for use in rechargeable lithium batteries [16-20]. Titania crystal lattice has the ability to accommodate charge in the form of small foreign ions, such as  $\text{H}^+$  and  $\text{Li}^+$  [21]. These ions can be inserted and extracted from  $\text{TiO}_2$  electrodes using an electric field as driving force through a process referred to as intercalation. The insertion of positively charged ions has to be balanced with an uptake of electrons to preserve overall charge neutrality [21]. For practical devices, the extent, reversibility and speed of intercalation are of prime importance. A common way to meet these demands is by using nano-structured electrodes. The large effective surface area provides a concomitant large number of adsorption sites for the intercalating ions [21].

Titania coatings have been studied for a wide variety of uses, such as antifouling, antibacterial, de-odourising and in wet type solar cells [11]. Because of high refractive index, dielectric constant, good oil absorption ability, tinting strength and chemical stability, even under strongly acidic or basic conditions,  $\text{TiO}_2$  is used in optical coatings, beam splitters and in antireflection coatings [22-25]. The fabrication and characterization of titania thin films have attracted the attention of many researchers [26&27].

In view of its chemical stability, high refractive index and high dielectric constant, it has also got applications in opto-electronic devices,[28] optical wave-guides,[29] filters [29] and  $\text{NO}_2$  gas sensors.[30] Because of its wide chemical stability and non-stoichiometric phase region, it shows different electrical characteristics with oxygen partial pressure, which makes it suitable for use in high temperature oxygen and humidity sensors in pure form or mixed with other metal oxides,[31-33] with enhanced mechanical properties

[34]. Titania based oxygen sensors can be used to monitor automobile engine performance and the feed back from the detector can control the air fuel ratio to give optimum low pollution performance [9].

Titania nano particles are widely used for the preparation of micro porous membranes,[35] which are used for the separation, with or without chemical reaction.[36&37] Layered hydrated titania ( $H_2Ti_4O_9 \cdot nH_2O$ ) and some titanates can readily inter change with some alkali or alkaline earth metals,[38-40] because of which they find application in ion-exchange materials. The possibility of using hydrated titania as an ion-exchange agent for treatment of liquid radioactive wastes from nuclear reactor installations and for the separations of uranium from seawater has also been reported.[41&42]

Synthetic gems have been produced from rutile, since its refractive index is significantly higher than that of diamond, which makes it a very spectacular gem.[43] Strontium titanate gems under various trade names, viz. Fabulite and Wellington, are available in the world market.[9] Gemstone grade  $SrTiO_3$  was first developed at the National Lead Company in mid 1950s.[44]

In recent years, significant developments took place in titania. These include ultrafine titanium dioxide for UV blocks in cosmetics and plastics, and novel optical effects, and high purity titanium dioxide for electro ceramics and catalysis. the traditional uses of titanium dioxide in ceramics are in vitreous enamels and in thread guides for the fibre industry. These applications have traditionally used pigmentary type titanium dioxide. Electro ceramic applications have imposed increasingly demanding specifications on titanium dioxide. These applications are based mainly on alkaline earth



titanates. Barium titanate ceramics can have exceptionally high dielectric constants and are used as high performance capacitors capable of withstanding high voltage surges. Suitably doped titanate ceramics have large positive temperature coefficients of resistance and are widely used in positive temperature coefficient (PTC) thermistors which are incorporated in heaters, power controls and to control currents. Typical products are made by the hydrolysis of high purity titanium tetrachloride.

Titanates, like barium titanate, lead titanate, lead zirconate titanate (PZT), lead lanthanum zirconate titanate (PLZT), barium strontium titanate (BST), strontium bismuth titanate (SBT), etc have found applications in ultrasonic transducers, radio and communication filters, medical diagnostic transducers, stereo tweeters, buzzers, gas igniters, positive temperature coefficient sensors, ultra sonic motors, electro-optic light valves, thin film capacitors and ferroelectric thin film memories.[45] The wide applications of  $\text{BaTiO}_3$  include multi layer capacitor, thermistor, piezo electric actuator, non-linear resistor, thermal switch, passive memory storage device,[46] chemical sensor (due to its surface sensitivity to gas adsorption),[47] etc.

Titania has gained much attention in catalyst industry due to its applications as a catalyst or catalyst support for metal or metal oxide catalysts used in heterogeneous catalysis including photo catalysis of industrially and environmentally important reactions. Anatase is generally catalytically and photo catalytically more active than rutile, and for most of these applications anatase is used. The starting material may be derived from pigment production but careful control of sulphate and phosphate levels and dedicated calcination facilities are usually necessary. The growing demands for more efficient catalysts justify the consequent costs.

#### 1.4 Properties of Titania.

The first successful attempt to produce relatively pure  $\text{TiO}_2$  was made by Rossi in U.S.A in 1908. In 1912 Barton and Rossi undertook a systematic research programme to investigate titanium compounds for making pigments. They produced a composite  $\text{BaSO}_4$  and  $\text{CaSO}_4$  pigment containing about 25%  $\text{TiO}_2$ . Their efforts were immediately a commercial success [7].

As the stable dioxide,  $\text{TiO}_2$  exists in three polymorphs, corresponding to the naturally occurring mineral anatase, rutile and brookite respectively. The word rutile comes from the latin rutilus, which means reddish. The name is fitting because rutile is commonly a brilliantly red or black mineral. Out of these, rutile is the thermodynamically most stable form. Anatase and brookite are meta stable, which readily get transformed to rutile on calcinations at higher temperature [8]. All three forms exist as minerals, though brookite is rare. Because of their high refractive index, lack of absorption of visible light, ability to be produced in the correct size range, chemical stability and non-toxicity, both anatase and rutile are produced commercially and have become the world's predominant white pigments. Brookite can be synthesized hydrothermally but has no technological importance as it has no advantages to compensate for the more difficult synthesis.

The crystal form of rutile and anatase has arrangement in which titanium atoms are surrounded by six oxygen atoms in approximately regular but slightly different octahedral arrangement and each oxygen atom is surrounded by three adjacent titanium atoms and have the formula  $\text{TiO}_2$ . In the rutile structure, octahedra are turned through 90 degrees and a twist of 45 degrees from one layer to the next, where as in anatase structure they retain their orientation in all layers. Because of their tetragonal symmetry, both anatase

and rutile are anisotropic. The important properties of anatase and rutile in crystal form are summarized in Table 1.2

**Table 1.2. The important properties of anatase and rutile [6,8&48]**

Sl.No	Property	Anatase	Rutile
1	Crystal structure	Tetragonal	Tetragonal
	a, nm	0.3785	0.4593
	c, nm	0.9514	0.2959
2	Density, (gm m <sup>-3</sup> )	3.84-3.87	4.24-4.26
3	Refractive index		
	Air	2.5	2.7
	Water	1.9	2.1
	Oil	1.7	1.8
4	Dielectric constant	48	114
5	Hardness	5-6	6-7
6	Band gap (ev)	3.25	3.05
7	Chalking Resistance	Poor	Good
8	Tinting Strength	1200-1300	1650-1900
9	Melting point	Converts to rutile	1830-1850

The predominant commercial phase of titanium dioxide is anatase, although it is rarely found in ore form. Anatase has a tetragonal crystal structure in which the Ti-O octahedra share four corners, as shown in figure 1.1A. Rutile has a crystal structure similar to that of anatase, with the exception that the octahedra share four edges instead of four corners. This leads to the formation of chains which are subsequently arranged in a four fold symmetry, as shown in figure 1.1B

A comparison of two crystal structures shows that rutile is more densely packed than anatase. As a point of reference, the densities of the anatase and rutile phases are known to be  $3.899\text{g/cm}^3$  and  $4.250\text{g/cm}^3$ , respectively [49]

Figure.1.1A. Crystal structure of Anatase.

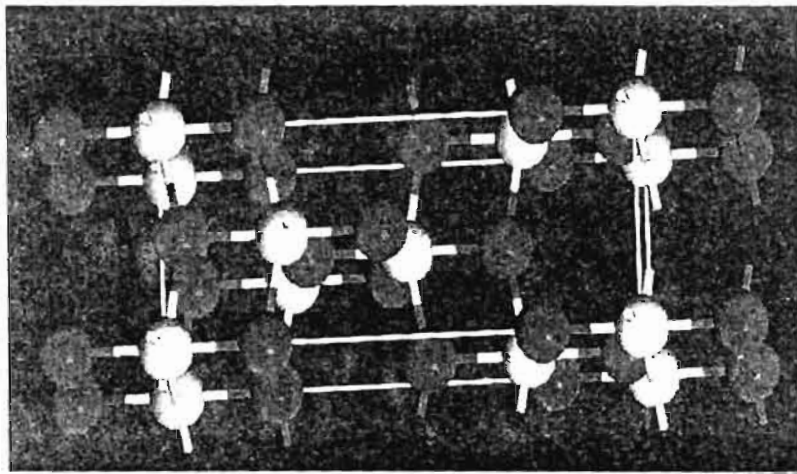
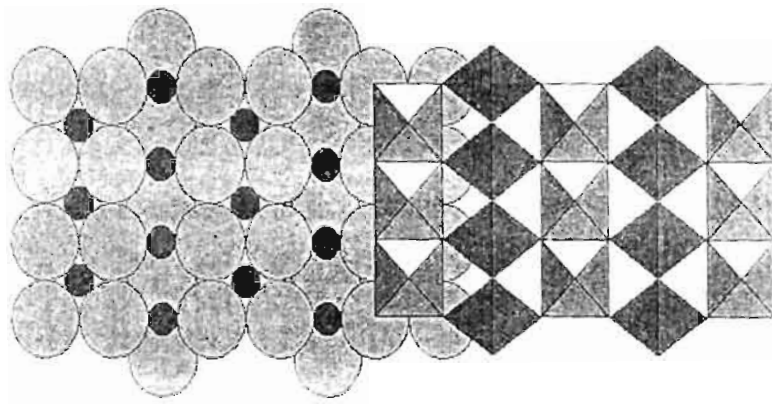


Figure. 1.1B. Crystal structure of rutile



Brookite has an ortho rhombic crystal and spontaneously transforms to rutile around 750<sup>0</sup>C. Its mechanical properties are very similar to those of rutile.

A Variety of solids exhibit transformation from one crystal structure to another as the temperature or pressure is varied. This phenomenon is known as polymorphism. It was reported that nano crystalline solids which occur as polymorphs of low density can be expected to transform to a dense polymorphic form at high pressure and temperature. [50] As mentioned earlier, titania also exhibits polymorphism, i.e. it exists in three crystal modifications, viz. anatase, brookite and rutile. [51] The structural differences between anatase and rutile make the transformation irreversible.

Anatase to rutile transformation in titania is very important in deciding its applicability as a catalyst support. Also the properties of the titania are determined by the phase composition and the particle size of each phase. The phase composition and the particle size evolve as functions of time during heat treatment. Quantitative analysis of the transformation kinetics of amorphous titania to anatase has only been attempted in liquid media under hydrothermal conditions.[52] The rate for the transformation of amorphous titania particles in air is different from that in liquid media.[53]

The anatase to rutile transformation involves an over all contraction of the oxygen structure and a movement of ions, so that a co-operative rearrangement of Ti<sup>4+</sup> and O<sup>2-</sup> ions occurs. To say more specifically, two of the six Ti – O bonds of anatase break and re-unite in a slightly distorted manner, to form rutile structure. It has been proposed that [54-56] the removal of oxygen ions, which generates lattice vacancies, accelerates the transformation and hence, the cations, having the valency less than four, which

correspondingly increase the oxygen vacancy, would enhance the transformation.[54] Because of its irreversible nature, there is no phase equilibria involved in this transformation and hence, does not have any specific transition temperature.[51]

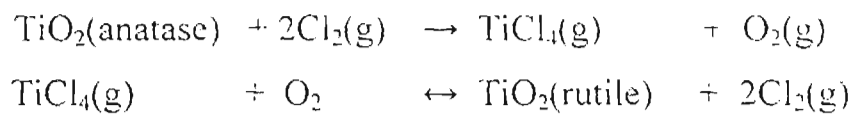
Depending upon the characteristics of anatase, its preparation method, impurity contents,[57-63] deviation from stoichiometry,[59] atmosphere of calcination,[54-56&62] etc, a wide variation in rutilation temperature is reported. The high temperature diffusion technique used to form homogeneously doped  $\text{TiO}_2$  easily causes the complete structural transformation of anatase to rutile. [64] Investigations on the effect of dopants on this transformation revealed that, normally, anions like sulfate and nitrate would inhibit rutilation, while phosphate and chloride enhance the same.[6] The alkaline [54&57] and some transition metal cations like  $\text{Fe}^{3+}$ , [51, 57, 61, 62,65&66] $\text{Cu}^{2+}$ , [54,57&67]  $\text{Mn}^{4+}$  [57,65&67]  $\text{Co}^{2+}$ , [65] $\text{Ni}^{2+}$ , [65]  $\text{Zn}^{2+}$  [68]etc are reportedly enhancing the transformation. Addition of  $\text{AlCl}_3$  enhanced rutilation by increasing the primary particle size and rate of sintering.[63] Dopants like  $\text{SnCl}_4$  enhanced rutilation, since both tin and titanium are in octahedral coordination with oxygen and also due to the formation of  $\text{SnO}_2$  with rutile structure during calcination, which in turn acts as rutile nuclei.[63] According to Ding *et al*,[66]  $\text{SnO}_2$  enhances rutilation by reducing either the onset temperature or the transformation temperature range. Most of the authors unanimously agreed [54,56,57,61&62] that the enhancement or inhibiting effect of additives is dependent on their ability to enter  $\text{TiO}_2$  lattice, there by creating oxygen vacancies or interstitial  $\text{Ti}^{3+}$  ions respectively. The colour change observed in pure anatase during rutilation is an indication of oxygen loss to form lattice defects.[6] These lattice defects act as colour centers.[56]

Riyas *et al* [69] reported that both NiO and Fe<sub>2</sub>O<sub>3</sub> enhance rutilation in the order NiO > Fe<sub>2</sub>O<sub>3</sub>. The activation energies for the transformation were found lowered very much while doping NiO and Fe<sub>2</sub>O<sub>3</sub>.

Several researchers have investigated the effects of different atmospheres on the anatase-rutile transformation, with somewhat conflicting results. Studies have shown that in vacuum conditions, the transformation was inhibited due to the presence of interstitial Ti<sup>3+</sup> ions.[54&56] Lida *et al* [65] have reported that the transformation rate was increased in hydrogen atmosphere due to the formation of oxygen vacancies. MacKenzie found that reducing atmospheres such as steam, a H<sub>2</sub>/N<sub>2</sub> mixture (5%-95% respectively), and vacuum (10<sup>-1</sup>Pa) yield the formation of large aggregates of rutile.[70] MacKenzie's results are contradicted by those of Czanderna *etal*, who found that the rate of the anatase-rutile transformation was unaffected by the presence of a vacuum. Furthermore, Shannon and Pask reported that the anatase-rutile transformation was retarded in vacuum. [71] They proposed that titanium interstitials were created rather than oxygen vacancies, thus inhibiting the transformation instead of facilitating it.

Gamboa and Pasquevich reported on the effect of air/argon and Cl<sub>2</sub>/argon atmosphere on the anatase-rutile transformation. [72] The samples were calcined in different atmospheres for a range of time intervals. At 950<sup>o</sup>C the anatase-rutile transformation was found to be 300 times slower in the air/argon atmosphere than in the Cl<sub>2</sub>/argon atmosphere. Gamboa and Pasquevich reported that after four hours in either air or argon, only up to 5% of the anatase transformed to rutile, and even after 48 hours the transformation was not complete. This is contradicted in part by the studies of MacKenzie that show 10 – 15% transformation to rutile within 30 minutes in an air-argon

atmosphere, at 1000°C. Gamboa and Pasquevich proposed that chlorine assists both vapor mass transport, which is a possible mechanism for nucleation on the solid surface, and oxygen vacancy formation, which assists nucleation and growth in the bulk material. They proposed that when the chlorine partial pressure is sufficiently high, it might assist dissolution of anatase and recrystallization of rutile by the following mechanism:



The idea of oxygen vacancy formation catalyzing the anatase-rutile transformation was discussed earlier, and this again was the mechanism proposed by Gamboa and Pasquevich to explain the observed effects of adsorbed chlorine on the system.

Similar observations were put forward by many authors.[54-56] Gennari *et al* [61&62] claimed an enhanced rutilation in presence of Fe<sub>2</sub>O<sub>3</sub> in air, and chloride atmospheres. In general chemically reducing atmosphere enhances the transition by formation of oxygen vacancies in the anatase lattice, which in turn favours the rupture of Ti—O bonds necessary for crystallographic rearrangement.[54,56&67] Significant grain growth has been reported in TiO<sub>2</sub> during this transformation by different authors.[75-77,56&57,65-68,73&74] Mackenzie *et al* [74] have shown that those reaction atmospheres, which favour the formation of rutile also favour the particle growth. Yoganarasimhan and Rao[59] claimed a marked increase in crystallite size and particle size in the region of transformation due to the expansion of unit cell of anatase prior to the transformation. According to them smaller particle size and larger surface area would favour the transformation. Rao[78] classified this transformation under nucleation and growth mechanism.



Gamboa *et al* [56] also agreed with this mechanism. Reddy *et al* [79] demonstrated that the formation of gaseous  $\text{TiCl}_4$  is responsible for  $\text{TiO}_2$  grain growth occurring at a faster rate in chloride atmosphere than in air. Nobile jr [73] concluded by his studies on iron doped  $\text{TiO}_2$  that the  $\text{TiO}_2$  grain growth and rutilation are simultaneous processes and are inter-related. He argued with the support of a mechanism that, the  $\text{Ti}^{3+}$  ions formed on the surface of  $\text{TiO}_2$  were responsible for enhancement of rutilation. Many authors.[54,59,61&67] also investigated the kinetics of anatase to rutile transformation.

Study of the effects of preparation method and titanium precursor on the resulting titania crystal structure has not been comprehensive. The effects of sulfate and chloride solutions were studied and reported by Wilska in 1954 [80]. He found that although the initially dried products were always amorphous, the first crystalline forms present varied with preparation method and precursor solution. Samples originating from sulfate solutions always gave the anatase structure, while samples produced from the boiling of chloride solutions always gave the rutile structure. Other methods of synthesis such as hydrolysis of phosphate solutions or hydrolysis at room temperature gave either the anatase structure or a mixture of both the anatase and the rutile structure. Wilska found that an amorphous phase always existed prior to the crystalline phase, even in the cases of direct rutile formation. No mechanism was proposed to explain the different effect of sulfate and chloride precursors on the phase transformation.

A kinetic effect of particle size on the anatase-rutile phase transformation has been proposed by Gribb and Banfield [81]. The critical size effect applicable to titanium dioxide is summarized by Kumar [82], who used it to explain the initiation of the anatase-rutile transformation. Kumar found

that both the grain sizes of rutile and the rutile content increased with increasing time and temperature of calcination. They found significant particle-size effect on the anatase-rutile transformation rate in nanocrystalline titania whereby an increase in reaction rate was associated with a decrease in particle size. Three rate-limiting factors were offered as explanation, each relating particle size to a change in reaction rate:

1) Potential Nucleation Sites: Due to purely geometrical effects, the overall number of potential surface nucleation sites per unit volume increases with a decrease in particle size. As the number of potential sites per unit volume increases, it would logically follow that the number of surface nuclei increases, increasing the rate of phase transformation.

2) Driving Force: The driving force for a phase transformation is the difference in free energies between the reactant and product phases. Gribb and Banfield cited experimental evidence suggesting that anatase has a lower surface energy than rutile and therefore would imply that as crystallite size decreases, so does the driving force, which would result in a reduced reaction rate. This is inconsistent with the experimental data provided by Gribb and Banfield and was therefore discounted as a reasonable explanation.

3) Strain Energy: Since the molar volume of rutile is 8-10% less than that of anatase, there is likely to be strain energy associated with the phase transformation. Because of differences in surface tension and hydrostatic-like pressure on smaller crystallites, this strain energy may be affected by particle size. As particle size decreases, the surface tension and hydrostatic-like pressures would potentially reduce the strain energy, reducing one of the barriers to transformation. Upon consideration of experimental data that included the examination of both nanocrystalline and macrocrystalline

titanium dioxide, Gribb and Banfield concluded that the number of nucleation sites was the most probable cause of the increase in reaction rate with decreasing particle size.

Synthesis methods for the production of nanostructured materials vary widely between laboratories and researchers. One common approach, however, is to combine a metal salt solution with a precipitating agent. The result is a precipitant slurry containing a mixture of solid particles suspended in a liquid. In the conventional case, the particles are an oxide precursor, such as a hydroxide, which can then be converted to the oxide by calcining at elevated temperatures [83&84]. One method that can potentially produce nanometer-sized grains in the solid oxide involves exposing those particles to a tremendous amount of shear stress and in situ calcination. The effect of shear is to produce a nanometer-sized, fine, crystalline solid. In situ calcination causes the decomposition of any residual salts such as sulfates, nitrates, and chlorides [84]. The result is a metal oxide slurry which can be dried to a powder. Most of the research conducted in order to accomplish this strategy has focused on the use of cavitation to provide both the shear force and the in situ calcination.

Suslick and co-workers [85] performed much of the early work exploring the effects of acoustic cavitation on materials synthesis. Using ultrasound, Suslick generated acoustic waves to produce the desired cavitation effects. His studies provide insight into the microscopic effects of cavitation on solid particles. Suslick asserts that the effects of ultrasonic-induced cavitation on metal powders are radical changes in particle morphology, significant agglomeration of particles, and a reduction in passivating surface oxide coatings. Cavitation in liquids generates implosive

bubble collapse and associated shock waves. If the bubbles collapse near an extended solid surface, localized high-speed jets of liquid impinge on the surface of the solid. If small solid particles exist in a slurry these smaller particles do not interrupt the cavitation process. Essentially the solid is suspended on the surface of the bubble before the bubble implodes. Normal cavitation collapse occurs. As this occurs, solid particles suspended on the surface of the bubble collide. The collisions that occur as results of cavitation afford a tremendous amount of in situ thermal treatment and an exceptional degree of shear leading to good mixing.

Suslick reports temperatures as high at 5000°C when using a high powered ultrasonic probe to induce cavitation effects [85]. Cavitation has also been shown by Moser to produce smaller grain sizes in a variety of oxide systems, but only in the case of mechanically induced cavitation, not acoustic [83]. The effect of acoustic cavitation on the grain size of nanostructured metal oxides was studied in depth by Emerson et al [84] using a synthesis technique similar to the one used by Moser. Emerson found that while acoustic cavitation generally has a minor effect on the grain size and phase purity of most metal oxide catalysts, it has a more dramatic, yet still minor, effect on the grain size of titania. The observed effect was a 1- 2 nm reduction in grain size upon exposure to the ultrasound. Since this contradicts other results in the literature, Emerson offered a few explanations for his observations. Firstly, the rate of precipitation in the studied systems is very high. Since one of the major benefits of acoustic cavitation is an increased precipitation rate, acoustic cavitation would be less effective on a system with an already high precipitation rate. Secondly, acoustic waves from the tip of the ultrasonic probe have a tendency to propel objects away from the tip, so it is not

inconceivable that precipitates are pushed from the probe and avoid the effects of cavitation [84].

Hence, it is currently an important and active topic of research among material scientists, even though there exists a vast number of literature dealing with the basic aspects of this transformation. The anatase - rutile transformation has been shown in the literature to be affected by a large number of processing variables, including dopants and impurities, atmosphere, precursor, particle size, and synthesis method. However, this review of the literature showed that results from previous studies are often contradictory. Furthermore, the relative influence of each of these variables appears to have been not studied. Therefore, the focus of this work was the exploration of these variables and their individual as well as group effects on the phase transformation.

In spite of large number of literature available on this transformation, there is no systematic data available dealing with anatase to rutile transformation in presence of different percentages of dopants prepared under different methods. Also most of the studies were carried out by impregnating the metal ions on to crystalline  $\text{TiO}_2$  and in some cases, [51,59,61&67] a smaller percentage of rutile was already present in  $\text{TiO}_2$  even before loading metal oxides. All these would undoubtedly affect the investigation.

### **1.5 Some catalytic Reactions of metal oxides supported on titania.**

Catalyzed reactions form the basis of many industrial chemical processes. Catalyst manufacture is itself a rapidly growing industrial process.

#### **1.5.1. Hydro de sulfurisation (HDS)**

The removal of sulfur from sulfur containing feedstock, as  $\text{H}_2\text{S}$  is known as hydro de-sulfurisation, which is an important process used in

petroleum industry and is one of the most widely studied branches of catalysis. The most common catalysts employed are molybdena-alumina catalyst.[86] Molybdena supported on  $\text{TiO}_2$  is reported by a few researchers[87-89] for this reaction. It has been shown that at low molybdena loading, titania supported catalysts are more active than alumina supported ones. Takeuchi *et al* [90&91] reported HDS of thiophene in naphtha on Ni-Mo- $\text{TiO}_2$  catalyst and is reported to be more active than alumina supported ones. Matsuda *et al*[92] used  $\text{MoO}_3/\text{TiO}_2$  catalyst for  $\text{H}_2\text{S}$  adsorption and removal from waste gas streams or from natural gas. The important advantage, they claimed was that, the adsorbent can be regenerated easily by passing oxygen through the adsorbent bed. One of the important advantages of  $\text{TiO}_2$  based catalyst in commercial HDS processes is that, usually, a commercial HDS catalyst is sulfided prior to use, but  $\text{TiO}_2$  based catalyst showed a high activity without pre-sulfidation.

### 1.5.2. Partial oxidation (Selective oxidation)

Partial oxidation is an interesting and promising approach for producing synthesis gas from methane and oxygen or air to give hydrogen and CO with a ratio suitable for Fischer-Tropsch synthesis and methanol synthesis. Ir/ $\text{TiO}_2$  is reported to be a better catalyst for this reaction.[93]

The effect of  $\text{TiO}_2$  supported catalysts in selective catalytic oxidation of hydrocarbons is currently a topic of investigation. There have been numerous investigations on  $\text{V}_2\text{O}_5/\text{TiO}_2$  catalysts. This catalyst was reported for selective oxidation of furan to maleic acid.[94] The selectivity was determined by the number of  $\text{V}_2\text{O}_5$  layers on the support. A high selectivity was reported with five layers of  $\text{V}_2\text{O}_5$  over  $\text{TiO}_2$ . [93]  $\text{V}_2\text{O}_5/\text{TiO}_2$  possesses high activity and selectivity in processes of industrial importance, such as, oxidation of o-xylene[95-99] and naphthalen [100] to phthalic anhydride. Conversion of buta

diene[95] and benzene[101&102] to maleic anhydride, and oxidative ammonolysis of various hydrocarbons[103-105] are also reported over this catalyst. Reddy *et al* [106] reported that, this catalyst is quite superior to other alternatives due to their high activity and resistance to SO<sub>2</sub> poisoning. It is generally accepted that the active phase is the vanadia part of the catalyst and the most appropriate support is anatase.[96-99] Many scientists, put several hypotheses forward to explain the unique activity of this catalyst. Thus, Vejux and Courtine [107] have noted that there is crystallographic fitting between the (010) face of V<sub>2</sub>O<sub>5</sub> and the prevailing anatase planes (001), (100) and (010). Thus there is a possibility of epitaxial growth of V<sub>2</sub>O<sub>5</sub> during its deposition with predominant exposure of the (010) vanadia face, characterized by the presence of V = O groups[108] and these groups are responsible for the enhancement of selective oxidation.[108] Bond *et al* [109] proposed that at low vanadia content, isolated tetrahedral hydroxo vanadyl groups are formed. The peculiar catalytic properties of this catalyst are due to the joint effect of an easily reducible V = O bond and an acid hydroxyl group from the same active centers.[98] Spectroscopic studies of sub monolayer coverages of vanadia on titania have shown that the dispersed vanadia is present as a combination of monomeric vanadyl and polymeric vanadate species,[110-114] with distribution of both these structures varying with vanadia loading[114] and when the vanadia loading was raised above the dispersive capacity of the titania support, crystallites of V<sub>2</sub>O<sub>5</sub> were formed.[111-113&115]

V<sub>2</sub>O<sub>5</sub> supported on TiO<sub>2</sub>-ZrO<sub>2</sub>[116] or TiO<sub>2</sub>-SiO<sub>2</sub> [106] mixed oxides was also proposed for the improved selective catalytic oxidation reactions. Murakami *et al* [101] and Inomata *et al* [102] reported the benzene oxidation over titania and alumina supported ones with the following order V<sub>2</sub>O<sub>5</sub>/TiO<sub>2</sub> >

$V_2O_5$  >  $V_2O_5/Al_2O_3$  and the activation energy for this reaction on  $V_2O_5/TiO_2$  was reported to be much smaller (ca. 80 KJ/mol) than that on unsupported  $V_2O_5$  (ca. 92 KJ/mol) or on  $V_2O_5/Al_2O_3$  (ca.120 KJ/ mol). These data indicate the promoting effect of  $TiO_2$  support. In spite of the catalyst containing  $V_2O_5$  on titania has been the subject of considerable interest due to its successful application in selective catalytic oxidation reactions; the nature of active species taking part in the reaction is still controversial.

### 1.5.3. Carbon monoxide hydrogenation

Catalytic hydrogenation of CO is a profoundly important reaction widely exploited by many chemical industries for the production of gasoline, alcohol, methane and other higher hydrocarbons. This reaction for the synthesis of long chain hydrocarbon is referred to as Fischer-Tropsch synthesis. Group VIII metals supported on silica, alumina or titania are generally used.[117] But depending on the metal used, the product would be different. The selectivity of this reaction varied with support material.[118]

Carbon monoxide hydrogenation using  $Fe/TiO_2$  catalyst led to the formation of methane.[119-121] while  $Rh/TiO_2$  gave methanol and other hydrocarbons. Methane was reported to be formed over Ni catalyst.[118] Sebatier won Nobel prize in 1912 for the successful production of methane over unsupported Ni catalyst.[118] Sen *et al* [122] and Vannice *et al* [123] reported  $Ni/TiO_2$  catalyst with better activity for methanation than unsupported one and  $Ni/SiO_2$ . Smith *et al* [124] also strongly supported the above observation.

The CO and hydrogen chemisorption behaviour of  $Ni/TiO_2$  was investigated by many researchers [124-127]. The chemisorption was reported to be decreasing in the catalyst reduced at high temperature (ca.> 500<sup>0</sup>C). The



peculiar behaviour of this catalyst was due to SMSI as discussed earlier, which was induced during high temperature reduction.[124] The titania moieties migrated to the Ni surface during reduction would reduce the sticking coefficient of CO adsorption.[124&126] So, it is very clear that the rate of CO adsorption is strongly dependent on the support material [124] and change of support would change the rate of CO hydrogenation.[124]. Rabo *et al* [128] investigated the methanation using Ni over a range of supports and made a conclusion that the specific activity for hydrogenation would be in the order  $\text{Ni/TiO}_2 > \text{Ni/Al}_2\text{O}_3 > \text{Ni/SiO}_2\text{-Al}_2\text{O}_3 > \text{Ni/SiO}_2$ .

Many researchers have reported high activity in CO hydrogenation to synthesize gasoline, over alloy catalysts, like 42Ni29Fe29Co and 50Co50Ni supported on  $\text{TiO}_2$ . [129-132]

#### **1.5.4. Selective catalytic reduction of $\text{NO}_x$ (SCR)**

The emission of  $\text{NO}_x$  from power plants, nitric acid plant and from other industries caused serious environmental problem. So, the removal of  $\text{NO}_x$  is particularly important from a standpoint of pollution control.

Selective catalytic reduction using  $\text{NH}_3$  is the most commonly used method to abate  $\text{NO}_x$  emission and was commercialized in recent years. By the end of 1982, about hundred plants have been constructed and are operating in Japan.[133] In early stages of development of the  $\text{NO}_x$  reduction process, several base metal oxide catalysts, such as oxides of Fe, Fe-Cr and Fe/Al, were reported[133] with high activity. These catalysts, however, lost their activity in a few hundred hours, due to  $\text{SO}_x$  poisoning, which was present along with  $\text{NO}_x$ . Hence, the commercialization of SCR of  $\text{NO}_x$  was not realized until the advent of  $\text{TiO}_2$  based catalysts, which are resistant to sulfur poisoning and were reported to be maintaining their activity for more than five years.[133]

So, now,  $\text{TiO}_2$  has become a catalyst support of choice for this reaction. A number of Japanese[134&135] and US[136] patents available on  $\text{TiO}_2$  based  $\text{NO}_x$  reduction catalyst disclose this fact more clearly.

The SCR catalysts are mainly composed of  $\text{TiO}_2$  and the second component selected from  $\text{V}_2\text{O}_5$ ,  $\text{MoO}_3$ ,  $\text{Fe}_2\text{O}_3$ ,  $\text{CoO}$ ,  $\text{NiO}$ ,  $\text{MnO}_2$ ,  $\text{Cr}_2\text{O}_3$ ,  $\text{CuO}$ , etc. On the whole, a catalyst composed of  $\text{TiO}_2$  and one of the n-type semiconductor ( $\text{V}_2\text{O}_5$ ,  $\text{MoO}_3$ ,  $\text{Fe}_2\text{O}_3$ , etc) showed high activity for  $\text{NO} - \text{NH}_3$  reaction, while a catalyst composed of  $\text{TiO}_2$  and one of the p-type semiconductor ( $\text{CoO}$ ,  $\text{NiO}$ , etc) showed high activity for  $\text{NO}_2 - \text{NH}_3$  reaction.[133] But,  $\text{NO}_2 - \text{NH}_3$  reaction was also reported on  $\text{V}_2\text{O}_5/\text{TiO}_2$  catalyst.[137] A large number of literature are available on the investigation of the surface structure of  $\text{V}_2\text{O}_5/\text{TiO}_2$  catalyst and its  $\text{NO}_x$  reduction capacity.[137-152] The high activity of this catalyst is attributed to the nature of the adsorption sites on the catalyst surface.

Inomatha and co-workers[138-141] found that the sites responsible for the catalytic activity of bulk as well as supported vanadia towards the  $\text{NO} - \text{NH}_3$  reaction in presence of oxygen are the  $\text{V}^{5+} = \text{O}$  groups, whose concentration is directly related with activity. On the basis of isotopic transient studies Janssen *et al* [142&143] proposed dual site mechanism for this reaction with the participation of two neighbouring  $\text{V}^{5+} = \text{O}$  species as active sites. On the other hand, Gasier *et al* [144] concluded that not the  $\text{V} = \text{O}$  species, but the acid hydroxyl group, i.e.  $\text{V} - \text{OH}$  group, present on vanadia surface could be the active site. But, Topsoe *et al* [145] noted that the  $\text{V} = \text{O}$  species are also involved in this reaction along with  $\text{V} - \text{OH}$  group. Some others believe, on the contrary, that amorphous disordered multiple layer of  $\text{V}_2\text{O}_5$  are present on the whole surface.[141,146&147] Isolated monovanadate

structures have been detected at low vanadia coverage on  $\text{SiO}_2$ ,  $\text{Al}_2\text{O}_3$ ,  $\text{TiO}_2$ ,  $\text{ZrO}_2$  and  $\text{HfO}_2$  supported vanadia catalysts by some authors.[111,148&149] According to them,  $\text{VO}_x$  species condense into chain or 2D domains and ultimately into bulk  $\text{V}_2\text{O}_5$  crystallites as  $\text{VO}_x$  loading was increased. Eckert *et al* [111] and Coustemer *et al*,[150] by spectroscopic studies revealed that  $\text{V}^{5-}$  centers evolve from tetrahedral coordination at low coverage to octahedral coordination at higher coverage on  $\text{TiO}_2$  and  $\text{Al}_2\text{O}_3$ . In spite of these investigations on this catalyst, there is still no agreement on the nature of the active sites and the mechanism of the  $\text{NO}_x$  reduction process,[150] but, it is generally accepted that the vanadia part of the catalyst is essential for this reaction.

#### 1.5.5. Coal liquefaction

Concern about the supply of clean burning fuels has stimulated interest in coal liquefaction process. The conversion of coal to liquid fuel involves increasing the hydrogen content of the material. In the liquefaction process it is not sufficient to break down the coal structure into the basic condensed ring units, but it must be broken to yield a product that is liquid at room temperature.[75]

Tanabe *et al* [76] reported direct hydrogenation of coal using various metal oxide catalysts, including  $\text{TiO}_2$  based ones, such as,  $\text{MoO}_3/\text{TiO}_2$  and  $\text{Fe}_2\text{O}_3/\text{TiO}_2$ . Hydrogenation of coal was carried out under a pressure of 100  $\text{Kg/cm}^3$  and a temperature of  $400^\circ\text{C}$ . The ratio of benzene soluble fraction from hydrogenated coal reached 68% for  $\text{MoO}_3/\text{TiO}_2$  compared to 51% for  $\text{MoO}_3/\text{SiO}_2$ . These results suggest that  $\text{TiO}_2$  is not only acting as a support, but also promoting the hydro cracking activity.

### 1.5.6. Ammonia synthesis

The gas phase equilibrium reaction between hydrogen and nitrogen to form  $\text{NH}_3$  is well known to chemists as the basis of the famous Haber - Bosch process, which represents the typical example for a heterogeneously catalyzed reaction. Practical catalysts are multifunctional catalysts, which consist mainly of the reduced form of  $\text{Fe}_3\text{O}_4$  doped with small percentage of  $\text{Al}_2\text{O}_3$ ,  $\text{K}_2\text{O}$ ,  $\text{CaO}$ ,  $\text{SiO}_2$  and  $\text{MgO}$ . [118]

Aika *et al*, [77] who studied the ammonia synthesis over Ru supported on several supports, found the activity to depend strongly on the type of support used. These authors attributed this to variations in the electronic interaction of the metal with the support. Sueiras *et al* [153] also support this conclusion.

Santos *et al*, [154] who studied ammonia synthesis over  $\text{Fe}/\text{TiO}_2$  catalyst found that a small degree of surface poisoning by titania caused a drastic decrease of activity. Nobile jr [155] investigated the kinetics of  $\text{NH}_3$  synthesis over  $\text{Fe}/\text{TiO}_2$ , hydrazine pre treated  $\text{Fe}/\text{TiO}_2$  and K or Cs promoted  $\text{Fe}/\text{TiO}_2$ . The pre-treatment of  $\text{Fe}/\text{TiO}_2$  catalyst with hydrazine increased the ammonia synthesis turn over frequency by more than an order of magnitude than untreated one, because of inhibition of onset of  $\text{Fe}-\text{TiO}_2$  interaction by hydrazine. Alkali promotion also increased the activity.

### 1.5.7. Isomerization

Hattori *et al* [156&157] and Itoh *et al* [158] reported the isomerization of butene over  $\text{TiO}_2$  and  $\text{TiO}_2/\text{SiO}_2$  catalyst. Maximum activity was obtained for a catalyst with 9:1  $\text{TiO}_2$ :  $\text{SiO}_2$  composition. The acidic properties are reported to be responsible for the activity. [156-162] Some authors [158-160] also reported the isomerization of 1-butene and  $\beta$ -pinene over pure  $\text{TiO}_2$ .

Sohn *et al* [161] investigated the isomerization of 1-butene to cis and trans 2-butene over NiO/TiO<sub>2</sub> catalysts modified by anions like SO<sub>4</sub><sup>2-</sup>, PO<sub>4</sub><sup>3-</sup>, SeO<sub>4</sub><sup>2-</sup> and BO<sub>3</sub><sup>3-</sup> and showed the order of activity NiO-TiO<sub>2</sub>/SO<sub>4</sub><sup>2-</sup> >> NiO-TiO<sub>2</sub>/PO<sub>4</sub><sup>3-</sup> > NiO-TiO<sub>2</sub>/BO<sub>3</sub><sup>3-</sup> > NiO-TiO<sub>2</sub>/SeO<sub>4</sub><sup>2-</sup> > NiO-TiO<sub>2</sub>. According to them the higher activity of SO<sub>4</sub><sup>2-</sup> modified one is due to the improved acidic properties of this catalyst. Similar was the order of activity for ethylene dimerization carried out using these catalysts.[161&162]

### 1.5.8. Carbon monoxide oxidation

Carbon monoxide oxidation to CO<sub>2</sub> is an extremely important reaction from environmental point of view, since this reaction is applicable in automotive exhaust decontamination. This reaction is readily catalyzed by transition metals, particularly Pt group metals. The CO oxidation can be performed on Pt catalyst supported on either Al<sub>2</sub>O<sub>3</sub> or TiO<sub>2</sub>. [133] If the reaction gas contains even trace amount of SO<sub>x</sub>, Pt/Al<sub>2</sub>O<sub>3</sub> catalyst is deactivated in a short time. A drastic decrease in specific surface area and pore volume takes place, resulting from the formation of aluminium sulfate. [133] An advantage of using TiO<sub>2</sub> based catalyst, is that it is resistant to SO<sub>x</sub> poisoning. Matsuda *et al* [133] made this conclusion by investigating CO oxidation in presence and absence of SO<sub>2</sub> over Pt/TiO<sub>2</sub>, Pd/TiO<sub>2</sub> and Ru/TiO<sub>2</sub>. An inhibition of the reaction due to the presence of SO<sub>2</sub> was observed with all the catalysts. The effect, however, was smallest in the case of Pt/TiO<sub>2</sub>, which had maintained its initial activity even in presence of 500 ppm SO<sub>2</sub> for a longer period.

Tanaka and White [163-165] studied, in detail, the CO adsorption and CO<sub>2</sub> dissociation on Pt/TiO<sub>2</sub> catalyst. Akubuiro *et al* [166] carried out the kinetic study of this reaction over Pt/TiO<sub>2</sub>. Lane and Wolf [167] investigated

the effect of  $\text{TiO}_2$  crystal phases on this reaction over  $\text{Pt}/\text{TiO}_2$  catalyst. They convincingly argued that, the crystalline form of support plays a dominant role in determining the activity, where as the reduction temperature plays only a minor role. After low ( $200^\circ\text{C}$ ) or high ( $500^\circ\text{C}$ ) temperature reduction, the rutile supported Pt exhibited greater activity than  $\text{SiO}_2$  or anatase supported ones. Though the reason for this better activity of rutile supported one was not clear, a speculative oxygen transfer mechanism from the support is presented (here the rutile support acts as an oxygen source and provides a means for oxygen transfer to the adsorbed  $\text{CO}$ ). These authors argued that the rutile support tends to give up its oxygen, more freely, since it has 19 Kcal/mole lower energy for oxygen desorption compared to anatase.[167]

#### 1.5.9. Miscellaneous

Metals or metal oxides supported on  $\text{TiO}_2$  are reported [168] to be used in catalytic conversion of chloro fluoro carbon (CFC). By considering the hazardous nature of CFC, this reaction is of vital importance.  $\text{Pd}/\text{TiO}_2$ ,  $\text{CeO}_2/\text{TiO}_2$ ,  $\text{La}_2\text{O}_3/\text{TiO}_2$ ,  $\text{Pt}/\text{TiO}_2$ ,  $\text{NiO}/\text{TiO}_2$  and  $\text{CoO}/\text{TiO}_2$  were the catalysts used.[168]

Enantio selective hydrogenation of prochiral  $\text{C} = \text{C}$  bonds using heterogeneous chiral catalyst is a challenging subject in organic synthesis. (E)- $\alpha$ -phenyl cinnamic acid was hydrogenated to yield (S)-(+)-2,3-diphenyl propionic acid on cinchonidine modified  $\text{Pt}/\text{TiO}_2$  catalyst, with much higher optical yield than palladium supported on activated carbon.[169-172]

$\text{Ir}/\text{TiO}_2$  is reported for hydrogenation of n-butane and 2,2, dimethyl propane.[173] The same catalyst was reported for partial oxidation of  $\text{CH}_4$  to synthesis gas ( $\text{CO}$  and  $\text{H}_2$ ).[93]

Catalytic oxidation process plays an important role in the industrial production of fine chemicals and several other commodities. Propylene oxidation to acrolein is reported [174] over Fe-Sb-Ti mixed oxide catalyst with higher activity. Liquid phase epoxidation of olefins is known to proceed in the presence of hydro peroxides as oxidant over catalytic system that contain titanium.[175]

Micro porous crystalline titano silicates are another class of titanium containing catalysts, which are reported to be catalyzing the oxidation of unsaturated hydrocarbons with aqueous  $H_2O_2$ , oxidation of alcohols to ketone, hydroxylation of aromatic hydrocarbon and amines to oxime.[175] Another titano silicate,[176] called titanium- $\beta$ , is a suitable catalyst for oxidation of branched and cyclic alkenes in presence of organic hydroperoxides with high selectivity. The development of titano silicates,[175] which are ZSM type molecular sieves, are interesting due to their hydrophobic nature, which favours the diffusion of non-polar substrates to the active sites. The hydrophobic micro pores of this catalyst are assumed to exclude water from its voids and thus protect the catalyst from deactivation.

### **1.6. Photo catalysis**

Photo catalysis is a process in which there is a combination of photochemistry and catalysis and implies that light and a catalyst are necessary to bring about a chemical reaction. The photocatalytic experiments were generally carried out by exposing aqueous  $TiO_2$  suspensions (1.25mg P25 Degussa  $TiO_2$  Per ml solution) to the light of a 450 W XBO Xe lamp. During the early 1980's Ollis and co-workers [177-182] showed that in the presence of near UV illuminated  $TiO_2$  suspensions, common chlorinated aliphatic hydrocarbon contaminants in water were not only dechlorinated but

totally mineralized and it is clear that near UV illuminated  $\text{TiO}_2$  suspensions provide a powerful wet oxidation method of general applicability. There are different types of  $\text{TiO}_2$  used as photo catalyst: Degussa P25 (30nm diameter particle, 80% anatase & 20% rutile), Aldrich anatase (500 nm diameter particle) and Platinized Aldrich anatase( $\text{Pt-TiO}_2$ ).

The metal oxide semiconductors  $\text{SrTiO}_3$  and  $\text{TiO}_2$  have been frequently studied for applications in photo electrolysis cells and for toxic waste water treatment. Metal oxide photo catalysts have possible applications in water electrolysis, toxic waste remediation and in organic synthesis.[183-185] One of the most interesting aspects in  $\text{TiO}_2$  based photo catalysis is the mineralization process by which halogenated organic compounds can be converted in to the inorganic substrates  $\text{CO}_2$  and halide ions. This has been documented in quite number of elegant and informative studies pioneered in particular by Ollis and Matthews.[178,186-188]

Photo catalysis has been extensively studied over the past two decades. The literature reports a variety of photo catalytic reactions involving  $\text{TiO}_2$ ,  $\text{ZnO}$ ,  $\text{Fe}_2\text{O}_3$ ,  $\text{WO}_3$ ,  $\text{CdS}$  as commonly used photo catalysts for a variety of organic contaminants. These materials have the advantage of an absorption spectrum reaching through the UV and extending near the visible spectral domain. However when factors concerning photo stability, toxicity, cost, availability and redox efficiencies are all considered,  $\text{TiO}_2$  becomes the photo catalyst of choice. It has been recognized that  $\text{TiO}_2$  is the most efficient photo catalyst for many industrially and environmentally important reactions.[189] Photo oxidation of salicylic acid is reported by Dagan *et al* [190] on pure  $\text{TiO}_2$ . Photo decomposition of tri chloro acetic acid and  $\text{CHCl}_3$  over  $\text{TiO}_2$  were reported by Wang *et al*. [191] Reductive dehalogenation of 1,1,2- tri chloro



fluoro ethane (CFC113) took place upon illumination of air free suspension of  $\text{TiO}_2$  containing formate ions.[192] Photo reduction of  $\text{CCl}_4$  and  $\text{CHBr}_3$  occurred in suspensions of  $\text{TiO}_2$ . [193&194] Kutty *et al*[195] studied the photo degradation of phenol over nano sized  $\text{TiO}_2$  (anatase) powder.

Kominami *et al* [196&197] put forward a couple of conditions to obtain better photo activity, viz. titania should necessarily possess large surface area to adsorb substrates and high crystallinity to diminish electron - hole recombination. They investigated the photo mineralization of acetic acid in presence of air. They claimed better activity for their catalysts prepared by hydrothermal crystallization in presence of organic solvents, compared to commercially available Degussa p-25 and Ishihara ST-01.

The photo degradation of metal - EDTA complexes, especially that of Cu, Fe and Zn over  $\text{TiO}_2$  were studied by Kagaya *et al* [198] with complete removal of metal ions. This reaction is profound in the treatment of industrial effluent containing metal ions. Photo oxidation of mono chloro acetic acid and pyridine in presence of oxygen and ozone over  $\text{TiO}_2$  were reported with activity and much lower specific energy consumption in presence of ozone. [199]

Lee *et al* [200] carried out the photo degradation of 1,4 - dichloro benzene. The irradiation of aqueous solutions of 1,2,4- trichloro benzene in the presence of titanium dioxide leads to the formation of several products. Rutile was reported by Sopyan *et al* [201] for the photo oxidative decomposition of gaseous acetaldehyde. It is reported that reduction of  $\text{O}_2$  and oxidation of  $\text{CHCl}_3$  take place at rutile  $\text{TiO}_2$  Surface[202]. Muneer *et al* [203] studied the photo degradation of acid blue 40, a textile dye, in aqueous suspension of

TiO<sub>2</sub>. Addition of some anions, like SO<sub>4</sub><sup>2-</sup> and PO<sub>4</sub><sup>3-</sup> enhanced the photo degradation of paraquat, a very toxic herbicide.[204&205]

Iron doped TiO<sub>2</sub> is reported for photo reduction of molecular N<sub>2</sub>, which has ecological significance and is a part of natural N<sub>2</sub> -cycle. [206] Fe<sub>2</sub>O<sub>3</sub>/TiO<sub>2</sub> mixed oxide catalyst was found to be used in photo detoxification of water containing dichloro acetic acid.[207] Titania supported on SiO<sub>2</sub> or Al<sub>2</sub>O<sub>3</sub> is reported for photo decomposition of salicylic acid and phenol [208] with improved activity than pure TiO<sub>2</sub>. Titania species anchored within the micro pores of Y-zeolite and meso porous zeolites exhibited a high and unique photo activity for the reduction of CO<sub>2</sub> with water at 55<sup>o</sup>C.[209&210] which is known as reductive fixation of CO<sub>2</sub>. The titano silicalite is used for the photo decomposition of NO into N<sub>2</sub>, O<sub>2</sub> and N<sub>2</sub>O at 22<sup>o</sup>C. [211] Photo degradation of aceto phenone in aqueous medium is reported by Xu et al [212] on TiO<sub>2</sub> supported on micro porous zeolite X and Y and on meso porous molecular sieves. Ti exchanged clays are reported for photo degradation of dichloro methane with improved activity than pure TiO<sub>2</sub>. [213]

Crystal structure of TiO<sub>2</sub> is important factor determining its photo catalytic efficiency. It has been known that anatase is more efficient catalyst than rutile. [214] However there is a great variety in the photo catalytic efficiency even among the same crystal form. Increasing the photo catalyst surface area appears to be the most obvious means of improving the efficiency of photo catalytic oxidation reactions. K.Tanaka *et al* reported[215&216] that the addition of H<sub>2</sub>O<sub>2</sub> accelerated the degradation rate of many pollutants considerably. This effect of H<sub>2</sub>O<sub>2</sub> is also influenced by crystal structure of TiO<sub>2</sub>.

### 1.7. Scope and objective of the present investigation

It is evident from the literature that the preparation of fine metal oxides, especially  $\text{TiO}_2$ , has been the subject of many scientific studies during the last two decades, considering their particular demand for use in catalysis. Hence, now, the preparation of fine  $\text{TiO}_2$  powder is a subject of profound importance, in basic as well as applied research. As we know, the catalytic activity of titania is highly dependent on the phase anatase/rutile and its preparation is of fundamental importance to obtain desired properties, necessarily required to catalyze a particular reaction.

Only limited methods are available in literature for the preparation of metal oxide doped  $\text{TiO}_2$ . The methods utilizing titanium tetra alkoxides or tetra chlorides are described in literature. But, it is very difficult to handle these compounds of titanium, as they vigorously hydrolyze even in presence of atmospheric moisture and phase pure  $\text{TiO}_2$  anatase cannot be prepared in presence of chloride ions. Non-availability of commercial catalytic grade titania is the major concern of many of the catalyst industries, as the  $\text{TiO}_2$  manufacturers are aiming only at the pigmentary properties rather than any other physical properties.

The present investigation is therefore carried out with the following objectives.

- To prepare titania doped with different percentages of some transition metal oxides.
- To characterize the transition metals doped titania prepared by co-precipitation using hydrazine hydrate and by wet-impregnation method and to evaluate their properties.

- To examine thoroughly the onset and completion temperatures of anatase to rutile phase transformation in presence of different percentages of  $\text{Fe}_2\text{O}_3$ ,  $\text{NiO}$ ,  $\text{Cr}_2\text{O}_3$ ,  $\text{MnO}_2$  and  $\text{CuO}$  during the heating.
- To study the phase transformation in titania under air, inert and reducing atmospheres.
- To carry out detailed investigation on the photo catalytic activity of all these samples.

With these objectives,  $\text{Fe}_2\text{O}_3/\text{TiO}_2$ ,  $\text{NiO}/\text{TiO}_2$ ,  $\text{Cr}_2\text{O}_3/\text{TiO}_2$ ,  $\text{MnO}_2/\text{TiO}_2$  and  $\text{CuO}/\text{TiO}_2$  systems with different percentages of transition metal oxides were prepared through two different methods and characterized. Photo catalytic oxidation of toluene to benzoic acid was also carried out using all the five systems with different phase content of titania.

The present investigations were done using the uncalcined hydrated titanium hydroxide (titania pulp-amorphous material) containing 82%  $\text{TiO}_2$  produced by the Travancore Titanium Products .Ltd., Trivandrum, Kerala, India. The various transition metal oxides are doped with the titania using co-precipitation and wet-impregnation methods. The details and results of these investigations are given in the following chapters.

---

---

*Experimental*

---

---

## CHAPTER 2

### MATERIALS AND EXPERIMENTAL METHODS

In this chapter, a brief description of the reagents used and the procedural details of the preparation of metal oxides doped TiO<sub>2</sub> namely Fe<sub>2</sub>O<sub>3</sub>/TiO<sub>2</sub>, NiO/TiO<sub>2</sub>, Cr<sub>2</sub>O<sub>3</sub>/TiO<sub>2</sub>, CuO/TiO<sub>2</sub> and MnO<sub>2</sub>/TiO<sub>2</sub> systems are given. The details of instruments used and the analytical methods adopted for the physico-chemical characterization of the above samples as well as the transformation and catalytic properties are also outlined.

#### 2.1. Materials used

##### Chemicals used

All the chemicals used were of analytical grade. The following chemicals were used:

- Aluminium foil (s.d. fine - chem Ltd)
- Ammonia (s.d. fine - chem Ltd)
- Ammonium Sulfate (s.d. fine - chem Ltd)
- Ammonium thiocyanate (s.d. fine - chem Ltd)
- Barium chloride (RANBAXY)
- Chromium trioxide (s.d. fine – chem. Ltd)
- Cupric nitrate (s.d. fine – chem. Ltd)
- Dimethyl glyoxime (MERCK)
- Diphenyl amine sulfonate (s.d. fine - chem Ltd)
- Ethanol (RANBAXY)
- Ferric nitrate (s.d. fine - chem Ltd)
- Hydrazine hydrate (99% - s.d. fine - chem Ltd)

Hydrochloric acid (s.d. fine - chem Ltd)  
Hydrofluoric acid (RANBAXY)  
Hydrogen peroxide (30% - s.d. fine - chem Ltd)  
Manganous sulfate (s.d. fine - chem Ltd)  
Manganese dioxide (s.d. fine - chem Ltd)  
Mercuric chloride (s.d. fine - chem Ltd)  
Nickel nitrate (MERCK)  
Phosphoric acid (s.d. fine - chem Ltd)  
Phenolphthalein indicator ( s.d. fine - chem. Ltd)  
Potassium bisulfate (s.d. fine - chem Ltd)  
Potassium dichromate (s.d. fine - chem Ltd)  
Sodium bicarbonate(s.d. fine - chem Ltd)  
Sodium hydroxide (s.d. fine - chem Ltd)  
Stannous chloride (s.d. fine - chem Ltd)  
Sulfuric acid (s.d. fine - chem Ltd)  
Sulfurous acid (CDH)  
Titanium dioxide (un calcined hydrated titania pulp containing 82% TiO<sub>2</sub> obtained from Travancore Titanium products. Ltd, Trivandrum, Kerala, India.  
Toluene (99% - RANBAXY).

**Gases used**

Argon (IOL, Mumbai)  
Hydrogen (Sterling Gases, Kochi)  
Helium (IOL, Mumbai)  
Nitrogen (West Coast Industries Gases, Kochi)

## **2.2. Experimental procedure**

### **2.2.1. Preparation of Fe<sub>2</sub>O<sub>3</sub>/TiO<sub>2</sub>**

Titania with two different compositions of Fe<sub>2</sub>O<sub>3</sub> were prepared through two different methods.

#### **2.2.1.1. Co-precipitation**

Pure hydrated titania (34.7g) was dissolved in conc. H<sub>2</sub>SO<sub>4</sub> (712.5ml) and (NH<sub>4</sub>)<sub>2</sub>SO<sub>4</sub> (570g) by boiling. Boiling was continued till a clear solution was obtained. It was then cooled, diluted 4 times with distilled water and kept in an ice bath. Ferric nitrate (8.2g) dissolved in distilled water (20ml) was added to the above titanium sulfate solution and mixed well. Hydrazine hydrate (99%) was added drop by drop to this solution with continuous stirring till the precipitation was complete (pH became 9 at this stage). It was then kept aside for 3hrs to settle down the precipitate and the supernatant liquid was decanted. Distilled water (approx. 500ml) was added to the precipitate, stirred well and decanted after settling. This was repeated till the washings were free from sulfate ions (tested using 2% BaCl<sub>2</sub> solution). The precipitate was filtered using Whatman No: 42 filter paper and oven dried at 110<sup>o</sup>C for 8hrs. This oven dried sample was divided into different portions and calcined at different temperatures viz. 700<sup>o</sup>C, 800<sup>o</sup>C and 900<sup>o</sup>C for different time in order to investigate the phase changes during calcination. The sample was labelled as 5%Fe<sub>2</sub>O<sub>3</sub>/TiO<sub>2</sub>(c.p) and were also prepared similarly by taking 31.1g hydrated titania and 22.8g of ferric nitrate respectively. The sample was labeled as 15%Fe<sub>2</sub>O<sub>3</sub>/TiO<sub>2</sub>(c.p).

#### **2.2.1.2. Wet-impregnation**

Hydrated titania (34.7g) was taken in a 250ml beaker. Ferric nitrate (8.2g) dissolved in distilled water (20ml) was added to the hydrated titania,



stirred well and evaporated to dryness on a hot plate with intermittent stirring. The residue was then oven dried at  $110^{\circ}\text{C}$  for 8hrs and calcined at different temperatures, viz.  $800^{\circ}\text{C}$ ,  $850^{\circ}\text{C}$  and  $900^{\circ}\text{C}$  for different time. This sample was labeled as  $5\%\text{Fe}_2\text{O}_3/\text{TiO}_2(\text{w.i})$  By adopting the same procedure, the sample  $15\%\text{Fe}_2\text{O}_3/\text{TiO}_2(\text{w.i})$  was also prepared using 31.1g hydrated titania and 22.8g of ferric nitrate .

### **2.2.2. Preparation of NiO/TiO<sub>2</sub>**

Two different samples of NiO doped titania were prepared by the following methods.

#### **2.2.2.1. Co-precipitation**

The samples of  $5\% \text{NiO} / \text{TiO}_2$ , and  $15\% \text{NiO} / \text{TiO}_2$  (c.p) were prepared by adopting the procedure described in section 2.2.1.1. using 8.2 and 27.3g nickel nitrate (dissolved in 20ml distilled water) respectively. The samples were oven dried at  $110^{\circ}\text{C}$  for 8hrs and finally calcined at  $700^{\circ}\text{C}$ ,  $750^{\circ}\text{C}$ ,  $800^{\circ}\text{C}$  and  $850^{\circ}\text{C}$  for different time.

#### **2.2.2.2. Wet-impregnation**

The wet-impregnation was carried out by the same procedure given in section 2.2.1.2. The samples prepared by using 8.2 and 27.3g nickel nitrate (dissolved in 20ml distilled water) were labeled as 5 and 15%  $\text{NiO} / \text{TiO}_2(\text{w.i})$  respectively. These samples were calcined at  $850^{\circ}\text{C}$ ,  $875^{\circ}\text{C}$  and  $900^{\circ}\text{C}$  for different time intervals.

### **2.2.3. Preparation of Cr<sub>2</sub>O<sub>3</sub>/TiO<sub>2</sub>**

Two different samples of  $\text{Cr}_2\text{O}_3$  loaded  $\text{TiO}_2$  were prepared using the following procedure.

### **2.2.3.1. Co-precipitation**

The co-precipitation was carried out as described in section 2.2.1.1 Here the samples 5 and 15% Cr<sub>2</sub>O<sub>3</sub>/TiO<sub>2</sub>(c.p) were prepared using 1.38 and 4.61 g of chromium trioxide (dissolved in 20ml distilled water) respectively. The calcination was done at 600<sup>0</sup>C, 700<sup>0</sup>C, 800<sup>0</sup>C, 850<sup>0</sup>C and 900<sup>0</sup>C for different time.

### **2.2.3.2. Wet-impregnation**

The procedure adopted was similar to that described in the section 2.2.1.2. The samples were prepared using 1.38 and 4.61g of chromium trioxide (dissolved in 20ml distilled water) and labeled as 5 and 15% Cr<sub>2</sub>O<sub>3</sub>/TiO<sub>2</sub>(w.i). These samples were calcined at 900<sup>0</sup>C, 925<sup>0</sup>C and 950<sup>0</sup>C for different time.

### **2.2.4. Preparation of MnO<sub>2</sub>/TiO<sub>2</sub>**

The samples of MnO<sub>2</sub> loaded titania were prepared as follows.

#### **2.2.4.1. Co-precipitation**

Co-precipitation was carried out as explained in section 2.2.1.1 using 4.31 and 13.6g of manganese sulphate (dissolved in 20 ml distilled water). The samples were marked as 5 and 15% MnO<sub>2</sub>/TiO<sub>2</sub> (c.p) respectively. They were calcined at 650<sup>0</sup>C, 675<sup>0</sup>C, 700<sup>0</sup>C and 750<sup>0</sup>C for different time.

#### **2.2.4.2. Wet-impregnation**

5 and 15% MnO<sub>2</sub>/TiO<sub>2</sub> (w.i) Samples were prepared under this method as described earlier using 2.1 and 7.0 g manganese Dioxide respectively. These samples were calcined at 700<sup>0</sup>C, 750<sup>0</sup>C, 800<sup>0</sup>C and 850<sup>0</sup>C for different time.

### **2.2.5. Preparation of CuO/TiO<sub>2</sub>**

The samples of CuO doped titania were prepared as follows.

### 2.2.5.1. Co-precipitation

Co-precipitation was carried out as explained in section 2.2.1.1 using 7.9 and 21.25g of cupric nitrate (dissolved in 20 ml distilled water ). The samples were marked as 5 and 15% CuO/TiO<sub>2</sub> (c.p) respectively. They were calcined at 700<sup>0</sup>C, 750<sup>0</sup>C, 800<sup>0</sup>C and 850<sup>0</sup>C for different time.

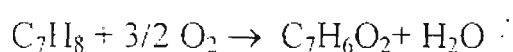
### 2.2.5.2. Wet-impregnation

5 and 15% CuO/TiO<sub>2</sub> (w.i) Samples were prepared under this method as described earlier using 7.9 and 21.25g cupric nitrate respectively. These samples were calcined at 750<sup>0</sup>C, 800<sup>0</sup>C and 850<sup>0</sup>C for different time.

## 2.3. Photo Catalytic oxidation of Toluene to benzoic acid (liquid phase)

The toluene oxidation activity studies were carried out using Fe<sub>2</sub>O<sub>3</sub>/TiO<sub>2</sub>, NiO/TiO<sub>2</sub>, Cr<sub>2</sub>O<sub>3</sub>/TiO<sub>2</sub>, MnO<sub>2</sub>/TiO<sub>2</sub> and CuO/TiO<sub>2</sub> samples calcined at different temperatures as per the procedure described below.

0.250 g of above metal oxide doped TiO<sub>2</sub> samples with different phase content was taken in a photo reactor and 238 ml distilled water and 10 ml hydrogen peroxide also were added. It was then kept on a magnetic stirrer and oxygen was bubbled continuously. 2.7 ml of toluene was then added to the mixture and irradiation was done using 125 Watt medium pressure Hg-arc lamp fitted with annular water cooling jackets fabricated from glass not transmitting light of wave length < 300 nm, for different durations. After each one hour, sample was taken and analysed for benzoic acid formation. The benzoic acid formed was estimated by titrating against standard 0.1N NaOH solution using phenolphthalein as indicator as per the procedure cited in reference.[217] The proposed reaction is:



#### 2.4. Crystallite size calculation

The crystallite size (not the particle size) of anatase was calculated using a computer program based on Scherrer relation. For this purpose, the width at half height of the peak corresponding to [101] plane of anatase was measured. The Scherrer relation states that the XRD peak broadening is inversely proportional to crystallite size [218] and the crystallite size can be calculated from the equation  $D = 0.9\lambda / \beta \cos \theta$ . Where,  $D$  = crystallite size,  $\lambda$  = wavelength used,  $\beta$  = corrected half width of the peak and  $\theta$  = angle of diffraction.

#### 2.5. Rutile percentage calculation

The rutile percentage in each sample was calculated using the equation  $(1 + 0.794 I_A/I_R)^{-1}$  multiplied by 100. Where,  $I_A$  and  $I_R$  are the peak intensities of [101] and [110] planes of anatase and rutile respectively. [219]

#### 2.6. Chemical analysis

A brief description of chemical analysis methods adopted for the estimation of  $TiO_2$ , [220]  $Fe_2O_3$ , [221]  $NiO$ , [222]  $Cr_2O_3$ , [223],  $MnO_2$ , [224] and  $CuO$  [225] is given below.

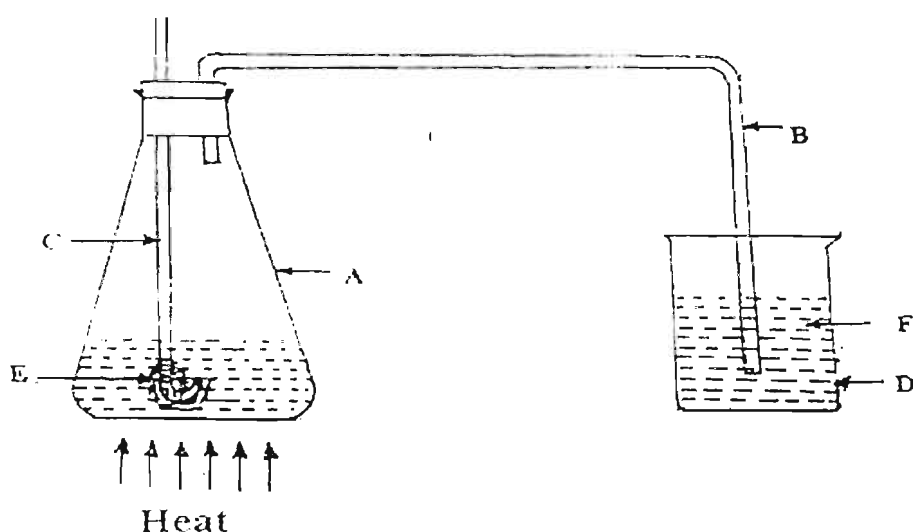
##### 2.6.1. Estimation of $TiO_2$

Aluminium reduction method

The estimation was carried out using the procedure described in literature. [221] The sample (0.2g) was fused with excess amount of potassium bisulfate (15g). The mass was cooled and dissolved in 20%  $H_2SO_4$  (150ml) and the solution was made up to 250ml in a standard flask. A known volume of the made up solution was pipetted into a 500ml Erlenmeyer flask and conc.  $HCl$  (30ml) was added to it. The solution was boiled well and removed from the heating mantle. High purity aluminium foil (2g) was

attached to the glass rod of the reaction setup. The rubber stopper carrying the glass rod with aluminium foil and the delivery tube was immediately inserted into the Erlenmeyer flask. The other end of the delivery tube was placed below the level of saturated sodium bicarbonate solution taken in a beaker, to prevent the re-oxidation as shown below in figure 2.1.

**Figure 2.1: Apparatus for the reduction for the estimation of Titanium dioxide.**



A. 500ml Erlenmeyer Flask  
C. Glass Rod  
E. Aluminium Foil

B. Glass tube  
D. 250ml Beaker  
F. Sodium Bicarbonate Solution

The flask was heated again. Towards the end of the reaction, the flask was swirled to ensure complete mixing and reduction. When the aluminium foil was completely dissolved, the solution was gently boiled for 3-5 minutes keeping the delivery tube immersed in the sodium bicarbonate solution. The solution was cooled to a temperature less than  $60^{\circ}\text{C}$ . As the solution was cooled, the sodium bicarbonate solution was drawn inside the flask and the  $\text{CO}_2$  evolved would give the necessary protective atmosphere. The solution

was cooled and titrated against standard N/16 ferric alum solution using ammonium thiocyanate solution as indicator.

### 2.6.2. Estimation of $\text{Fe}_2\text{O}_3$

$\text{Fe}_2\text{O}_3$  was estimated as per the standard procedure.[222] The sample (0.2g) was fused with potassium bisulfate, dissolved in dilute  $\text{H}_2\text{SO}_4$  and made up to 250ml, as described in section 2.8.1. A known volume of the made up solution was pipetted out into a 250ml Erlenmeyer flask, conc. hydrochloric acid (5ml) was added and heated for 5 minutes. Stannous chloride (6%, 2-3 drops) was added till the yellow colour disappeared and then one drop in excess was added. The excess  $\text{SnCl}_2$  was removed by adding saturated  $\text{HgCl}_2$  solution (15ml). Then 10ml of acid mixture (150 ml  $\text{H}_2\text{SO}_4$  and 150 ml  $\text{H}_3\text{PO}_4$  in 700 ml distilled water) and 10ml of Zimmermann solution (this solution was prepared by adding a cooled mixture of 100 ml conc.  $\text{H}_2\text{SO}_4$  and 300ml water to a solution of 50g of  $\text{MnSO}_4 \cdot 4\text{H}_2\text{O}$  in 250ml water. 100ml of syrupy phosphoric acid was also added.) was added. It was then titrated against standard 0.1N potassium dichromate solution after adding 3 drops of diphenyl amine sulfonate indicator to a violet end point.

### 2.6.3. Estimation of NiO

Nickel estimation was done as per the standard procedure.[223] The sample (0.5g) was fused with potassium bisulfate (38g). The mass was cooled and dissolved in 20%  $\text{H}_2\text{SO}_4$  (300ml).  $\text{TiO}_2$  was precipitated out by adding ammonia. The filtrate was collected and was made acidic by adding conc. hydrochloric acid (10ml). The solution was then heated to 70-80<sup>o</sup>C and 1% ethanolic solution of dimethyl glyoxime (25ml) was added. Dilute ammonia solution was added drop wise with constant stirring until the precipitation began and then in slight excess. The precipitate was filtered

through a sintered glass crucible and washed with cold water until free from chloride and sulfate. Completion of precipitation was tested by adding dimethyl glyoxime to the filtrate. The residue was dried at  $110^{\circ}\text{C}$  for 1hr and weighed.

#### **2.6.4. Estimation of $\text{Cr}_2\text{O}_3$**

$\text{Cr}_2\text{O}_3$  was estimated as per the procedure.[224] The sample (0.5g) was fused with potassium bisulfate, dissolved in dilute  $\text{H}_2\text{SO}_4$  and made up to 250ml, as described in  $\text{TiO}_2$  estimation. A known volume of the made up solution was pipetted out into a 600ml beaker and added 50 ml of sulphuric acid and 10 drops of hydro fluoric acid (48%) using a plastic dropper. Oxidized by drop wise addition of Conc.  $\text{HNO}_3$  and evaporated the solution to fumes of  $\text{SO}_3$ . Cooled, diluted to 300ml and warmed on a hotplate until completely dissolved. Removed from the hot plate and added 10ml of 0.25%  $\text{AgNO}_3$  solution and 25ml of 15% ammonium persulphate solution. Brought to boiling and added one or two drops of  $\text{KMnO}_4$  solution. Boiled for 10 minutes. To the boiling solution added 5ml of  $\text{HCl}$ . Boiled for 5 minutes again (to remove the permanganate colour present) and added 3ml  $\text{HCl}$  and boiled for 10 minutes after the solution turned yellow. Removed from the hot plate and diluted to 200ml with distilled water, cooled to room temperature. Added from the burette a measured excess of 0.05 N ferrous ammonium sulphate solution and titrated the excess ferrous ammonium sulphate with 0.05N permanganate. From the values obtained, the amount of  $\text{Cr}_2\text{O}_3$  was calculated.

#### **2.6.5. Estimation of $\text{MnO}_2$**

Manganese estimation was done as per the standard procedure.[225] The sample (0.5g) was fused with potassium bisulfate (38g). The mass was cooled and dissolved in 20%  $\text{H}_2\text{SO}_4$  (300ml).  $\text{TiO}_2$  was

precipitated out by adding ammonia. The filtrate was collected and made acidic by adding about 40ml of 4N sulphuric acid solution and 40 ml of standard oxalic acid was buretted out into the solution. The mixture was gently heated to about 70<sup>0</sup>C and titrated against standard potassium permanganate solution till the end point. From the results, manganese dioxide was calculated.

#### **2.6.6. Estimation of CuO**

Copper estimation was done as per the standard procedure.[226] The sample (0.5g) was fused with potassium bisulfate (38g). The mass was cooled and dissolved in 20% H<sub>2</sub>SO<sub>4</sub> (300ml). TiO<sub>2</sub> was precipitated out by adding ammonia. The filtrate was collected and was made acidic by adding a few drops of dilute hydrochloric acid and then added a slight excess (about 20-30 ml as required) of freshly prepared saturated sulphurous acid solution. (Prepared by diluting to 10 times its volume, the commercial concentrated solution, which has a specific gravity of 1.33 and contains about 54% SO<sub>2</sub>)

Diluted the cold liquid to 150-200ml, heated nearly to boiling, and added freshly prepared 10% ammonium thiocyanate solution, slowly with constant stirring, from a burette until present in slight excess. The precipitate of copper(I) thiocyanate was white and the mother liquor was colourless and smell of SO<sub>2</sub> was present. Allowed to stand for settling over night. Filtered through a weighed sintered glass crucible and washed the precipitate 10 to 15 times with cold solution prepared by adding to every 100ml of water 1ml of a 10% solution of ammonium thiocyanate and 5-6 drops of saturated sulphurous acid solution and finally several times with 20% ethanol to remove ammonium thiocyanate. Dried the precipitate to constant weight at 110-120<sup>0</sup>C and weighed as CuSCN. From the weight obtained, the amount of CuO was calculated.



## **2.7. Instrumental methods employed**

### **2.7.1. Surface area analyzer**

Surface area measurements were done by BET method of nitrogen adsorption at liquid nitrogen temperature using Gemini 2360 V4.01 instrument by taking accurately 0.5g of the sample.

### **2.7.2. photo catalytic reactor**

The catalytic reactor was made of pyrex glass . It has 25cm height and 30mm and 18 mm outer and inner diameters respectively. It is fitted with annular water cooling jackets fabricated from glass not transmitting light of wave length < 300 nm.

### **2.7.3. Furnace and temperature programmer**

A vertical tube furnace with a temperature programmer (Century Systems CS 7533) was used in these studies. Ordinary muffle furnace was used for calcination purpose.

### **2.7.4. X - Ray Diffractometer**

Philips automatic powder diffractometer, PW 1710 with  $\text{CuK}\alpha$  wavelength was used for XRD studies.

### **2.7.5. Scanning Electron Microscope**

JSM-5600 instrument was used for SEM analysis. 0.1g of the sample was dispersed in acetone by sonication and one drop was placed on a copper stud, dried and gold sputtered. Then the SEM analysis was carried out.

EDAX analysis was also made simultaneously using the same equipment with attachments.

---

---

*RESULTS AND DISCUSSION*

---

---

## CHAPTER 3

### STUDIES ON Fe<sub>2</sub>O<sub>3</sub> DOPED TiO<sub>2</sub>

The catalytic activity of TiO<sub>2</sub> support is determined by physical properties such as surface area, crystallinity etc. which mainly depend on the preparative conditions. Many efforts have been made for preparing highly dispersed Fe catalysts on high surface area TiO<sub>2</sub>. But, unfortunately, only a few methods for the preparation of these catalysts are available in literature. The polymorphism occurring during the heat treatment is very important in selecting TiO<sub>2</sub> as a catalytic support.

In order to study the effect of amount of Fe<sub>2</sub>O<sub>3</sub> and reaction atmospheres TiO<sub>2</sub> doped with different percentages of Fe<sub>2</sub>O<sub>3</sub> was prepared using two methods, as described in Chapter 2. The transformation was studied in air, argon and hydrogen atmospheres as a function of temperature and time using XRD, Surface area measurements and SEM.

#### 3.1. Chemical analysis

The composition of samples was determined by chemical analysis using standard procedures as described in chapter 2. The percentage of Fe<sub>2</sub>O<sub>3</sub> in each sample is as given in Table 3.1.

**Table 3.1: Results of Chemical analysis of Fe<sub>2</sub>O<sub>3</sub> doped TiO<sub>2</sub> prepared through different methods.**

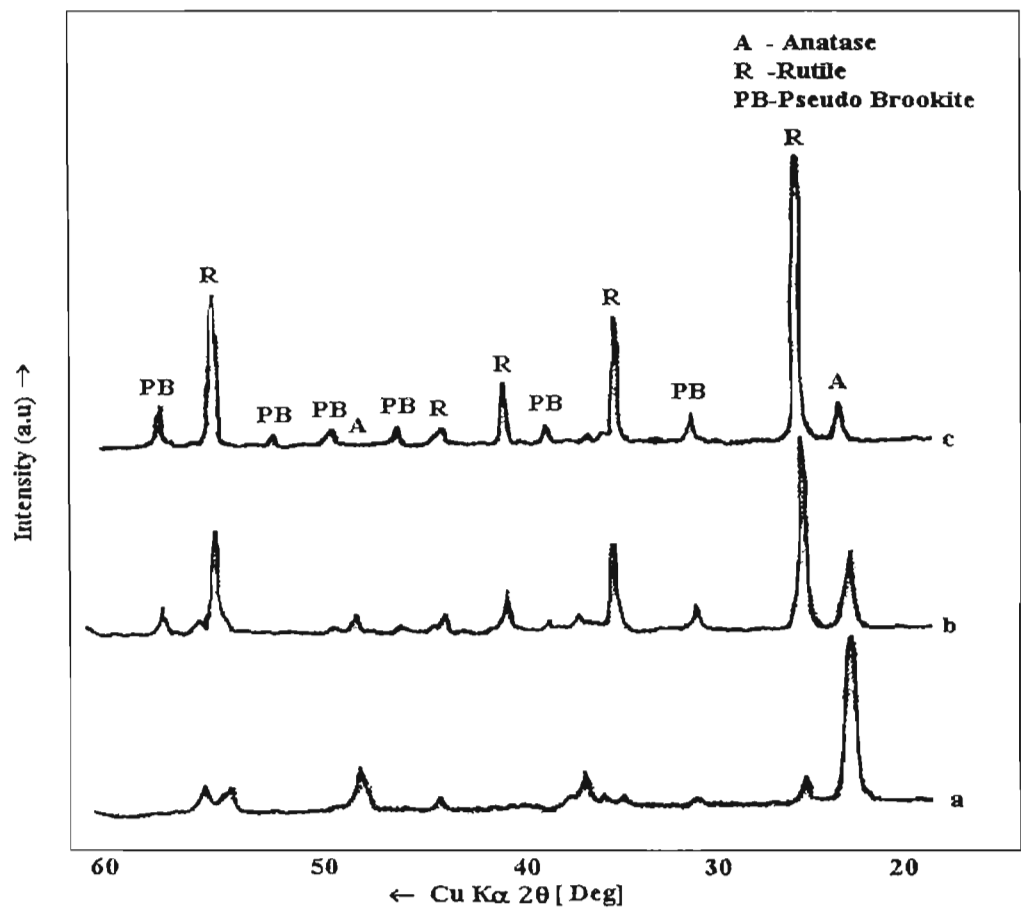
Method of Preparation	Expected Fe <sub>2</sub> O <sub>3</sub> (%)	Experimental Composition	
		Fe <sub>2</sub> O <sub>3</sub> (%)	TiO <sub>2</sub> (%)
Co-precipitation	5	4.84	94.3
	15	14.39	84.4
Wet-Impregnation	5	4.80	93.8
	15	14.80	84.2

### 3.2. XRD studies

XRD pattern of co-precipitated and wet-impregnated samples calcined in air at different temperatures and time showed that these samples are crystalline above  $550^{\circ}\text{C}$ , where as phase transformations are different in co-precipitated and wet-impregnated one.

X-ray Diffraction patterns of the co-precipitated  $\text{Fe}_2\text{O}_3$  doped  $\text{TiO}_2$  after calcination in air at different temperatures are shown in figures 3.1 and 3.2.

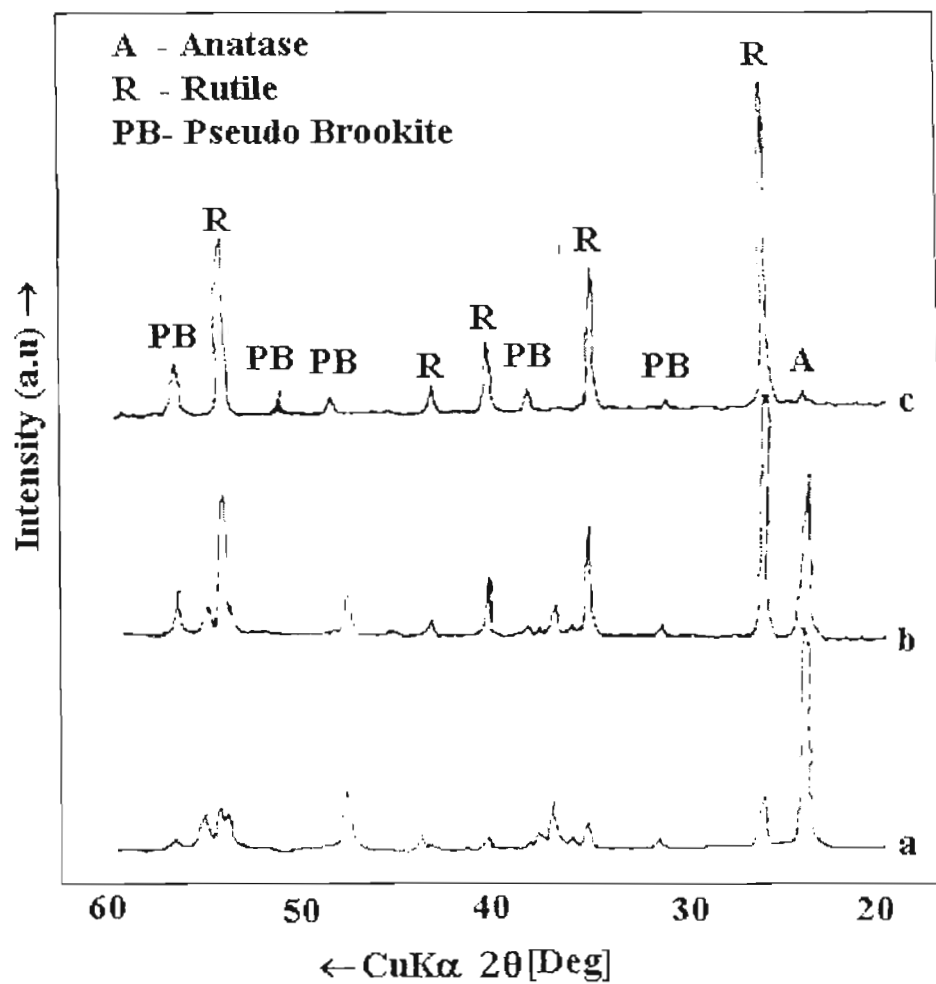
Figure 3.1: XRD Patterns of co-precipitated 5%  $\text{Fe}_2\text{O}_3/\text{TiO}_2$  heated at different temperatures. (a)  $700^{\circ}\text{C}$  (b)  $800^{\circ}\text{C}$  (c)  $900^{\circ}\text{C}$



In all the patterns there were peaks due to anatase and rutile phase of  $\text{TiO}_2$  and no peaks due to  $\text{Fe}_2\text{O}_3$  appeared, obviously due to the fineness of

iron oxide particles. Also there were peaks corresponding to pseudobrookite ( $\text{Fe}_2\text{TiO}_5$ ) which indicates that  $\text{Fe}_2\text{O}_3$  has reacted with  $\text{TiO}_2$  during heating to form iron titanate.

Figure 3.2: XRD Patterns of co-precipitated 15%  $\text{Fe}_2\text{O}_3/\text{TiO}_2$  heated at different temperature. (a)  $700^\circ\text{C}$  (b)  $800^\circ\text{C}$  (c)  $900^\circ\text{C}$



Peaks of rutile appeared in the pattern at  $700^\circ\text{C}$  and on further increase, the rutile peaks became more intense and anatase peaks disappeared from the pattern, The various amounts of rutile formed during



heating of co-precipitated  $\text{Fe}_2\text{O}_3$  doped samples are given in tables 3.2 and 3.3.

**Table 3.2: % of rutile formed during heating of co-precipitated 5%  $\text{Fe}_2\text{O}_3/\text{TiO}_2$  at different temperatures and time.**

Time of heating (hrs)	Rutile formed (%)		
	700 <sup>0</sup> C	800 <sup>0</sup> C	900 <sup>0</sup> C
1	1.5	13.2	34.9
2	3.1	24.5	57.6
3	4.6	34.5	72.4
4	6.2	43.1	82.1
5	7.7	50.6	88.3
6	9.2	57.1	92.4
7	10.6	62.7	95.1
8	12.2	67.6	96.8
9	13.5	71.9	97.9
10	14.8	75.6	98.9

In 5%  $\text{Fe}_2\text{O}_3$  doped  $\text{TiO}_2$ , on calcination at 700<sup>0</sup>C for 8 hrs 12% rutile was formed and at the same time 15% doped sample gave 26% rutile, on heating at same conditions.

The influence of altrivalent cation doping on  $\text{TiO}_2$  on its phase transition and grain growth has been investigated. It was reported that dopants like  $\text{Si}^{4+}$ ,  $\text{V}^{5+}$  and  $\text{Ru}^{3+}$  affect the phase transition temperature of the titania host. It was reported that on doping  $\text{TiO}_2$  with 10%  $\text{Fe}_2\text{O}_3$  and  $\text{NiO}$ , the anatase-rutile transformation is altered much. [69]

**Table 3.3: % of rutile formed during heating of co-precipitated 15% Fe<sub>2</sub>O<sub>3</sub>/TiO<sub>2</sub> at different temperatures and time**

Time of heating (hrs)	Rutile formed (%)		
	700 <sup>0</sup> C	800 <sup>0</sup> C	900 <sup>0</sup> C
1	3.7	16.1	43.6
2	7.2	29.5	68.2
3	10.6	40.8	82.1
4	14.1	50.3	89.9
5	17.2	58.6	94.3
6	20.2	65.2	96.8
7	23.4	70.8	98.2
8	26.1	75.4	98.9
9	28.9	79.7	99.4
10	31.4	82.6	99.7

It is clear from the table that increasing the calcination temperature gives higher rutile % for the 15% doped samples than for 5%. The increase in rutilation is due to the difference in concentration of Fe<sub>2</sub>O<sub>3</sub>.

Un doped TiO<sub>2</sub> does not undergo any phase transformation on heating up to 900<sup>0</sup>C. At 1000<sup>0</sup>C, anatase peaks disappeared giving only rutile peaks indicating that rutilation was complete. The patterns are as given in figure 3.3.

Figure 3.3: XRD patterns of undoped  $\text{TiO}_2$  heated at different temperatures.  
 (a)  $800^\circ\text{C}$  (b)  $900^\circ\text{C}$  (c)  $1000^\circ\text{C}$



Therefore it is evident that the anatase-rutile transformation in undoped  $\text{TiO}_2$  takes place between  $900\text{--}1000^\circ\text{C}$ . This clearly indicates that the presence of  $\text{Fe}_2\text{O}_3$  enhances the crystallographic rearrangement in  $\text{TiO}_2$ . Also in presence of  $\text{Fe}_2\text{O}_3$ , the crystallization temperature has been altered to



550<sup>0</sup>C as compared to 700<sup>0</sup>C for undoped sample. So, the presence of Fe<sub>2</sub>O<sub>3</sub> has a strong influence on the crystallization of the co-precipitated sample.

The variation of rutile percentage with time at different temperatures during calcinations of Fe<sub>2</sub>O<sub>3</sub> doped TiO<sub>2</sub> samples is given in figures 3.4 and 3.5. It was found that rutilation increases with durations of calcination. This variation in rutilation is different for different percentages of Fe<sub>2</sub>O<sub>3</sub>.

**Figure 3.4:** Variation of rutile % with time at different temperatures in co-precipitated 5% Fe<sub>2</sub>O<sub>3</sub>/TiO<sub>2</sub>.

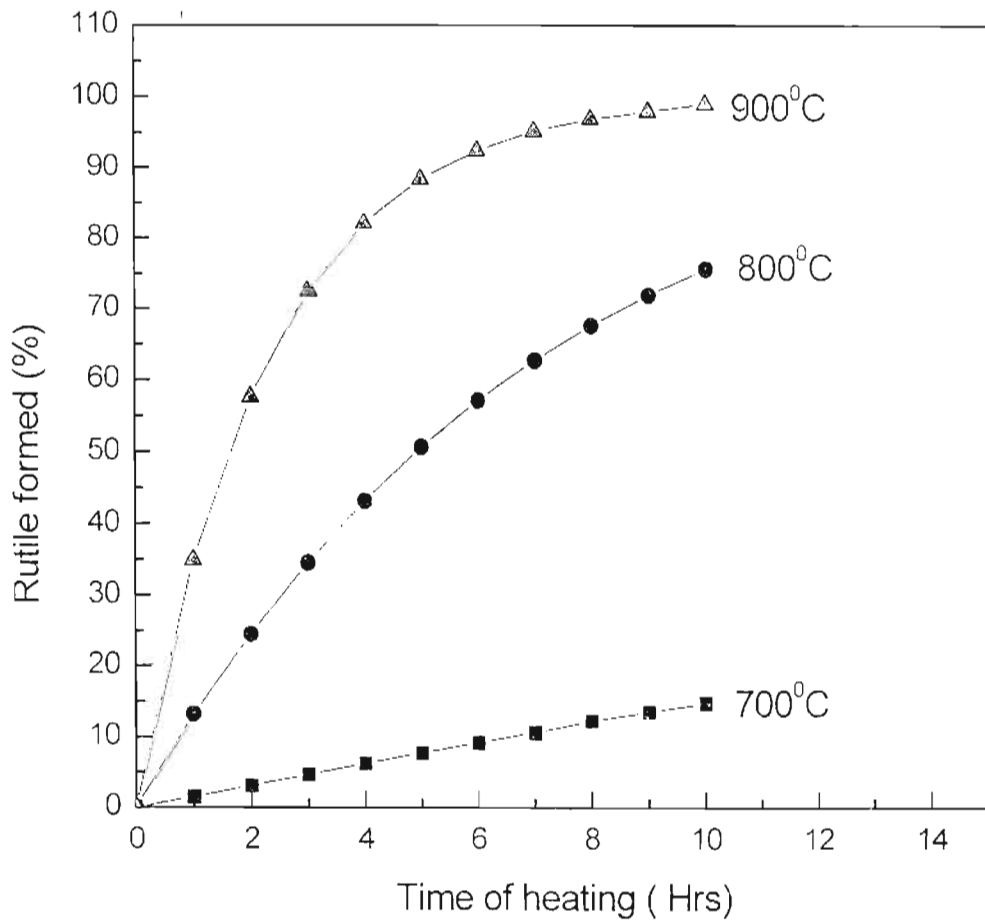
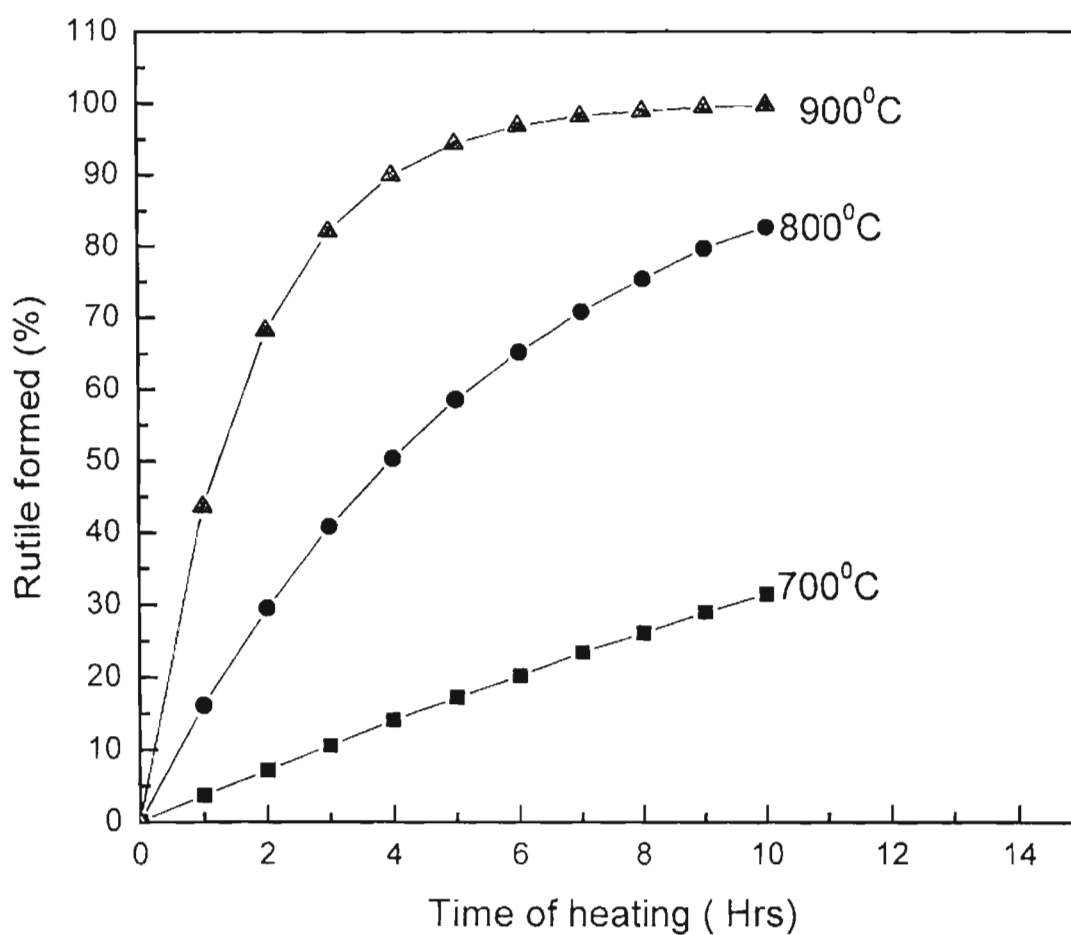
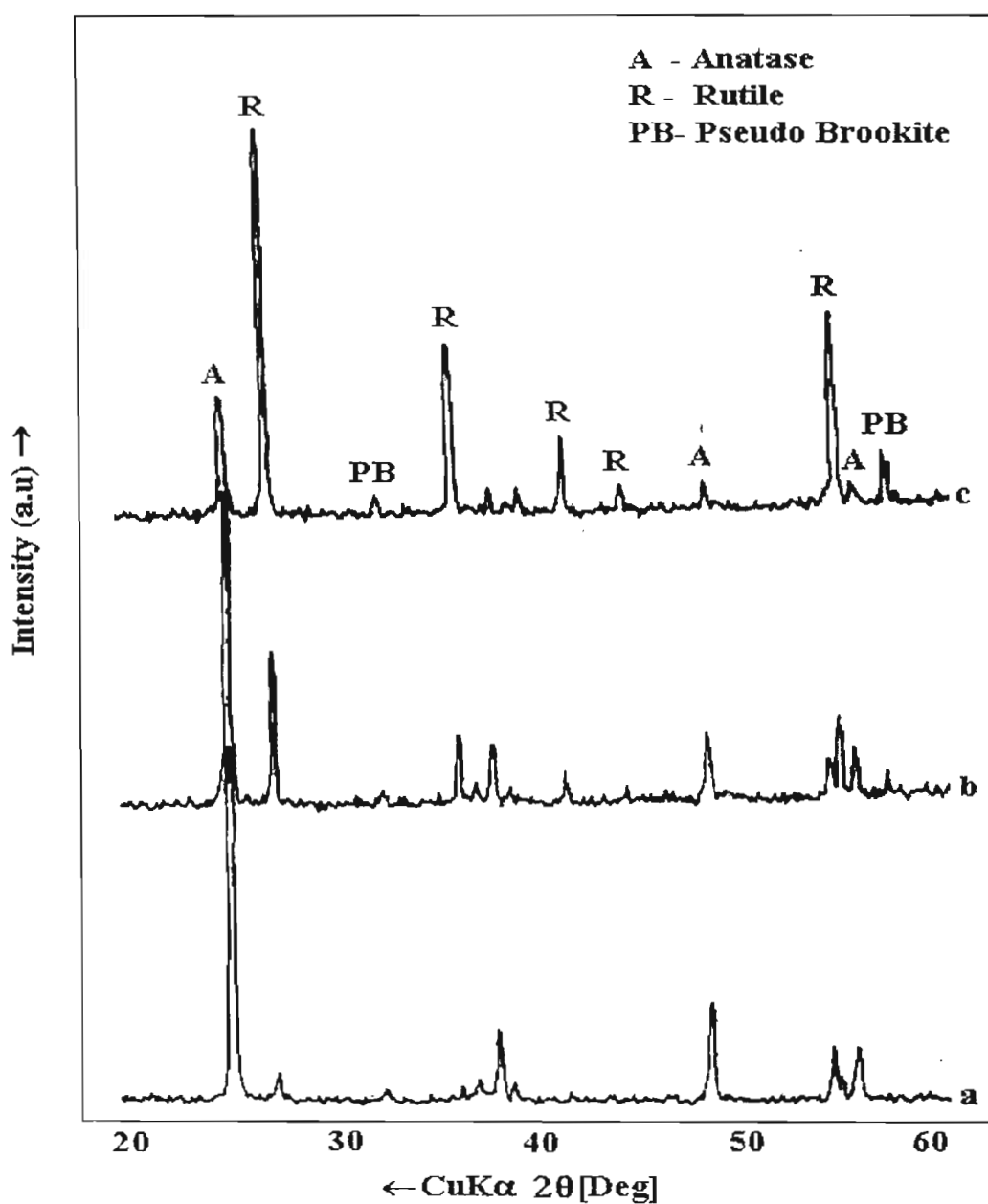


Figure 3.5: Variation of rutile % with time at different temperatures in co-precipitated 15%Fe<sub>2</sub>O<sub>3</sub>/TiO<sub>2</sub>.



The wet-impregnated samples behaved differently during the heat treatment even though the effect of different percentages is same as in the case of co-precipitated samples. The XRD patterns of wet-impregnated samples are given in figures 3.6 and 3.7.

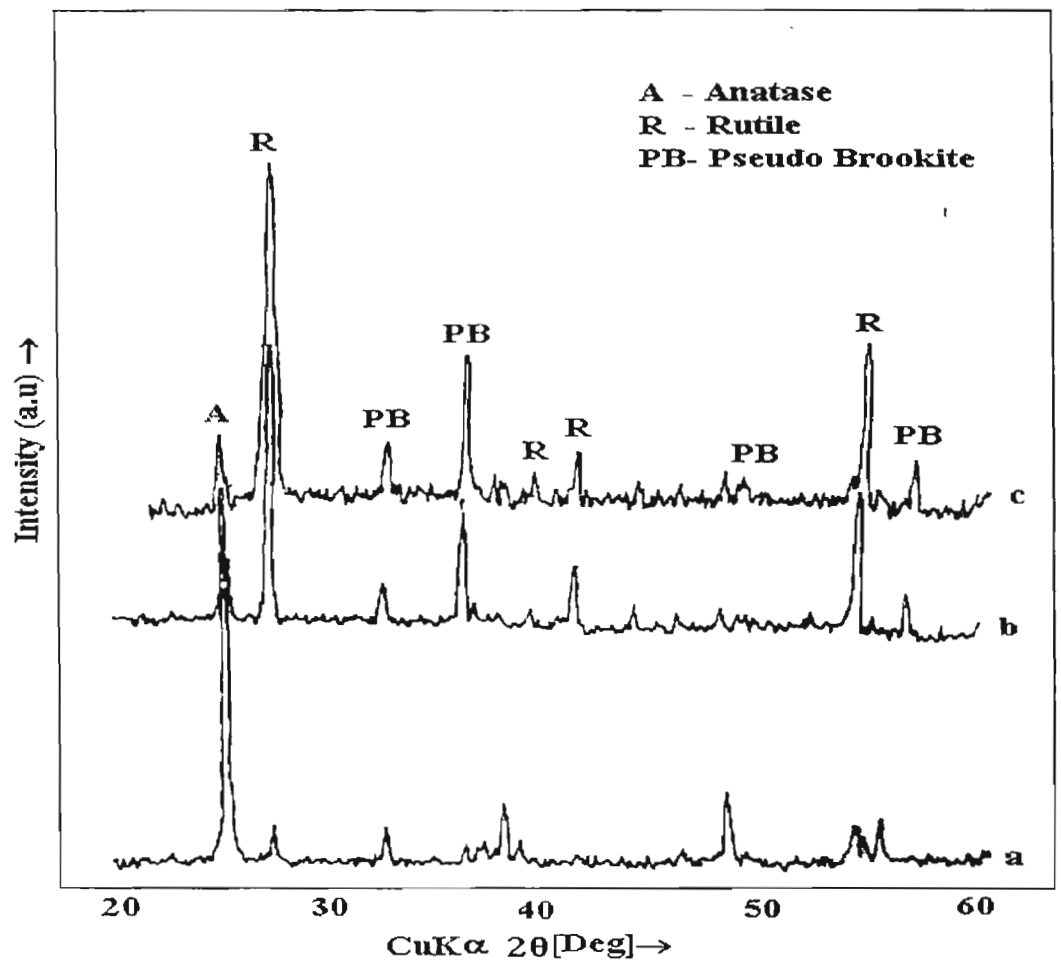
Figure 3.6: XRD Patterns of wet-impregnated 5% Fe<sub>2</sub>O<sub>3</sub>/TiO<sub>2</sub> heated at different temperatures. (a) 800<sup>o</sup>C (b) 850<sup>o</sup>C (c) 900<sup>o</sup>C



15% doped sample got rutilated almost completely at 900<sup>o</sup>C in 10 hrs, where as in the 5% loaded system, the rutilation started only at 800<sup>o</sup>C for 5 hrs heating and only 87% completed at 900<sup>o</sup>C for 10 hrs

heating. It is believed that  $\text{Fe}^{3+}$  introduces the oxygen vacancies in the anatase lattice, which favour the rutile nucleation.

**Figure 3.7: XRD Patterns of wet-impregnated 15%  $\text{Fe}_2\text{O}_3/\text{TiO}_2$  heated at different temperatures. (a)  $800^\circ\text{C}$ (b)  $850^\circ\text{C}$ (c)  $900^\circ\text{C}$**



An increase in the concentration of  $\text{Fe}^{3+}$  will favour a greater diffusivity because mass transport in  $\text{TiO}_2$  is controlled by oxygen diffusion. This leads to a more rapid growth of rutile, which is in agreement with general theory of the vacancy diffusion mechanism [61]. When the temperature raises  $\text{Fe}^{3+}$  dissolution, the concentration of oxygen vacancies

and diffusivity in  $\text{TiO}_2$  increase. Thus, the nucleation and growth of rutile is favoured by increasing temperature.

Rutile conversion in wet-impregnated samples on calcinations at different temperatures and time are given in tables 3.4 and 3.5.

**Table.3.4: % of rutile formed during heating of wet-impregnated 5% $\text{Fe}_2\text{O}_3/\text{TiO}_2$  at different temperatures and time**

Time of heating (hrs)	Rutile formed (%)		
	800	850	900 <sup>o</sup> C
1	0	7.4	18.9
2	0	14.2	34.3
3	0	20.6	46.7
4	0	30.9	61.8
5	4.7	35.5	69.9
6	5.6	39.4	73.2
7	9.3	42.3	75.3
8	10.6	46.1	81.4
9	11.8	50.3	84.9
10	13.2	53.6	87.7

So, it is obvious from all these observations that  $\text{Fe}_2\text{O}_3$  influences the rutile phase formation to different extents in samples prepared through different routes. The rutile percentages against time of heating at different temperatures of samples prepared by co-precipitation and wet-impregnation are given in Figures 3.8 and 3.9. The onset and completion temperatures of rutilation were much lower in co-precipitated ones as compared to wet-impregnated. The  $\text{Fe}_2\text{O}_3$  influences noticeably the rutilation temperature in co-precipitated samples.

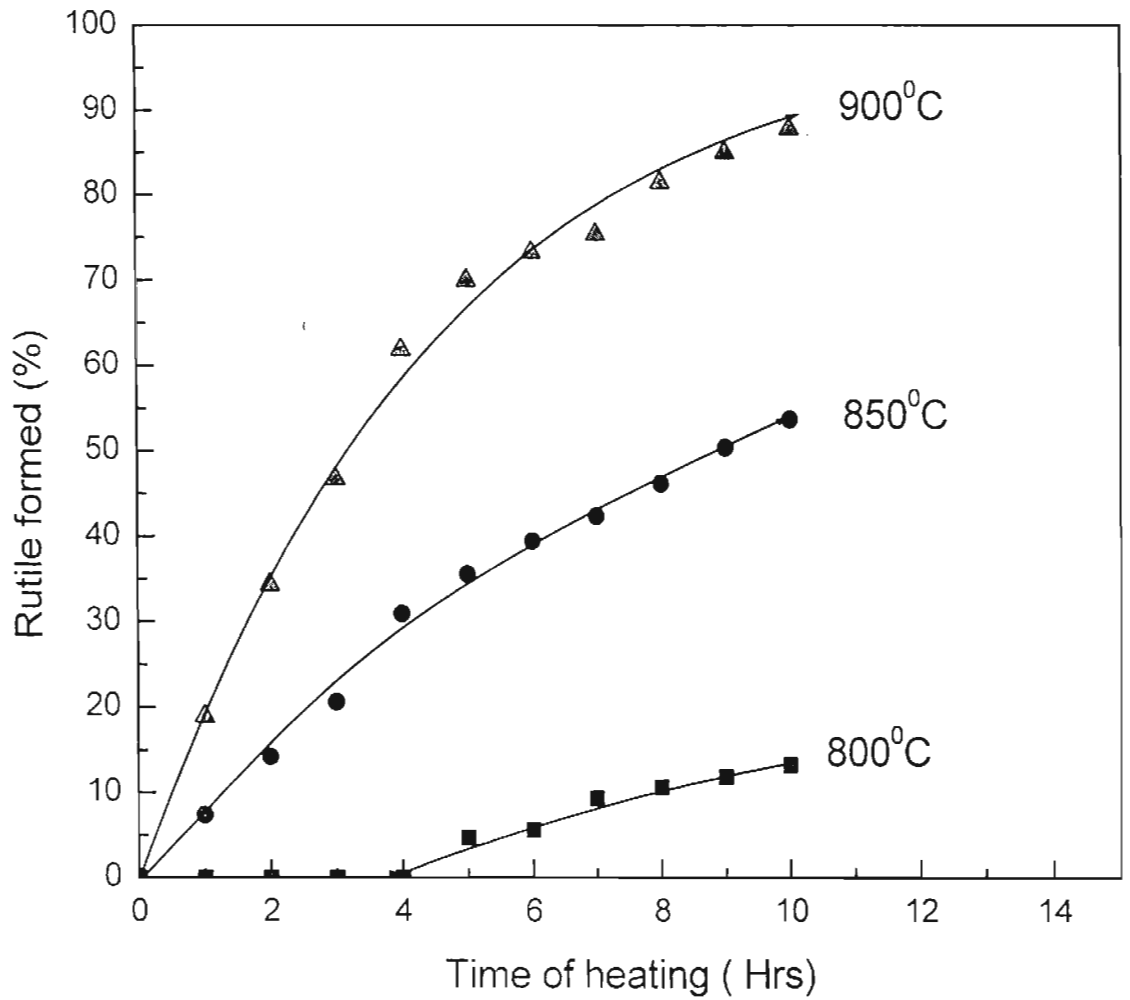
**Table 3.5: % of rutile formed during heating of wet-impregnated 15% Fe<sub>2</sub>O<sub>3</sub>/TiO<sub>2</sub> at different temperatures and time**

Time of heating (hrs)	Rutile formed (%)		
	800	850	900 <sup>o</sup> C
1	2.5	8.8	24.1
2	4.9	16.9	42.4
3	7.4	24.3	56.2
4	9.7	39.8	69.9
5	12.1	43.5	74.9
6	14.3	49.8	81
7	16.4	55.2	85.5
8	18.58	60	89
9	20.6	64.4	91.6
10	22.65	68.26	93.69

It can be inferred that the presence of Fe<sub>2</sub>O<sub>3</sub> during the crystallization of TiO<sub>2</sub> would enhance the formation of rutile, to different extents depending on the method of preparation. If the distribution of Fe<sub>2</sub>O<sub>3</sub> were more uniform, the chance for rutilation would also be higher. In wet-impregnated samples distribution of Fe<sub>2</sub>O<sub>3</sub> is not uniform, which may be the cause for lower rutilation as compared to co-precipitated samples.

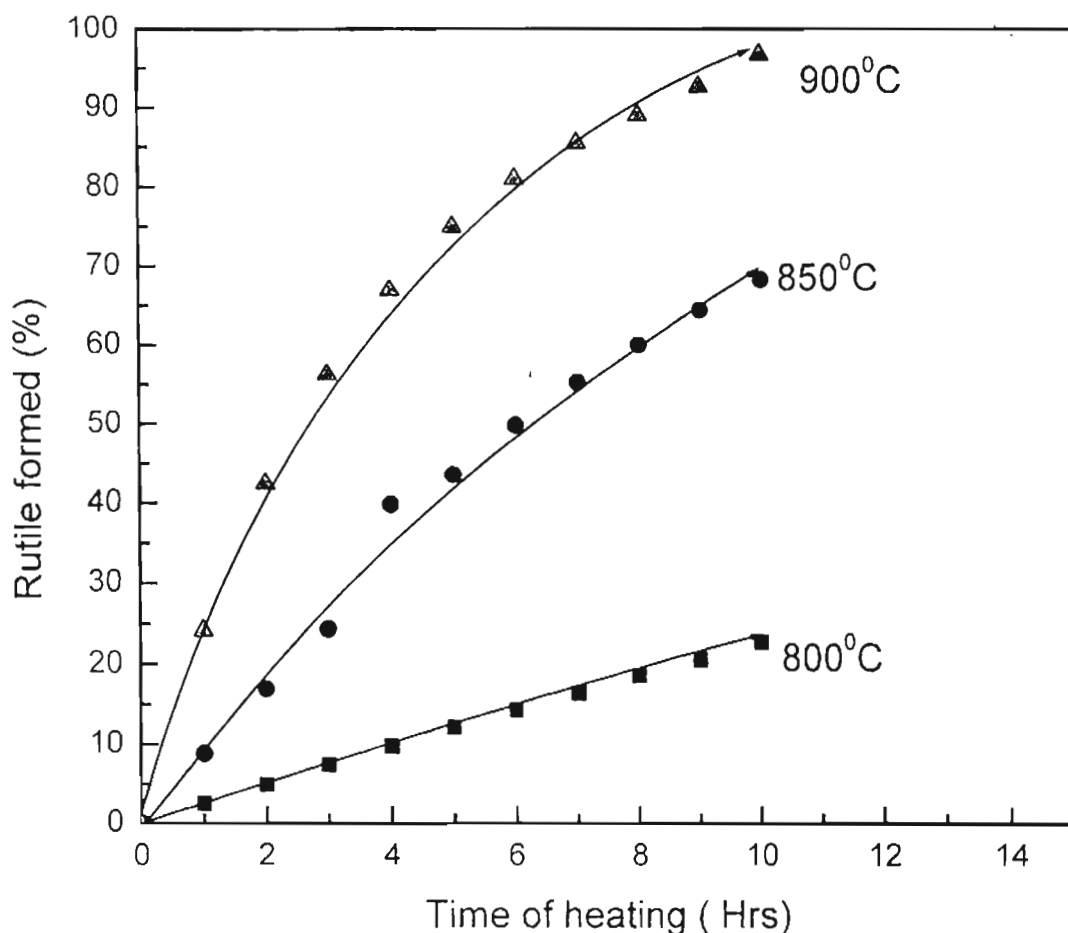
The activation energy for the anatase-rutile transformation was calculated and is given in table 3.6. The activation energy calculated for the transformation in co-precipitated samples in presence of 5% Fe<sub>2</sub>O<sub>3</sub> is found to be 38.3 while in presence of 15% Fe<sub>2</sub>O<sub>3</sub> 28.9k cal / mol. In case of wet-impregnated samples the activation energy for the transformation was found to be 63.6 in presence of 5% Fe<sub>2</sub>O<sub>3</sub> while in presence of 15% it is 59.9 k cal/mol. For undoped TiO<sub>2</sub>, activation energy for anatase-rutile transformation was reported to be ~90 K cal/mol. But among 5 & 15% Fe<sub>2</sub>O<sub>3</sub> 15% has more lowering of activation energy and hence it is more accelerating.

Figure 3.8: Variation of rutile % with time at different temperatures in wet-impregnated 5% Fe<sub>2</sub>O<sub>3</sub>/TiO<sub>2</sub>



It is clear that the lowering of activation energy is different in wet-impregnated system as compared to co-precipitated ones. So an analysis of the activation energy values determined is useful in understanding the relative accelerating effect of Fe<sub>2</sub>O<sub>3</sub> doping. Hence it is clear that in presence of Fe<sub>2</sub>O<sub>3</sub>, the activation energy is lowered much as compared to undoped.

Figure 3.9: Variation of rutile % with time at different temperatures in wet-impregnated 15%  $\text{Fe}_2\text{O}_3/\text{TiO}_2$ .



The crystallite size of anatase calculated from XRD data is given in Table 3.7. The crystallite size was found to increase with temperature and rutilation, depending on the method of preparation. On increasing percentage of  $\text{Fe}_2\text{O}_3$  in co-precipitated and wet-impregnated samples, Crystallite size also increased. The crystallite size increased more than that of pure  $\text{TiO}_2$ . The rutilation starts in 5% doped co-precipitated samples when the anatase crystallites grow to a size of 17.6 nm, while in the case of 5% wet-



impregnated ones the transformation happens at 14.4 nm. In 15% doped samples it is at 18.8 and 15.8 nm respectively.

**Table 3.6: Activation energies for the anatase-rutile transformation in Fe<sub>2</sub>O<sub>3</sub> doped TiO<sub>2</sub>.**

Method of Preparation	Fe <sub>2</sub> O <sub>3</sub> (%)	Activation energy K cal/mol
Co-precipitation	5	38.3
	15	28.9
Wet-Impregnation	5	63.6
	15	59.9

### 3.3. Surface area studies

The surface area values of undoped and Fe<sub>2</sub>O<sub>3</sub> doped samples calcined at different temperatures are given in table 3.7.

The effect on increasing Fe<sub>2</sub>O<sub>3</sub> percentage is more pronounced. In the case of co-precipitated samples, surface area was 13.4 m<sup>2</sup>/g, and 12.9 m<sup>2</sup>/g respectively for 5 and 15% doped samples heated at 700<sup>0</sup>C for 8 hrs. Undoped titania under the same conditions gave 27.2 m<sup>2</sup>/g. The surface area decreased drastically with rutilation observed at 800 and 900<sup>0</sup>C for 5 and 15% doped samples respectively. Similarly, for wet-impregnated samples it was 16.2 and 14.4 m<sup>2</sup>/g in 5 and 15% doped system after heating at 800<sup>0</sup>C. It became 2.53 and 2.96 m<sup>2</sup>/g at 900<sup>0</sup>C. This is in agreement with crystallite size of anatase, which is found to increase with increasing Fe<sub>2</sub>O<sub>3</sub> percentage.

**Table 3.7: Crystallite size and surface area values of un doped and Fe<sub>2</sub>O<sub>3</sub> doped TiO<sub>2</sub> Samples heated at different temperatures for 8 hrs**

Sample	Heating Temperature (°C)	Surface area (m <sup>2</sup> /g)	Crystallite size of anatase (nm)
Undoped TiO <sub>2</sub>	110	162.58	a*
	300	109.59	a*
	700	27.2	4.8
	900	9.13	14.2
	1000	2.54	b*
Co-precipitated 5% Fe <sub>2</sub> O <sub>3</sub> /TiO <sub>2</sub>	700	13.4	17.1
	800	9.9	18.8
	900	2.41	22.6
Co-precipitated 15% Fe <sub>2</sub> O <sub>3</sub> /TiO <sub>2</sub>	700	12.9	17.6
	800	4.3	19.9
	900	1.32	23.7
Wet-impregnated 5% Fe <sub>2</sub> O <sub>3</sub> /TiO <sub>2</sub>	800	16.2	14.4
	850	8.43	17.3
	900	2.53	22.3
Wet-impregnated 15% Fe <sub>2</sub> O <sub>3</sub> /TiO <sub>2</sub>	800	14.4	15.8
	850	7.93	17.6
	900	2.96	21.4

\* a- Amorphous TiO<sub>2</sub>    \* b- Anatase phase absent

Crystallite size of anatase seems to have some relation with surface area. Surface area decreased on increase of crystallite size. So, Fe<sub>2</sub>O<sub>3</sub> has a significant influence on the surface area of these samples. The decrease in

surface area with increase in rutile percentage was also larger in presence of  $\text{Fe}_2\text{O}_3$ . This indicates that anatase-rutile transformation involves a collapse of the open structure to a closed rutile structure. This process takes place by the rupture of two of the six Ti-O bonds of the titanium co-ordination octahedral in anatase to form new bonds in rutile as said earlier.

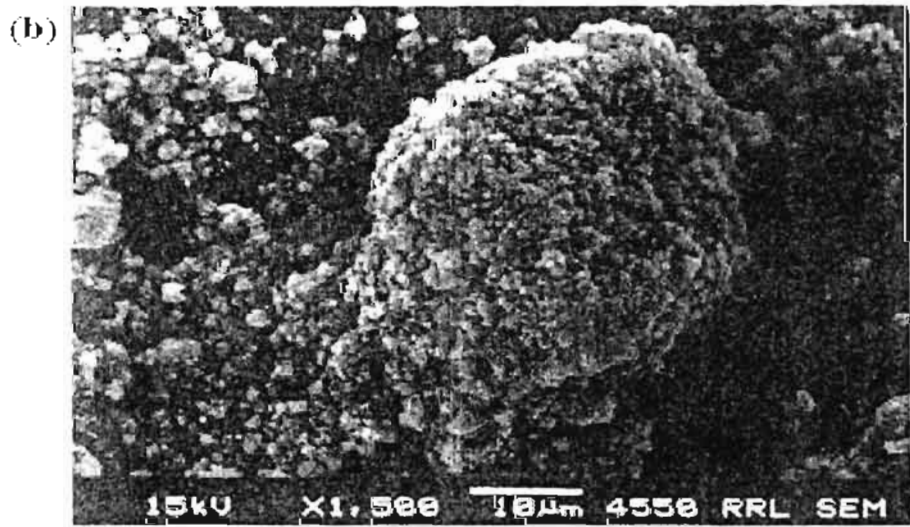
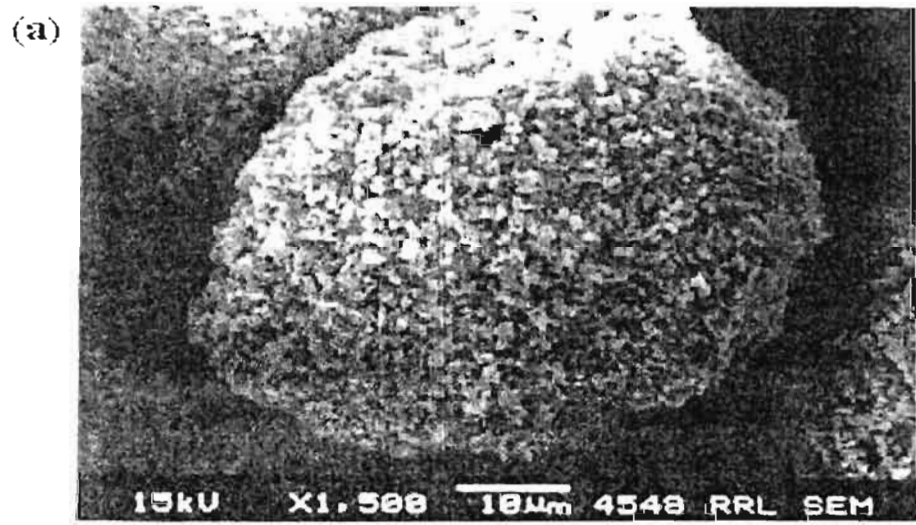
Therefore it can be believed that the anatase-rutile transformation in the presence of  $\text{Fe}_2\text{O}_3$  is more rapid than in pure  $\text{TiO}_2$ . The formation of pseudobrookite is independent of the phase transition because it took place on  $\text{Fe}_2\text{O}_3$  particles [61]

#### **3.4. Scanning Electron Microscopic studies.**

To understand the morphological changes of the titania doped with  $\text{Fe}_2\text{O}_3$ , Scanning Electron Microscopic studies on the samples were performed. Scanning Electron Micrographs of undoped  $\text{TiO}_2$  before heating (containing anatase) and after heating at  $1000^\circ\text{C}$  for 8 hrs (containing rutile) are shown in Figures 3.9. Here Titania particles were found to be aggregated in the pure form (anatase). On heating at  $1000^\circ\text{C}$  for 8 hrs, some rearrangement occurs to form rutile. During this conversion, the aggregates of particles would be converted into agglomerates where the particles are rigidly joined. Also there is no appreciable change in the particle size during the conversion in undoped  $\text{TiO}_2$ . The surface of both anatase and rutile samples were found to be rough before doping. Micrographs of  $\text{Fe}_2\text{O}_3$  doped  $\text{TiO}_2$  shown in figure 3.10 reveal that it becomes very fine on doping  $\text{Fe}_2\text{O}_3$ . The surface of particles becomes smooth during the anatase rutile transformation. The surface morphology of  $\text{Fe}_2\text{O}_3$  doped  $\text{TiO}_2$  changes with rutilation. The distribution of  $\text{Fe}_2\text{O}_3$  is uniform in co-precipitated samples and not in wet-impregnated system. This is identified from the EDAX analysis of

the samples prepared. This is the reason for lower rutilation in wet-impregnated system. This observation is in close agreement with XRD studies.

Figure 3.9: Scanning Electron Micrographs of undoped  $\text{TiO}_2$   
(a) pure anatase (b) pure rutile



(b)

Figure: 3.10. Scanning Electron Micrographs of  $\text{Fe}_2\text{O}_3/\text{TiO}_2$  before rutilation (a) Co-precipitated (b) Wet-impregnated.

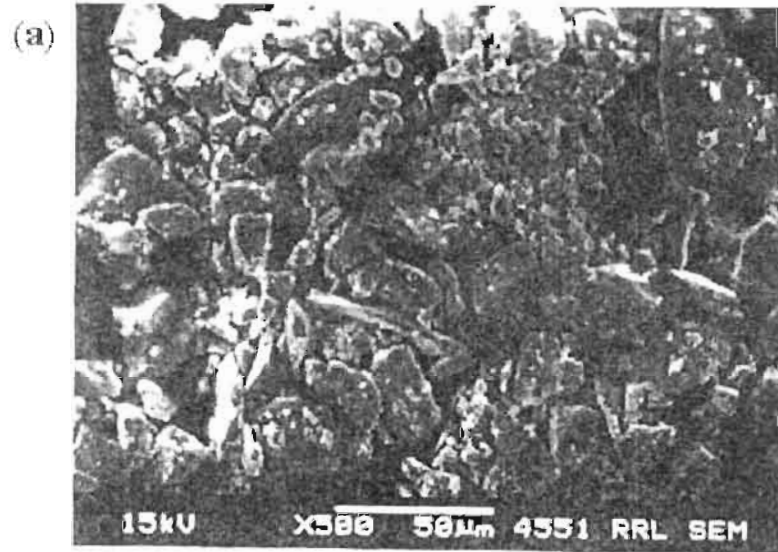
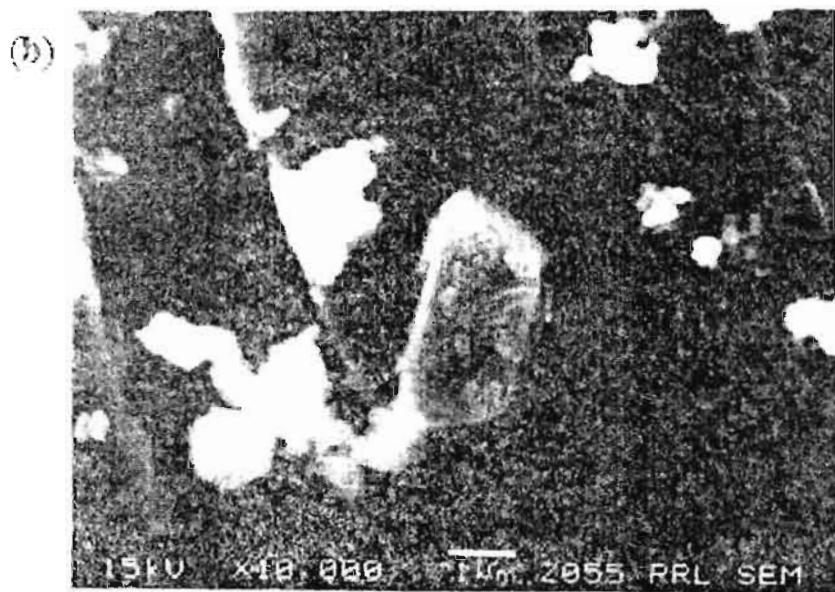


Figure: 3.11. Scanning Electron Micrographs of  $\text{Fe}_2\text{O}_3/\text{TiO}_2$  after rutilation (a) Co-precipitated (b) Wet-impregnated.



### 3.5. Transformation in Argon and Hydrogen atmospheres.

The anatase rutile transformations in different atmospheres were studied to understand the effect of different reaction atmospheres on the anatase-rutile transformation. Argon (inert) and hydrogen (reducing) atmospheres are used in the investigations.

Figure.3.11.represents the XRD patterns of  $\text{Fe}_2\text{O}_3/\text{TiO}_2$  heated in argon atmosphere at  $700^\circ\text{C}$ . The anatase-rutile conversion was found to be amazingly accelerated in argon than in air.

The percentages of rutile formed in co-precipitated 5 and 15%  $\text{Fe}_2\text{O}_3/\text{TiO}_2$  at different temperatures are tabulated in table 3.8. ( tables 3.2 and 3.3 explain the transformation in air atmosphere)

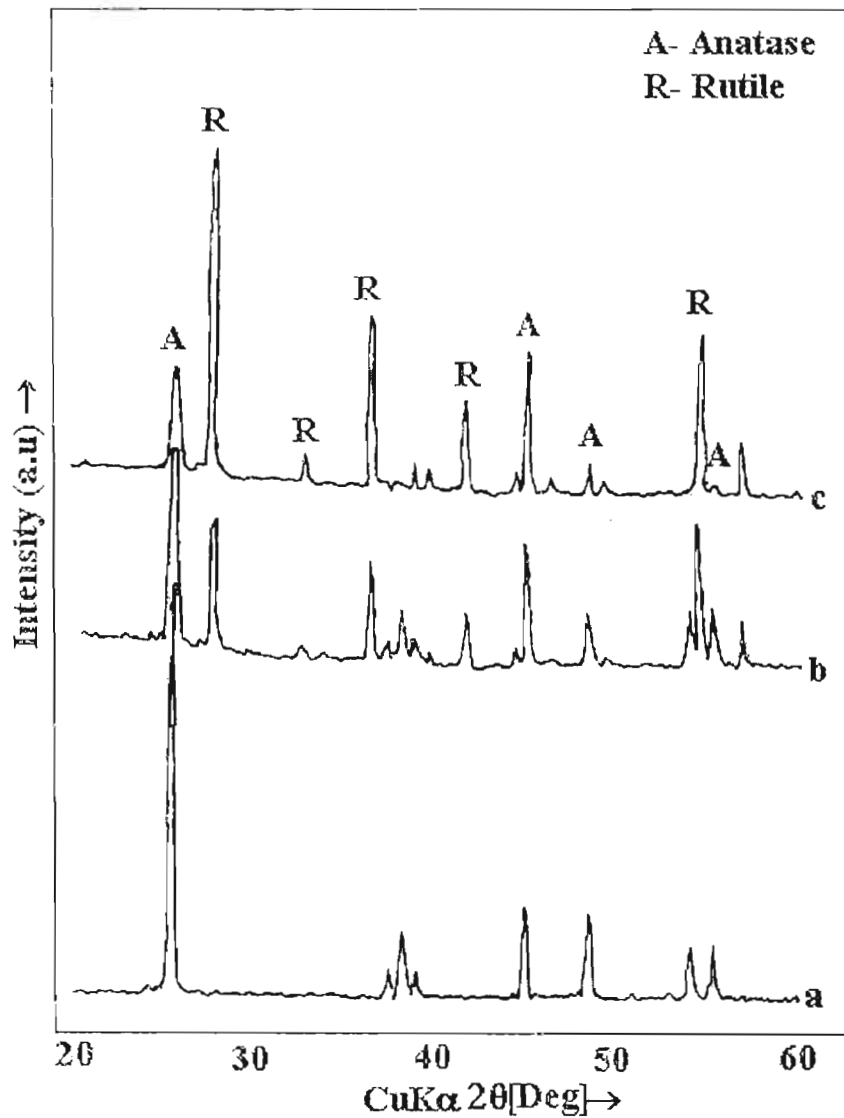
Table 3.8:% of rutile formed in co-precipitated  $\text{Fe}_2\text{O}_3/\text{TiO}_2$  samples heated in argon atmosphere at different temperatures for 0.5 hrs.

Temperature ( $^\circ\text{C}$ )	Rutile formed	
	5% $\text{Fe}_2\text{O}_3/\text{TiO}_2$	15% $\text{Fe}_2\text{O}_3/\text{TiO}_2$
650	7.8	14.4
675	18.6	35.8
700	48	91.5
750	98.2	100

In presence of argon the onset of rutilation was lowered to  $650^\circ\text{C}$  in co-precipitated 5%  $\text{Fe}_2\text{O}_3/\text{TiO}_2$ . The fraction of rutile formed is 7.8% in argon atmosphere for 0.5 hrs heating. In air atmosphere at the same conditions, no rutilation was found. Heating at  $800^\circ/6\text{hrs}$  produced 57.1% rutile in air

atmosphere. Thus the anatase rutile conversion is different in argon than that in air atmosphere. In argon at  $750^{\circ}\text{C}$ , the rutilation was found to be nearly complete (98.2%) but in air, rutilation was found to be complete at  $900^{\circ}\text{C}$  and 10 hrs (98.9).

Figure.3.11: XRD Patterns of co-precipitated  $\text{Fe}_2\text{O}_3/\text{TiO}_2$  samples heated in argon atmosphere at  $700^{\circ}$  for 0.5 hrs.  
(a)Undoped  $\text{TiO}_2$  (b) 5%  $\text{Fe}_2\text{O}_3/\text{TiO}_2$  (c)15%  $\text{Fe}_2\text{O}_3/\text{TiO}_2$

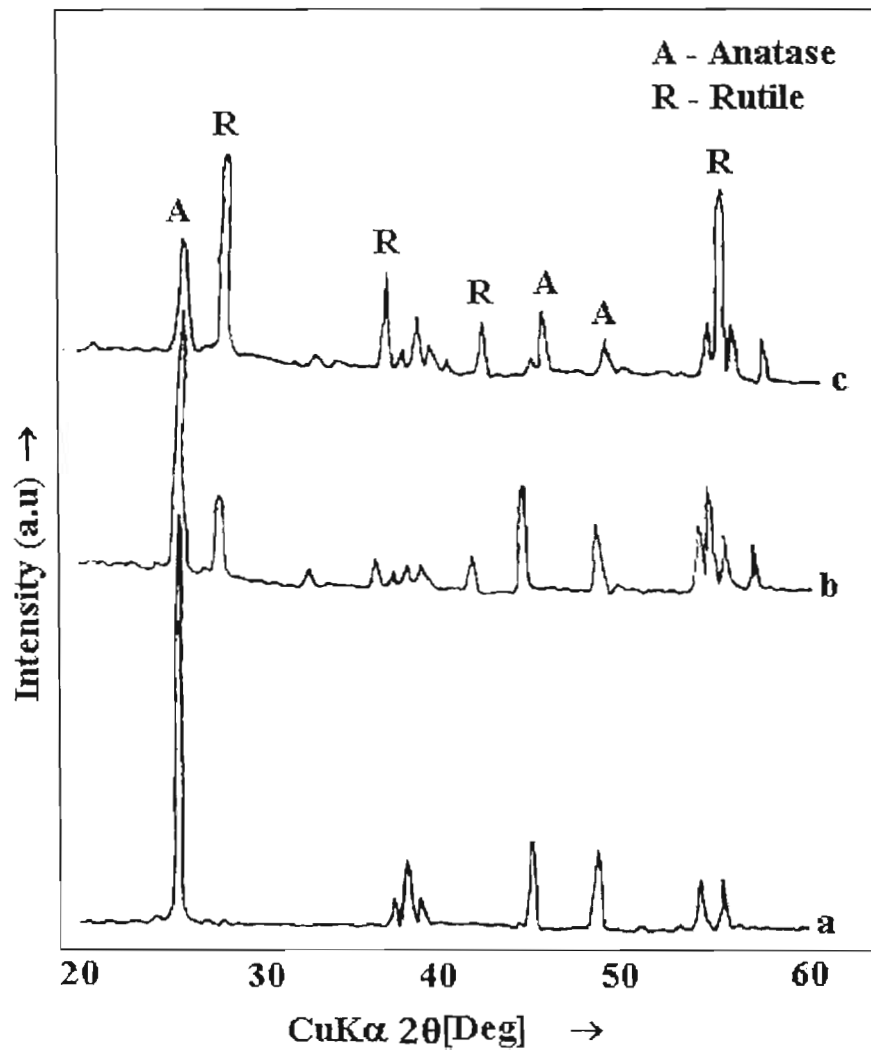




In the case of 15%  $\text{Fe}_2\text{O}_3/\text{TiO}_2$  samples, the phase transformation is achieved by 0.5 hrs heating. The extent of acceleration is different in this case as compared to air. The amount of rutile formed is higher at each temperature as compared to 5% doped samples as evident from the table.

In wet-impregnated samples onset of rutilation is shifted to  $700^\circ\text{C}$ . The XRD patterns are shown in figure 3.12.

**Figure.3.12: XRD Patterns of wet-impregnated  $\text{Fe}_2\text{O}_3/\text{TiO}_2$  samples heated in argon atmosphere at  $700^\circ$  for 0.5 hrs.**  
 (a) Undoped  $\text{TiO}_2$  (b) 5%  $\text{Fe}_2\text{O}_3/\text{TiO}_2$  (c) 15%  $\text{Fe}_2\text{O}_3/\text{TiO}_2$



The effect of temperature is same as that in co-precipitated one. Different amounts of rutile formed in wet-impregnated samples are summarized in table 3.9.

**Table 3.9: Fraction of rutile formed in wet-impregnated  $\text{Fe}_2\text{O}_3/\text{TiO}_2$  samples heated in argon atmosphere at different temperatures for 0.5 hrs.**

Temperature ( $^{\circ}\text{C}$ )	Rutile formed	
	5% $\text{Fe}_2\text{O}_3/\text{TiO}_2$	15% $\text{Fe}_2\text{O}_3/\text{TiO}_2$
700	23.2	39.8
750	48.4	78.7
800	79.3	100
825	100	100

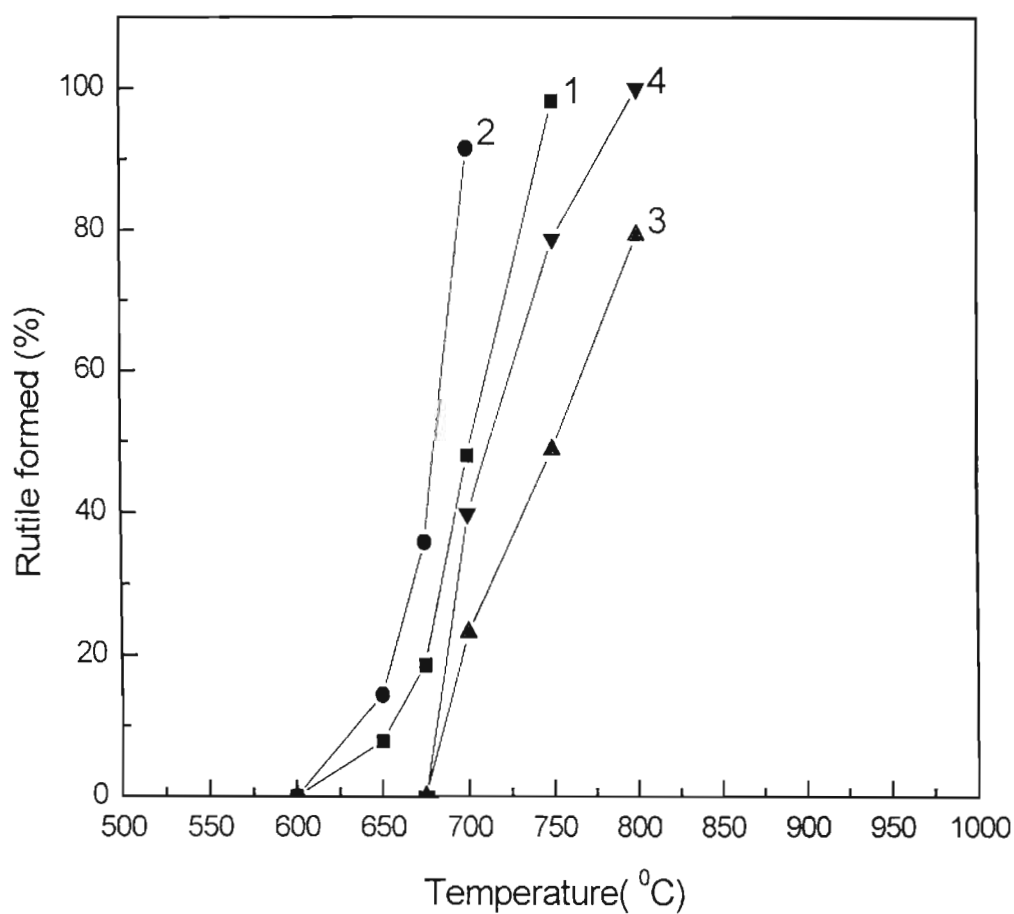
The variation of rutilation during heating in argon atmosphere in  $\text{Fe}_2\text{O}_3/\text{TiO}_2$  samples is evident in figure 3.13. Here the transformation is accelerated but the extent of acceleration strongly depends on the method of preparation. The lower distribution in wet-impregnated samples may be the cause for the variation in transformation.

The activation energies for the transformation in argon are calculated to be 37.8 and 29.1 kcal/mol for co-precipitated 5 and 15%  $\text{Fe}_2\text{O}_3$  doped  $\text{TiO}_2$  and 62.8 and 60.1 kcal/mol for wet-impregnated 5 and 15% doped samples respectively. It is seen that there is not much difference in the activation energies in presence of air or argon. Hence the lowering of activation energy is not the reason for the enhancement of rutilation.

The importance of oxygen vacancies on the phase transition rate of  $\text{TiO}_2$  in the presence of  $\text{Fe}_2\text{O}_3$  seems to be also confirmed by a more rapid transformation in argon than in air. Hence it can be concluded that argon atmosphere increases oxygen vacancies concentration and thus it favours the anatase-rutile transformation.

**Figure 3.13: Variation of rutilation in  $\text{Fe}_2\text{O}_3/\text{TiO}_2$  samples heated in argon atmosphere for 0.5 hrs at different temperatures.**

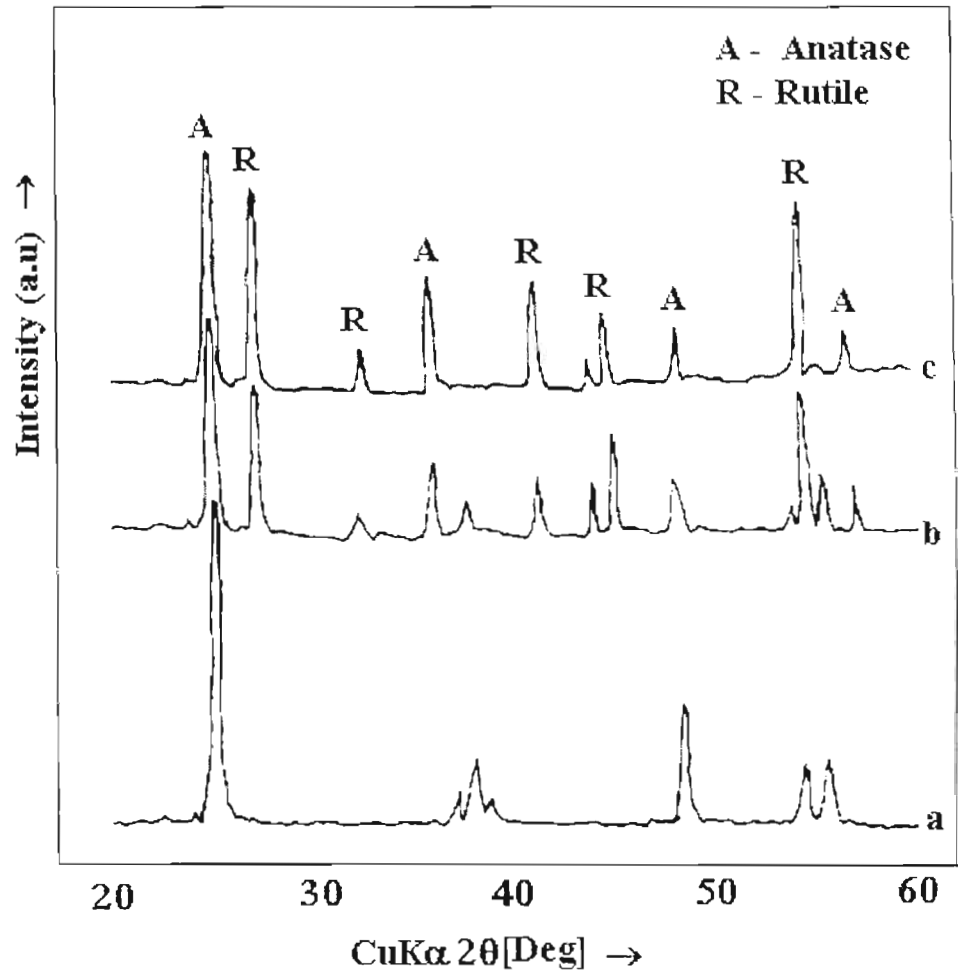
1. 5%  $\text{Fe}_2\text{O}_3/\text{TiO}_2$  2. 15%  $\text{Fe}_2\text{O}_3/\text{TiO}_2$  (Co-precipitated)  
3. 5%  $\text{Fe}_2\text{O}_3/\text{TiO}_2$  4. 15%  $\text{Fe}_2\text{O}_3/\text{TiO}_2$  (Wet-impregnated)



In hydrogen atmosphere, the anatase-rutile transformation was found to be low as compared to that in inert atmosphere. The XRD patterns of co-

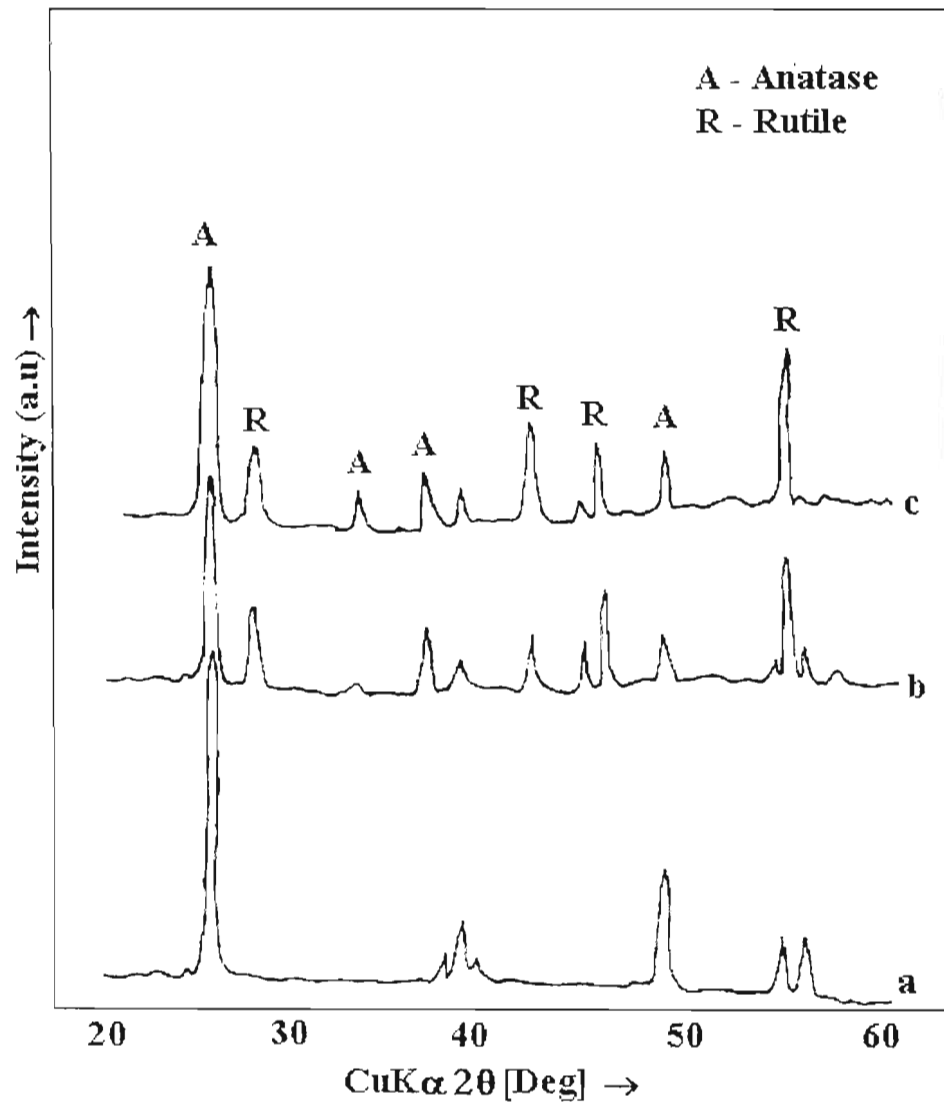
precipitated and wet-impregnated samples of different compositions are given in figures 3.14 and 3.15.

**Figure.3.14:** XRD Patterns of co-precipitated  $\text{Fe}_2\text{O}_3/\text{TiO}_2$  samples heated in hydrogen atmosphere at  $700^\circ$  for 2hrs.  
(a) Undoped  $\text{TiO}_2$  (b) 5%  $\text{Fe}_2\text{O}_3/\text{TiO}_2$  (c) 15%  $\text{Fe}_2\text{O}_3/\text{TiO}_2$



It is observed that onset of rutilation is shifted to  $700^\circ\text{C}$  for 2 hrs heating, which is higher temperature than that in argon atmosphere.

Figure.3.15: XRD Patterns of wet-impregnated  $\text{Fe}_2\text{O}_3/\text{TiO}_2$  samples heated in hydrogen atmosphere at  $750^\circ$  for 2hrs.  
 (a) Undoped  $\text{TiO}_2$  (b) 5%  $\text{Fe}_2\text{O}_3/\text{TiO}_2$  (c) 15%  $\text{Fe}_2\text{O}_3/\text{TiO}_2$



The 5% doped samples gave 12.2 % of rutile and 22.4% rutilation was observed in 15% doped sample for 2 hrs heating at  $700^\circ\text{C}$ . Tables 3.10 and

3.11 give the different fractions of rutile formed in co-precipitated and wet-impregnated systems (tables 3.2 and 3.3 represent the transformation in air)

**Table 3.10: % of rutile formed in co-precipitated  $\text{Fe}_2\text{O}_3/\text{TiO}_2$  system during heating in hydrogen atmosphere for 2 hrs.**

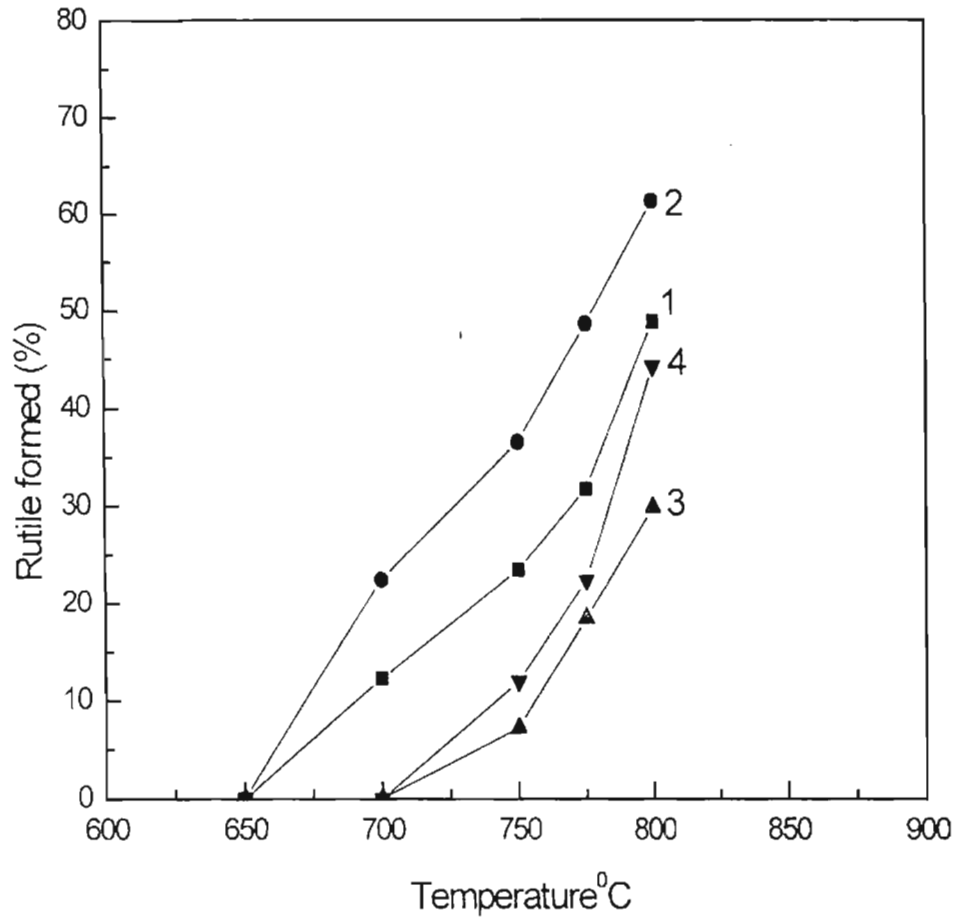
Temperature $^{\circ}\text{C}$	Rutile formed (%)	
	5% $\text{Fe}_2\text{O}_3/\text{TiO}_2$	15% $\text{Fe}_2\text{O}_3/\text{TiO}_2$
700	12.2	22.4
750	23.4	36.5
775	31.7	48.6
800	48.8	61.3

**Table 3.11: % of rutile formed in wet-impregnated  $\text{Fe}_2\text{O}_3/\text{TiO}_2$  system during heating in hydrogen atmosphere for 2 hrs.**

Temperature $^{\circ}\text{C}$	Rutile formed (%)	
	5% $\text{Fe}_2\text{O}_3/\text{TiO}_2$	15% $\text{Fe}_2\text{O}_3/\text{TiO}_2$
700	0	0
750	7.2	11.9
775	18.4	22.3
800	29.8	44.2

In wet-impregnated samples rutilation was slow as compared to co-precipitated. The variation in rutilation with temperature in  $\text{Fe}_2\text{O}_3/\text{TiO}_2$  samples heated in hydrogen atmosphere is shown in figure 3.16.

Figure 3.16: Variation in rutilation of  $\text{Fe}_2\text{O}_3/\text{TiO}_2$  samples heated in Hydrogen atmosphere for 2 hrs at different temperatures.  
 1. 5% $\text{Fe}_2\text{O}_3/\text{TiO}_2$ . 2. 15% $\text{Fe}_2\text{O}_3/\text{TiO}_2$ . (Co-precipitated)  
 3. 5% $\text{Fe}_2\text{O}_3/\text{TiO}_2$ . 4. 15% $\text{Fe}_2\text{O}_3/\text{TiO}_2$ . (Wet-impregnated)



5% doped sample on heating for 2 hrs at 750°C produced 7.2% rutile while 15% has given 11.9% rutile at the same conditions. There occurs some lattice defects in the sample during the heat treatment in reducing atmospheres. This is observed as colour changes to the samples. The colour changes may also be due to the reduction of  $\text{Fe}_2\text{O}_3$  to its lower oxidation state in hydrogen atmosphere. The intensity of colour depends on the amount of dopants. This clearly indicates the effect of concentration of  $\text{Fe}_2\text{O}_3$  is more

important in the phase transformation. This is observed in air and argon atmospheres.

Hence it can be concluded that the anatase-rutile transformation in  $\text{Fe}_2\text{O}_3$  doped  $\text{TiO}_2$  strongly depends on the concentration of dopants, method of preparation and the atmosphere of calcination.

### 3.6. Conclusions

The following conclusion can be arrived at from the results of the above investigations.

- ☐ In  $\text{Fe}_2\text{O}_3$  doped  $\text{TiO}_2$  anatase-rutile transformation takes place at lower temperature than pure  $\text{TiO}_2$ .
- ☐ The phase transformation depends on method of preparation of doped samples
- ☐ On increasing percentage of  $\text{Fe}_2\text{O}_3$  the transformation is accelerated in co-precipitated and wet-impregnated samples.
- ☐ The activation energy for the transformation is lowered much on doping  $\text{TiO}_2$  with  $\text{Fe}_2\text{O}_3$ .
- ☐ Pseudobrookite phase was formed during heating at higher temperatures.
- ☐ The formation of Pseudobrookite phase is independent of anatase-rutile transformation.
- ☐ The percentage of  $\text{Fe}_2\text{O}_3$  and method of preparation play major role on surface area and crystallite size of  $\text{TiO}_2$ .
- ☐ Crystallite size of anatase increases and surface area decreases markedly upon  $\text{Fe}_2\text{O}_3$  loading and rutilation.



- ☐ Surface morphology of  $\text{TiO}_2$  changes much on doping  $\text{Fe}_2\text{O}_3$  and also with rutilation.
- ☐ Both argon and hydrogen atmospheres enhance the anatase-rutile transformation
- ☐ Argon atmosphere was found to be more accelerating than hydrogen.

## CHAPTER 4

### STUDIES ON NiO DOPED TiO<sub>2</sub>

Extensive work has been reported recently on Ni supported on TiO<sub>2</sub> as a catalyst for CO hydrogenation with better activity compared to the other supports. Traditional methods like, wet-impregnation and ion exchange on crystalline TiO<sub>2</sub> were found to be employed in most of the investigations. In both the above methods, Ni atoms are introduced in to the TiO<sub>2</sub> crystal lattice by heating crystalline TiO<sub>2</sub> in presence of nickel salt solution at different temperatures, These methods would obviously reduce the surface area of TiO<sub>2</sub>, enhance the phase transformation and affect adversely on the homogeneous dispersion of the active metal on it.

Hydrazine hydrate precipitation is a new method described in literature for the preparation of nano sized metal oxides used for electronic applications. Hydrazine hydrate can quantitatively precipitate certain metals by complexing with them. These complexes undergo decomposition upon calcination resulting in high surface area metal oxides. Titania, in the amorphous state possesses high surface area and hence can incorporate large quantities of other metal oxides. Also, while loading metal oxides on crystalline titania, there is an increased chance for rutilation. Hence, amorphous titania was used for Co-precipitation and wet-impregnation methods. The phase in which TiO<sub>2</sub> exist during the calcination temperature is an important factor for deciding its applicability as a catalyst support. In this chapter polymorphism in TiO<sub>2</sub> doped with different percentages of NiO

prepared by two methods such as co-precipitation and wet-impregnation, as described in Chapter 2. The transformation was studied in air, argon and hydrogen atmospheres as a function of temperature and time using XRD, Surface area measurements and SEM.

#### 4.1. Chemical analysis.

The composition of the samples were established through chemical analysis using standard procedures as explained in chapter 2. The results are as given in Table 4.1.

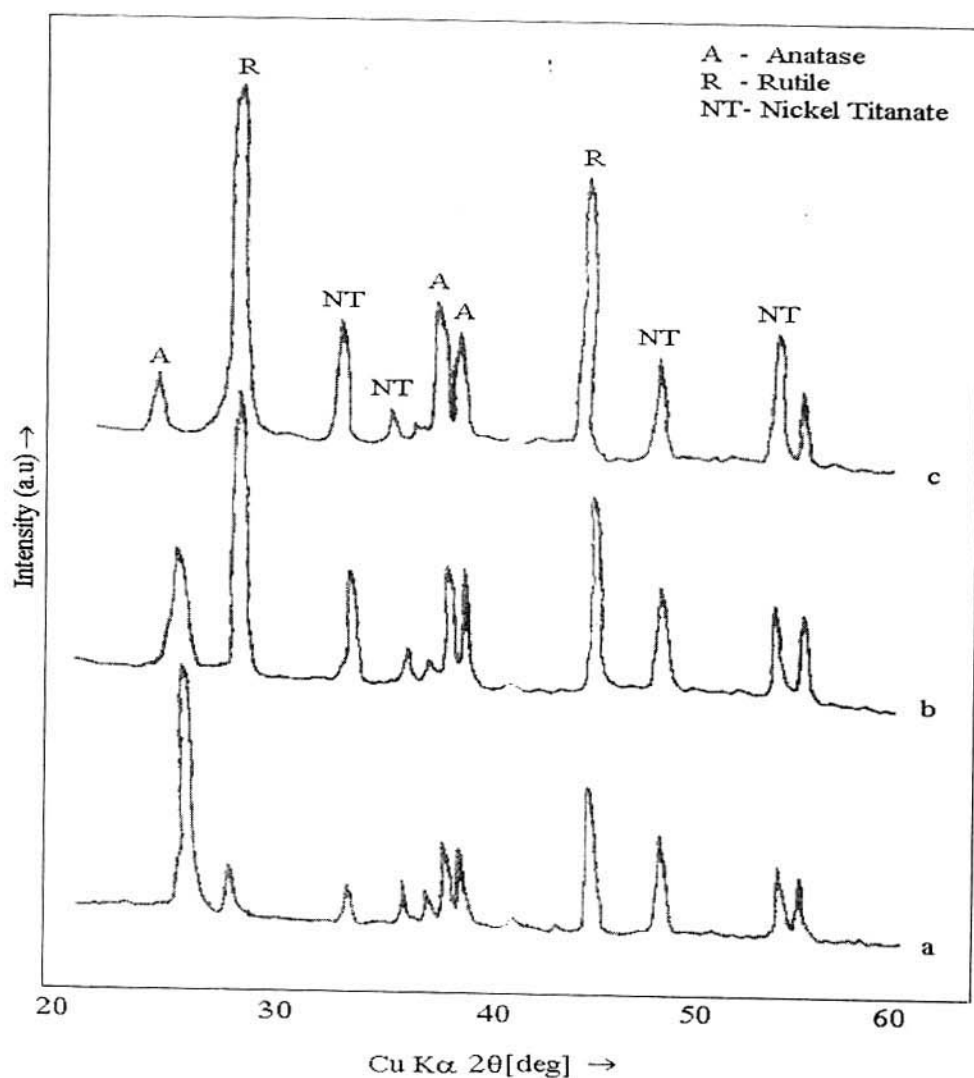
**Table.4.1: Results of Chemical analysis of NiO doped TiO<sub>2</sub> prepared through different methods.**

Method of preparation	Expected NiO (%)	Experimental Composition	
		NiO	TiO <sub>2</sub>
Co-Precipitation	5	4.88	94.73
	15	14.72	84.89
Wet-impregnation	5	4.79	94.82
	15	14.78	84.92

#### 4.2. XRD studies

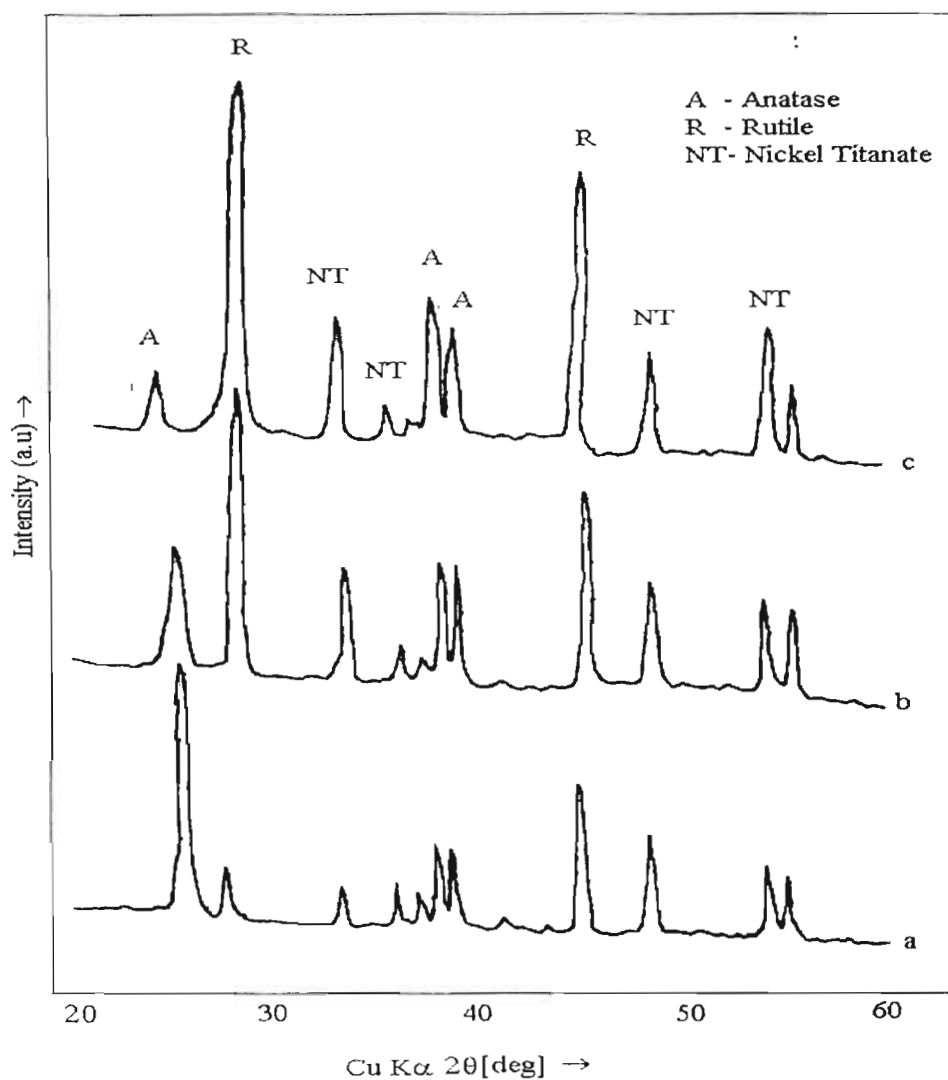
XRD patterns of co-precipitated NiO doped TiO<sub>2</sub> heated at different temperatures in air for different durations are given in figures 4.1 and 4.2. It was found that well defined and sharp peaks were obtained for samples calcined at 700<sup>0</sup>C for 6 hrs, but one heated below 600<sup>0</sup> was amorphous. It has become crystalline only at 700<sup>0</sup>C.

Figure. 4.1: XRD Patterns of co-precipitated 5% NiO/TiO<sub>2</sub> Samples heated at different temperatures.  
 (a) 700<sup>0</sup>C. (b) 800<sup>0</sup>C. (c) 850<sup>0</sup>C.



Marked changes could be seen in the characteristic peaks of anatase at  $d$ -value  $3.52\text{\AA}$  and that of rutile at  $d$ -value  $3.23\text{\AA}$ . All the peaks were those of anatase, rutile and no peak of NiO are observed. There were peaks due to NiTiO<sub>3</sub> in sample containing rutile, which shows that reaction between NiO and TiO<sub>2</sub> has started forming NiTiO<sub>3</sub>.

Figure 4.2: XRD Patterns of co-precipitated 15% NiO/TiO<sub>2</sub>  
Samples heated at different temperatures.  
(a) 700°C (b) 800°C (c) 850°C



The absence of NiO peaks clearly discloses the fine nature of NiO, which can't be detected using XRD technique. On comparing with crystallization temperatures of pure TiO<sub>2</sub> prepared by hydrazine

precipitation and thermal hydrolysis, there is a change in crystallization temperature in presence of NiO.

In order to investigate the effect of NiO on rutilation, the XRD analysis of all the samples calcined at different temperatures were carried out. The percentage of rutile formed at different temperatures were calculated and the various amounts of rutile formed in co-precipitated 5 and 15% doped samples are summarized in tables 4.2 and 4.3

**Table 4.2: % of rutile formed in co-precipitated 5% NiO doped TiO<sub>2</sub> Samples at different temperatures and durations.**

Time of heating (hrs)	Rutile formed (%)		
	700 <sup>0</sup> C	800 <sup>0</sup> C	850 <sup>0</sup> C
1	0	13.2	30.8
2	1.6	26.9	52.2
3	2.4	35.4	66.9
4	3.2	39.8	77.1
5	4.1	44.1	84.2
6	4.9	46.8	89.1
7	5.6	49.7	92.4
8	6.4	51.9	94.7
9	7.2	54.7	96.4
10	8.0	62.4	97.5

The rutile peaks appeared after calcination at 700°C. So, it is apparent from the XRD data that the onset temperature of rutilation was lower in co-precipitated 5% doped ones than in pure TiO<sub>2</sub>.

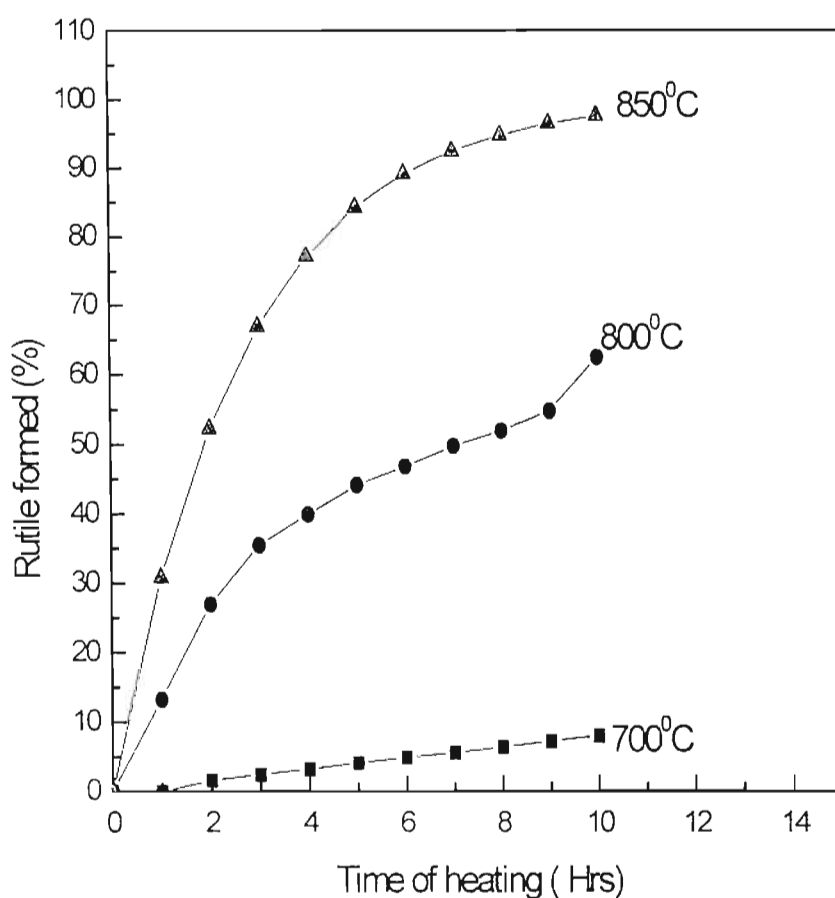
**Table 4.3: % of rutile formed in co-precipitated 15% NiO doped TiO<sub>2</sub> Samples at different temperatures and durations.**

Time of heating (hrs)	Rutile formed (%)		
	700°C	750°C	800°C
1	1.2	26.8	52.5
2	2.5	31.9	61.3
3	3.7	38.0	72.4
4	4.9	42.7	80.6
5	6.2	45.4	84.6
6	7.4	48.8	90.2
7	8.5	53.0	97.6
8	9.7	54.1	99.9
9	10.8	55.4	100
10	12.3	61.6	100

When the calcination temperature was increased to 800°C, the intensity of rutile peaks increased and that of anatase decreased in 5% doped sample while in 15% doped sample, rutilation is found to be complete at about 9 hrs. On increasing further to 850°C 5% doped system gave 97.5% rutile formation at 10 hrs calcination. The plot of

rutile percentage against time at different temperatures of calcinations is given in figures 4.3 and 4.4.

**Figure.4.3: The plot of rutile percentage against time at different temperatures of calcination in co-precipitated 5% NiO doped TiO<sub>2</sub>.**

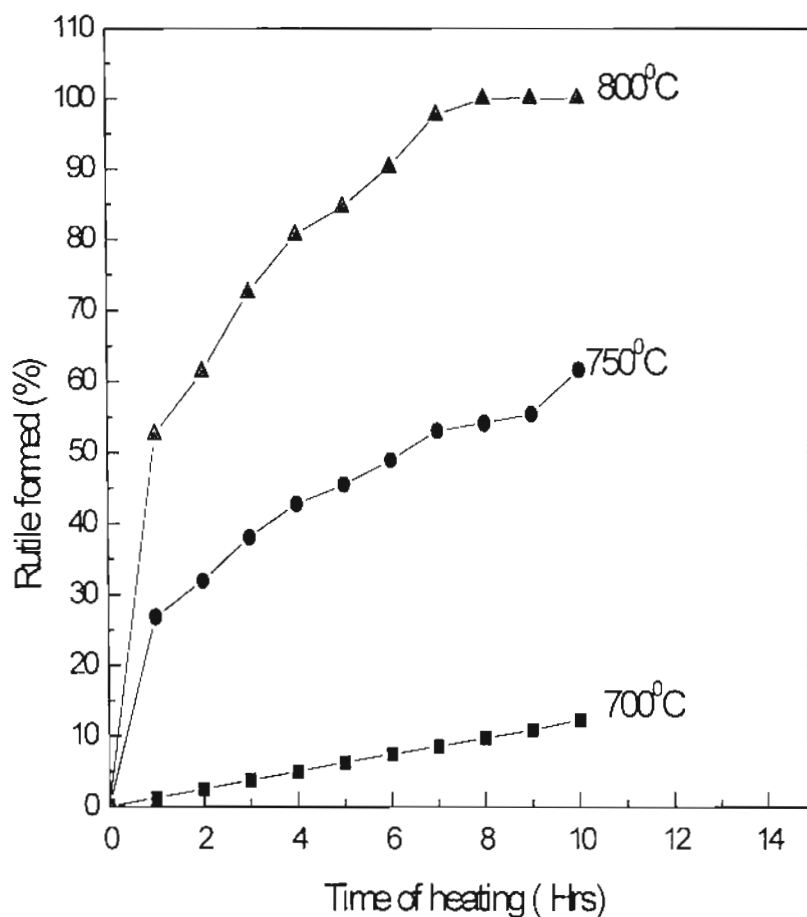


In 5% doped system, at 850°C the anatase peaks disappeared and rutile peaks became more predominant while in 15% doped case, it happens at 800°C. On comparing with pure TiO<sub>2</sub>, where the onset and completion temperatures of rutilation were in between 900°C to 1000°C, in co-precipitated NiO doped TiO<sub>2</sub> prepared by hydrazine



precipitation rutilation temperature has been reduced. It is very clear that NiO has important effect on the onset and completion of rutilation.

**Figure.4.4: The plot of rutile percentage against time at different temperatures of calcination in co-precipitated 15% NiO doped TiO<sub>2</sub>.**



It is noteworthy that, at the onset of rutilation, some peaks due to NiTiO<sub>3</sub> were also present in the pattern. On increasing the calcination temperature, the intensity of these peaks also increased. This suggests that at higher temperatures, NiO reacts with TiO<sub>2</sub> to form the titanate.

The XRD patterns of wet-impregnated 5 and 15% loaded samples shown in figures 4.5 and 4.6 reveal that the above said samples behaved differently from co-precipitated ones. Here the onset and completion of rutilation were altered much. No phase changes could be observed up to 800<sup>0</sup>C in any of the wet-impregnated ones. This reflects the thermal stability of these systems under the conditions adopted.

Figure 4.5: XRD Patterns of wet-impregnated 5% NiO/TiO<sub>2</sub> Samples heated at different temperatures. (a) 850<sup>0</sup>C (b) 875<sup>0</sup>C (c) 900<sup>0</sup>C

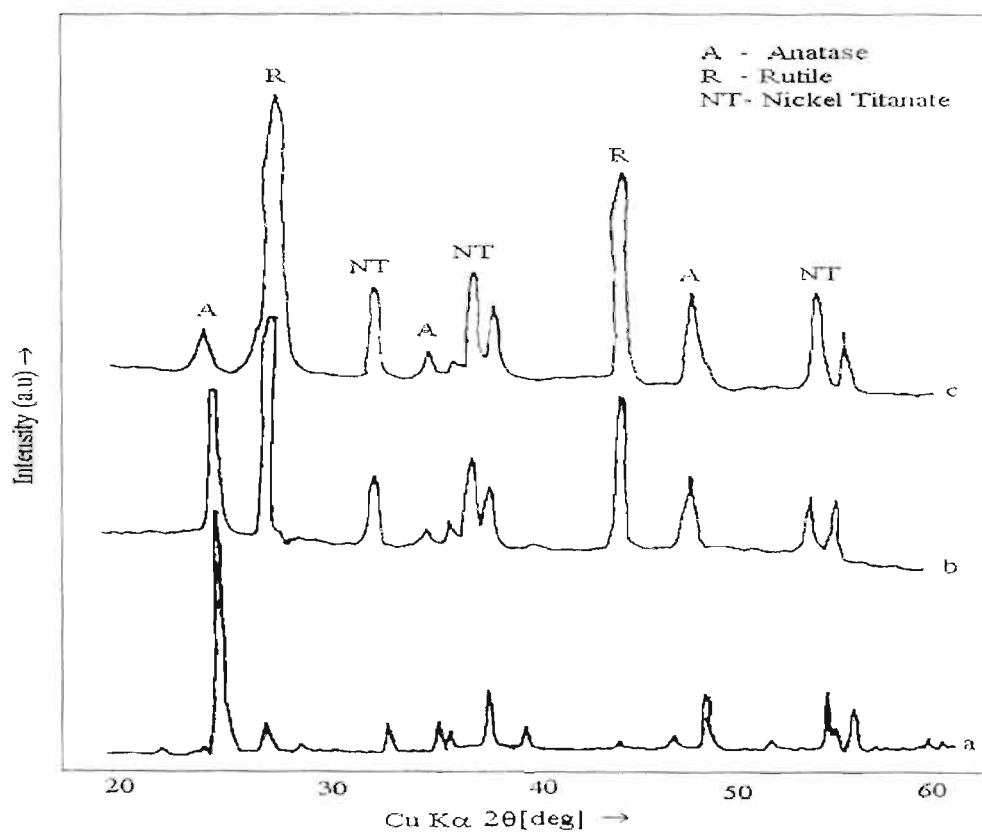
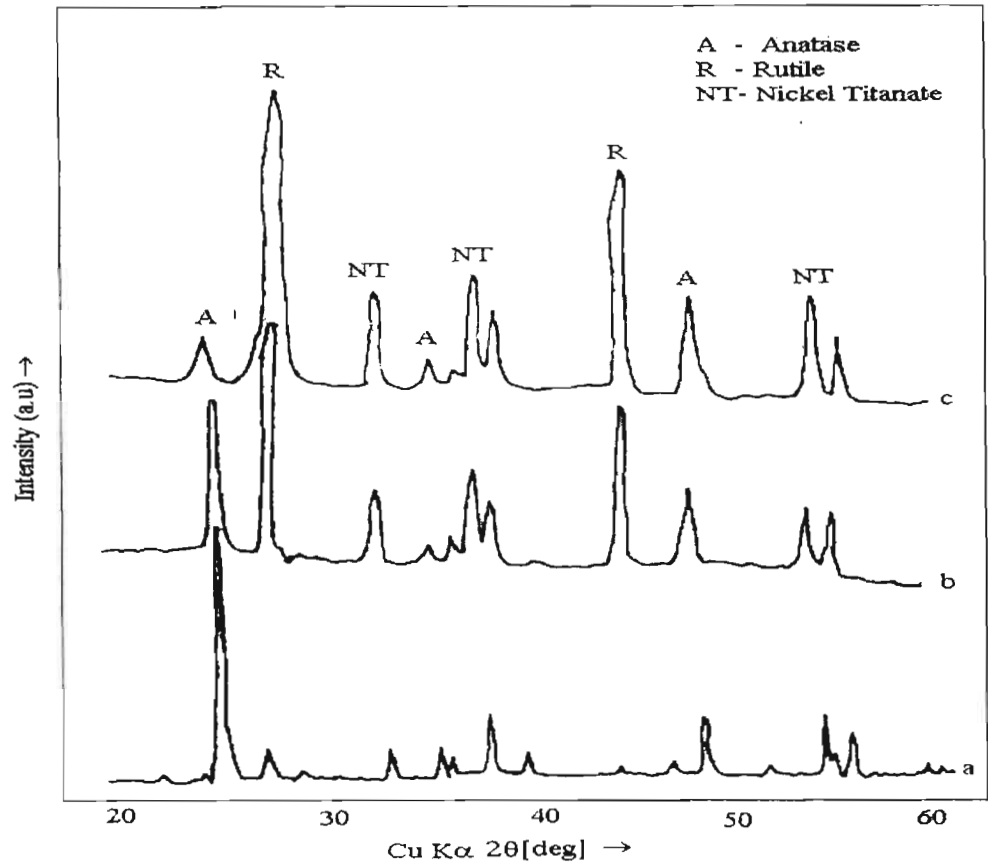


Figure 4.6: XRD Patterns of wet-impregnated 15% NiO/TiO<sub>2</sub> Samples heated at different temperatures.  
(a) 850<sup>0</sup>C (b) 875<sup>0</sup>C (c) 900<sup>0</sup>C



The amount of rutile formed in wet-impregnated NiO doped TiO<sub>2</sub> heated at different temperatures is calculated from the XRD patterns using the equation given in chapter 2. The various percentages of rutile obtained are given in tables 4.4 and 4.5.

**Table 4.4: % of rutile formed in wet-impregnated 5% NiO doped TiO<sub>2</sub> Samples**

Time of heating (hrs)	Rutile formed (%)		
	850 <sup>0</sup> C	875 <sup>0</sup> C	900 <sup>0</sup> C
1	1.7	9.2	22.6
2	3.3	17.6	40.1
3	4.8	25.3	53.7
4	6.6	32.2	64.2
5	8.2	38.5	72.3
6	9.8	44.2	78.6
7	11.3	49.3	83.4
8	12.8	54.2	87.1
9	14.3	58.3	90.1
10	15.7	62.1	92.3

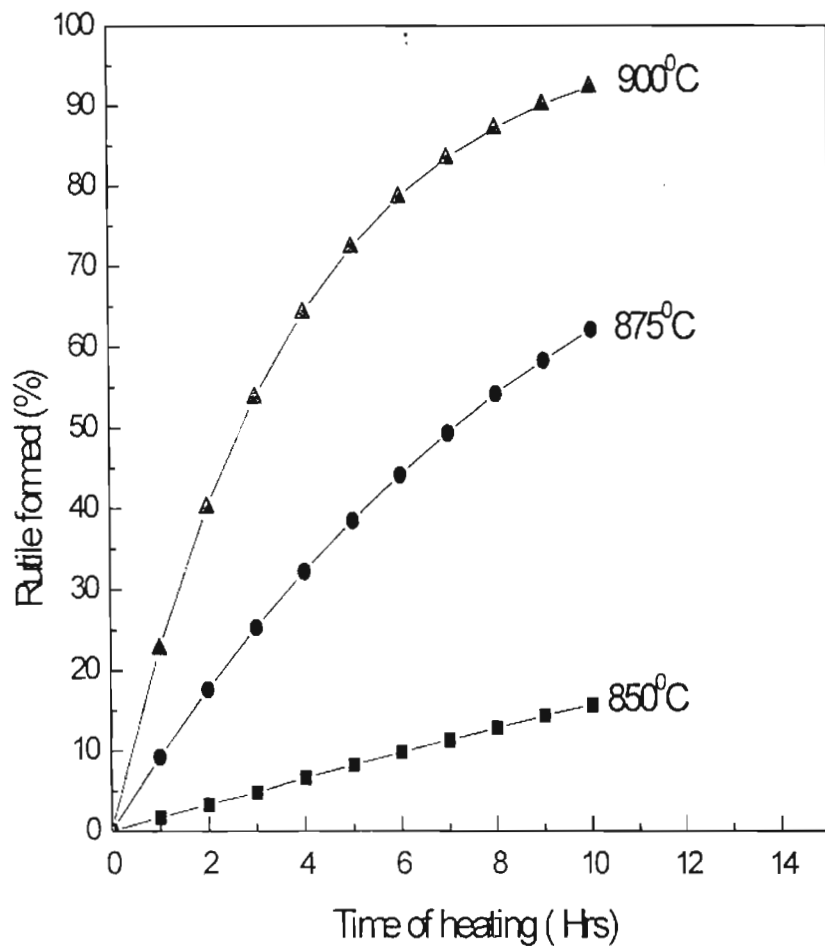
It is obvious that rutilation in sample containing 5% NiO begins at 850<sup>0</sup>C, 9.8% rutile was formed on 6hrs heating, while in 15% 44.8% rutilation was observed at the same conditions. The variation of rutilation with temperature is different for different percentages of NiO. The conversion strongly depends on the amount of NiO and method of preparation of NiO doped TiO<sub>2</sub> samples.

**Table 4.5: % of rutile formed in wet-impregnated 15% NiO doped TiO<sub>2</sub> samples**

Time of heating (hrs)	Rutile formed (%)		
	850 <sup>o</sup> C	875 <sup>o</sup> C	900 <sup>o</sup> C
1	9.4	16.3	43.6
2	17.9	29.9	68.2
3	25.7	41.4	82.1
4	32.7	50.9	89.9
5	39.1	59.2	94.3
6	44.8	65.7	96.8
7	50.3	71.3	98.1
8	54.7	75.9	100
9	58.9	79.9	100
10	62.8	83.1	100

From the table it is clear that the rutile formed at different temperatures strongly depends on the amount of NiO. As compared to co-precipitated samples, rutilation in wet-impregnated samples are low. This may be due to lower distribution of NiO over TiO<sub>2</sub> in wet-impregnated samples. The graphical representations of rutile formation versus time are shown in figures 4.7 and 4.8.

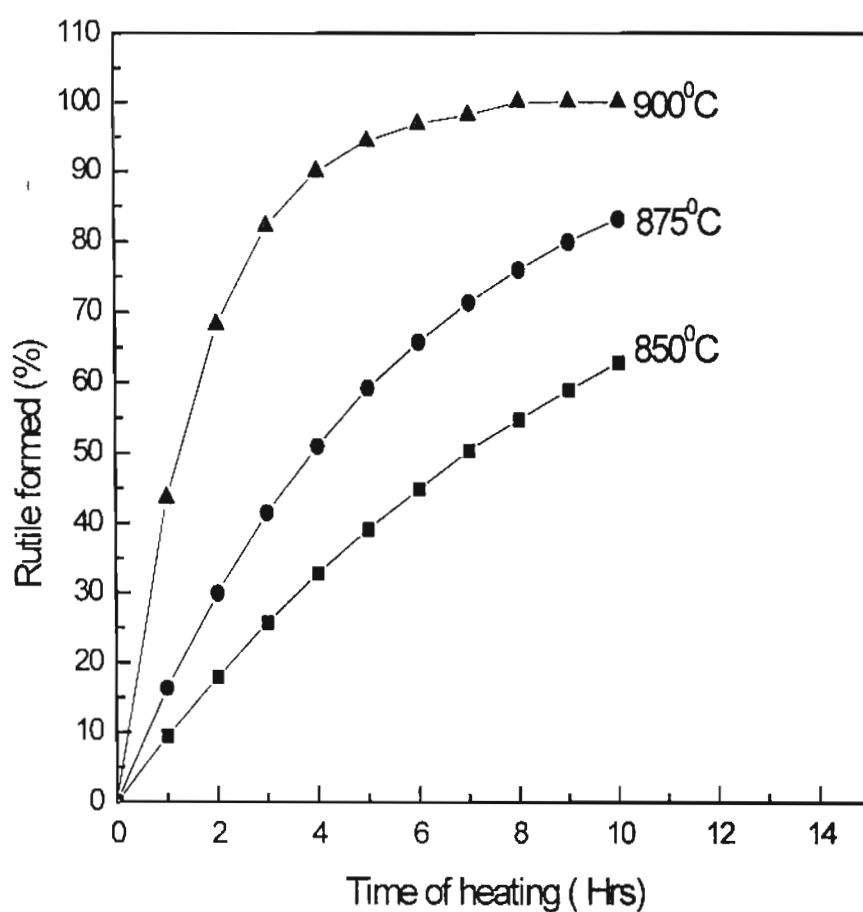
Figure.4.7: The plot of rutile percentage against time at different temperatures of calcination in wet-impregnated 5% NiO doped TiO<sub>2</sub>.



The activation energy for the anatase-rutile transformation was calculated and is given in table 4.6. The activation energy calculated for the transformation in co-precipitated sample in presence of 5% NiO is found to be 44.4 k cal/mol while in presence of 15% NiO 36.6k cal / mol. In case of wet-impregnated samples the activation energy for the transformation was found to be 68.3 in presence of 5% NiO while in presence of 15% it is 59.4 k cal/ mol. For undoped TiO<sub>2</sub>, activation

energy for anatase-rutile transformation was reported to be  $\sim 90$  K cal/mol. Here also among 5 & 15% NiO 15% has more lowering of activation energy and hence it is more accelerating.

**Figure.4.8. The plot of rutile percentage against time at different temperatures of calcination in wet-impregnated 15% NiO doped  $\text{TiO}_2$ .**



It is clear that the lowering of activation energy is different in wet-impregnated system as compared to co-precipitated ones. So an analysis of the activation energy values determined is useful in understanding the relative accelerating effect of NiO doping. It is clear

that in presence of NiO, the activation energy is lowered much as compared to undoped.

**Table: 4.6: Activation energies for the anatase-rutile transformation in NiO doped TiO<sub>2</sub>.**

Method of preparation	NiO (%)	Activation Energy K cal/mol
Co-precipitation	5	44.4
	15	36.6
Wet-impregnation	5	68.3
	15	59.4

On increasing the calcination temperature, the crystallite size was also increased in all the samples, but to different extents. In 5% NiO doped TiO<sub>2</sub> co-precipitated ones, at the onset of rutilation, the crystallite size was 9.4 nm, while in 15% doped one it was 11.8 nm. So, the rutilation takes place after the enlargement of anatase crystallites and the growth in crystallite size is highly dependent on method of preparation. The anatase crystallites are larger in NiO loaded samples than that in pure titania. In wet-impregnated samples, crystallite size was found to be 13.9 and 17.3 nm respectively in 5 and 15% NiO doped systems. Thus the crystallite size increased on increasing NiO percentage. It would be due to the suppression of titania grain growth by extremely fine NiO particles distributed on TiO<sub>2</sub>.



**Table.4.7: Crystallite size and surface area values of un doped and NiO doped TiO<sub>2</sub> Samples heated at different temperatures for 8 hrs**

Sample	Temperature (°C)	Surface area (m <sup>2</sup> /g)	Crystallite size of anatase(nm)
Undoped TiO <sub>2</sub>	110	162.58	a*
	300	109.59	a*
	700	27.2	4.8
	900	9.13	14.2
	1000	2.54	b*
Co-precipitated 5% NiO/TiO <sub>2</sub>	110	137.7	a*
	700	13.8	9.4
	850	6.8	27.7
Co-precipitated 15% NiO/TiO <sub>2</sub>	110	192.7	a*
	700	11.2	11.8
	800	1.9	31.6
Wet-impregnated 5% NiO/TiO <sub>2</sub>	110	103.5	a*
	850	17.7	13.9
	900	9.2	19.3
Wet-impregnated 15% NiO/TiO <sub>2</sub>	110	125.2	a*
	850	13.8	17.3
	900	6.2	22.1

\* a- Amorphous \*b-Anatase absent

Among all the samples, the co-precipitated one has highest rutile percentage at any temperature and lowest for wet-impregnated one. So, the preparation method and NiO percentage have marked influence on rutile phase formation. The crystallite size of anatase calculated from XRD data are given in table 4.6. Crystallite size calculations were done only at certain calcination temperatures at which drastic changes occurred.

### 4.3. Surface area studies

The results of surface area measurements are tabulated in Table 4.6. It was observed that on increasing calcination temperature, there occurred a marked decrease in surface area in all the samples. When the calcination temperature was increased to 700<sup>0</sup>C, in co-precipitated samples the surface area became 13.8 and 11.2 m<sup>2</sup>/g from 137.7 and 192.7 m<sup>2</sup>/g for 5 and 15% NiO doped systems. Like wise, in the case of wet-impregnated samples at 850<sup>0</sup>C, it became 17.7 and 13.8 m<sup>2</sup>/g respectively for 5 and 15% doped samples. Before calcination in these samples surface area was found to be 103.5 and 125.3 m<sup>2</sup>/g for 5 and 15%. It again decreased at 800<sup>0</sup>C at which the rutilation was found to be increased. In 5% NiO doped co-precipitated samples the surface area was 6.8 m<sup>2</sup>/g at 850<sup>0</sup>C when rutilation was complete and in 15% it was 1.9m<sup>2</sup>/g when rutilation was complete at 800<sup>0</sup>C.

In wet-impregnated samples at 900<sup>0</sup>C, when the NiO doped TiO<sub>2</sub> was fully converted to rutile, surface area was found to be 9.2 and 6.2 m<sup>2</sup>/g in 5 and 15% doped samples. Even though no direct relation between crystallite size and surface area could be made, surface area decreased significantly along with marked increase in

crystallite size. It is also evident that a very small change in crystallite size does not always necessarily involve a change in surface area. The decrease in surface area is due to rutilation, sintering and fusion of  $\text{TiO}_2$  and NiO, to form  $\text{NiTiO}_3$ , which is in agreement with XRD data.

On comparing with surface area of pure  $\text{TiO}_2$  surface area decreased on loading NiO. It is obvious from the above observations that the surface area decreased drastically during rutilation, which in turn is dependent on method of preparation, calcination temperature and NiO percentage. The decrease in surface area during rutilation was also greater in presence of NiO compared to pure  $\text{TiO}_2$ . The change in surface area with increase in NiO percentage is highly influenced by preparation method.

#### **4.4 Scanning Electron Microscopic studies.**

To understand the morphological changes occurring with rutilation, the samples before and after rutilation were subjected to SEM analysis. The micrographs were compared with the micrograph of undoped pure anatase and rutile shown in chapter 3. The micrographs are shown in Figs 4.9 and 4.10.

In all the micrographs only titania particles could be seen, which mirrors the presence of NiO as very fine particles, as supported by XRD and EDAX studies. The particles were all in a irregular shapes and were aggregated.

An appreciable change in particle size was observed between the samples prepared through different methods, even though the surface area values and other physical properties were different. So, it is apparent that a very small change in particle size detected in SEM, can

cause a larger alteration in surface area. Particles in wet-impregnated samples appear to be finer in the micrographs. The particles were in much more agglomerated state (i.e. assemblages of particles which are rigidly joined) when the  $\text{TiO}_2$  was fully converted to rutile, which would be due to cementation and sintering of individual particles, which is in agreement with XRD and surface area studies.

Figure.4.9 : Scanning Electron Micrographs of NiO doped  $\text{TiO}_2$  before rutilation (a)Co-precipitated (b)Wet-impregnated.

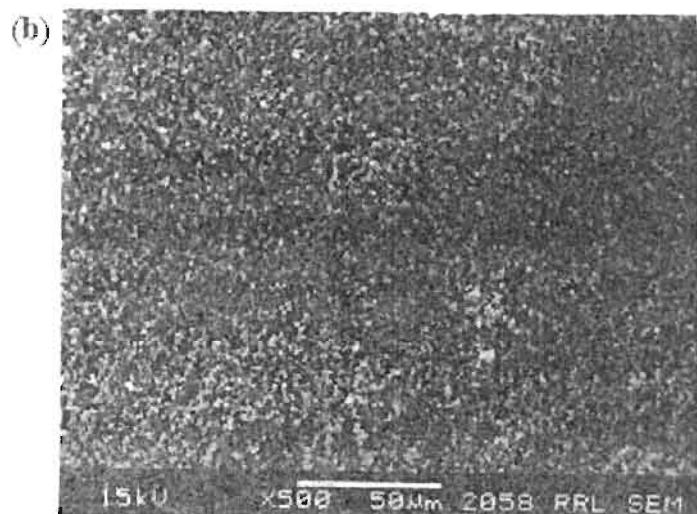
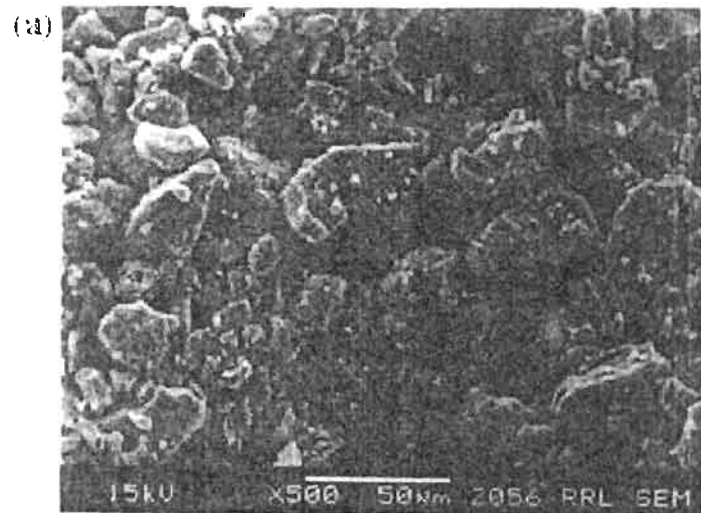
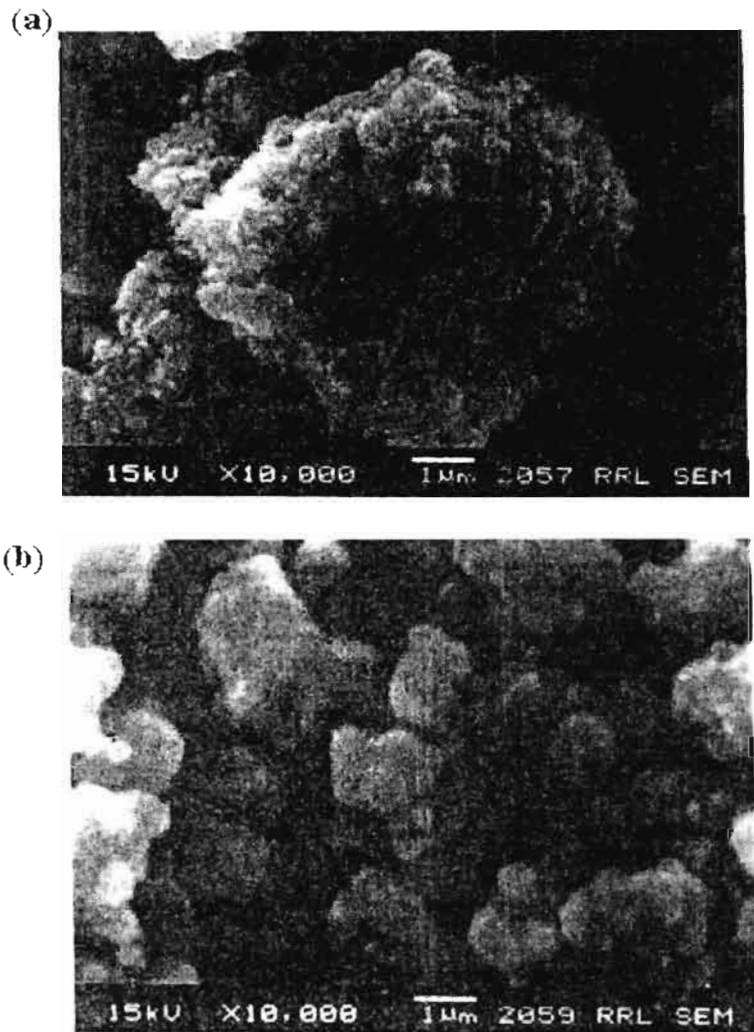


Figure.4.10 : Scanning Electron Micrographs of NiO doped TiO<sub>2</sub> after rutilation (a) Co-precipitated (b)Wet-impregnated.



Individual particles are also finer in wet-impregnated sample. The aggregation of particles is an evidence for the fineness of the sample, because it has been reported that<sup>281</sup> the individual particles in a fine powder would be in an aggregated form (i.e. assemblages of particles which are loosely coherent).

#### 4.5 Transformations in Argon and Hydrogen atmospheres.

The anatase rutile transformations in different atmospheres were studied to understand the effect of different reaction atmospheres on the anatase-rutile transformation. Argon (inert) and hydrogen (reducing) atmospheres are used in the investigations.

Figure.4.11. represents the XRD patterns of NiO doped TiO<sub>2</sub> heated in argon atmosphere at 700<sup>0</sup>C. The anatase-rutile conversion was found to be accelerated in argon than in air.

The percentages of rutile formed in co-precipitated 5 and 15% NiO doped TiO<sub>2</sub> at different temperatures are tabulated in Table.4.8.

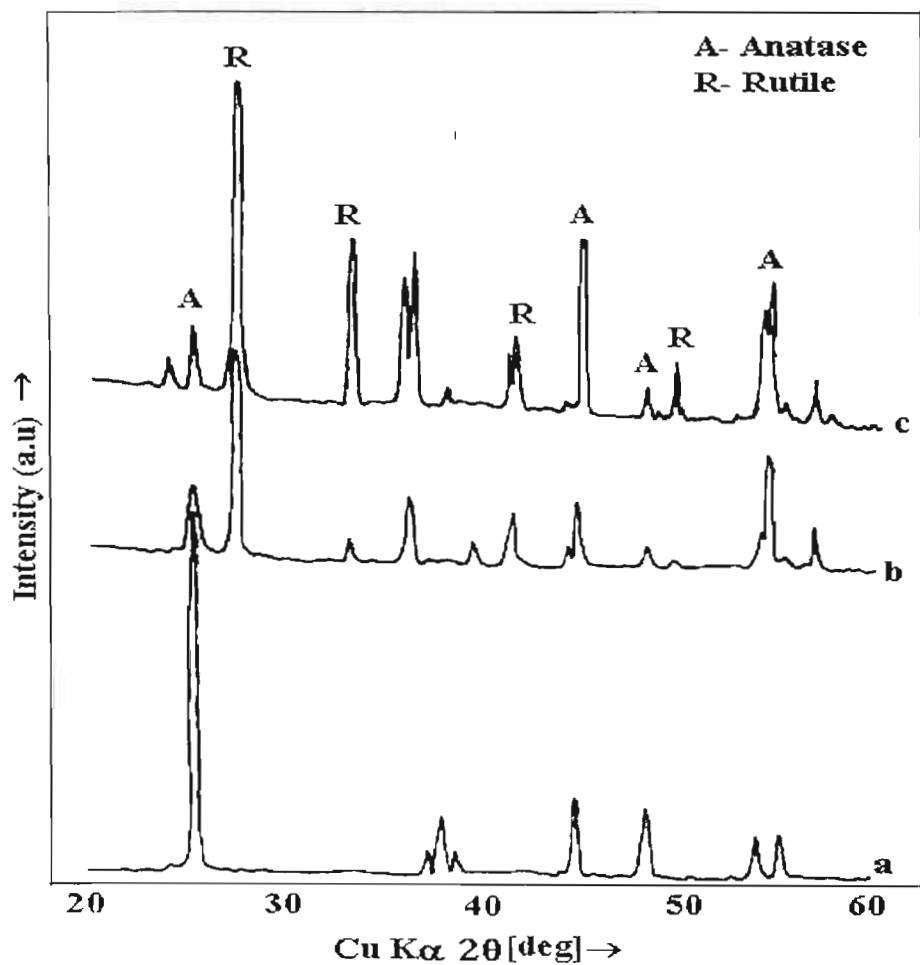
**Table.4.8: % of rutile formed in co-precipitated NiO doped TiO<sub>2</sub> samples heated in argon atmosphere at different temperatures for 0.5 hrs.**

Temperature ( <sup>0</sup> C)	Rutile formed	
	5% NiO/TiO <sub>2</sub>	15% NiO/TiO <sub>2</sub>
650	23.8	32.4
675	51.3	61.8
700	76.9	88.7
750	98.2	100

In presence of argon atmosphere, the onset of rutilation was lowered to 650<sup>0</sup>C in co-precipitated 5% NiO/TiO<sub>2</sub>. The fraction of rutile formed is 23.8 % in argon atmosphere for 0.5 hrs heating. In air atmosphere at the same conditions, no rutile was formed. At 800<sup>0</sup>/6hrs heating produced 57.1% rutile in air atmosphere. Thus the anatase

rutile conversion is different in argon than that in air atmosphere. In argon at  $750^{\circ}\text{C}$ , the rutilation was found to be more or less completed (98.2%) but in air rutilation was found to be completed at  $900^{\circ}\text{C}$  10 hrs (98.9).

Figure.4.11: XRD Patterns of co-precipitated NiO doped  $\text{TiO}_2$  samples heated in argon atmosphere at  $700^{\circ}$  / 0.5 hrs. (a) Undoped  $\text{TiO}_2$  (b) 5% NiO/ $\text{TiO}_2$  (c) 15% NiO/ $\text{TiO}_2$

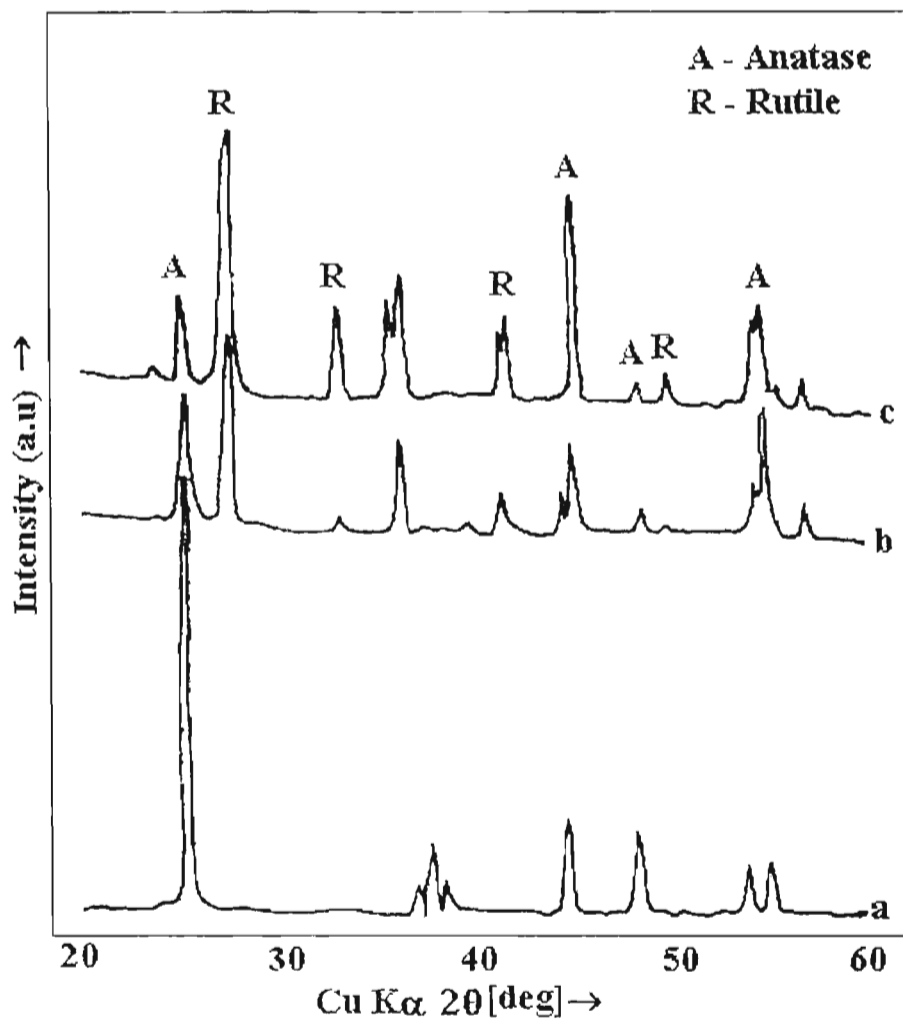


In the case of 15% NiO/ $\text{TiO}_2$  samples, the phase transformation is achieved by 0.5 hrs heating at  $650^{\circ}\text{C}$ , where 32.4 % rutilation was found. The extent of acceleration is different in this case as compared

to air. The amount of rutile formed is higher at each temperature as compared to 5% doped samples as evident from the table 4.8.

In wet-impregnated samples on set of rutilation is same as in co-precipitated samples but the amount of conversion is different. At 650°C, 5% NiO doped TiO<sub>2</sub> sample gave 12.8% rutile while 15% doped sample produced 24.7%. The XRD patterns are shown in figure 3.12.

Figure.4.12: XRD Patterns of wet-impregnated NiO doped TiO<sub>2</sub> samples heated in argon atmosphere for 0.5 hrs.  
(a)Undoped TiO<sub>2</sub> (b) 5% NiO/TiO<sub>2</sub> (c) 15% NiO/TiO<sub>2</sub>





The effect of temperature is same as that in co-precipitated one. Different amounts of rutile formed in wet-impregnated samples are summarized in table:4.9.

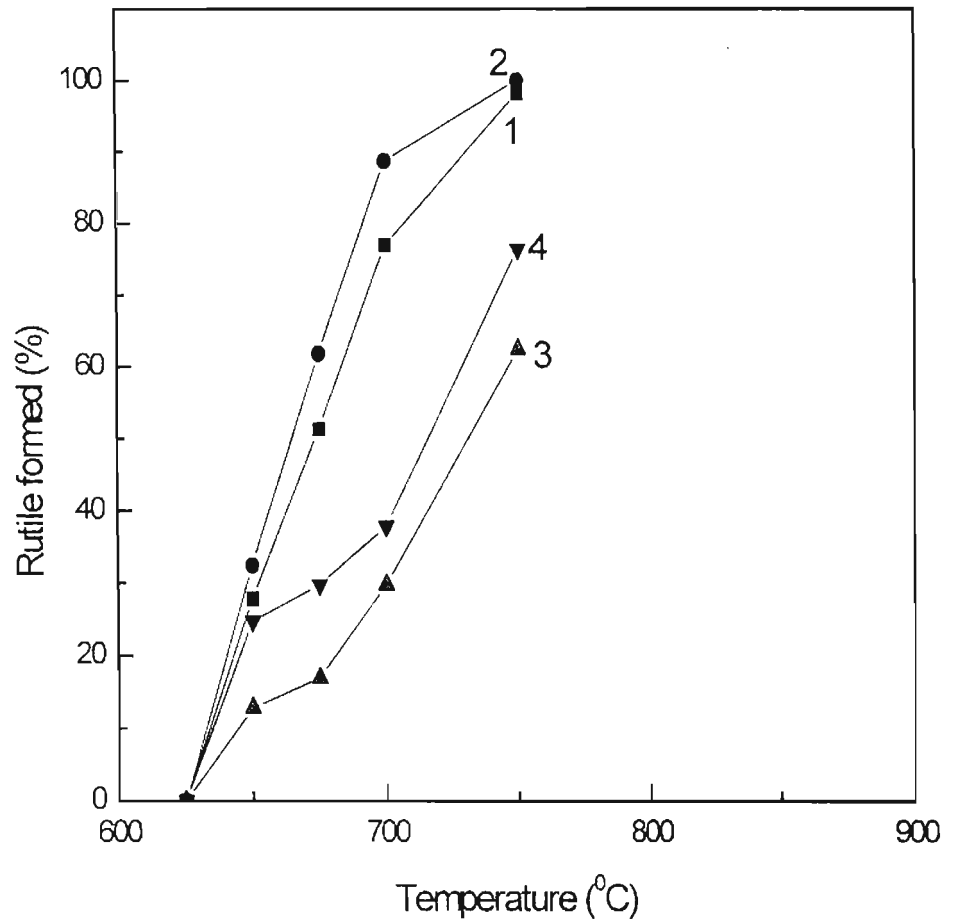
**Table.4.9: % of rutile formed in wet-impregnated NiO doped TiO<sub>2</sub> samples heated in argon atmosphere at different temperatures for 0.5 hrs.**

Temperature (°C)	Rutile formed	
	5% NiO/TiO <sub>2</sub>	15% NiO/TiO <sub>2</sub>
650	12.8	24.7
700	29.7	37.8
750	62.4	76.3

The variation of rutilation during heating in argon atmosphere in NiO/TiO<sub>2</sub> samples is evident in figure 4.13. Here the transformation is accelerated but the extent of acceleration strongly depends on the method of preparation. The lower distribution in wet-impregnated samples may be the cause for the variation in transformation.

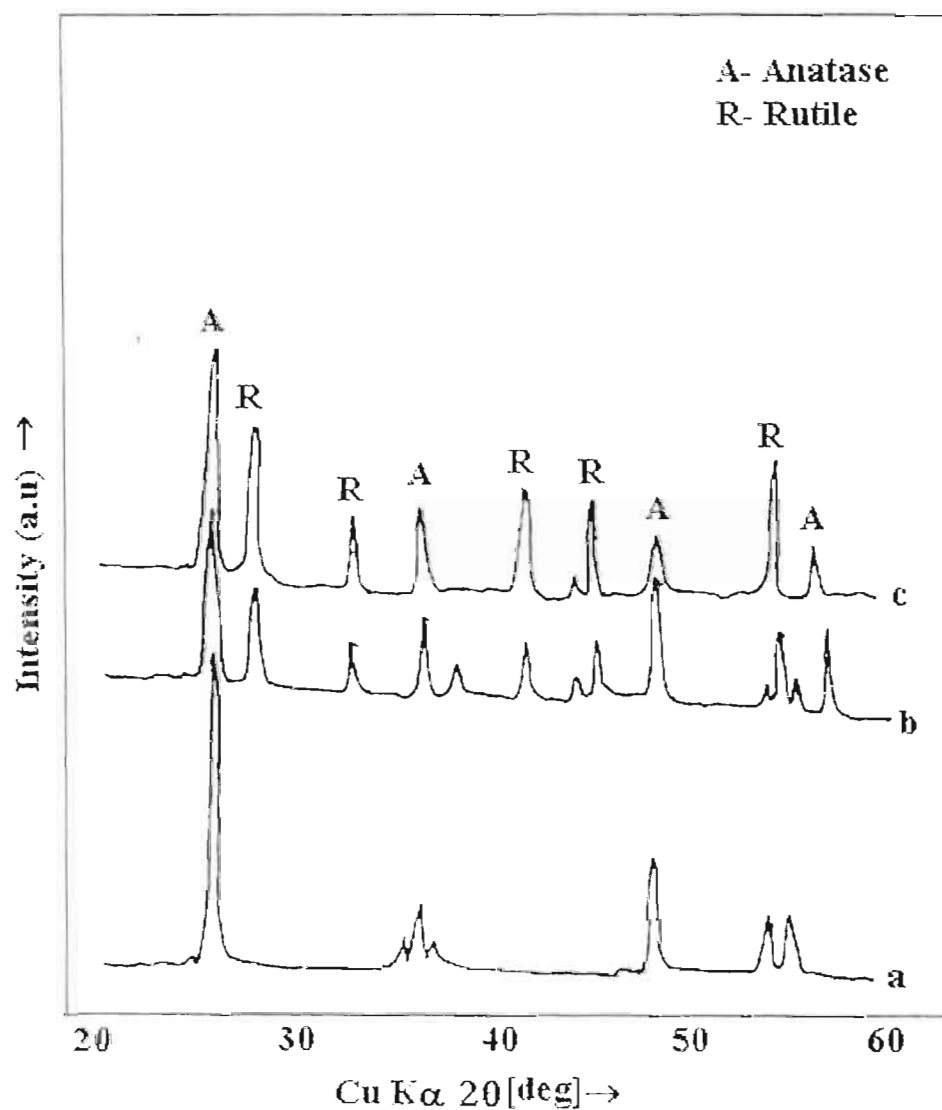
The importance of oxygen vacancies on the phase transition rate of TiO<sub>2</sub> in the presence of NiO seems to be also confirmed by a more rapid transformation in argon than in air. Hence it can be concluded that argon atmosphere increases oxygen vacancies concentration and thus it favours the anatase-rutile transformation.

Figure.4.13: Variation of rutilation in NiO/TiO<sub>2</sub> samples heated in argon atmosphere for 0.5 hrs at different temperatures.  
 1 - 5%NiO/TiO<sub>2</sub>, 2 - 15%NiO/TiO<sub>2</sub>, (Co-precipitated)  
 3 - 5%NiO/TiO<sub>2</sub>, 4 - 15%NiO/TiO<sub>2</sub>, (Wet-impregnated)



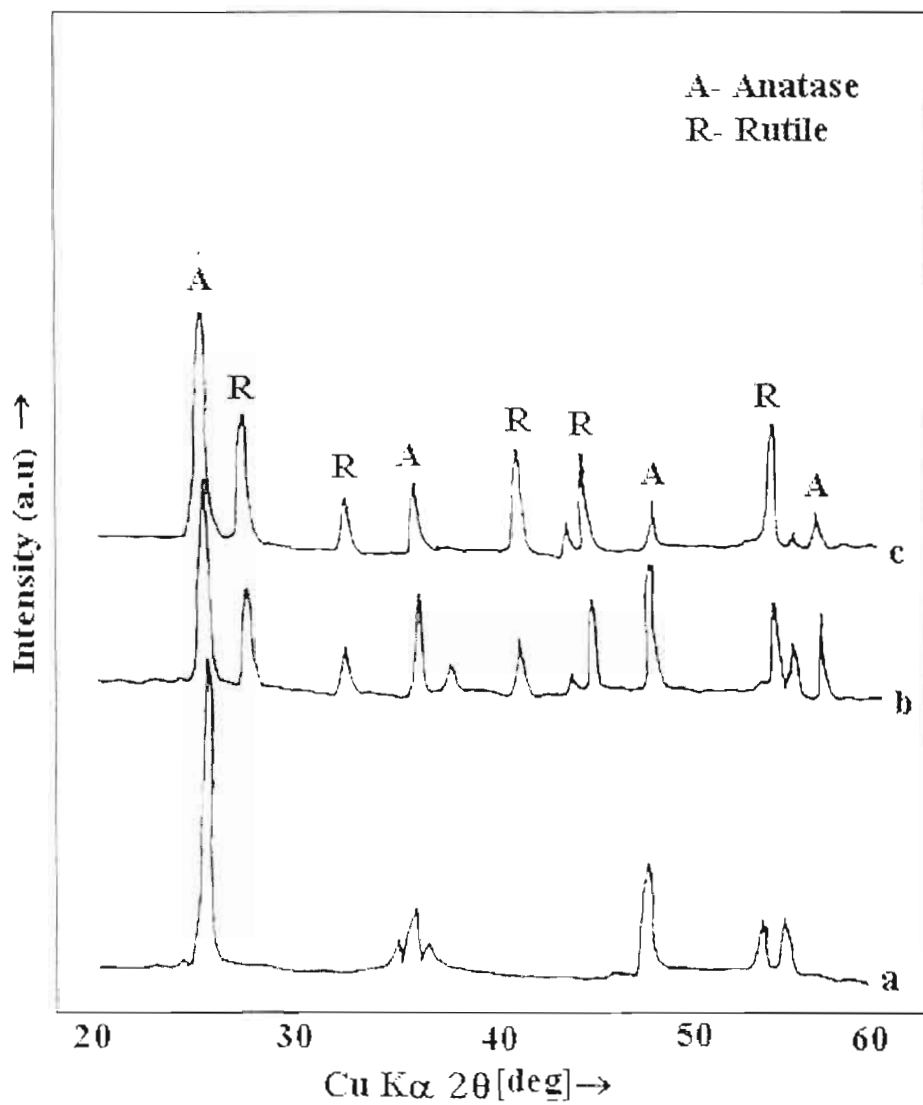
In hydrogen atmosphere, the anatase-rutile transformation was found to be low as compared to that in inert atmosphere. The XRD patterns of co-precipitated and wet-impregnated samples in different compositions are given in figures 4.14 and 4.15.

Figure.4.14: XRD Patterns of co-precipitated NiO/TiO<sub>2</sub> samples heated in hydrogen atmosphere at 700<sup>o</sup>/2hrs.  
(a) Undoped TiO<sub>2</sub> (b) 5% NiO/TiO<sub>2</sub> (c) 15% NiO/TiO<sub>2</sub>



In co-precipitated samples, it is observed that on set of rutilation is shifted to 700<sup>o</sup>C for 2 hrs heating, which is higher temperature than that in argon atmosphere.

Figure.4.15: XRD Patterns of wet-impregnated NiO-doped  $\text{TiO}_2$  samples heated in hydrogen atmosphere at  $750^\circ/2\text{hrs}$ .  
 (a) Undoped  $\text{TiO}_2$  (b) 5% NiO/ $\text{TiO}_2$  (c) 15% NiO/ $\text{TiO}_2$



The 5% doped samples gave 16.7 % of rutile at  $700^\circ\text{C}$  and 22.3% rutilation was observed in 15% doped sample for 2 hrs heating at the

same temperature. Tables 4.10 and 4.11 represent the different fractions of rutile formed in co-precipitated and wet-impregnated systems.

**Table.4.10:** % of rutile formed in co-precipitated NiO doped TiO<sub>2</sub> system during heating in hydrogen atmosphere for 2 hrs.

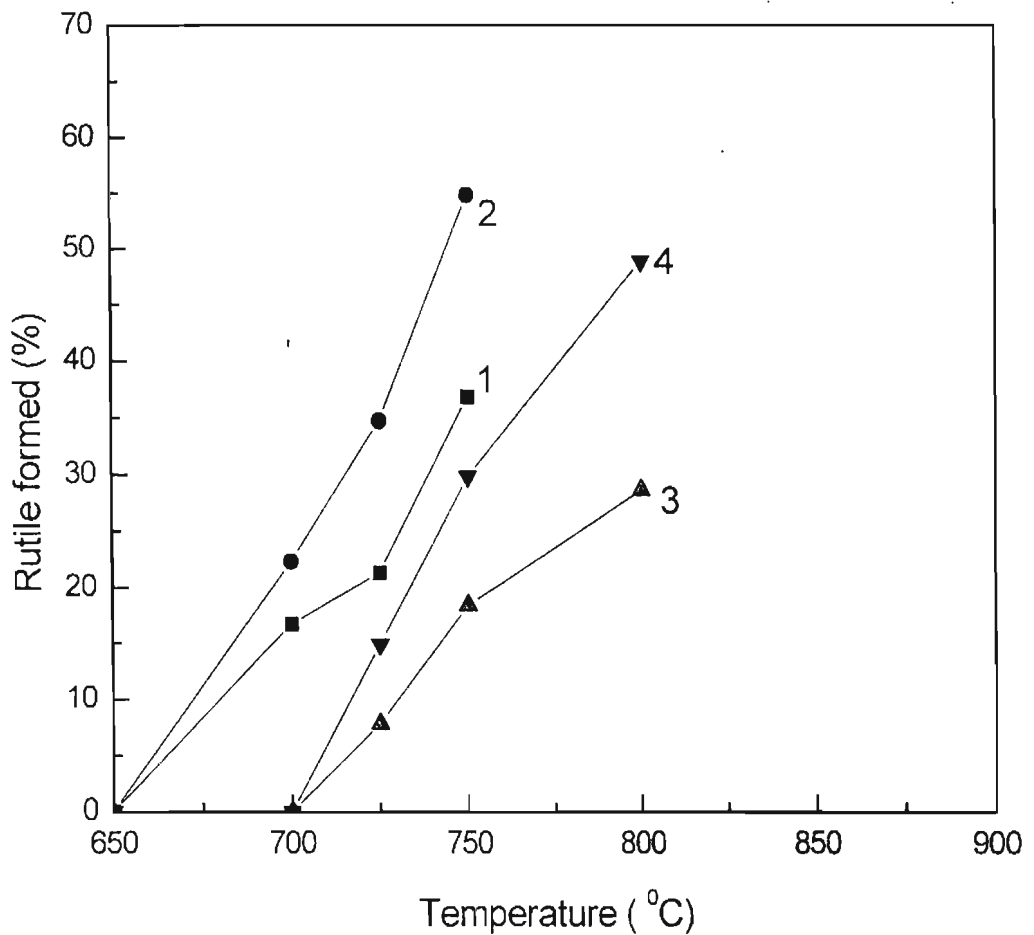
Temperature °C	Rutile formed (%)	
	5% NiO/TiO <sub>2</sub>	15% NiO/TiO <sub>2</sub>
650	0	0
700	16.7	22.3
725	21.3	34.7
750	36.8	54.8

**Table.4.11:** % of rutile formed in wet-impregnated NiO doped TiO<sub>2</sub> system during heating in hydrogen atmosphere for 2 hrs.

Temperature °C	Rutile formed (%)	
	5% NiO/TiO <sub>2</sub>	15% NiO/TiO <sub>2</sub>
700	0	0
725	7.8	14.9
750	18.4	29.8
800	28.6	48.9

In wet-impregnated samples rutilation started slowly as compared to co-precipitated. The variation in rutilation with temperature in NiO/TiO<sub>2</sub> samples heated in hydrogen atmosphere is shown in figures 4.16.

**Figure: 4.16: Variation in rutilation of NiO/TiO<sub>2</sub> samples heated in Hydrogen atmosphere for 2 hrs at different temperatures.**  
 1 - 5%NiO/TiO<sub>2</sub>, 2 - 15%NiO/TiO<sub>2</sub> (Co-precipitated)  
 3 - 5%NiO/TiO<sub>2</sub>, 4 - 15%NiO/TiO<sub>2</sub> (Wet-impregnated)



5% doped sample on 2 hrs heating at 750°C produced 18.4 % rutile while 15% has given 29.8 % rutile at the same conditions. There occurs some lattice defects in the samples during the heat treatment in reducing atmospheres. This is experienced as colour changes of the samples. The colour changes can also be due to the reduction of NiO to its lower oxidation state in hydrogen atmosphere. The intensity of

colour depends on the amount of dopant. This clearly indicates the effect of concentration of NiO is more important in the phase transformation. This is observed in air and argon atmosphere also. Hence it can be concluded that the anatase –rutile transformation in NiO doped TiO<sub>2</sub> strongly depends on the concentration of dopants, method of preparation and the atmosphere of calcination.

#### 4.6 Conclusions

- ☞ On heating NiO doped TiO<sub>2</sub>, anatase-rutile transformation takes place.
- ☞ Onset and completion temperatures of rutilation were found to vary with method of preparation.
- ☞ At the onset of rutilation NiTiO<sub>3</sub> phase is also formed.
- ☞ Better surface area are obtained with co-precipitated ones compared to wet-impregnation method.
- ☞ Calcination temperature and amount of NiO content have greater role in determining surface area.
- ☞ Crystallite size enlargement takes place during rutile phase formation.
- ☞ A morphological change occurs to TiO<sub>2</sub> during heating in presence of NiO and with rutilation.
- ☞ Atmosphere of calcination have major role in polymorphism in TiO<sub>2</sub>.
- ☞ Among air, argon and hydrogen atmospheres, the order of enhancing rutilation is Argon > Hydrogen > Air.

## CHAPTER 5

### STUDIES ON Cr<sub>2</sub>O<sub>3</sub> DOPED TiO<sub>2</sub>

The catalytic activity of the titania supported chromia system is owing to the stabilization of the anchored chromia species having multiple chemical and molecular states on the surface. Many transition metal ion dopants have been investigated for the TiO<sub>2</sub> system. Chromium doped TiO<sub>2</sub> is studied for the photo degradation of methylene blue dye.

Therefore in order to study the effect of Cr<sub>2</sub>O<sub>3</sub> and reaction atmospheres on anatase-rutile transformation in TiO<sub>2</sub>, it is doped with 5 and 15 percentages of Cr<sub>2</sub>O<sub>3</sub> using co-precipitation and wet-impregnation methods, as described in Chapter 2. The transformation was studied in air, argon and hydrogen atmospheres as a function of temperature and time using XRD. Surface area measurements and SEM.

#### 5.1. Chemical analysis

The constitution of Cr<sub>2</sub>O<sub>3</sub>/ TiO<sub>2</sub> samples was established by chemical analysis using standard procedures available in literature. The percentage of Cr<sub>2</sub>O<sub>3</sub> in each sample is as given in Table 5.1.

**Table.5.1: Results of Chemical analysis of Cr<sub>2</sub>O<sub>3</sub> doped TiO<sub>2</sub> prepared through different methods.**

Method of Preparation	Expected Cr <sub>2</sub> O <sub>3</sub> (%)	Experimental Composition	
		Cr <sub>2</sub> O <sub>3</sub>	TiO <sub>2</sub>
Co-precipitation	5	4.94	94.8
	15	14.89	84.9
Wet-Impregnation	5	4.64	94.3
	15	14.39	84.7



## 5.2. XRD studies

XRD patterns of co-precipitated  $\text{Cr}_2\text{O}_3$  doped  $\text{TiO}_2$  heated in air are shown in Figures 5.1 and 5.2. It was found that there are peaks corresponding to anatase and rutile in samples heated at different temperatures. The appearance of peak and its intensity are different for samples containing different amounts of  $\text{Cr}_2\text{O}_3$ . In 5%  $\text{Cr}_2\text{O}_3$  doped  $\text{TiO}_2$  samples the percentage of rutile formed was lower as compared to 15%  $\text{Cr}_2\text{O}_3$ . In 5%  $\text{Cr}_2\text{O}_3$  doped  $\text{TiO}_2$ , on heating at  $800^\circ\text{C}$  for 8hrs, the anatase to rutile transformation occurs and 27.7% rutile was formed. On increasing temperature to  $850^\circ\text{C}$ , at 8 hrs, 60.6% rutile was formed and at  $900^\circ\text{C}$  for 10 hrs, rutilation was almost complete.

There are peaks corresponding to chromium titanate in samples heated above  $800^\circ\text{C}$ , the intensity of titanate peaks increased with rise of temperature. Hence at higher temperature  $\text{Cr}_2\text{O}_3$  reacts with titania to form its titanate. 15%  $\text{Cr}_2\text{O}_3$  doped  $\text{TiO}_2$  behaved differently from that of 5% doped samples, here rutilation started at  $600^\circ\text{C}$  itself, and 8 hrs heating at this temperature produced 72.3% rutile. This clearly indicates that amount of  $\text{Cr}_2\text{O}_3$  is a deciding factor of rutilation. On heating at  $800^\circ\text{C}$  for 8 hrs, 96.5% rutile formation was found in 15%  $\text{Cr}_2\text{O}_3$  doped  $\text{TiO}_2$ .

Figure 5.1: XRD Patterns of co-precipitated 5% Cr<sub>2</sub>O<sub>3</sub> doped TiO<sub>2</sub> heated at different temperatures for 8 hrs.  
(a) 800<sup>0</sup>C (b) 850<sup>0</sup>C (c) 900<sup>0</sup>C

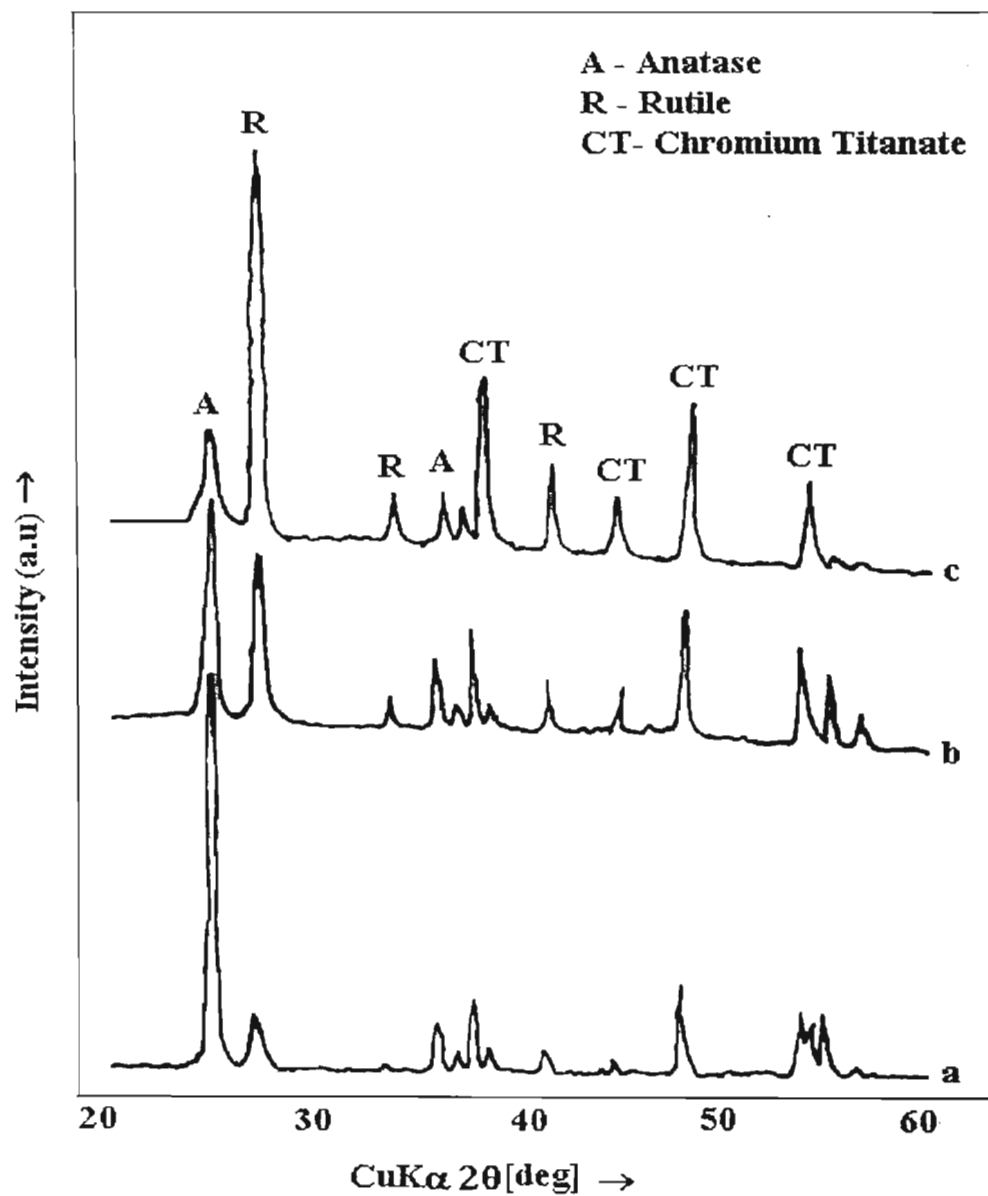
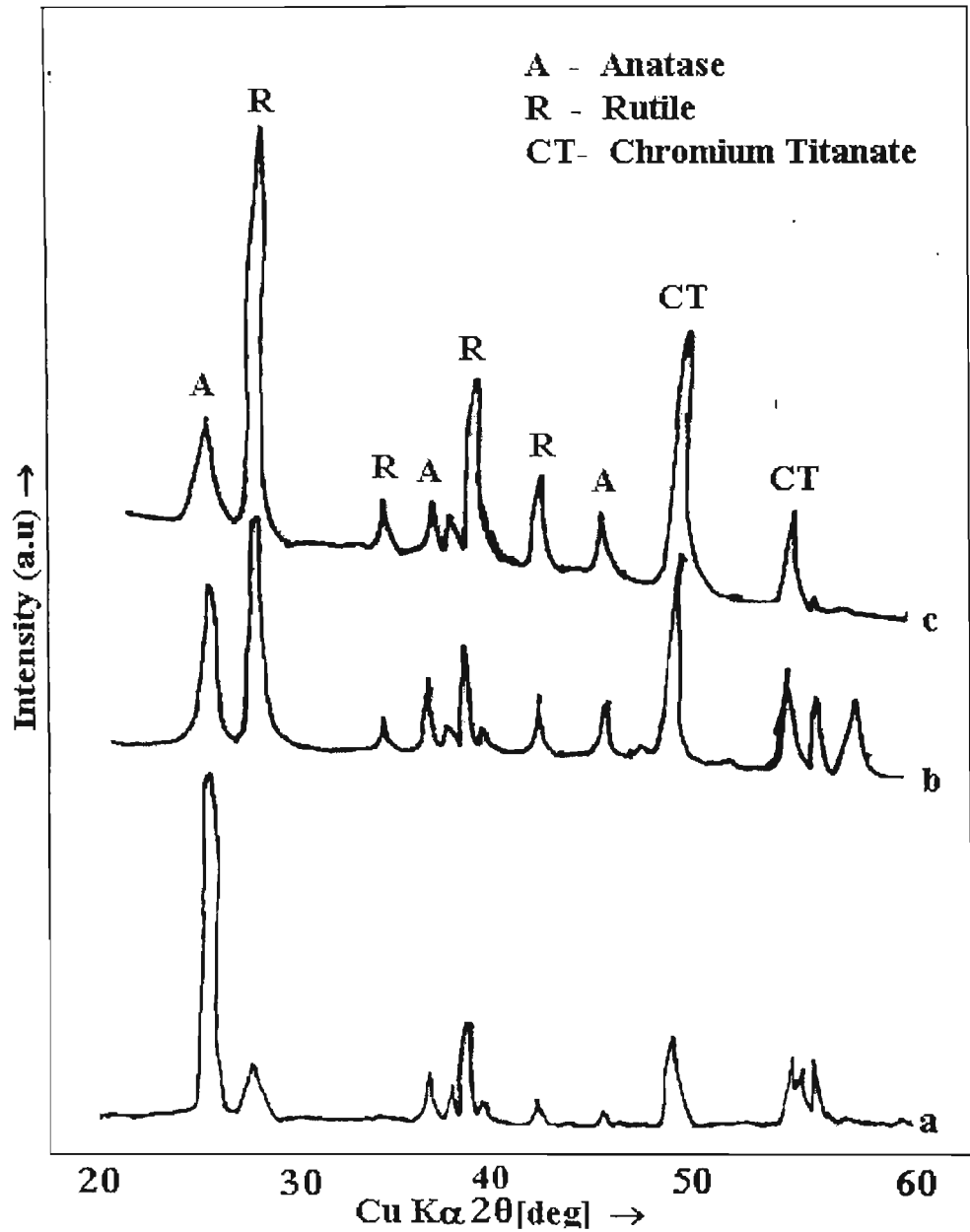


Figure.5.2: XRD Patterns of co-precipitated 15% Cr<sub>2</sub>O<sub>3</sub> doped TiO<sub>2</sub> heated at different temperatures for 8 hrs.  
(a) 600<sup>o</sup>C (b) 700<sup>o</sup>C (c) 800<sup>o</sup>C



In order to quantify anatase to rutile transformation, different percentages of rutile formed during heating of co-precipitated Cr<sub>2</sub>O<sub>3</sub>/TiO<sub>2</sub> at different temperatures and time are calculated using the standard equations given in chapter 2 and the values are given in tables 5.2 and 5.3.

Table.5.2: % of rutile formed during heating of co-precipitated 5%Cr<sub>2</sub>O<sub>3</sub> doped TiO<sub>2</sub> heated at different temperatures and time.

Time of heating (hrs)	Rutile formed (%)		
	800 <sup>0</sup> C	850 <sup>0</sup> C	900 <sup>0</sup> C
1	3.9	10.9	24.9
2	7.7	20.7	43.6
3	11.4	29.5	57.6
4	14.9	37.2	68.2
5	18.3	44.3	76.1
6	21.6	50.2	82.2
7	24.7	55.7	86.5
8	27.7	60.6	89.9
9	30.5	64.9	92.4
10	33.3	68.8	96.9

But undoped TiO<sub>2</sub> on calcination at 700<sup>0</sup>C for 8 hours has no rutile and only anatase phase was present as described in chapter 3. Hence it is clear that Cr<sub>2</sub>O<sub>3</sub> has higher enhancing effect on polymorphism in TiO<sub>2</sub> than Fe<sub>2</sub>O<sub>3</sub>. This reaction is highly temperature dependent and 15% Cr<sub>2</sub>O<sub>3</sub> has more enhancing effect than 5%.

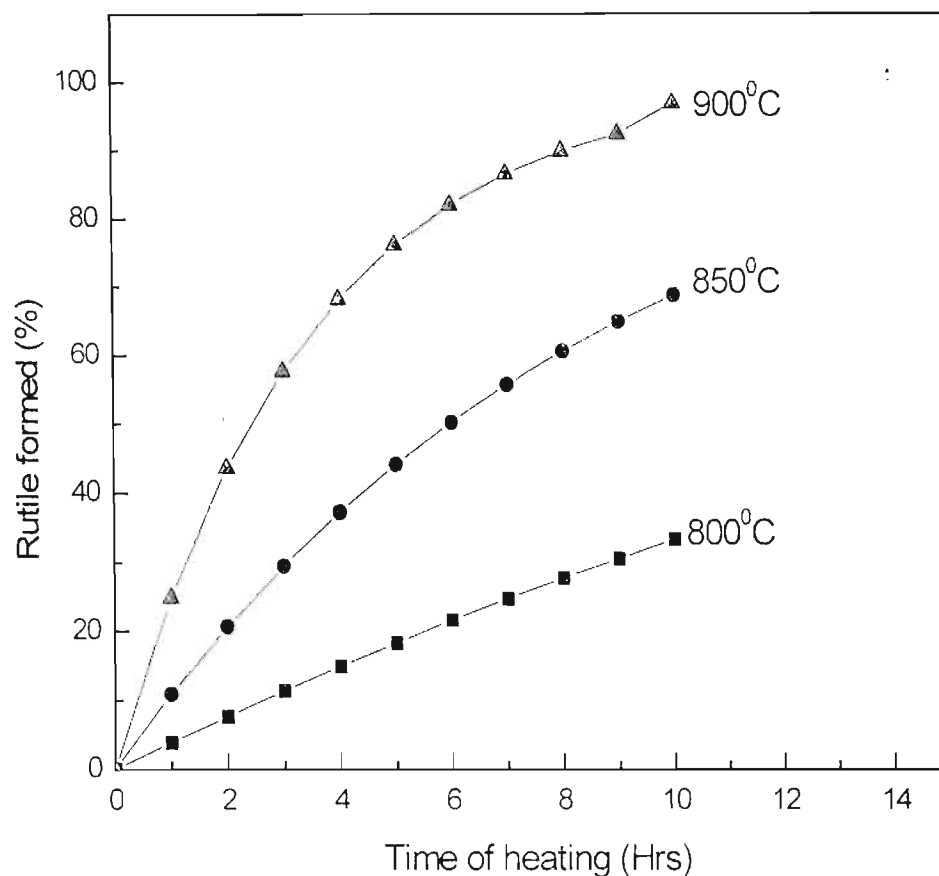
**Table.5.3: % of rutile formed during heating of co-precipitated 15% Cr<sub>2</sub>O<sub>3</sub> doped TiO<sub>2</sub> heated at different temperatures and time**

Time of heating (hrs)	Rutile formed (%)		
	600 <sup>0</sup> C	700 <sup>0</sup> C	800 <sup>0</sup> C
1	14.8	21.7	32.1
2	27.4	38.8	53.9
3	38.2	52.1	68.7
4	47.3	62.5	78.7
5	55.1	70.7	85.6
6	61.8	77.1	90.2
7	67.4	82.4	93.3
8	72.3	86.2	96.5
9	76.4	89.1	96.9
10	79.9	91.4	97.9

If we consider the defect formation by foreign ions in titania lattice, it can be assumed that ions, which enter in to the system substituting Ti<sup>4+</sup>, may either enhance or delay the transformation from anatase to rutile depending on whether the number of oxygen vacancies is increased or decreased.[227] In this case the oxygen vacancies created in anatase by the presence of Cr<sub>2</sub>O<sub>3</sub> act as nucleation site for the anatase to rutile phase transformation.[228]

The variation of rutile formation on heating at different temperature and time is shown in figures 5.3 and 5.4.

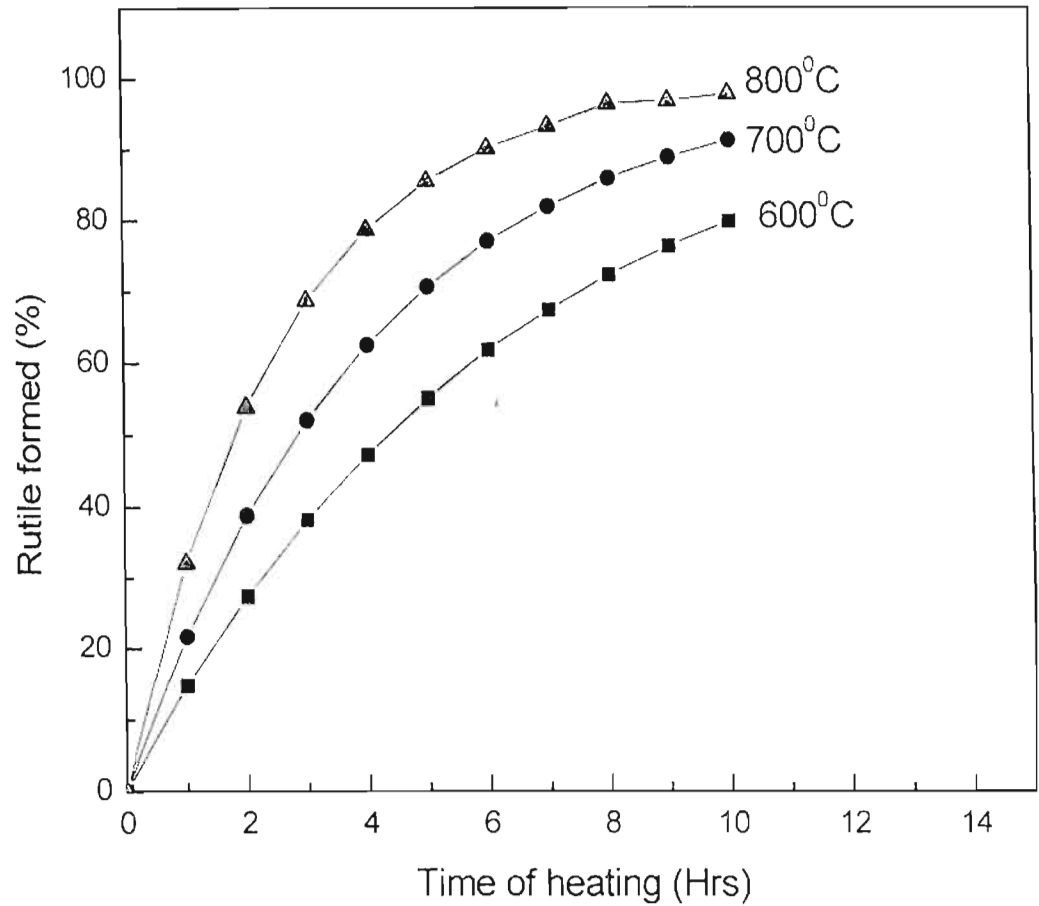
Figure.5.3: Variation of rutile % with time at different temperatures in co-precipitated 5% Cr<sub>2</sub>O<sub>3</sub> doped TiO<sub>2</sub>.



The graphs clearly show the increase of rutilation with increasing temperature and time of heating. The variation is different for 5 and 15% Cr<sub>2</sub>O<sub>3</sub> doped TiO<sub>2</sub> even though both are co-precipitated samples.

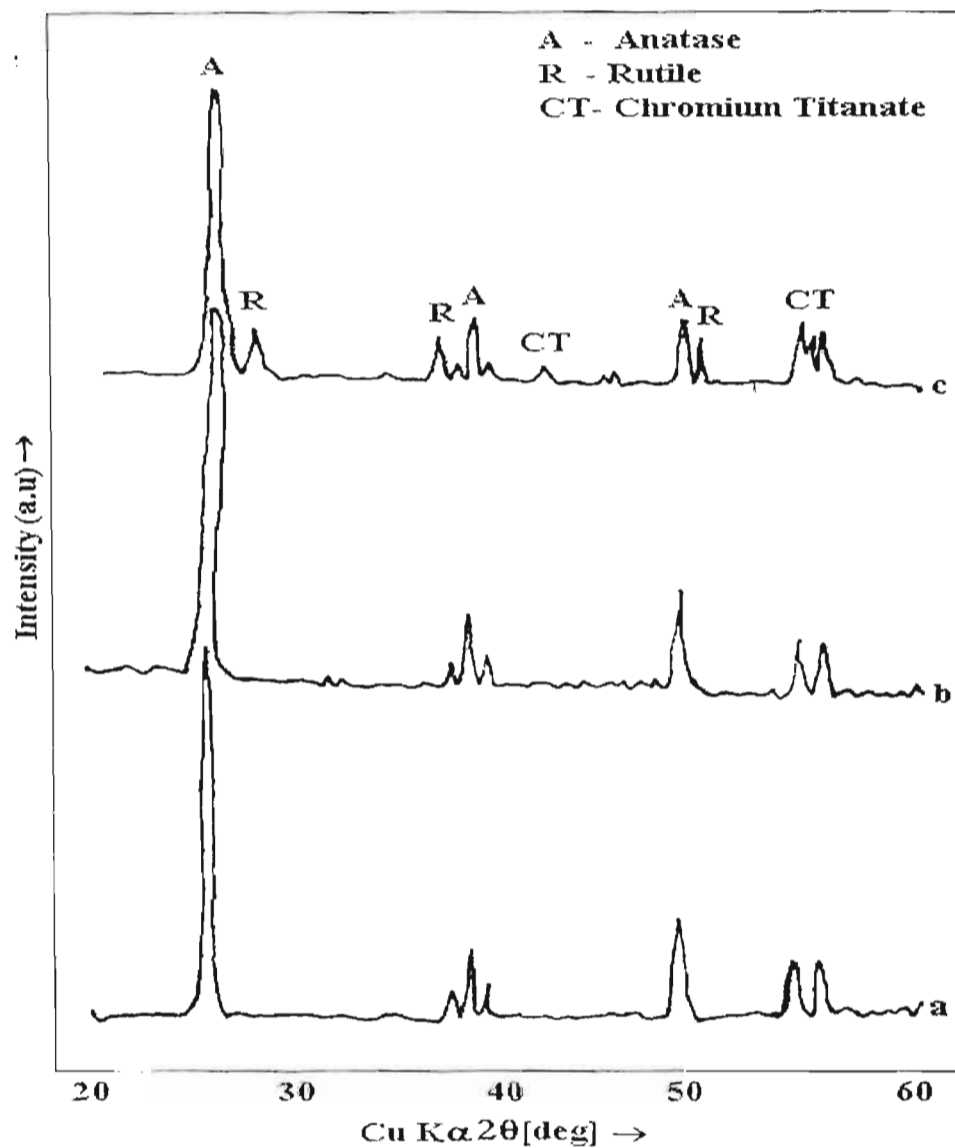
The transformation in wet-impregnated samples is found to be very low as compared to co-precipitated. The onset of rutilation in both 5 and 15% Cr<sub>2</sub>O<sub>3</sub> doped TiO<sub>2</sub> takes place at very high temperature compared to co-precipitated samples.

Figure.5.4: Variation of rutile % with time at different temperatures in co-precipitated 15% Cr<sub>2</sub>O<sub>3</sub> doped TiO<sub>2</sub>.



From the XRD patterns shown in figures 5.5 and 5.6, it is evident that rutilation started at 900°C in both 5 and 15% Cr<sub>2</sub>O<sub>3</sub> doped TiO<sub>2</sub> samples. In all the samples rutilation is not complete even at 950°C. The peaks corresponding to anatase and rutile were found in all the XRD patterns of the samples heated above 900°C. The intensity of anatase peak was found to be decreased while that of rutile increased with temperature and time of heating.

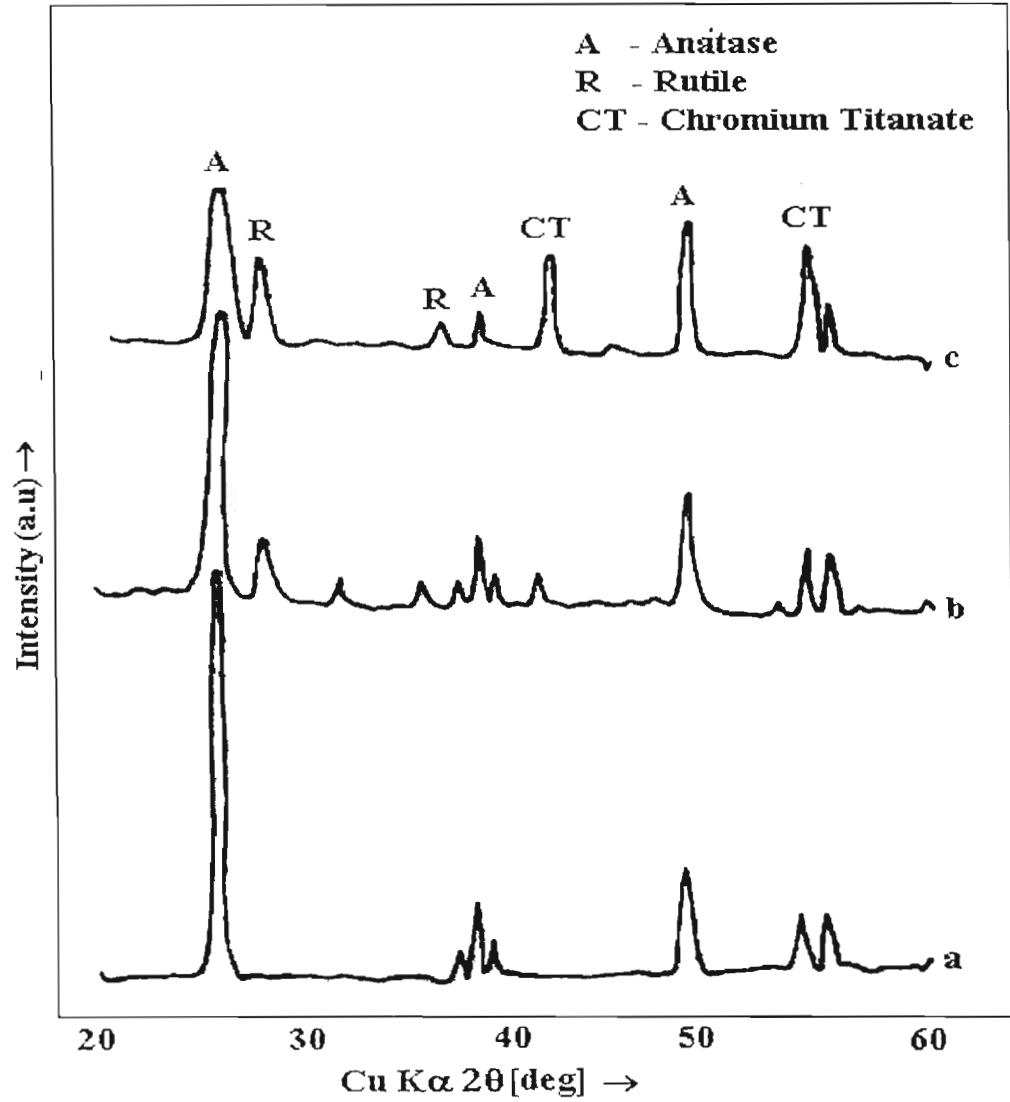
Figure.5.5: XRD Patterns of wet-impregnated 5%  $\text{Cr}_2\text{O}_3$  doped  $\text{TiO}_2$  heated at different temperatures for 8 hrs.  
 (a)  $700^\circ\text{C}$  (b)  $800^\circ\text{C}$  (c)  $900^\circ\text{C}$



In these samples also peaks corresponding to chromium titanate appeared in samples heated above  $900^\circ\text{C}$ . At higher temperature  $\text{Cr}_2\text{O}_3$  reacts with titania to form their titanate and its formation depends on the method of preparation of doped sample since the intensity of chromium titanate peak is low compared with co-precipitated systems.



Figure.5.6: XRD Patterns of wet-impregnated 15% Cr<sub>2</sub>O<sub>3</sub> doped TiO<sub>2</sub> heated at different temperatures for 8 hrs.  
 (a) 800<sup>0</sup>C (b) 900<sup>0</sup>C (c) 925<sup>0</sup>C



Various amounts of rutile formed in wet-impregnated samples heated at different temperatures and time are calculated from XRD patterns using standard method and are tabulated in tables 5.4 and 5.5.

Table.5.4: % of rutile formed during heating of Wet-impregnated 5% Cr<sub>2</sub>O<sub>3</sub> doped TiO<sub>2</sub> at different temperatures and time.

Time of heating (hrs)	Rutile formed (%)		
	900 <sup>0</sup> C	925 <sup>0</sup> C	950 <sup>0</sup> C
1	0	3.6	12.2
2	0	7.2	22.9
3	4.3	10.6	32.3
4	5.8	13.9	40.5
5	7.2	17.4	47.8
6	8.6	20.2	54.2
7	10.3	23.1	59.4
8	12.4	25.9	64.7
9	14.9	28.7	69.8
10	16.2	31.3	72.7

It was observed that at 950<sup>0</sup> for 6hrs heating 54.2% conversion has taken place in wet-impregnated 5% Cr<sub>2</sub>O<sub>3</sub> doped TiO<sub>2</sub>. In the case of 15% doped sample, 73.7% rutilation was seen at the same condition. At all other temperatures amount of rutile conversion is different in samples with different amounts of Cr<sub>2</sub>O<sub>3</sub>. Hence the transformation is highly dependent on the method of preparation of doped samples as well as the amount of dopent. In co-precipitated samples, the conversion occurs at lower temperature than in the wet-impregnated samples. It is due to the lower distribution of Cr<sub>2</sub>O<sub>3</sub> on TiO<sub>2</sub> in wet-impregnated samples. Also there are peaks for chromium titanate and no

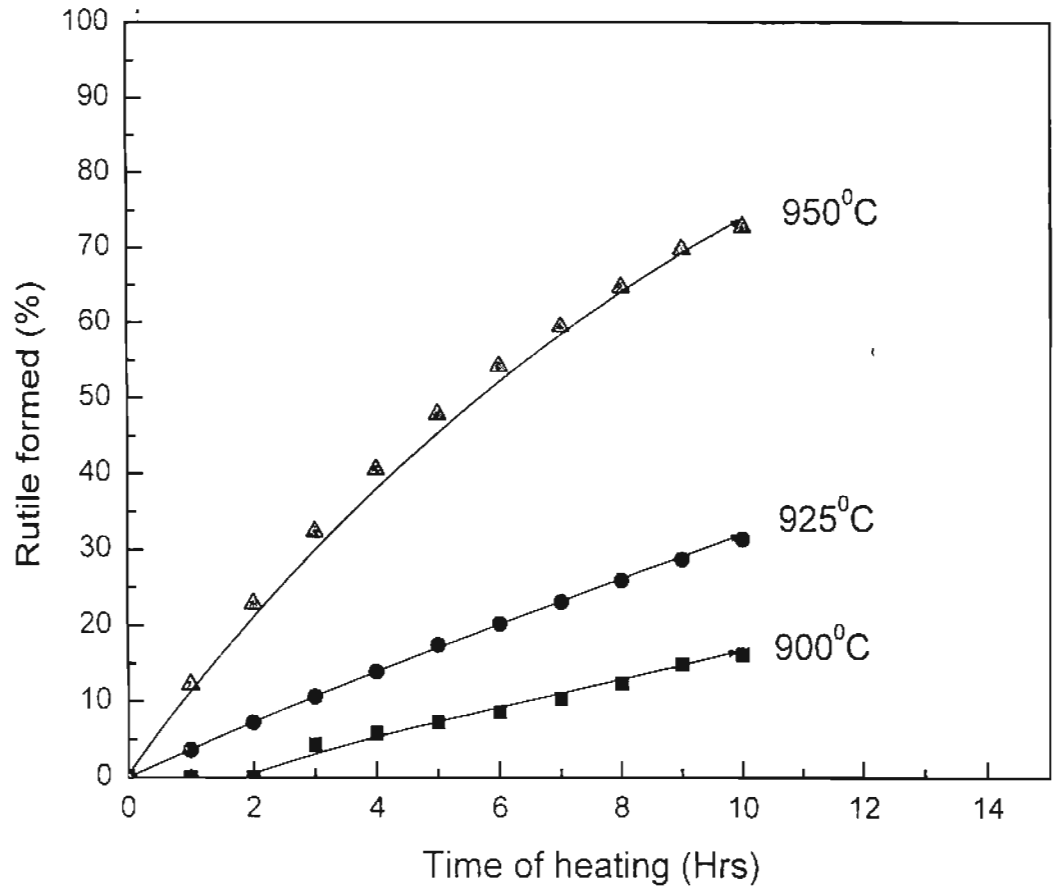
peak for  $\text{Cr}_2\text{O}_3$ , indicating that on heating at higher temperature  $\text{Cr}_2\text{O}_3$  reacts with  $\text{TiO}_2$  to form its titanate.

**Table.5.5: % of rutile formed during heating of Wet-impregnated  $15\%\text{Cr}_2\text{O}_3$  doped  $\text{TiO}_2$  at different temperatures and time.**

Time of heating (hrs)	Rutile formed (%)		
	$900^\circ\text{C}$	$925^\circ\text{C}$	$950^\circ\text{C}$
1	0	8.7	19.9
2	0	16.7	35.9
3	6.4	24.2	48.7
4	8.4	30.6	58.9
5	10.4	36.7	67.1
6	12.4	42.3	73.7
7	14.3	47.6	78.9
8	16.1	51.9	83.1
9	18.3	56.1	86.5
10	23.5	60.3	89.2

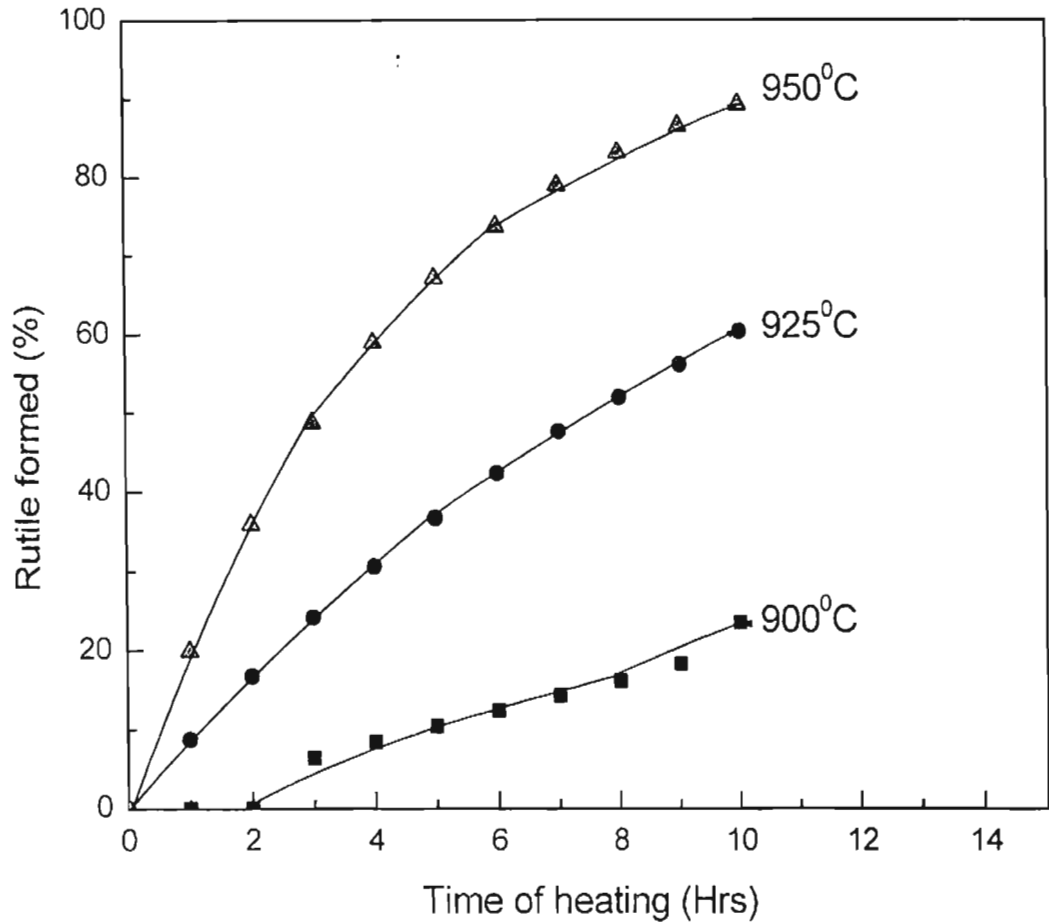
The plots of rutile percentage versus time at different temperatures are shown in figures 5.5 and 5.6. Like co-precipitated samples in wet-impregnated ones also the rutilation is accelerated by heating at higher temperature and time as evident from the graphs.

Figure.5.5: Variation of rutile % with time at different temperatures in wet-impregnated 5%  $\text{Cr}_2\text{O}_3$  doped  $\text{TiO}_2$ .



When anatase is transformed to rutile, chromium atoms are segregated from the rutile stable phase grains, thereby creating a thin  $\text{Cr}_2\text{O}_3$  film (in case of high  $\text{Cr}_2\text{O}_3$  loading) or small nano clusters (in the case of lower  $\text{Cr}_2\text{O}_3$  loading). At an intermediate stage, an anatase layer, which still contains chromium, remains at the exterior surface until the total transformation to rutile phase.[226]

Figure.5.6: Variation of rutile % with time at different temperatures in wet-impregnated 15%  $\text{Cr}_2\text{O}_3$  doped  $\text{TiO}_2$ .



The mechanism responsible for the transformation is the spatial disturbance of the oxygen ion framework. When  $\text{Cr}^{3+}$  ions enter in to  $\text{TiO}_2$ , the charge of the  $\text{Cr}^{3+}$  ions should be compensated for an increase in oxygen vacancies leading to the enhancement of the anatase to rutile transformation [227,229] and the shifting of the majority of  $\text{Ti}^{4+}$  ions by breaking two of the six Ti-O bonds to form new bonds. The function of  $\text{Cr}_2\text{O}_3$  is to lower the energy needed to break the bonds and to form the new bonds. There will be nucleation and growth of rutile during anatase to rutile transformation. This

process takes place rapidly in coprecipitated ones since there is uniform distribution of  $\text{Cr}_2\text{O}_3$  on  $\text{TiO}_2$  as both are precipitated together from a homogeneous solution. This distribution is low in wet impregnated ones, which is the reason for the lower transformation.

The crystallite size of  $\text{Cr}_2\text{O}_3/\text{TiO}_2$  calculated from XRD patterns are shown in Table 5.5. It is seen that crystallite size increases with increase of heating temperature. The rutilation taking place as the function of temperature may be the reason for the crystallite size enlargement. This increase is higher for 15%  $\text{Cr}_2\text{O}_3$  doped samples compared to 5% doped ones prepared by same method at any particular temperature as in the case of  $\text{Fe}_2\text{O}_3$  doped  $\text{TiO}_2$  system discussed in chapter 3. Rutilation begins in 5%  $\text{Cr}_2\text{O}_3$  doped coprecipitated samples when the anatase crystallites grow to a size of 9.8 nm, while in the case of 5% wet-impregnated ones the transformation happens at  $900^\circ\text{C}$ , where crystallite size was 10.2 nm. In the 15% doped samples also coprecipitated have larger crystallite size than wet-impregnated. Hence it is clear that the particle size and crystallite size of anatase increase markedly in the region of the crystal structure transformation. It was reported that the unit cell of anatase seems to expand prior to the transformation to rutile [51]

### 5.3. Surface area studies

The surface area values of undoped and  $\text{Cr}_2\text{O}_3$  doped samples calcined at different temperature are determined. It is clear that Surface area of both co-precipitated and wet-impregnated samples decreases on heating at higher temperature, which may be due to rutilation at these temperatures. The surface area decrease is more pronounced on increasing  $\text{Cr}_2\text{O}_3$  percentage. In the case of co-precipitated samples, surface area was  $45.4 \text{ m}^2/\text{g}$ , and  $39.1 \text{ m}^2/\text{g}$  respectively for 5 and 15% doped samples heated at  $700^\circ\text{C}$  for 6 hrs. Undoped

titania under the same conditions gave 27.2 m<sup>2</sup>/g. The surface area decreased drastically with rutilation. In 5% Cr<sub>2</sub>O<sub>3</sub> doped TiO<sub>2</sub> at 850<sup>0</sup>C for 6 hrs 23.9 m<sup>2</sup>/g surface area was obtained and for 15% Cr<sub>2</sub>O<sub>3</sub> doped TiO<sub>2</sub> containing 90.2% rutilation, surface area was 9.4 m<sup>2</sup>/g at 800<sup>0</sup>C for 6 hrs. Similarly in wet-impregnated samples it was 21.25 and 19.3 m<sup>2</sup>/g in 5 and 15% doped system on heating at 900<sup>0</sup>C for 6 hrs where rutilation started. It became 9.86 and 8.23 m<sup>2</sup>/g for heating at 950<sup>0</sup>C for 6 hrs.

In all the cases surface area decreased on increasing the percentage of Cr<sub>2</sub>O<sub>3</sub>. More predominant change was observed in co-precipitated ones. This is in agreement with crystallite size of anatase, which is found to increase on increasing Cr<sub>2</sub>O<sub>3</sub> percentage. At this point, it would be noteworthy that anatase to rutile transformation in Cr<sub>2</sub>O<sub>3</sub> doped TiO<sub>2</sub> system is accompanied by enlargement of crystallite size and lower surface area.

Crystallite size of anatase seems to have some relation with surface area. It decreased on increasing surface area in all the samples depending on the method of preparation. So, Cr<sub>2</sub>O<sub>3</sub> has a significant influence on the surface area of these samples. The decrease in surface area with increase in rutile percentage was also larger in presence of Cr<sub>2</sub>O<sub>3</sub>.

Table.5.5: Variation of Crystallite size and surface area in undoped and Cr<sub>2</sub>O<sub>3</sub> doped TiO<sub>2</sub> Samples heated for 6hrs.

Sample	Heating Temperature (°C)	Surface area (m <sup>2</sup> /g)	Crystallite size of anatase (nm)
Undoped TiO <sub>2</sub>	110	162.58	a*
	300	109.59	a*
	700	27.2	4.8
	900	9.13	14.2
	1000	2.54	b*
Co-precipitated 5% Cr <sub>2</sub> O <sub>3</sub> /TiO <sub>2</sub>	700	45.4	7.2
	850	23.9	13.4
	900	12.2	14.9
Co-precipitated 15% Cr <sub>2</sub> O <sub>3</sub> /TiO <sub>2</sub>	500	119.4	a*
	700	39.1	4.3
	800	9.4	10.3
Wet-impregnated 5% Cr <sub>2</sub> O <sub>3</sub> /TiO <sub>2</sub>	900	21.25	10.2
	925	13.47	11.2
	950	9.86	12.9
Wet-impregnated 15% Cr <sub>2</sub> O <sub>3</sub> /TiO <sub>2</sub>	900	19.3	11.4
	925	11.91	12.8
	950	8.23	13.9

\*a Amorphous \*b Anatase phase absent

The activation energy for the conversion in co-precipitated samples was calculated using standard methods explained in chapter 2 and values are 32.4 for



5% while in 15% it was 22.9 kcal / mol. For undoped  $\text{TiO}_2$ , activation energy for anatase-rutile transformation was reported to be  $\sim 90$  kcal/mol. Therefore  $\text{Cr}_2\text{O}_3$  decreases the activation energy for the transformation, this decrease is higher for 15%. In wet-impregnated samples activation energy for the transformation was calculated to be 82.4 for 5% while in 15% it was 78.7 kcal / mol. Here also the activation energy is lowered and the extent of lowering is low as compared to co-precipitated samples, which reflects as high onset temperature of rutilation ( $900^\circ\text{C}$ ). In wet-impregnated samples the distribution of dopant is not uniform compared to co-precipitation. This may be the reason for the wide variation in the transformation. Hence the anatase to rutile transformation strongly depends on the method of preparation of  $\text{Cr}_2\text{O}_3$  doped  $\text{TiO}_2$  samples as well as the amount of  $\text{Cr}_2\text{O}_3$ .

**Table.5.6: Activation energies for the anatase-rutile transformation in  $\text{Cr}_2\text{O}_3$  doped  $\text{TiO}_2$ .**

Method of preparation	$\text{Cr}_2\text{O}_3$ (%)	Activation Energy (kcal/mol)
Co-precipitation	5	32.4
	15	22.9
Wet-impregnation	5	82.4
	15	78.7

#### 5.4. Scanning Electron Microscopic studies.

SEM studies were done to understand the morphological changes of  $\text{Cr}_2\text{O}_3/\text{TiO}_2$  samples with rutilation. The micrographs are shown in figure 5.7. It is obvious that the surface morphology of  $\text{TiO}_2$  changes with rutilation. Also wet-impregnated samples differ from co-precipitated ones in their shape. Before rutilation particles are found to be agglomerated in wet-impregnated samples. After rutilation co-precipitated sample's surface becomes smooth and not porous and it is not agglomerated and most of the particles are fine (small).

In case of wet-impregnated samples, the surface becomes porous and not smooth like co-precipitated. It may be due to the agglomeration or aggregation of particles as prepared. Hence the morphological changes are different for samples prepared by co-precipitation and wet-impregnation. The lower rutilation in wet-impregnated samples may be due to this difference. However the surface morphology of  $\text{Cr}_2\text{O}_3$  doped  $\text{TiO}_2$  changes markedly during the anatase rutile transformation.

Thus we can say that some crystallographic changes occur in  $\text{TiO}_2$  during the heating in presence of  $\text{Cr}_2\text{O}_3$ , leading to the changes in surface morphology.

Figure.5.7: Scanning Electron Micrographs of  $\text{Cr}_2\text{O}_3$  doped  $\text{TiO}_2$  before rutilation (a) Co-precipitated (b) Wet-impregnated

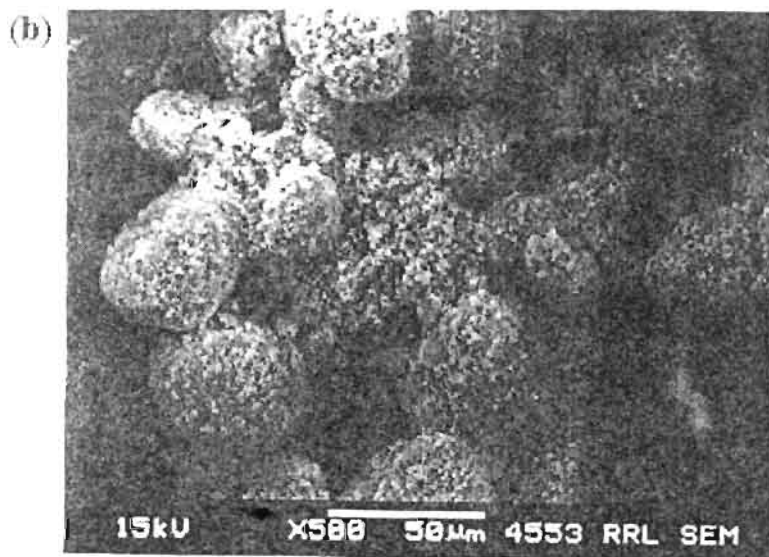
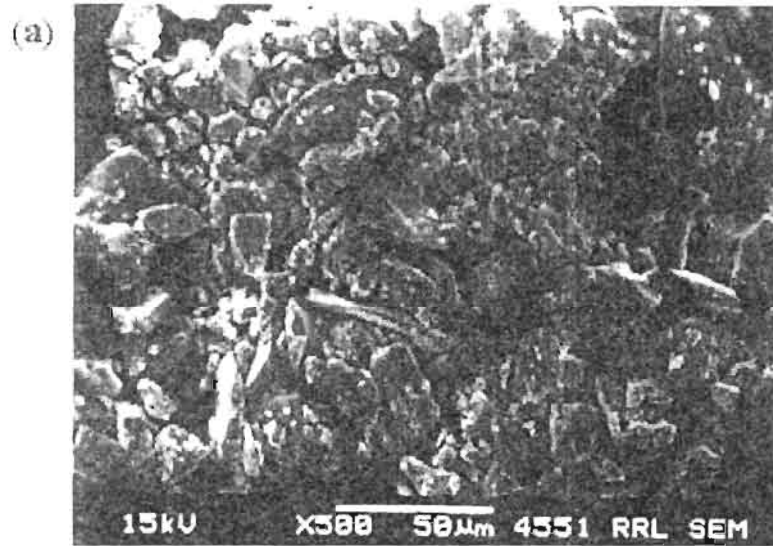
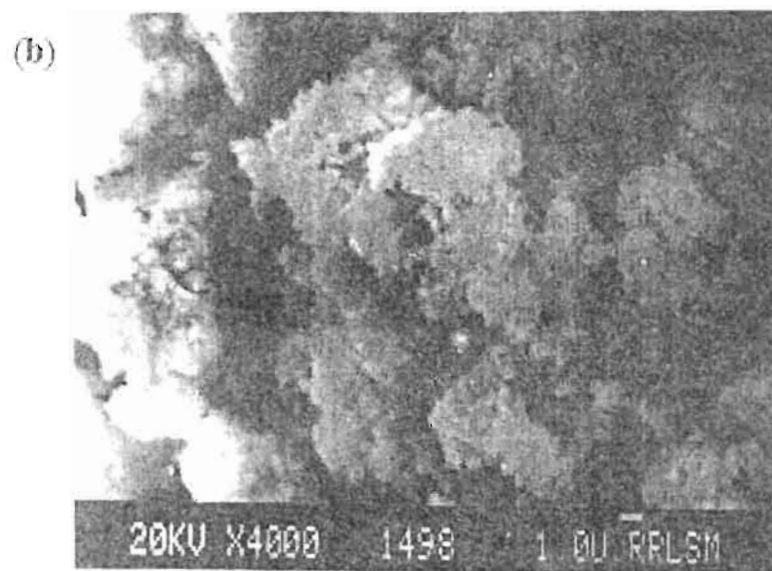
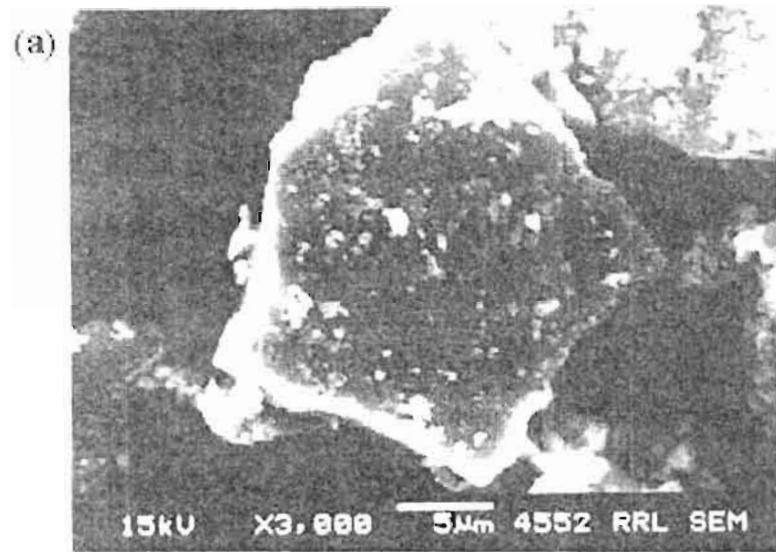


Figure.5.8: Scanning Electron Micrographs of  $\text{Cr}_2\text{O}_3$  doped  $\text{TiO}_2$  after rutilation (a) Co-precipitated (b) Wet-impregnated



### 5.5 Transformation in Argon and Hydrogen atmospheres.

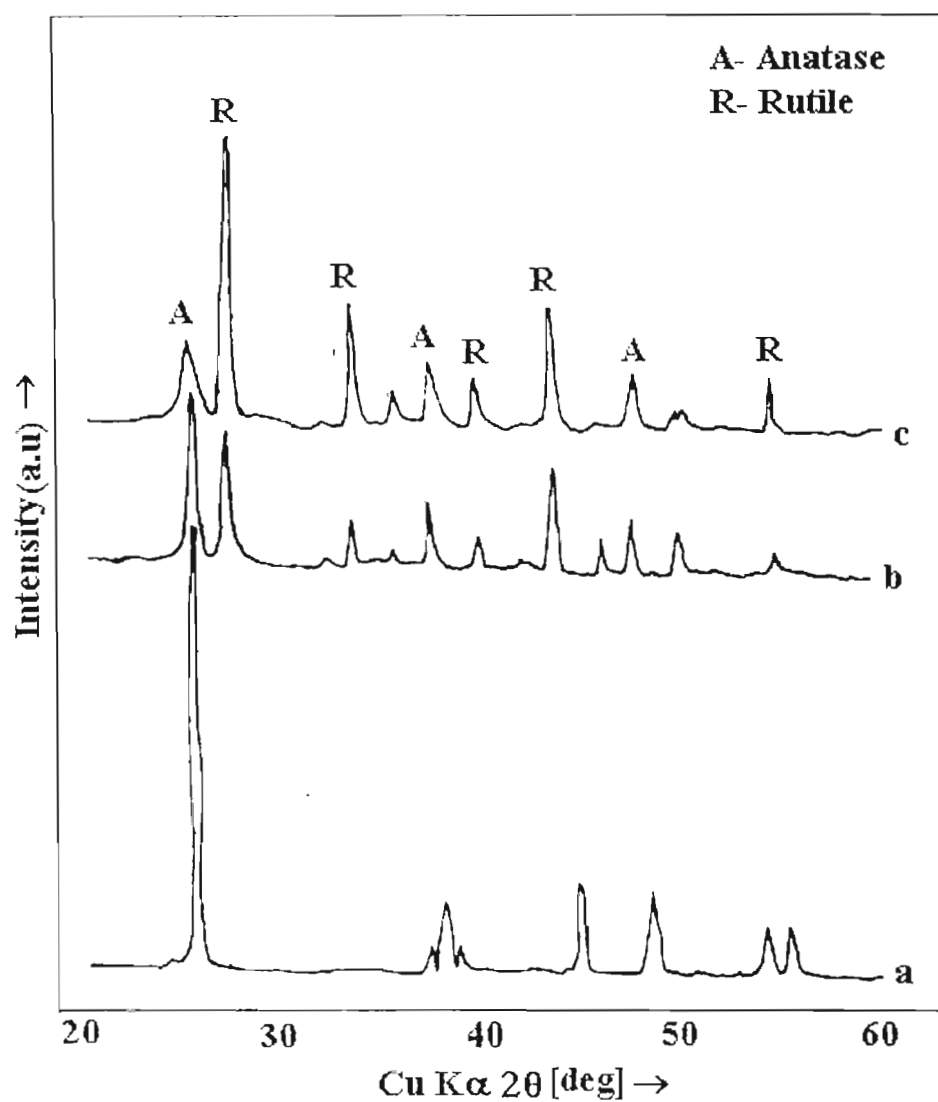
The anatase rutile transformations in Argon (inert) and hydrogen (reducing) atmospheres have been investigated. Figure 5.9 represents the XRD patterns of co-precipitated  $\text{Cr}_2\text{O}_3/\text{TiO}_2$  heated in argon atmosphere at  $700^\circ\text{C}$  for 0.5 hrs. The anatase-rutile transformation was found to be surprisingly accelerated in argon than in air.

In argon atmosphere, the onset of rutilation was lowered to  $700^\circ\text{C}$  in co-precipitated 5%  $\text{Cr}_2\text{O}_3$  doped  $\text{TiO}_2$ . The fraction of rutile formed is 9.3 % for 0.5 hrs heating. This is much different from that in air. At  $800^\circ\text{C}$ , the rutilation was found to be 88.9 %. 15%  $\text{Cr}_2\text{O}_3$  doped  $\text{TiO}_2$  even at  $600^\circ\text{C}$  for 0.5 hrs heating produced 34.8 % rutile and at  $750^\circ\text{C}$  for 0.5 hrs heating completed the rutilation. The fraction of rutile formed in co-precipitated 5 and 15%  $\text{Cr}_2\text{O}_3/\text{TiO}_2$  at different temperatures are tabulated in table 5.8. Hence the extent of acceleration is different in this case from that in air. The amount of rutile formed is higher at each temperature as compared to 5% doped samples as evident from the table 5.8.

**Table: 5.8: % of rutile formed in co-precipitated  $\text{Cr}_2\text{O}_3$  doped  $\text{TiO}_2$  samples heated in argon atmosphere at different temperatures for 0.5 hrs heating.**

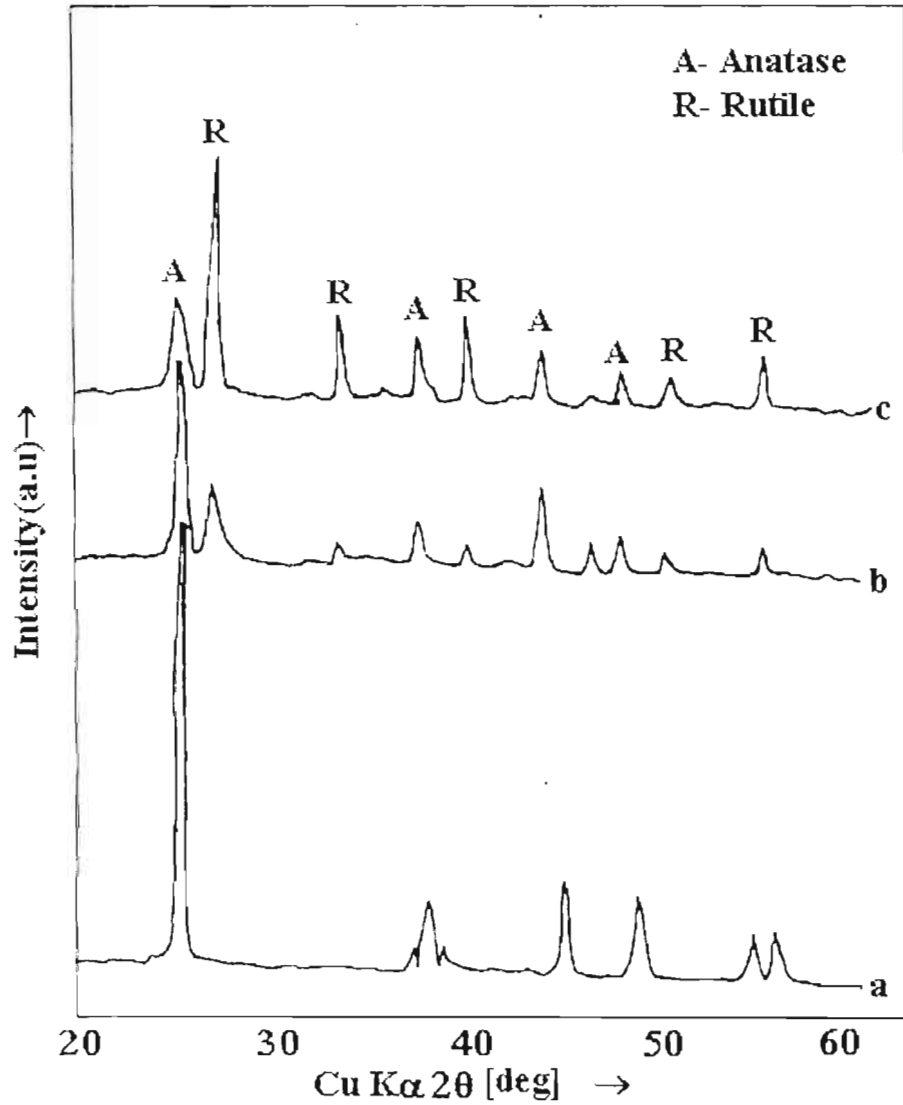
Temperature ( $^\circ\text{C}$ )	Rutile formed	
	5% $\text{Cr}_2\text{O}_3/\text{TiO}_2$	15% $\text{Cr}_2\text{O}_3/\text{TiO}_2$
600	0	34.8
700	9.3	78.9
750	44.9	100
800	88.9	100

Figure: 5.9: XRD Patterns of co-precipitated  $\text{Cr}_2\text{O}_3$  doped  $\text{TiO}_2$  samples heated in argon atmosphere at  $700^\circ$  for 0.5 hrs.  
 (a) Undoped  $\text{TiO}_2$  (b) 5%  $\text{Cr}_2\text{O}_3/\text{TiO}_2$  (c) 15%  $\text{Cr}_2\text{O}_3/\text{TiO}_2$



In wet-impregnated samples on set temperature of rutilation is changed and at  $800^\circ\text{C}$  for 0.5 hrs heating 5%  $\text{Cr}_2\text{O}_3$  doped samples gave 18.4 % rutile while 36.8% anatase to rutile conversion was found in 15% doped samples. The XRD patterns of wet-impregnated  $\text{Cr}_2\text{O}_3$  doped  $\text{TiO}_2$  heated in argon for 0.5 hrs at  $700^\circ\text{C}$  are shown in figure 5.10.

Figure.5.10: XRD Patterns of wet-impregnated  $\text{Cr}_2\text{O}_3$  doped  $\text{TiO}_2$  samples heated in argon atmosphere at  $700^\circ$  for 0.5 hrs.  
 (a) Undoped  $\text{TiO}_2$  (b) 5%  $\text{Cr}_2\text{O}_3/\text{TiO}_2$  (c) 15%  $\text{Cr}_2\text{O}_3/\text{TiO}_2$



The effect of higher temperature is same as that in co-precipitated one. The different amounts of rutile formed in wet-impregnated samples are summarized in table 5.9.

**Table.5.9: % of rutile formed in wet-impregnated Cr<sub>2</sub>O<sub>3</sub> doped TiO<sub>2</sub> samples heated in argon atmosphere at different temperatures for 0.5 hrs heating.**

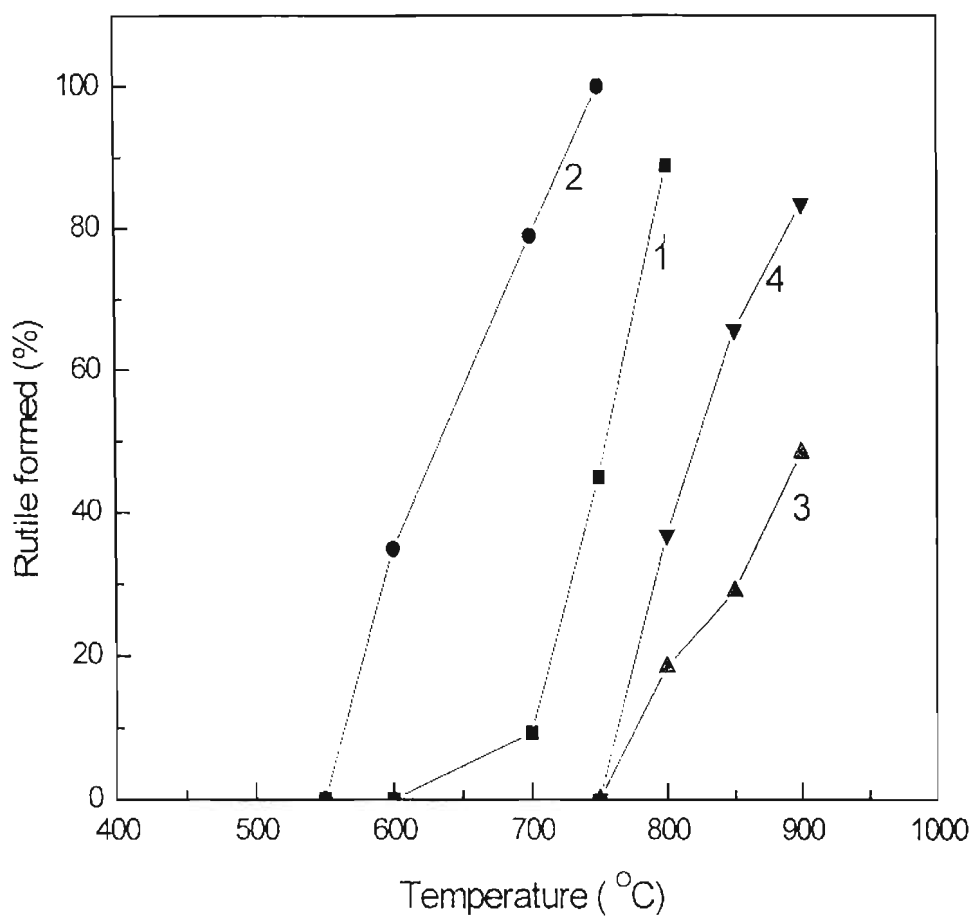
Temperature (°C)	Rutile formed (%)	
	5% Cr <sub>2</sub> O <sub>3</sub> /TiO <sub>2</sub>	15% Cr <sub>2</sub> O <sub>3</sub> /TiO <sub>2</sub>
700	0	0
800	18.4	36.8
850	28.9	65.7
900	48.3	83.4

The variation in rutilation during heating in argon atmosphere in Cr<sub>2</sub>O<sub>3</sub>/TiO<sub>2</sub> samples is shown in figure 5.11. Like in air atmosphere heating at higher temperature increases the rutilation in argon also. The difference is in the on set temperature and time. Here also the transformation strongly depends on the method of preparation and amount of Cr<sub>2</sub>O<sub>3</sub>. The lower distribution in wet-impregnated samples may be the cause for the differences in transformation.

The importance of oxygen vacancies in the phase transformation rate of TiO<sub>2</sub> in the presence of Cr<sub>2</sub>O<sub>3</sub> seems to be also confirmed by a more rapid transformation in argon than in air. Hence it can be concluded that argon atmosphere increases oxygen vacancies concentration and thus it favours the anatase-rutile transformation.

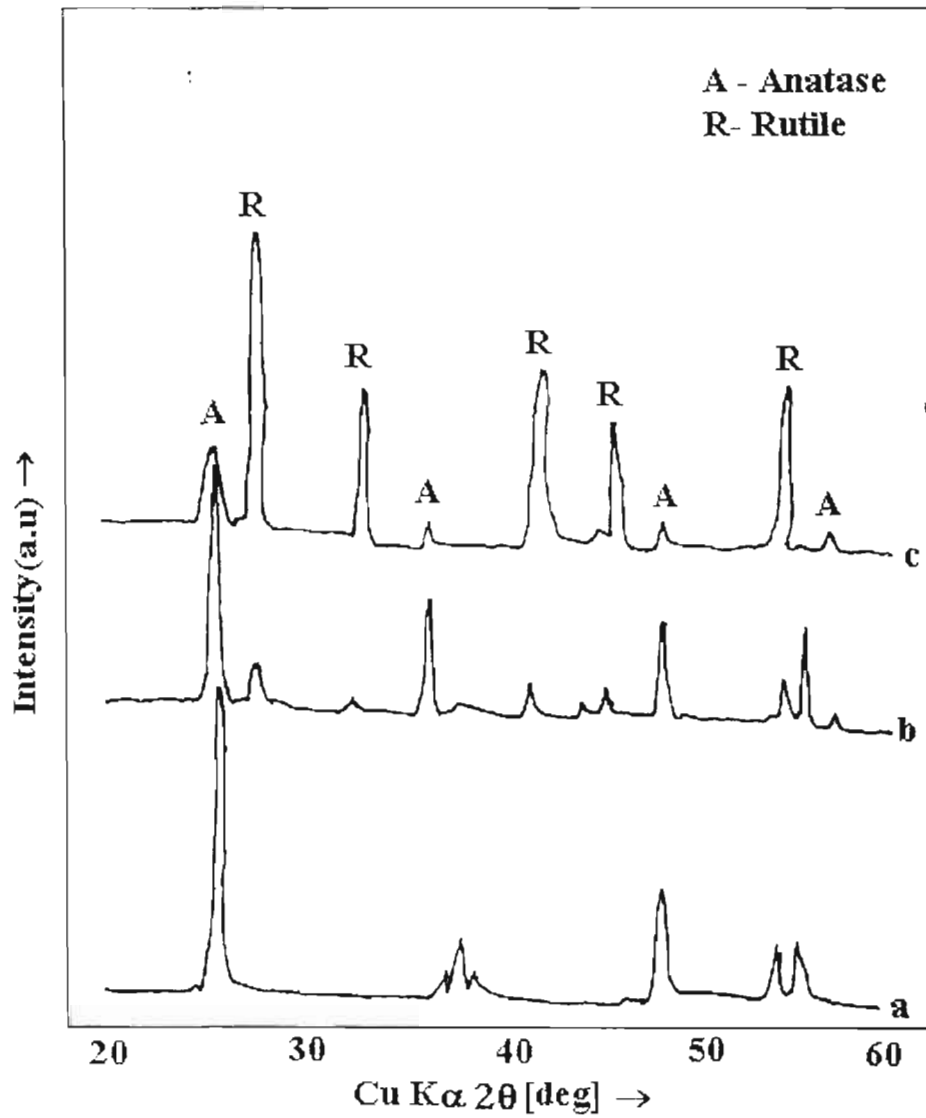


Figure.5.11: Variation of rutilation in  $\text{Cr}_2\text{O}_3/\text{TiO}_2$  samples heated in argon atmosphere for 0.5 hrs at different temperature.  
 1- 5%  $\text{Cr}_2\text{O}_3/\text{TiO}_2$ . 2 - 15%  $\text{Cr}_2\text{O}_3/\text{TiO}_2$ . (Co-precipitated)  
 3- 5%  $\text{Cr}_2\text{O}_3/\text{TiO}_2$ . 4 - 15%  $\text{Cr}_2\text{O}_3/\text{TiO}_2$ . (Wet-impregnated)



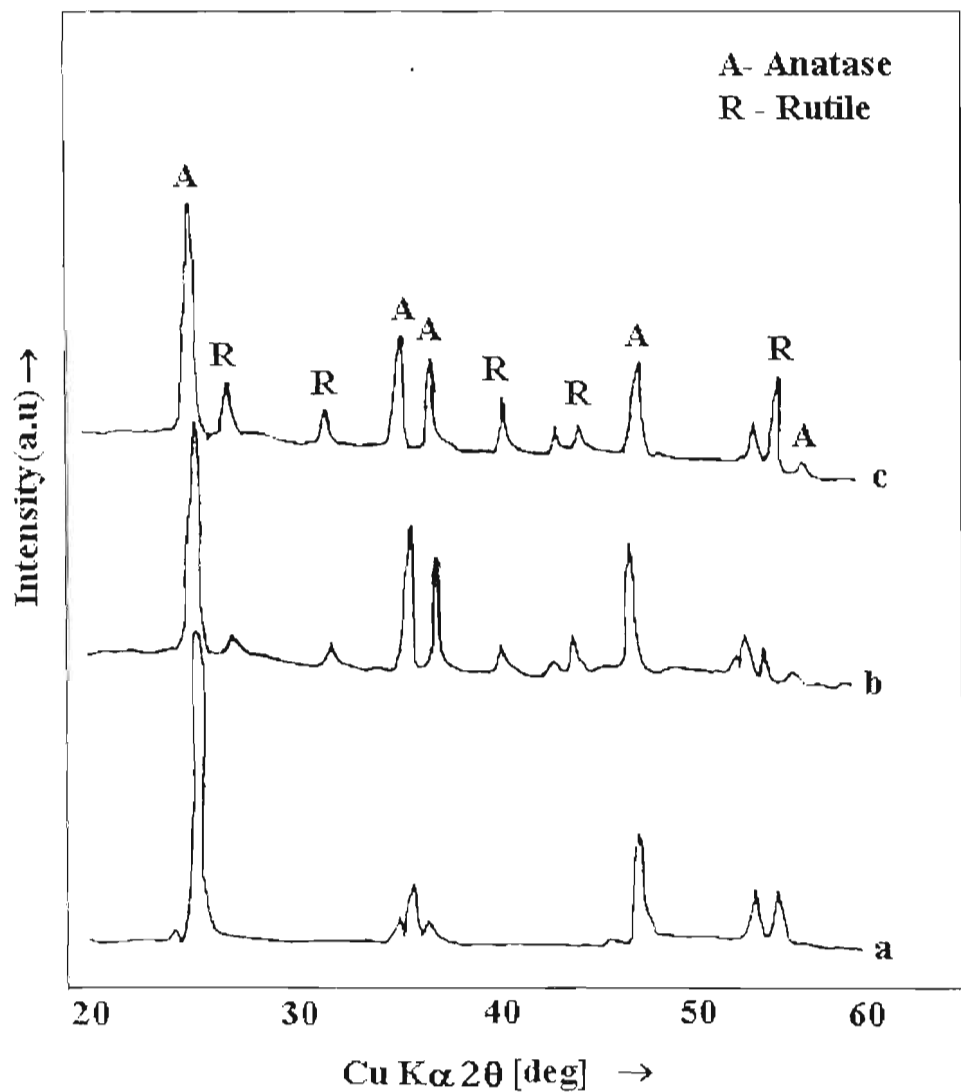
In hydrogen atmosphere, the anatase-rutile transformation was found to be different as compared to the transformation in air and inert atmosphere. The XRD patterns of co-precipitated and wet-impregnated samples of different compositions are given in figures 5.12 and 5.13.

Figure.5.12: XRD Patterns of co-precipitated  $\text{Cr}_2\text{O}_3/\text{TiO}_2$  samples heated in hydrogen atmosphere at  $650^\circ/2\text{hrs}$ .  
 (a) Undoped  $\text{TiO}_2$  (b) 5%  $\text{Cr}_2\text{O}_3/\text{TiO}_2$  (c) 15%  $\text{Cr}_2\text{O}_3/\text{TiO}_2$ .



It is observed that in co-precipitated samples on set of rutilation is shifted to  $650^\circ\text{C}$  for 2 hrs heating in 5% doped sample while in 15%  $\text{Cr}_2\text{O}_3$  doped  $\text{TiO}_2$  even at  $550^\circ\text{C}$  rutilation appeared which is widely different from than that in argon atmosphere. The 5% doped samples gave 12.4 % of rutile at  $650^\circ\text{C}$  for 2 hrs heating and 39.4% rutilation was observed in 15% doped sample for 2 hrs heating at  $550^\circ\text{C}$ .

Figure.5.13: XRD Patterns of wet-impregnated  $\text{Cr}_2\text{O}_3/\text{TiO}_2$  samples heated in hydrogen atmosphere at  $750^\circ\text{C}/2\text{hrs}$ .  
 (a) Undoped  $\text{TiO}_2$  (b) 5%  $\text{Cr}_2\text{O}_3/\text{TiO}_2$  (c) 15%  $\text{Cr}_2\text{O}_3/\text{TiO}_2$



In case of wet-impregnated samples heated in hydrogen atmosphere, rutilation started at  $750^\circ\text{C}$  in samples containing 5%  $\text{Cr}_2\text{O}_3$ . At  $700^\circ\text{C}$ , 15% doped samples gave rutile on 2 hrs heating. Different amounts of rutile formed are calculated from the XRD patterns and tables 5.10 and 5.11 represent the

different percentages of rutile formed in co-precipitated and wet-impregnated samples during the calcinations at different temperatures for 2 hrs.

**Table.5.10: % of rutile formed in co-precipitated  $\text{Cr}_2\text{O}_3$  doped  $\text{TiO}_2$  system during heating in hydrogen atmosphere for 2 hrs.**

Temperature $^{\circ}\text{C}$	Rutile formed	
	5% $\text{Cr}_2\text{O}_3/\text{TiO}_2$	15% $\text{Cr}_2\text{O}_3/\text{TiO}_2$
500	0	0
550	0	39.4
575	0	74.8
600	0	100
650	12.4	100
700	28.7	100
750	49.8	100

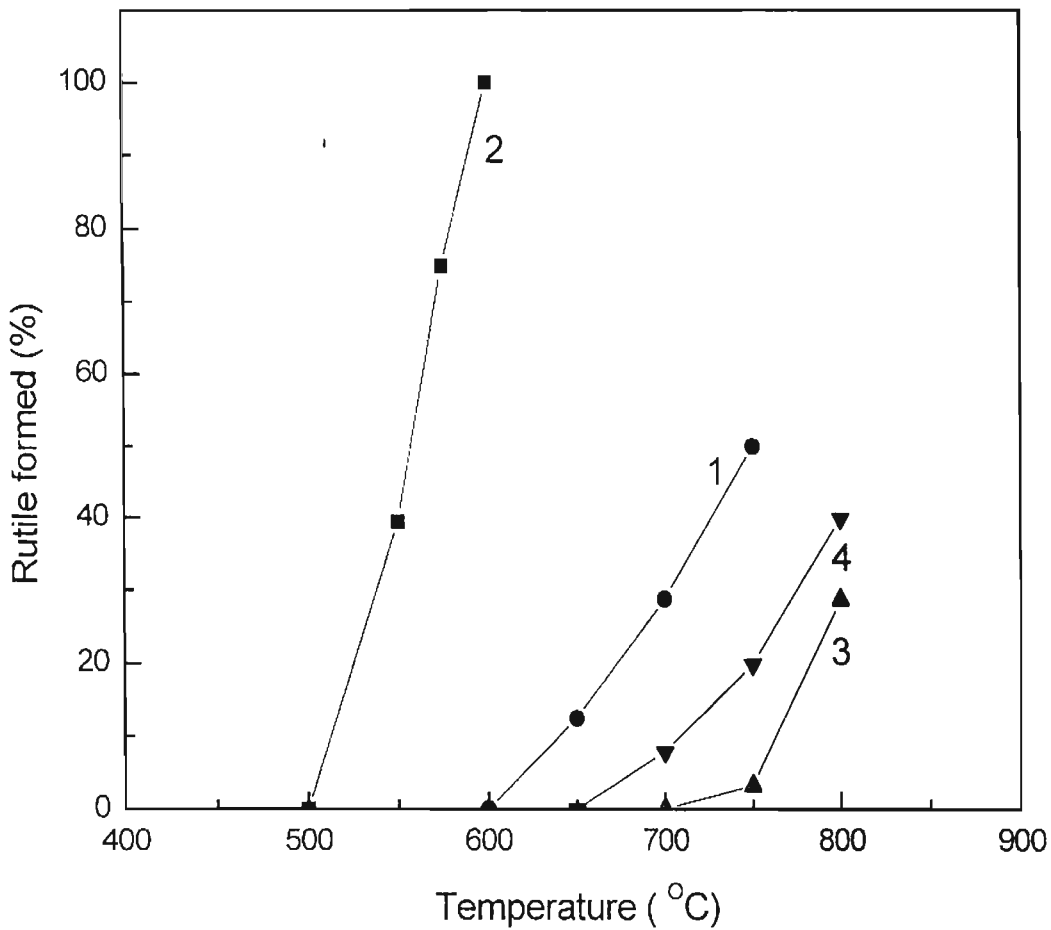
**Table.5.11: % of rutile formed in wet-impregnated  $\text{Cr}_2\text{O}_3$  doped  $\text{TiO}_2$  system during heating in hydrogen atmosphere for 2 hrs.**

Temperature $^{\circ}\text{C}$	Rutile formed.	
	5% $\text{Cr}_2\text{O}_3/\text{TiO}_2$	15% $\text{Cr}_2\text{O}_3/\text{TiO}_2$
700	0	7.8
750	3.2	19.8
800	28.6	39.8

Hence it is clear that in wet-impregnated samples rutilation started slowly as compared to co-precipitated which again confirms the importance of method of preparation on the phase transformation in  $\text{Cr}_2\text{O}_3$  doped  $\text{TiO}_2$ . The

variation of rutilation with temperature in  $\text{Cr}_2\text{O}_3$  doped  $\text{TiO}_2$  samples heated in hydrogen atmosphere is shown in figure.5.16.

**Figure.5.16: Variation of rutilation in  $\text{Cr}_2\text{O}_3/\text{TiO}_2$  samples heated in hydrogen atmosphere for 2 hrs at different temperature.**  
 1 - 5% $\text{Cr}_2\text{O}_3/\text{TiO}_2$ . 2 - 15% $\text{Cr}_2\text{O}_3/\text{TiO}_2$ . (Co-precipitated)  
 3 - 5% $\text{Cr}_2\text{O}_3/\text{TiO}_2$ . 4 - 15% $\text{Cr}_2\text{O}_3/\text{TiO}_2$ . (Wet-impregnated)



There occurs some lattice defects in the sample during the heat treatment, resulting in phase transformation. This clearly indicates that the role of  $\text{Cr}_2\text{O}_3$  is more important. This observation was seen in air and argon atmospheres also. Hence it can be concluded that the anatase to rutile transformation in  $\text{Cr}_2\text{O}_3$  doped

TiO<sub>2</sub> strongly depends on the concentration of dopants, method of preparation and the atmosphere of calcination.

## 5.6. Conclusions

The following conclusion can be arrived at from the results of the above investigations.

- ☐ In Cr<sub>2</sub>O<sub>3</sub> doped TiO<sub>2</sub> anatase-rutile transformation takes place at lower temperature as compared to pure TiO<sub>2</sub>.
- ☐ The onset and extent of phase transformation depend on the method of preparation of doped samples.
- ☐ On increasing the percentage of Cr<sub>2</sub>O<sub>3</sub> the transformation is increased in co-precipitated and wet-impregnated samples.
- ☐ The activation energy for the transformation is lowered much on doping TiO<sub>2</sub> with Cr<sub>2</sub>O<sub>3</sub>.
- ☐ Chromium titanate phase was formed during the heating of TiO<sub>2</sub> doped with Cr<sub>2</sub>O<sub>3</sub>.
- ☐ The percentage of Cr<sub>2</sub>O<sub>3</sub> and method of preparation play major role on surface area and crystallite size of TiO<sub>2</sub>.
- ☐ Crystallite size of anatase increases and surface area decreases markedly on Cr<sub>2</sub>O<sub>3</sub> loading and rutilation.
- ☐ Surface morphology of TiO<sub>2</sub> changes much while doping Cr<sub>2</sub>O<sub>3</sub> and also with rutilation.
- ☐ Atmosphere of calcination is very important in the anatase to rutile transformation in Cr<sub>2</sub>O<sub>3</sub> doped TiO<sub>2</sub>.
- ☐ Argon and hydrogen atmospheres are more accelerating than air.

## CHAPTER 6

### STUDIES ON CuO DOPED TiO<sub>2</sub>

Copper oxide supported on titania are profoundly important catalyst materials. In catalysis, catalytic properties are mostly affected by the phase modification of the supported titania. In order to understand the phase stability of titania on doping with different percentages of CuO, samples were prepared and studied and the results are discussed in this chapter.

Only a few methods are available in literature for preparing CuO doped TiO<sub>2</sub>. TiO<sub>2</sub> doped with 5 and 15% percentages of CuO was prepared using two different methods namely co-precipitation and wet-impregnation as described in Chapter 2. The transformations in air, inert (argon) and reducing (hydrogen) atmospheres were studied. The quantitative analysis of the phase compositions of the heated CuO/TiO<sub>2</sub> samples was done as follows.

#### 6.1. Chemical analysis

The composition of samples was determined by chemical analysis using standard procedures as described in chapter 2. The percentage of CuO in each sample is as given in Table 6.1.

Table 6.1: Results of Chemical analysis of CuO doped TiO<sub>2</sub> prepared through different methods.

Method of Preparation	Expected CuO(%)	Experimental Composition	
		CuO (%)	TiO <sub>2</sub> (%)
Co-precipitation	5	4.88	94.9
	15	14.92	84.88
Wet-Impregnation	5	4.91	94.8
	15	14.82	84.97

## 6.2 XRD studies

XRD analysis was done on the co-precipitated CuO doped samples calcined at different temperatures. Figure 6.1 gives the XRD pattern of 5% CuO doped and figure 6.2 shows the pattern of 15% doped samples heated in air.

Figure 6.1: XRD Patterns of co-precipitated 5% CuO/TiO<sub>2</sub> heated at different Temperatures for 6hrs (a) 750°C (b) 800°C (c) 850°C

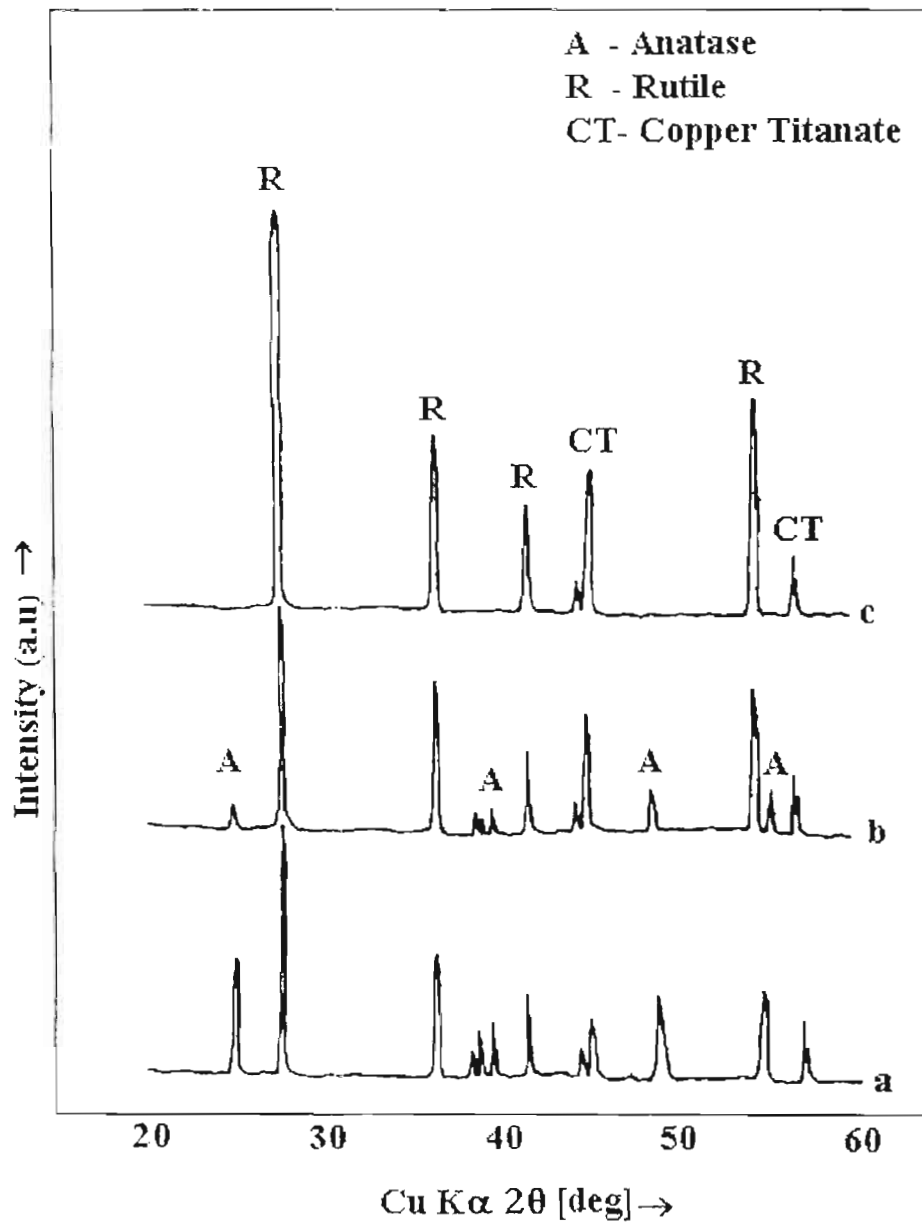
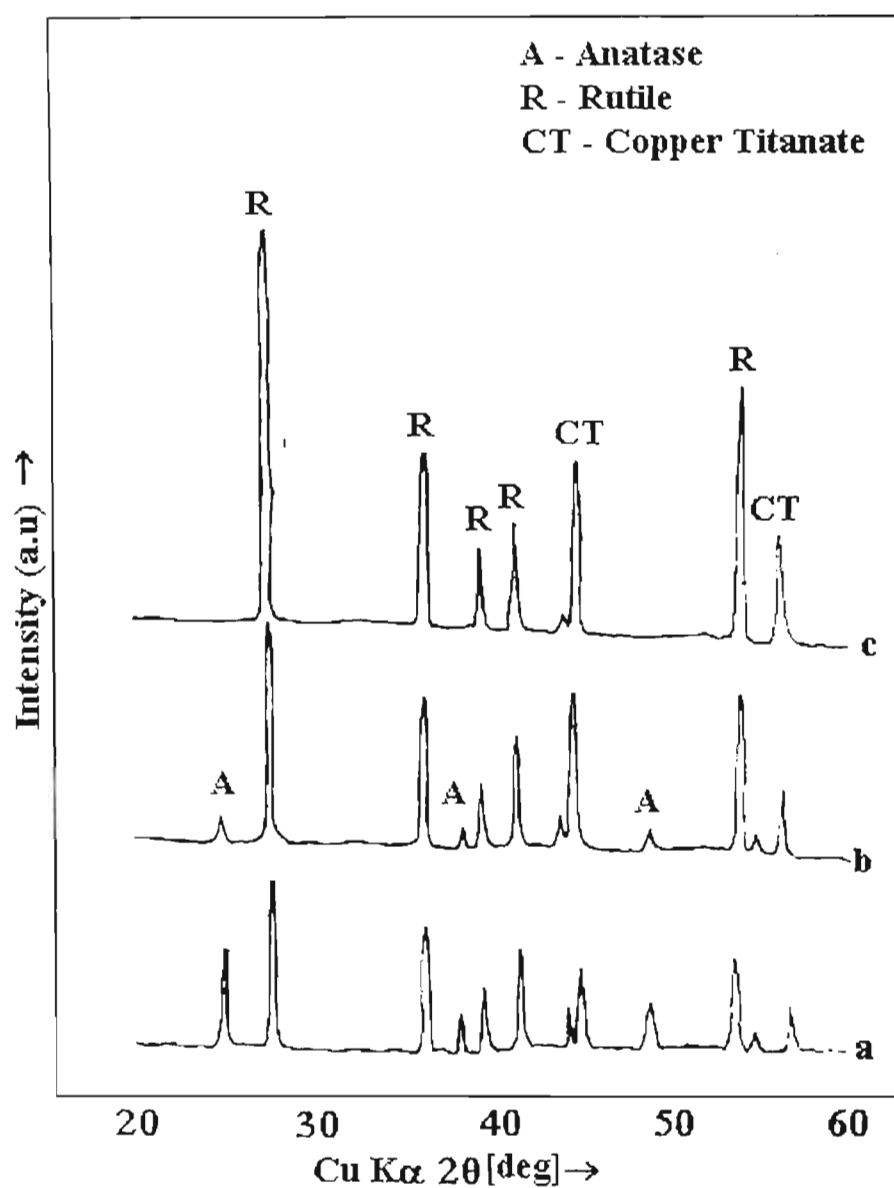




Figure 6.2: XRD Patterns of co-precipitated 15% CuO/TiO<sub>2</sub> heated at different temperatures for 6 hrs. (a) 700°C (b) 750°C (c) 800°C



It revealed that the amorphous nature of co-precipitated sample disappeared above 600°C and anatase phase appeared. At 750°C for 6 hrs heating, rutile phase emerges and 9.3% was formed for 6 hrs heating in 5%

CuO/TiO<sub>2</sub>. In the case of 15% doped samples, the rutile formation temperature was found to be 700°C and for 6 hrs heating 3.2 % rutile was present.

Peak intensities of anatase decreased during heating at higher temperatures in both 5 and 15% doped samples while the peak intensity for rutile was found to increase. This indicates the anatase rutile conversion during the calcinations. Also peaks corresponding to CuTiO<sub>3</sub> were observed above 700°C. Thus TiO<sub>2</sub> has reacted with CuO to form its titanate when the temperature is high enough. The various percentages of rutile formed in both the 5 and 15% doped samples are calculated and are tabulated in tables 6.2 and 6.3.

**Table 6.2: % of rutile formed during heating of co-precipitated 5% CuO/TiO<sub>2</sub> at different temperatures and time in air**

Time of heating (hrs)	Rutile formed (%)		
	750°C	800°C	850°C
1	1.6	9.8	25.7
2	3.2	18.8	44.8
3	4.7	26.8	59.1
4	6.3	34.2	69.5
5	7.8	40.6	77.3
6	9.3	46.5	83.2
7	10.7	51.7	87.5
8	12.2	56.5	90.7
9	13.6	60.8	93.1
10	15.2	64.7	94.8

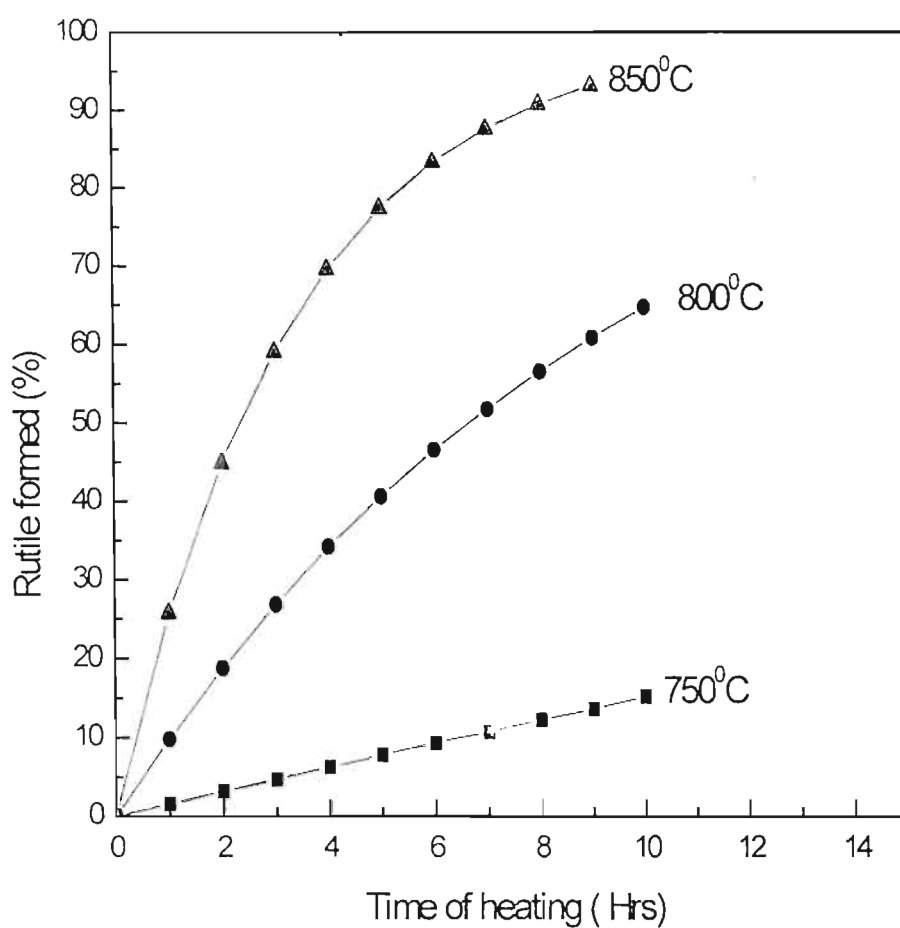
**Table 6.3: % of rutile formed during heating of co-precipitated 15% CuO/TiO<sub>2</sub> at different temperatures and time in air.**

Time of heating (hrs)	Rutile formed (%)		
	700 <sup>0</sup> C	750 <sup>0</sup> C	800 <sup>0</sup> C
1	0	12.8	56.2
2	0	24.1	80.8
3	1.5	33.8	91.6
4	2.1	42.3	96.3
5	2.5	49.7	97.4
6	3.2	56.2	99.3
7	3.9	61.8	100
8	4.8	66.7	100
9	7.9	71.2	100
10	10.8	74.8	100

The rutile percentage increased significantly in co-precipitated samples irrespective of the dopant concentration but the amount of rutile at a particular temperature and time depends on the amount of CuO present. At 800<sup>0</sup>C in 5% CuO doped sample, for 6 hrs heating 46.5% rutile was present and in 15% doped sample rutilation was complete at the same temperature and time. Onset of rutilation in 15% doped sample is 700<sup>0</sup>C, and at 750<sup>0</sup>C 8 hrs heating produced 66.7% rutile. At 850<sup>0</sup>C, the rutilation in 5% doped sample is 90.7% for 8 hrs heating.

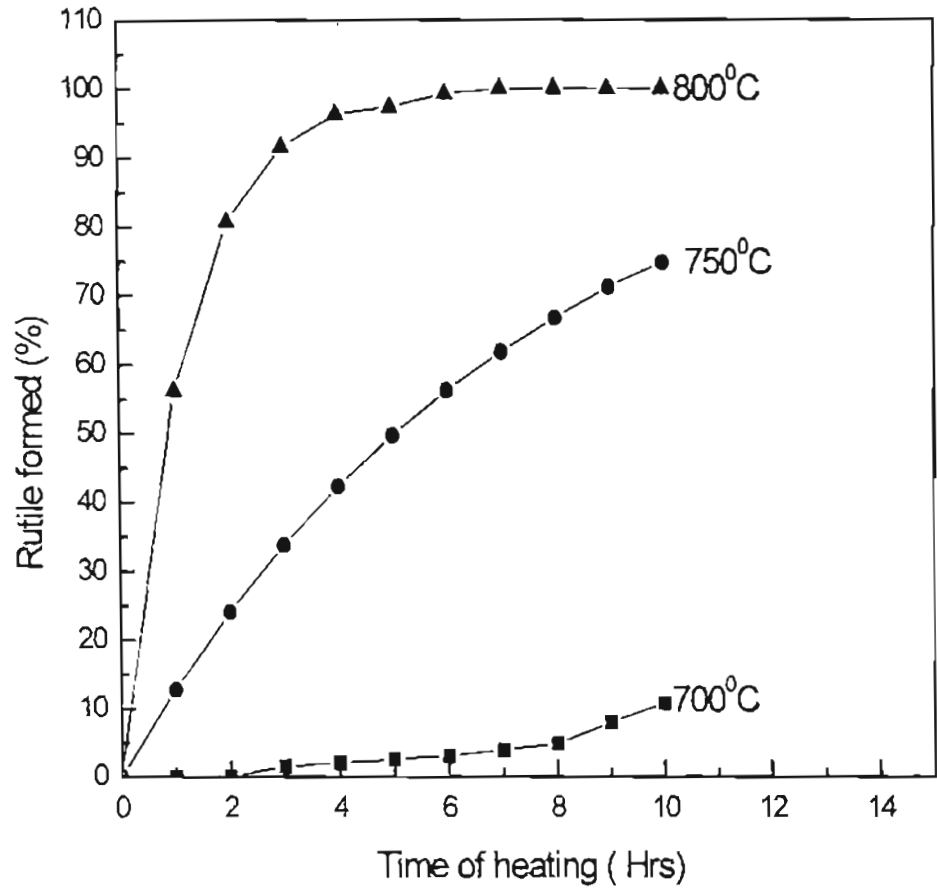
The variation in rutilation with time of heating at different temperatures are shown in figures 6.3 and 6.4.

Figure 6.3: Variation of rutile % with time at different temperatures in co-precipitated 5% CuO/TiO<sub>2</sub>.



At a particular temperature and time of heating, 15% CuO doped samples gave more rutile compared to 5%. Also the presence of CuO has marked influence on the anatase-rutile transformation in TiO<sub>2</sub> since in case of undoped TiO<sub>2</sub> there is no phase transformation on heating up to 900°C. At 1000°C, anatase peaks disappeared giving only rutile peaks indicating that rutilation was complete as evident from the patterns shown in figure 3.3 of chapter 3.

Figure 6.4: Variation of rutile % with time at different temperatures in co-precipitated 15% CuO/TiO<sub>2</sub>.

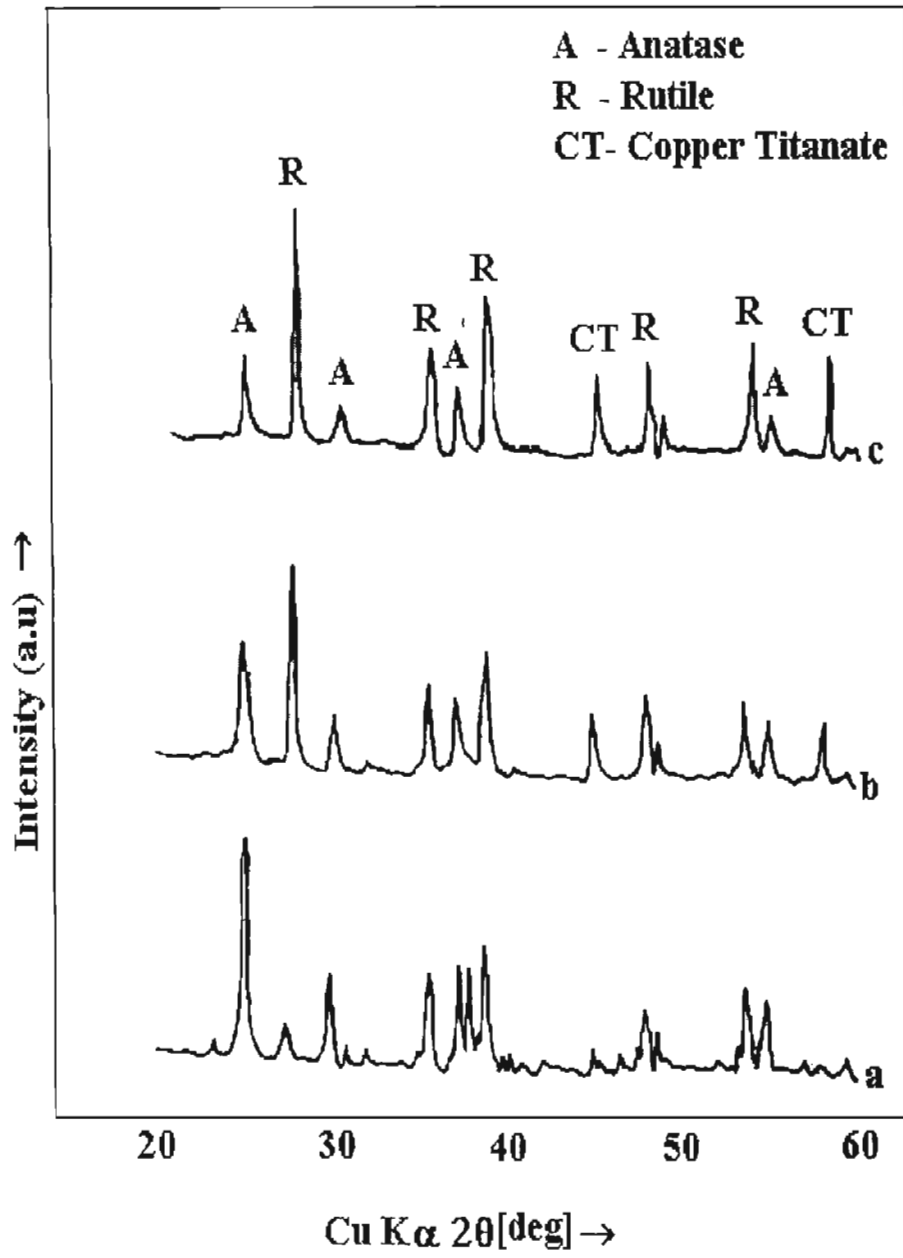


CuO has an influence on crystallization temperature of TiO<sub>2</sub> like other transition metal oxides. The onset temperature of rutilation was lowered by the presence of CuO in co-precipitated samples.

In wet-impregnated samples, the rutilation started at higher temperature compared to co-precipitated ones. This difference reveals that the method of preparation also influences the anatase to rutile transformation in CuO doped

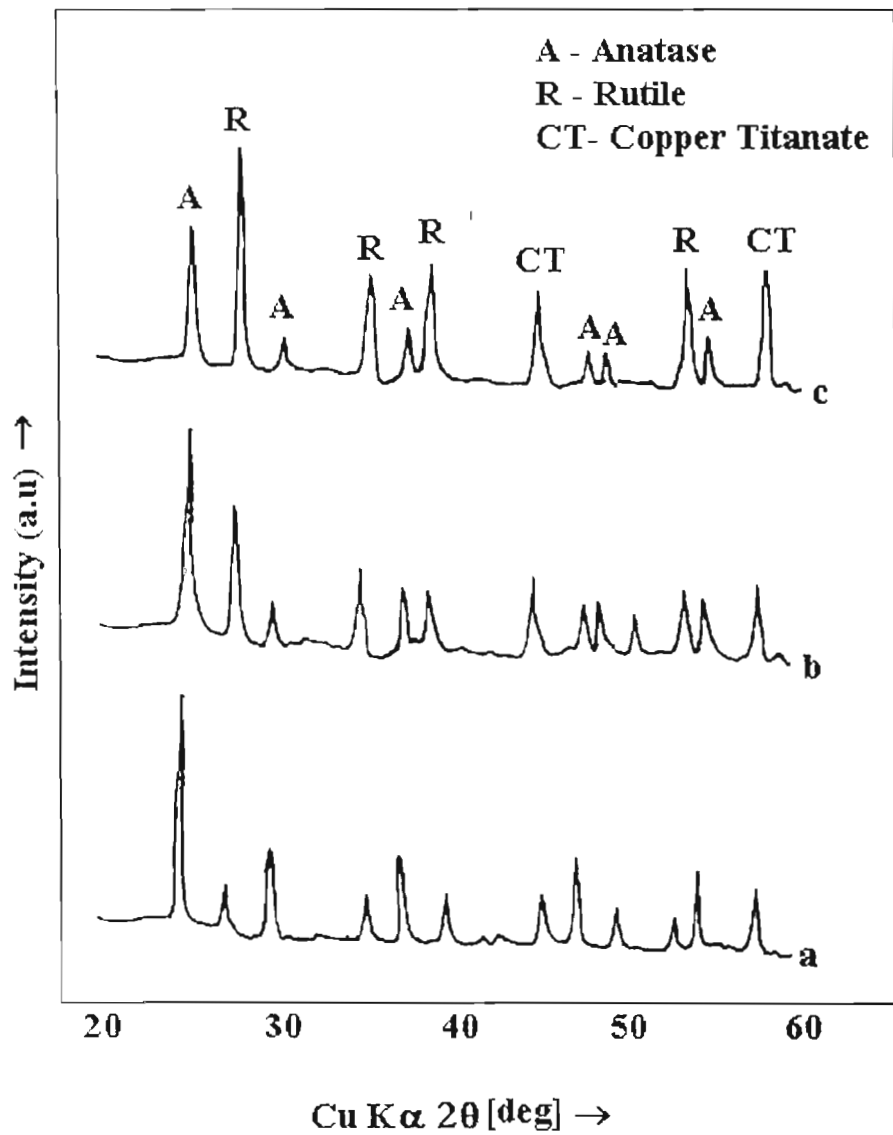
titania. XRD patterns of wet-impregnated 5 and 15% CuO doped TiO<sub>2</sub> heated at different temperatures are shown in figures 6.5 and 6.6.

Figure 6.5: XRD Patterns of wet-impregnated 5% CuO/TiO<sub>2</sub> heated at different temperatures. (a) 750°C (b) 800°C (c) 850°C



Rutilation in both 5 and 15% CuO doped TiO<sub>2</sub> wet-impregnated sample started at 750<sup>o</sup>C, and the rutilation was complete at 850<sup>o</sup>C. There is a rapid growth of rutile from anatase occurring in these samples.

Figure 6.6: XRD Patterns of wet-impregnated 15% CuO/TiO<sub>2</sub> heated at different temperatures for 6 hrs. (a) 750<sup>o</sup>C (b) 800<sup>o</sup>C (c) 850<sup>o</sup>C



Heating for 6hrs produced 5.9% rutile in 5% CuO doped TiO<sub>2</sub> and 11.9 % rutilation was present in 15% doped sample at 750<sup>0</sup>C. The different amounts of rutile formed in wet-impregnated CuO doped TiO<sub>2</sub> are tabulated in tables 6.4 and 6.5.

**Table.6.4: % of rutile formed during heating of wet-impregnated 5%CuO/TiO<sub>2</sub> at different temperatures and time.**

Time of heating (hrs)	Rutile formed (%)		
	750 <sup>0</sup> C	800 <sup>0</sup> C	850 <sup>0</sup> C
1	0	4.1	14.9
2	0	8.0	27.6
3	0	11.8	38.5
4	0	15.4	47.7
5	4.9	18.9	55.5
6	5.9	22.3	62.2
7	6.8	25.4	67.8
8	7.7	28.5	72.6
9	8.7	31.5	76.7
10	9.6	34.3	80.2

The rutilation in wet-impregnated 5% doped titania is different from that in 15% doped samples. The growth of rutile crystals is rapid after the onset of rutilation. Up to 750<sup>0</sup>C, the anatase phase is stable. When temperature is 850<sup>0</sup>C rutilation reaches 80% on 10 hrs heating. In the case of 15%, rutilation was almost complete at the same conditions.



The difference in behaviour of co-precipitated and wet-impregnated samples is due to the difference in distribution of CuO on TiO<sub>2</sub>, which is identified from the EDAX studies.

**Table.6.5: % of rutile formed during heating of wet-impregnated 15%CuO/TiO<sub>2</sub> at different temperatures and time**

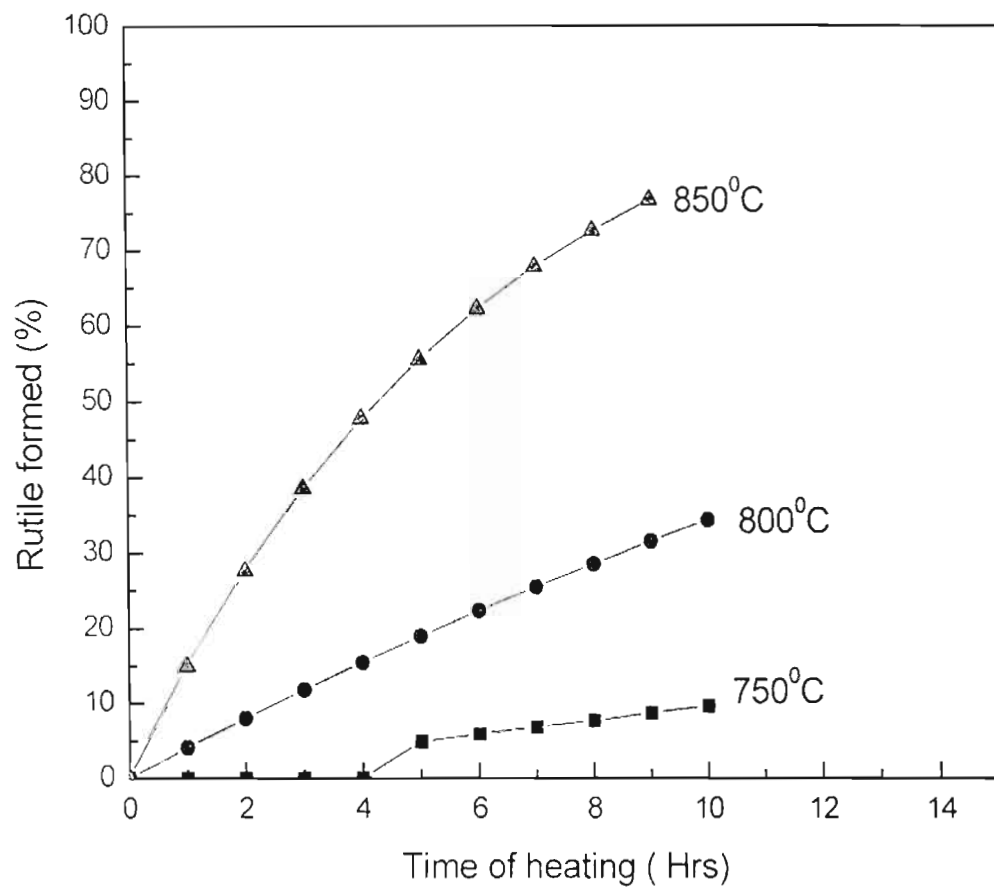
Time of heating (hrs)	Rutile formed (%)		
	750 <sup>o</sup> C	800 <sup>o</sup> C	850 <sup>o</sup> C
1	2.2	10.8	26.8
2	4.1	20.5	45.3
3	6.4	29.1	59.6
4	8.1	36.8	70.1
5	10.2	43.6	77.9
6	11.9	49.8	83.7
7	13.7	55.2	87.9
8	15.5	60.1	91.2
9	17.3	64.4	93.4
10	19.7	68.2	97.9

The variation in rutilation of co-precipitated and wet-impregnated CuO doped TiO<sub>2</sub> samples at different temperatures with time of heating are shown in figures 6.7 and 6.8.

At higher temperature, the peak for CuTiO<sub>3</sub> appeared, which shows that there is reaction between TiO<sub>2</sub> and CuO at higher temperatures. Hence it can be concluded that, CuO has noticeable effect on rutile phase formation in TiO<sub>2</sub>

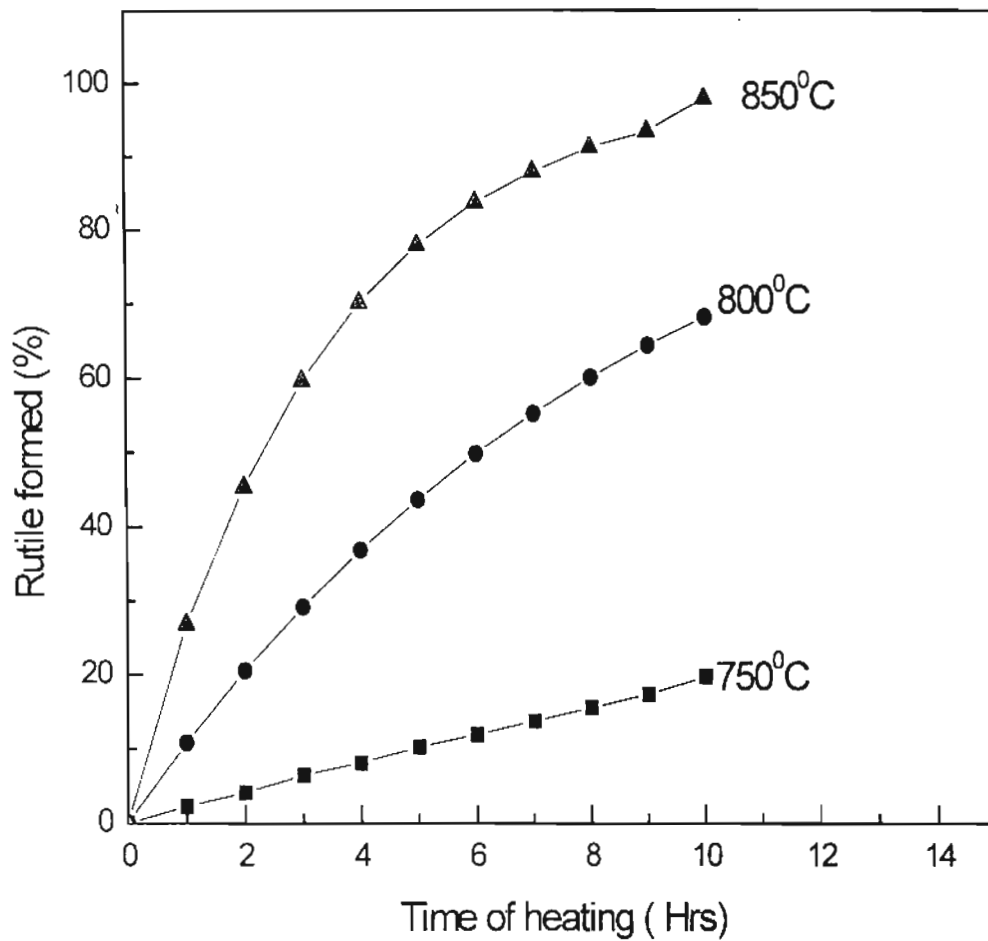
and the enhancement of rutilation by the metal oxide is strongly dependent on how the sample was prepared and the amount of the doped metal oxide.

Figure 6.7: Variation of rutile % with time at different temperatures in wet-impregnated 5% CuO/TiO<sub>2</sub>



In both samples rutilation increases with temperature and this crystallographic rearrangement is highly decided by the method of preparation and also the amount of CuO present in the doped samples.

Figure 6.8: Variation of rutile % with time at different temperatures in wet-impregnated 15% CuO/TiO<sub>2</sub>



The activation energy for the anatase-rutile transformation was calculated and is given in table 6.6. The activation energy calculated for the transformation in co-precipitated samples in presence of 5% CuO is found to be 33.93 k cal/mol while in presence of 15% CuO it is 30.59 k cal / mol. In

case of wet-impregnated samples the activation energy for the transformation was found to be 38.95 in presence of 5% CuO while in presence of 15% it is 33.22 kcal/mol. For undoped TiO<sub>2</sub>, activation energy for anatase-rutile transformation was reported to be ~90 K cal/mol as explained in the previous chapters. Here also among 5 & 15% CuO 15% has more lowering of activation energy and hence it is more accelerating. Also it is observed that the activation energy for the transformation was found to be very close to each other in co-precipitated 5% CuO/TiO<sub>2</sub> and wet-impregnated 15% CuO/TiO<sub>2</sub>.

Table 6.6: Activation energies for the anatase-rutile transformation in CuO doped TiO<sub>2</sub>.

Method of Preparation	CuO (%)	Activation energy K cal/mol
Co-precipitation	5	33.93
	15	30.59
Wet-Impregnation	5	38.95
	15	33.22

Table 6.7 shows the crystallite size of anatase present in the CuO doped TiO<sub>2</sub> samples at different calcination temperatures, Marked change was seen on increasing the CuO percentage, but it increased with increase in temperature. When the rutilation was started, the crystallite size of anatase attained a size of 11.6 nm in 5% doped co-precipitated samples and 2.39 nm in wet-impregnated ones. Hence, depending on the method of preparation, the crystallite size may vary and the growth in crystallite size with temperature is also determined by method of preparation. The crystallite size increased with rutilation and amount of CuO.

Table 6.7: Crystallite size and surface area values of un doped and CuO doped TiO<sub>2</sub> Samples heated at different temperatures for 8 hrs.

Sample	Heating Temperature (°C)	Surface area (m <sup>2</sup> /g)	Crystallite size of anatase (nm)
Undoped TiO <sub>2</sub>	110	162.58	a*
	300	109.59	a*
	700	27.2	4.8
	900	9.13	14.2
	1000	2.54	b*
Co-precipitated 5% CuO/TiO <sub>2</sub>	110	112.3	a*
	750	4.93	11.6
	850	1.34	17.76
Co-precipitated 15% CuO/TiO <sub>2</sub>	110	132.2	a*
	750	6.09	4.33
	850	0.092	31.54
Wet-impregnated 5% CuO/TiO <sub>2</sub>	110	92.7	a*
	750	12.3	2.39
	850	5.7	10.7
Wet-impregnated 15% CuO/TiO <sub>2</sub>	110	119.7	a*
	750	5.5	9.87
	850	2.77	15.3

\* a- Amorphous TiO<sub>2</sub> \* b- Anatase phase absent

### 6.3 Surface area studies

Surface area changes with percentage of CuO and calcination temperature. The surface area obtained for co-precipitated 5% CuO/TiO<sub>2</sub> was 112.3 m<sup>2</sup>/g, and for 15% doped sample it was 132.2 m<sup>2</sup>/g before calcination. In the case of wet-impregnated ones, the surface area was 92.7 m<sup>2</sup>/g and 119.7 m<sup>2</sup>/g in 5 and 15% CuO/TiO<sub>2</sub> samples respectively before heating.

Like other samples, here also, co-precipitated ones have much higher surface area. Out of all the samples, maximum surface area was obtained in sample containing 15% CuO before heating. The surface area decreased on rutilation in co-precipitated and wet-impregnated ones as in the case of other samples discussed in earlier Chapters.

Here also a sudden decrease in surface area was observed in co-precipitated and in wet-impregnated samples calcined at 850<sup>0</sup>C due to the onset of rutilation and titania particle enlargement. The crystallite size results are also in parallel with these observations. At temperatures when the TiO<sub>2</sub> was almost fully converted to rutile, the surface area became 1.34 m<sup>2</sup>/g, and 5.7 m<sup>2</sup>/g in 5% doped co-precipitated and wet-impregnated samples. In case of 15% doped samples, the surface area values are 0.092 m<sup>2</sup>/g, and 2.77 m<sup>2</sup>/g in co-precipitated and wet-impregnated samples respectively. The decrease in surface area was more severe in co-precipitated ones. So, like other samples discussed earlier, the method of preparation and percentage of CuO have a greater role in deciding the surface area of these samples. So, it is very clear that, CuO enlarges titania particle, which would occur on high temperature calcination. Formation of copper titanate also may be one reason.

#### 6.4 Scanning Electron Microscopic studies.

To understand the morphological changes of the titania doped with CuO. Scanning Electron Microscopic studies on the samples were performed. Scanning Electron Micrographs of undoped TiO<sub>2</sub> before heating (containing anatase) and after heating at 1000<sup>0</sup>C for 8 hrs (containing rutile) are shown in figure 3.9 of chapter 3. Titania particles were found to be aggregated in the pure form (anatase). On heating at 1000<sup>0</sup>C for 8 hrs, some rearrangement occurred to form rutile. During this conversion, the aggregates of particles were converted into agglomerates where the particles were rigidly joined. Also there was no appreciable change in the particle size during the conversion in undoped TiO<sub>2</sub>.

The surface of both anatase and rutile samples were found to be rough before doping. Micrographs of CuO doped TiO<sub>2</sub> prepared by co-precipitation and wet-impregnation are shown in figures 6.9 and 6.10. It was found that in wet-impregnated sample increase in particle size takes place on rutilation. before rutilation, the average particle size is about 2 $\mu$ m while after rutilation most of the particles are of more than 150  $\mu$ m size. The surface morphology also changes considerably. The surface becomes more or less smooth after rutilation. Morphology of co-precipitated sample is more or less same before and after heat treatment. The particle size is higher than that of wet-impregnated samples before rutilation. There is increase in particle size during the anatase rutile transformation.

Thus the surface morphology of CuO doped TiO<sub>2</sub> has some changes with rutilation. The distribution of CuO is uniform in co-precipitated samples and not in wet-impregnated system. This is identified from the EDAX analysis. This is the reason for lower rutilation in wet-impregnated system. Hence it is

clear that there occurs some rearrangement in  $\text{TiO}_2$  lattice. There is a crystallite size enlargement occurring on doping  $\text{CuO}$ , which reflects in lower surface area of the  $\text{CuO}$  doped sample. This process depends on the method of preparation of doped samples.

Figure: 6.9. Scanning Electron Micrographs of co-precipitated  $\text{CuO}/\text{TiO}_2$   
(a) Before rutilation (b) after rutilation.

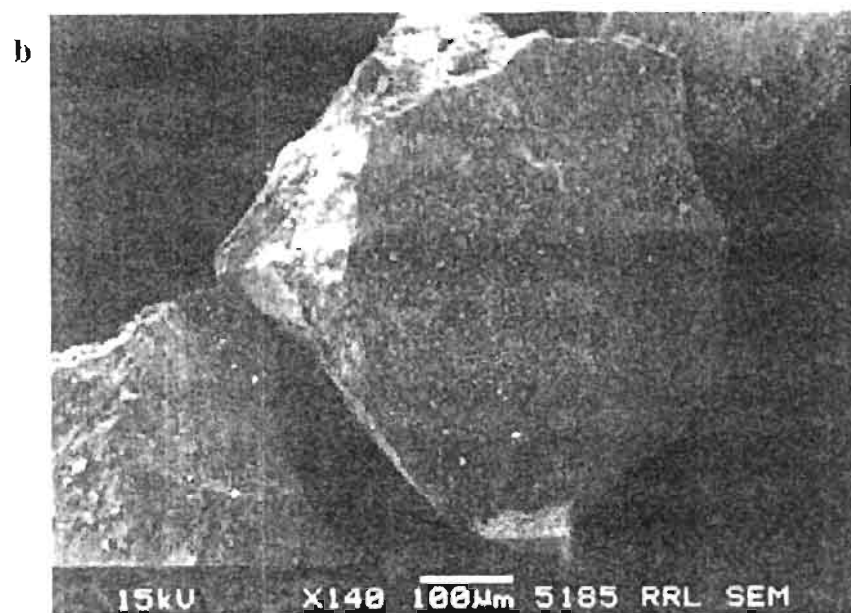
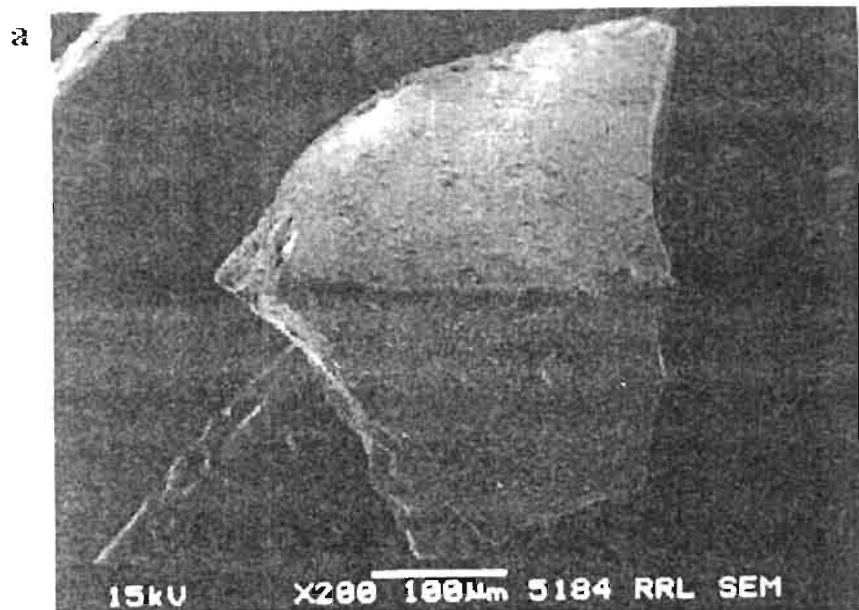
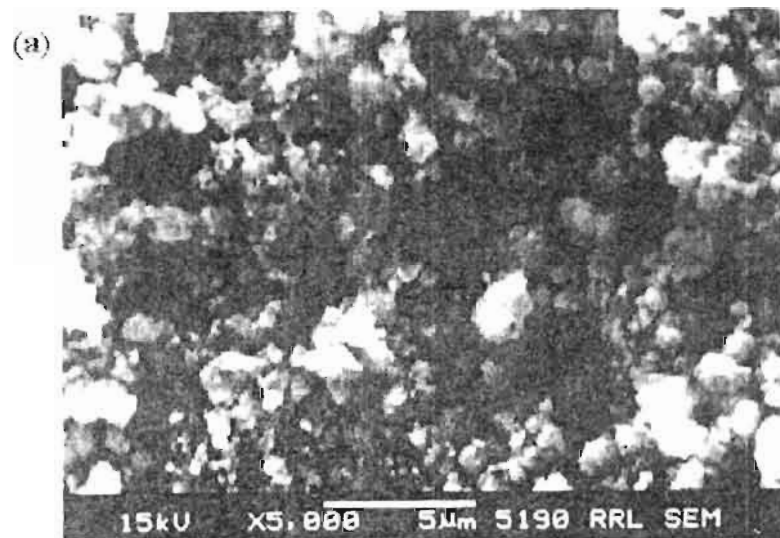




Figure: 6.10. Scanning Electron Micrographs of wet-impregnated  $\text{CuO}/\text{TiO}_2$   
(a) Before rutilation (b) After rutilation.

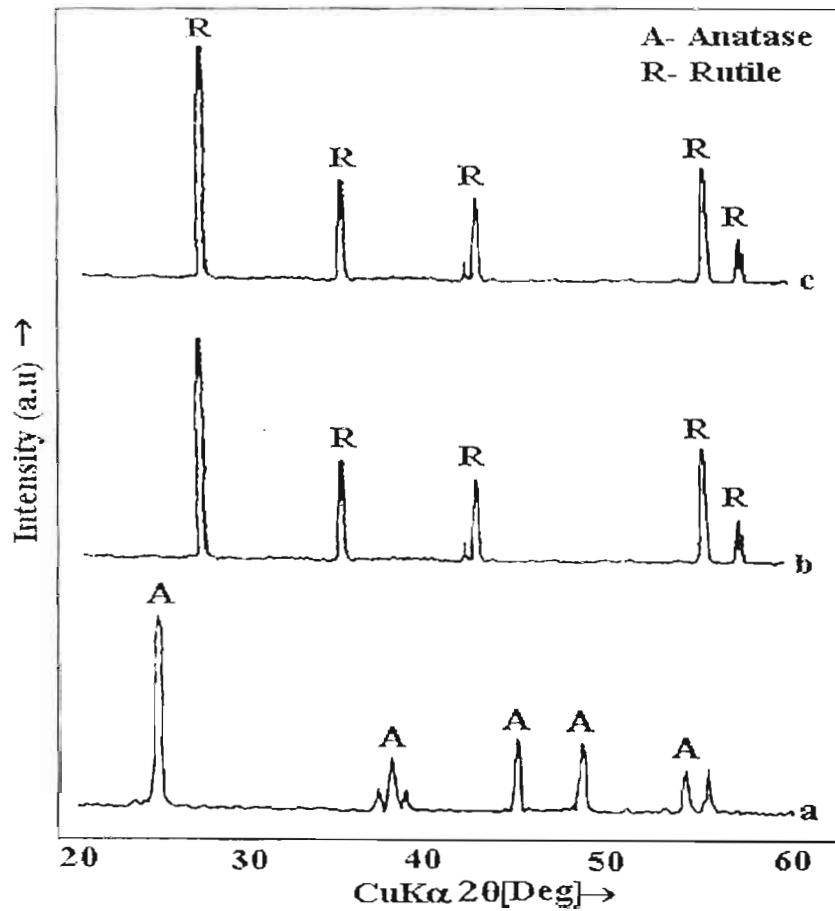


### 6.5 Transformation in Argon and Hydrogen atmospheres.

The anatase rutile transformation of CuO doped TiO<sub>2</sub> in different atmospheres were studied to understand the effect of different reaction atmospheres on the anatase rutile transformation. Argon (inert) and hydrogen (reducing) atmospheres are used in the investigations.

Figure.6.11. represents the XRD patterns of CuO doped TiO<sub>2</sub> heated in argon atmosphere at 700<sup>o</sup>C for 0.5 hrs. The anatase-rutile conversion was found to be different in argon compared to that in air.

Figure.6.11: XRD Patterns of co-precipitated CuO doped TiO<sub>2</sub> samples heated in argon atmosphere at 700<sup>o</sup>/ 0.5 hrs.  
(a) Undoped TiO<sub>2</sub> (b) 5% CuO/TiO<sub>2</sub> (c) 15% CuO/TiO<sub>2</sub>



In presence of argon atmosphere, the onset of rutilation was lowered and at 650<sup>0</sup>C in co-precipitated CuO/TiO<sub>2</sub>, the fraction of rutile formed is 39.8 % in 5% CuO doped TiO<sub>2</sub> for 0.5 hrs. In air atmosphere at the same conditions, no rutile was formed. In 15% doped sample, the rutile conversion was 54.8% at the same conditions. In both samples 700<sup>0</sup>/0.5hrs heating results in completion of rutilation in argon atmosphere. Thus the anatase rutile conversion is different in argon than that in air atmosphere. In air at 750<sup>0</sup>C, the rutilation was just started in 5% CuO/TiO<sub>2</sub> and in 15% doped sample it occurred at 700<sup>0</sup>C. The percentages of rutile formed in co-precipitated 5 and 15% CuO doped TiO<sub>2</sub> at different temperatures are tabulated in Table.6.8.

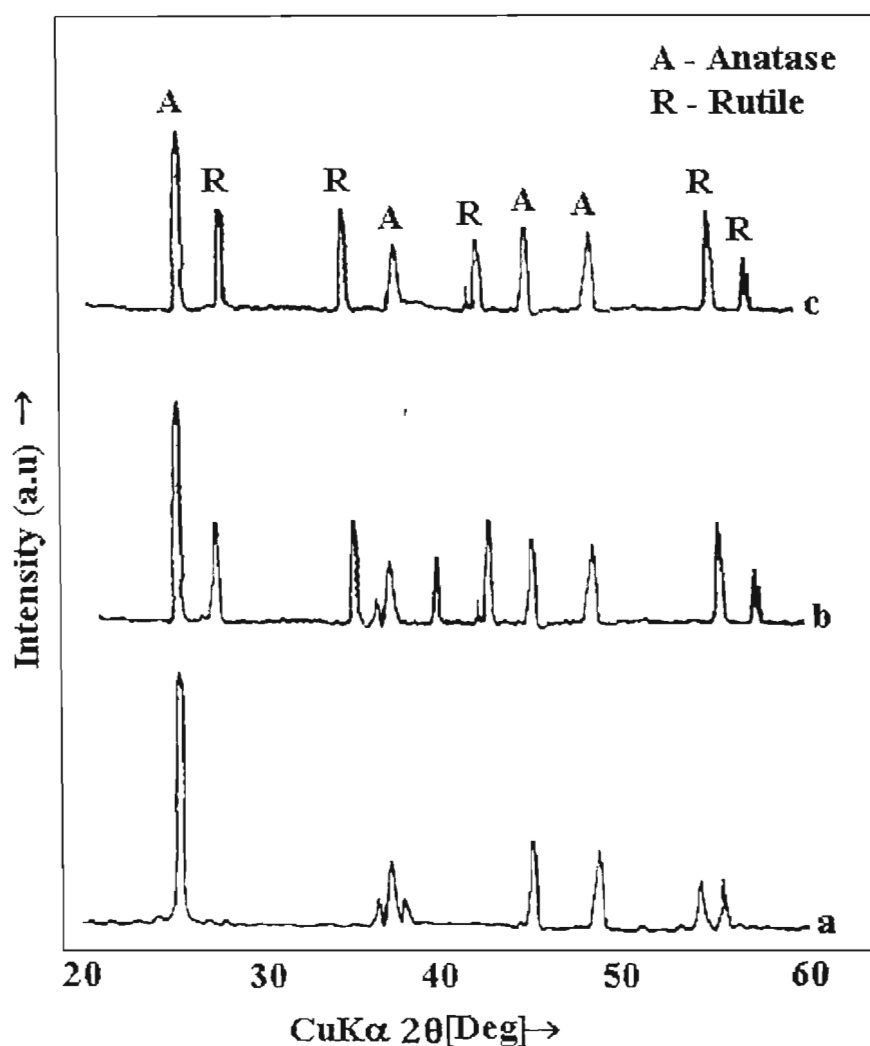
**Table.6.8: % of rutile formed in co-precipitated CuO doped TiO<sub>2</sub> samples heated in argon atmosphere at different temperatures for 0.5 hrs heating.**

Temperature ( <sup>0</sup> C)	Rutile formed (%)	
	5% CuO/TiO <sub>2</sub>	15% CuO/TiO <sub>2</sub>
650	39.8	54.8
675	74.6	88.7
700	100	100

The extent of acceleration is different in this case as compared to air. The amount of rutile formed is higher at any temperature for 15% sample as compared to 5% doped samples as evident from the table 6.8.

In wet-impregnated samples on set of rutilation is at around 650<sup>0</sup>C, 5% CuO doped TiO<sub>2</sub> sample gave 12.3% rutile while 15% doped sample produced 31.8% at the same temperature. The XRD patterns are shown in figure 6.12.

Figure.6.12: XRD Patterns of wet-impregnated CuO doped TiO<sub>2</sub> samples heated in argon atmosphere for 0.5 hrs.  
 (a)Undoped TiO<sub>2</sub> (b) 5% CuO/TiO<sub>2</sub> (c) 15% CuO/TiO<sub>2</sub>



The effect of temperature is same as that in co-precipitated one except that rutilation was not completed at 700<sup>0</sup>C for wet-impregnated samples. At 750<sup>0</sup>C, rutilation was 78.3 and 81.3% in 5 and 15% doped samples respectively. Different amounts of rutile formed in wet-impregnated samples heated in argon atmosphere are summarized in table 6.9.

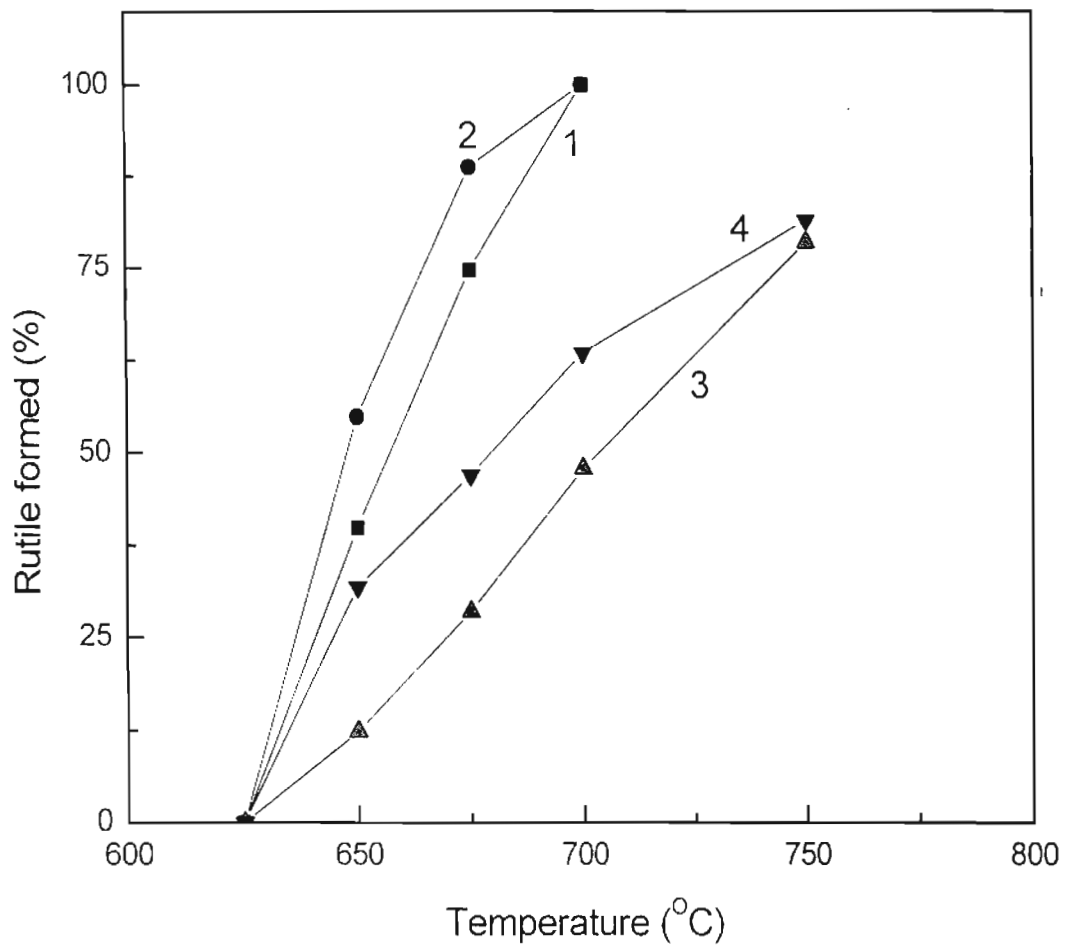
**Table.6.9: % of rutile formed in wet-impregnated CuO doped TiO<sub>2</sub> samples heated in argon atmosphere at different temperatures for 0.5 hrs.**

Temperature (°C)	Rutile formed	
	5% CuO/TiO <sub>2</sub>	15% CuO/TiO <sub>2</sub>
650	12.3	31.8
675	28.4	46.9
700	47.8	63.4
750	78.3	81.3

The variation of rutilation during heating in argon atmosphere in CuO/TiO<sub>2</sub> samples is evident in figure 6.13. Here the transformation is accelerated but the extent of acceleration strongly depends on the method of preparation. The lower distribution in wet-impregnated samples may be the cause for the variation in transformation.

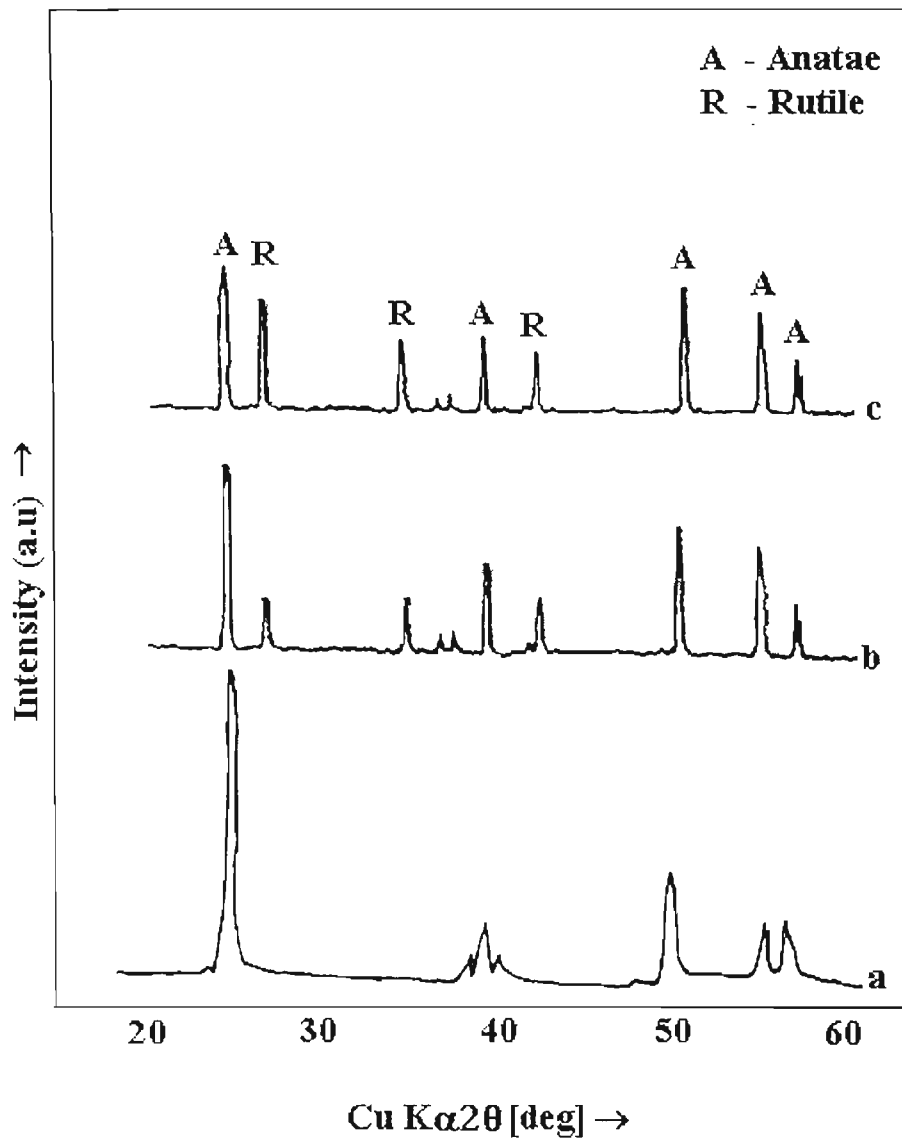
Here also the importance of oxygen vacancies on the phase transformation rate of TiO<sub>2</sub> in the presence of CuO seems to be confirmed by a more rapid transformation in argon than in air. Hence it can be concluded that argon atmosphere increases oxygen vacancies concentration and thus it favours the anatase-rutile transformation.

Figure.6.13: Variation of rutilation in CuO/TiO<sub>2</sub> samples heated in argon atmosphere for 0.5 hrs at different temperatures.  
 1 - 5%CuO/TiO<sub>2</sub>, 2 - 15%CuO/TiO<sub>2</sub> (Co-precipitated)  
 3 - 5%CuO/TiO<sub>2</sub>, 4 - 15%CuO/TiO<sub>2</sub> (Wet-impregnated)



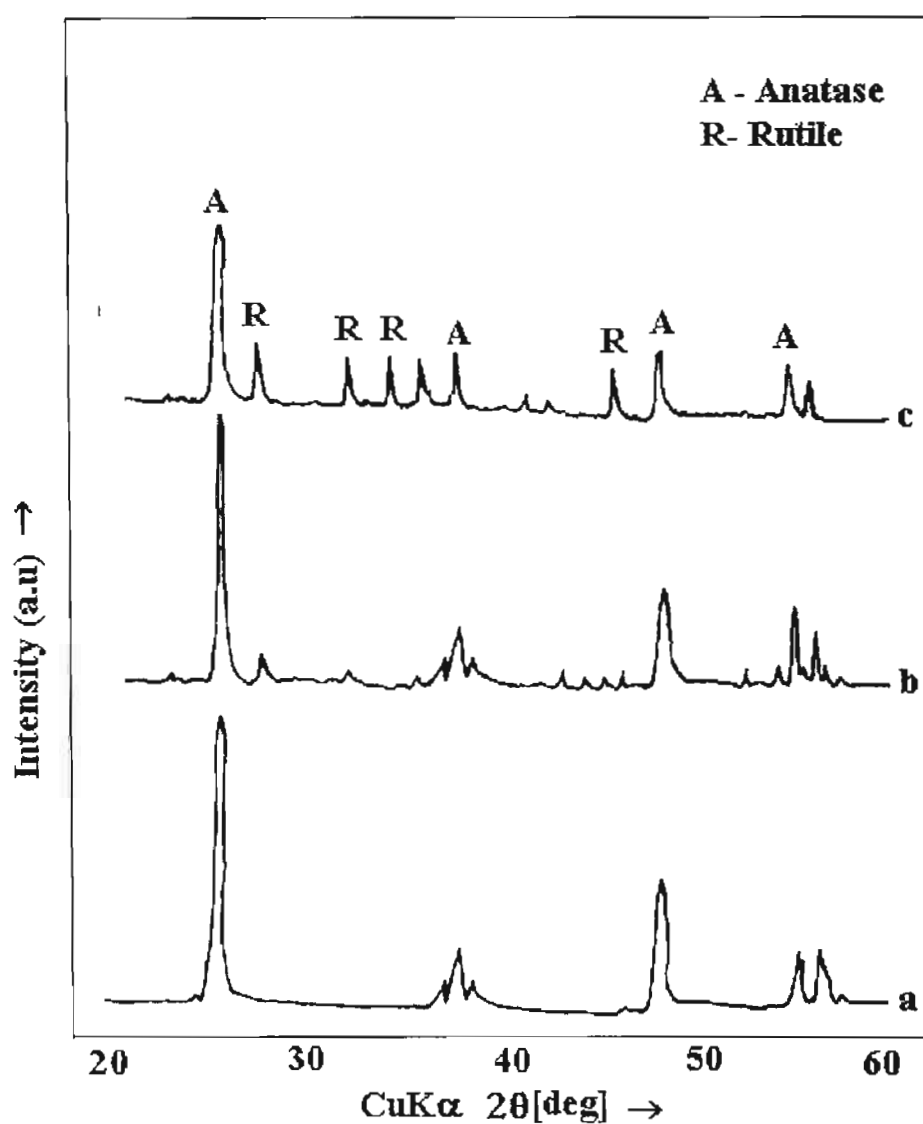
In hydrogen atmosphere, the anatase-rutile transformation was found to be low as compared to that in argon atmosphere. The XRD patterns of co-precipitated and wet-impregnated samples are given in figures 6.14 and 6.15.

Figure.6.14: XRD Patterns of co-precipitated CuO/TiO<sub>2</sub> samples heated in hydrogen atmosphere at 700<sup>o</sup>/2hrs.  
 (a) Undoped TiO<sub>2</sub> (b) 5% CuO/TiO<sub>2</sub> (c) 15% CuO/TiO<sub>2</sub>



In co-precipitated samples, it is observed that on set of rutilation is 700<sup>o</sup>C for 2 hrs heating. In wet-impregnated sample also rutilation was started at this temperature. This is higher temperature than that in argon atmosphere.

Figure.6.15: XRD Patterns of wet-impregnated CuO doped  $\text{TiO}_2$  samples heated in hydrogen atmosphere at  $700^\circ/2\text{hrs}$ .  
 (a) Undoped  $\text{TiO}_2$  (b) 5%  $\text{CuO}/\text{TiO}_2$  (c) 15%  $\text{CuO}/\text{TiO}_2$



The co-precipitated 5% doped samples gave 17.4 % rutile at  $700^\circ\text{C}$  and 29.8% rutilation was found in 15% doped sample for 2 hrs heating at the same temperature. At the same conditions, in wet- impregnated samples 4.3 and 12.8 % rutilation was found in 5 and 15%  $\text{CuO}$  doped  $\text{TiO}_2$  respectively. Tables



6.10 and 6.11 represent the different fractions of rutile formed in co-precipitated and wet-impregnated systems.

**Table.6.10: % of rutile formed in co-precipitated CuO doped TiO<sub>2</sub> system during heating in hydrogen atmosphere for 2 hrs.**

Temperature °C	Rutile formed (%)	
	5% CuO/TiO <sub>2</sub>	15% CuO/TiO <sub>2</sub>
650	0	0
700	17.4	29.8
725	36.6	53.7
750	49.3	65.8

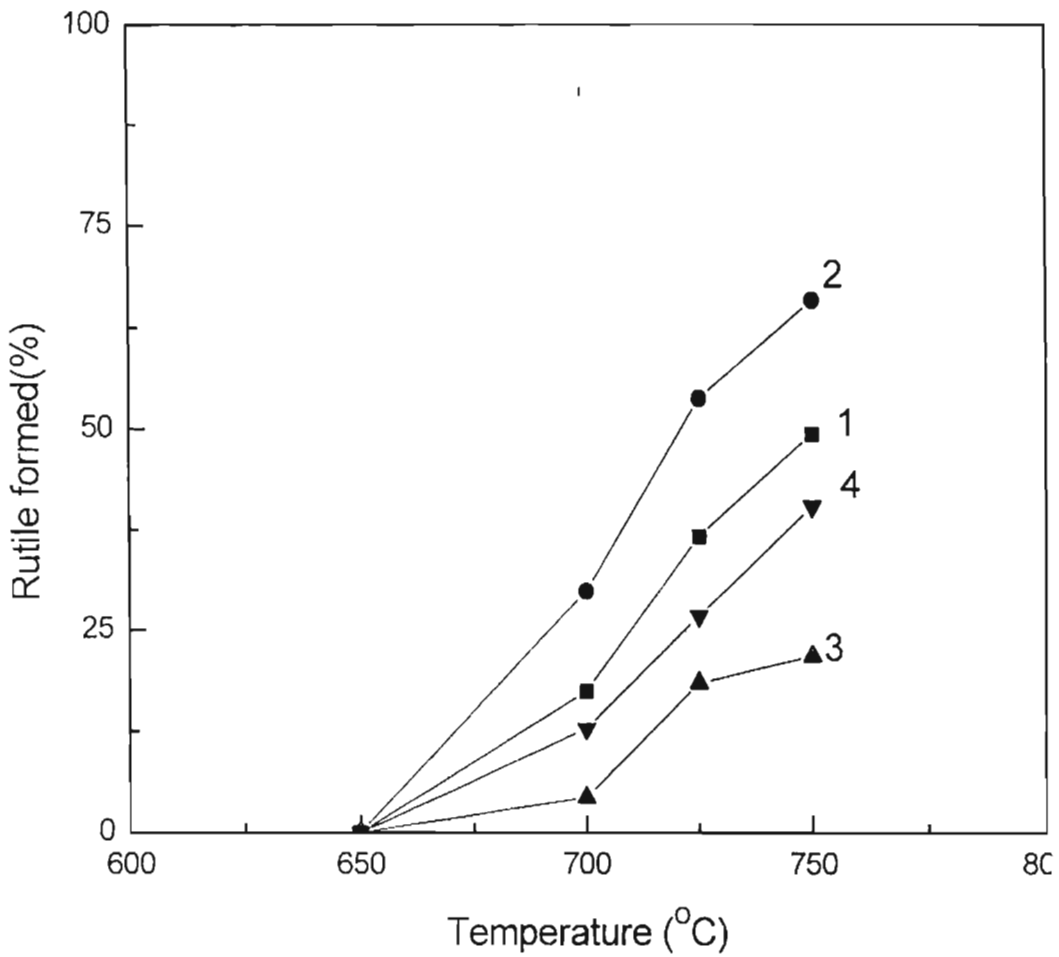
**Table.6.11: % of rutile formed in wet-impregnated CuO doped TiO<sub>2</sub> system during heating in hydrogen atmosphere for 2 hrs.**

Temperature °C	Rutile formed (%)	
	5% CuO/TiO <sub>2</sub>	15% CuO/TiO <sub>2</sub>
650	0	0
700	4.3	12.8
725	18.4	26.7
750	21.7	40.3

Eventhough in both the samples rutilation started at the same temperature in hydrogen atmosphere, the amount of conversion is different. At 750°C, 49.3% rutile is formed in co-precipitated 5% CuO doped TiO<sub>2</sub> sample while in 15% doped samples the rutile conversion was 65.8 for 2 hrs heating.

In case of wet-impregnated 5% CuO doped  $\text{TiO}_2$  sample rutilation was 21.7 % while in 15% doped samples it was 40.3% at the same conditions. Variation in rutilation with temperature in CuO/ $\text{TiO}_2$  samples heated in hydrogen atmosphere is shown in figure 6.16.

**Figure.6.16: Variation in rutilation of CuO doped  $\text{TiO}_2$  samples heated in Hydrogen atmosphere for 2 hrs at different temperatures.**  
 1 - 5%CuO/ $\text{TiO}_2$  2 - 15%CuO/ $\text{TiO}_2$  (Co-precipitated)  
 3 - 5%CuO/ $\text{TiO}_2$  4 - 15%CuO/ $\text{TiO}_2$  (Wet-impregnated)



Therefore it can be believed that there is some lattice defects in the samples during the heat treatment in reducing or inert atmospheres. This is experienced as colour changes of the samples. The intensity of colour depends on the

amount of dopant. Reduction of the oxides also may be taking place which also may be reason for colour change. This confirms the effect of concentration of CuO is more important in the phase transformation. This is observed in air and argon atmosphere also. Hence it can be concluded that the anatase –rutile transformation in CuO doped TiO<sub>2</sub> strongly depends on the concentration of dopants, method of preparation and the atmosphere of calcination.

## 6.6 Conclusions

The following are the conclusions made out of the above studies.

- ☐ Anatase to rutile transformation temperature is lowered, much on doping TiO<sub>2</sub> with CuO.
- ☐ The method of preparation, percentage of CuO and calcination temperature have marked effect on rutilation.
- ☐ CuTiO<sub>3</sub> phase is formed during heating in air.
- ☐ CuTiO<sub>3</sub> formation is independent of rutilation and depends only on the temperature.
- ☐ On loading CuO noticeable change in surface area and crystallization temperature were observed with rutilation.
- ☐ Surface area of CuO doped TiO<sub>2</sub> is decided by the amount of CuO and method of preparation of doped sample.
- ☐ Crystallite size of anatase increases on loading CuO and during rutilation.
- ☐ Surface morphology of titania doped with CuO is changed on heating.
- ☐ Argon atmosphere has more accelerating effect than hydrogen and air.

## CHAPTER 7

### STUDIES ON MnO<sub>2</sub> DOPED TiO<sub>2</sub>

In this Chapter studies on the effect of preparation method on rutilation and other properties like surface area changes, crystallite size variation and morphological changes are presented. In order to study the effect of amount of MnO<sub>2</sub> and reaction atmospheres TiO<sub>2</sub> doped with different percentages of MnO<sub>2</sub> was prepared using two methods, as described in Chapter 2. The transformation was studied in air, argon and hydrogen atmospheres as a function of temperature and time using XRD, Surface area measurements and SEM.

#### 7.1. Chemical analysis

The composition of MnO<sub>2</sub> doped TiO<sub>2</sub> samples was determined by chemical analysis using standard procedures as described in chapter 2. The percentage of MnO<sub>2</sub> in each sample is as given in Table 7.1.

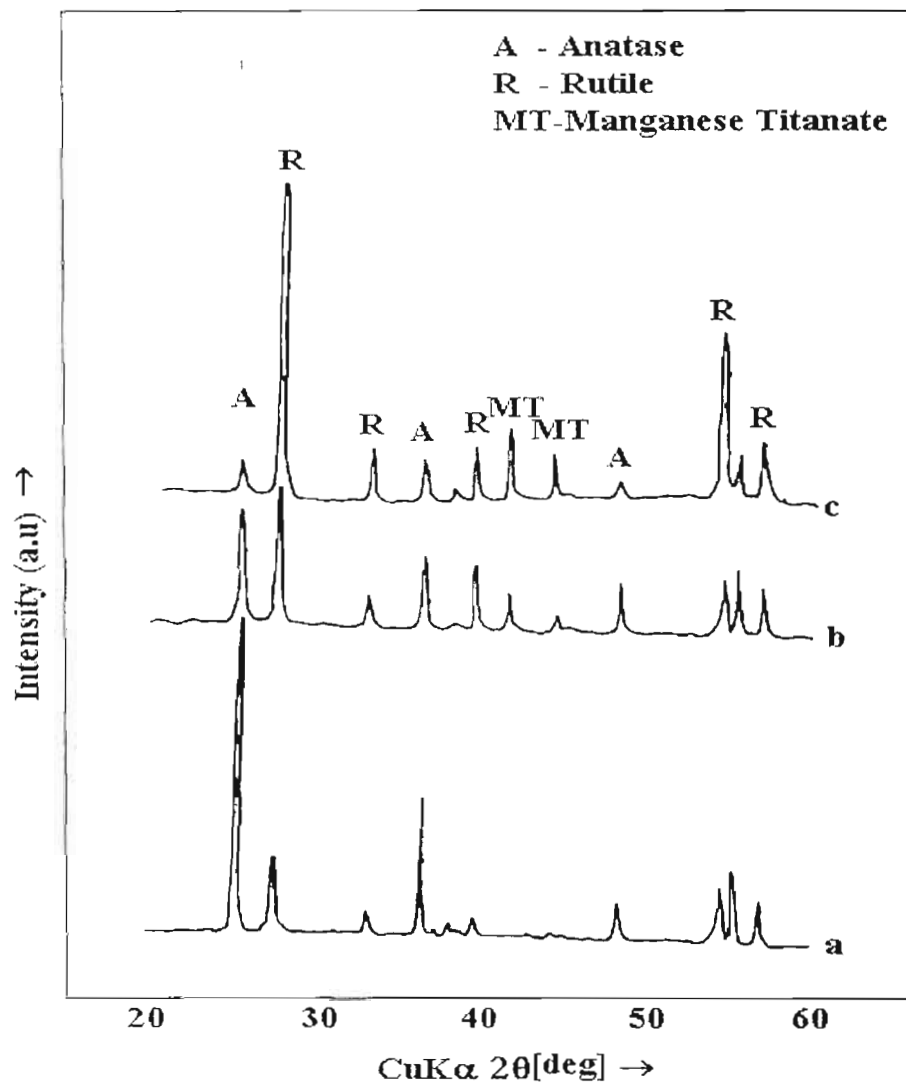
Table 7.1: Results of Chemical analysis of MnO<sub>2</sub> doped TiO<sub>2</sub> prepared through different methods.

Method of Preparation	Expected MnO <sub>2</sub> (%)	Experimental Composition	
		MnO <sub>2</sub> (%)	TiO <sub>2</sub> (%)
Co-precipitation	5	4.97	94.89
	15	14.87	84.93
Wet-Impregnation	5	4.88	94.87
	15	14.91	84.77

## 7.2 XRD studies

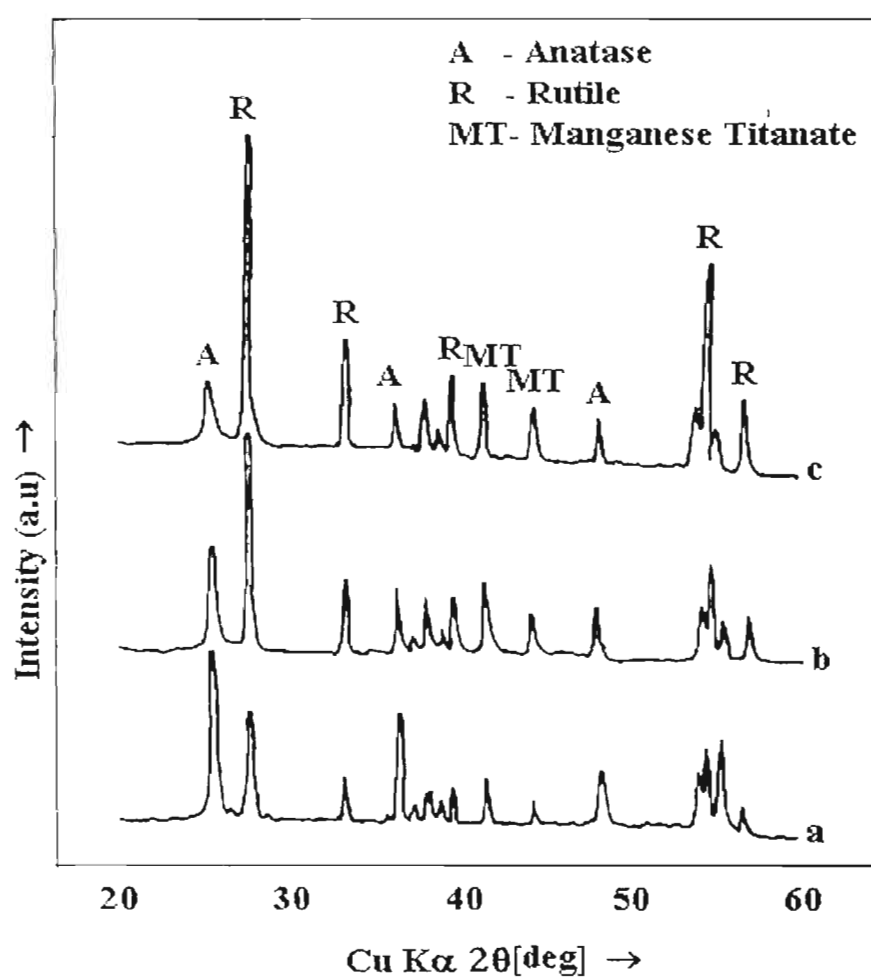
An interesting feature of these samples was that, the rutilation started at a lower temperature as compared to other transition metaloxide doped  $\text{TiO}_2$  studied. The XRD pattern of the co-precipitated samples heated at different temperatures in air for 6 hrs are given in figures 7.1 and 7.2.

Figure 7.1: XRD Patterns of co-precipitated 5%  $\text{MnO}_2/\text{TiO}_2$  heated at different temperatures for 6 hrs. (a)  $650^\circ\text{C}$  (b)  $700^\circ\text{C}$  (c)  $750^\circ\text{C}$



In both 5 and 15%  $\text{MnO}_2$  doped samples, rutilation started at  $650^\circ\text{C}$ . In 5%  $\text{MnO}_2$  doped sample, 4.1% rutile is formed for 4 hrs and in 15%, 8.5% rutile was formed at same time.

Figure 7.2: XRD Patterns of co-precipitated 15%  $\text{MnO}_2/\text{TiO}_2$  heated at different temperatures for 6 hrs. (a)  $650^\circ\text{C}$  (b)  $675^\circ\text{C}$  (c)  $700^\circ\text{C}$



In co-precipitated sample calcined at  $650^\circ\text{C}$ , anatase as well as rutile peaks appeared in the patterns. On increasing the calcination temperature, the

peak intensity of anatase decreased while that of rutile increased showing the anatase-rutile transformation during the heat treatment at different temperatures and time. At 650<sup>0</sup>C, 5% MnO<sub>2</sub> doped TiO<sub>2</sub> gave 6.2% rutile for 6 hrs heating while 12.6% rutilation was observed for 15% doped sample for the same duration. This clearly shows that the conversion depends on the amount of MnO<sub>2</sub> doped.

The different rutile percentages obtained at different temperatures and time of heating are summarized in tables 7.2 and 7.3.

**Table 7.2: % of rutile formed during heating of co-precipitated 5% MnO<sub>2</sub>/TiO<sub>2</sub> at different temperatures and time.**

Time of heating (hrs)	Rutile formed (%)		
	650 <sup>0</sup> C	700 <sup>0</sup> C	750 <sup>0</sup> C
1	0	12.9	28.4
2	0	24.2	48.8
3	0	34.0	63.3
4	4.1	42.5	73.8
5	5.3	50.0	81.2
6	6.2	56.5	86.6
7	7.1	62.1	90.4
8	8.2	67.0	93.1
9	9.1	71.3	95.0
10	10.3	75.0	96.4

Rutilation at 700<sup>0</sup>C for 5% MnO<sub>2</sub> doped TiO<sub>2</sub> was 56.5 for 6 hrs heating while 84.5% rutile was formed in 15% doped samples for the same time. In

15% doped sample almost complete anatase to rutile transformation was observed at 700<sup>0</sup>C 10 hrs heating.

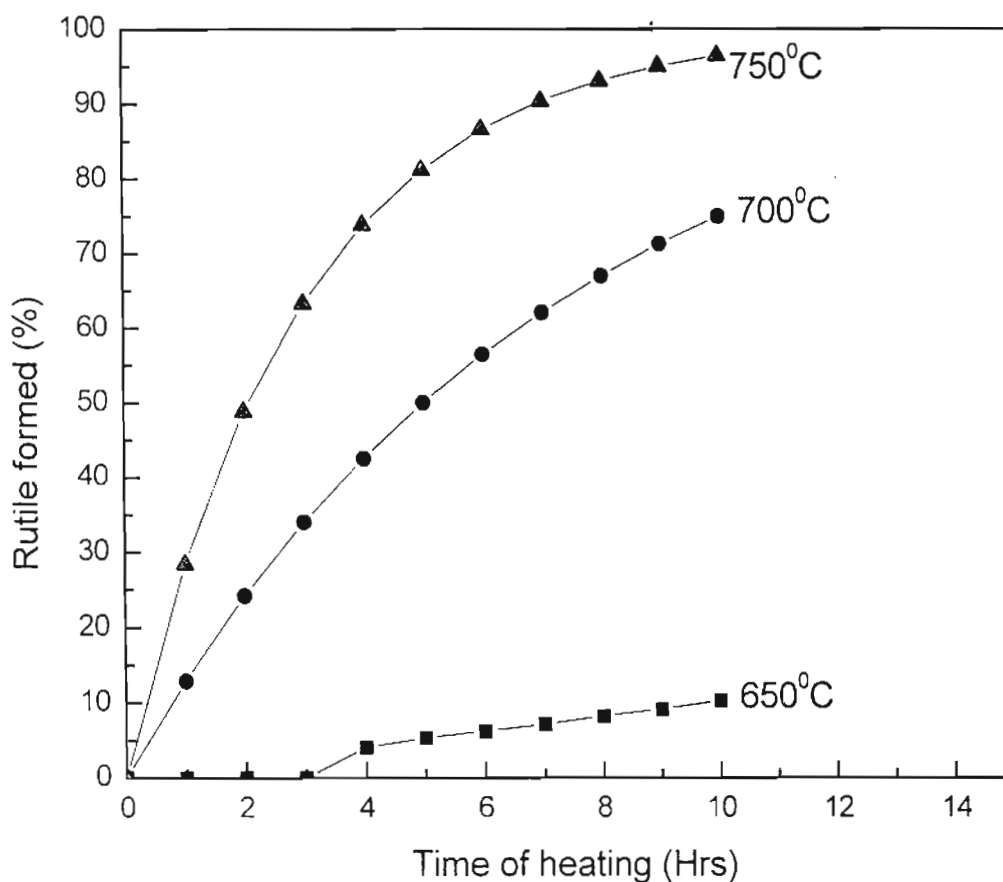
**Table 7.3: % of rutile formed during heating of co-precipitated 15% MnO<sub>2</sub>/TiO<sub>2</sub> at different temperatures and time.**

Time of heating (hrs)	Rutile formed (%)		
	650 <sup>0</sup> C	675 <sup>0</sup> C	700 <sup>0</sup> C
1	2.2	14.4	26.7
2	4.3	25.2	46.2
3	6.5	33.5	60.6
4	8.5	39.8	71.1
5	10.7	44.7	78.8
6	12.6	48.5	84.5
7	14.5	51.5	88.6
8	16.4	53.9	91.6
9	18.2	56.2	93.8
10	20.1	57.8	95.5

The variation in rutilation with time of heating at different temperatures in 5 and 15% MnO<sub>2</sub> doped TiO<sub>2</sub> co-precipitated samples is shown in figures 7.3 and 7.4 respectively. The 15% doped co-precipitated sample was converted almost completely to rutile at 700<sup>0</sup>C for 10 hrs. In these samples, rutilation was started and completed at lower temperatures as compared to pure TiO<sub>2</sub>. Hence, it is obvious that MnO<sub>2</sub> has a marked effect on rutilation.



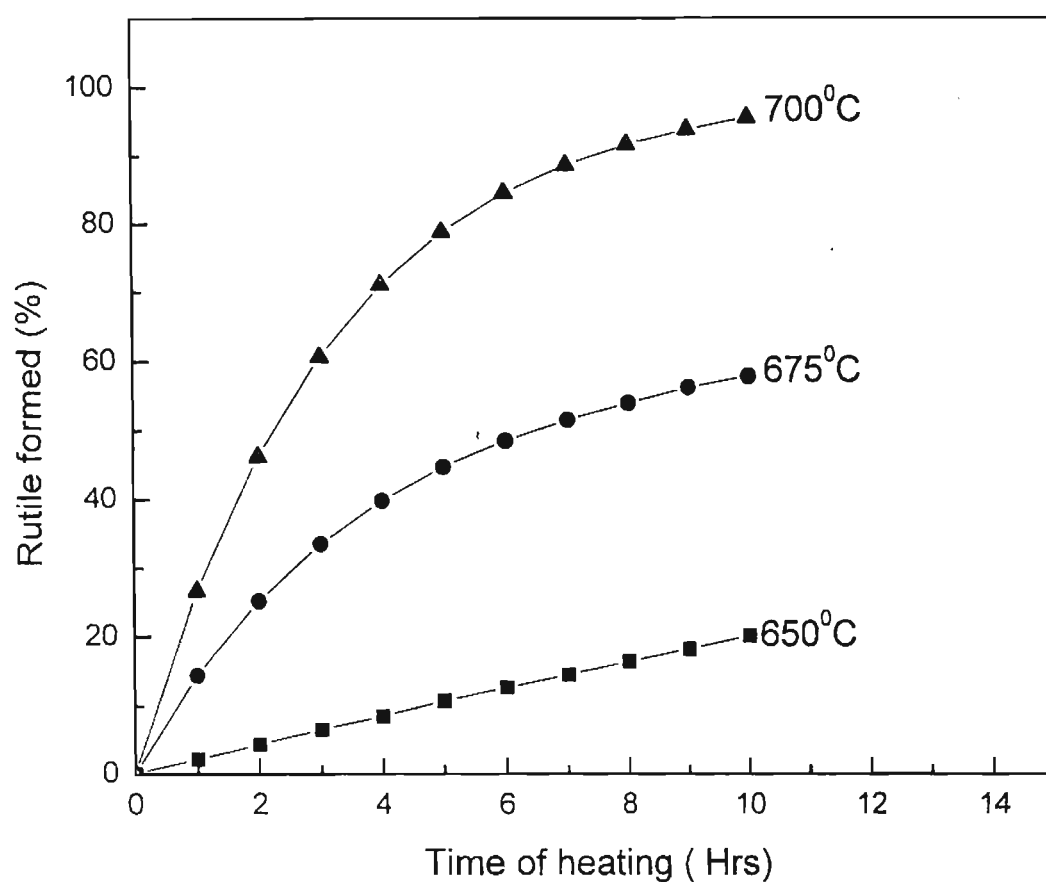
Figure 7.3: Variation of rutile % with time at different temperatures in co-precipitated 5% $\text{MnO}_2/\text{TiO}_2$ .



It was found that the rutile formation is enhanced by heating at higher temperatures. Also the time of heating determines the amount of rutile at any particular temperature. Among 5 and 15% doped samples, 15% doped ones produces more rutile compared to 5% at any particular temperature and time.

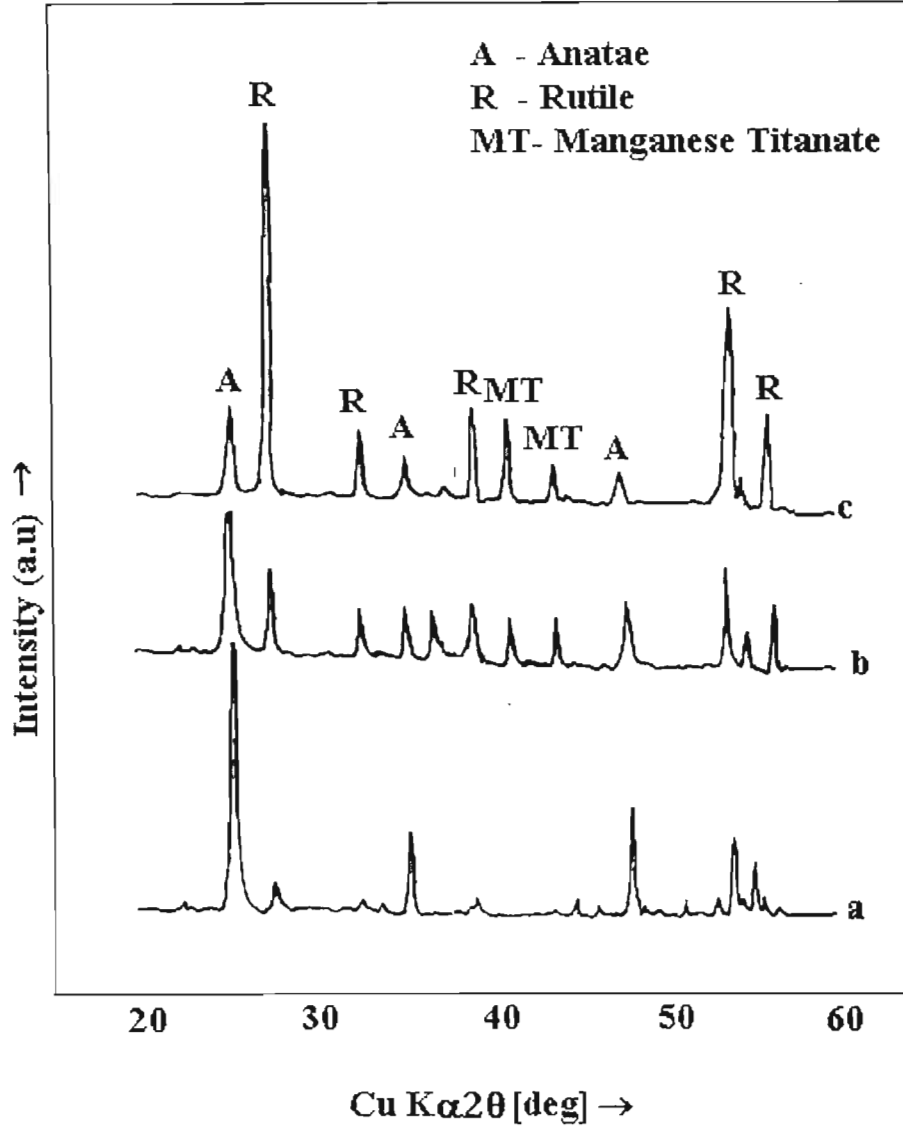
Thus it is clear that the amount of  $\text{MnO}_2$  plays a major role in deciding the phase transformation in  $\text{TiO}_2$ .

Figure 7.4: Variation of rutile % with time at different temperatures in co-precipitated 15% MnO<sub>2</sub>/TiO<sub>2</sub>.



The wet-impregnated samples behaved differently from that of co-precipitated one during the heat treatment even though the effect of different percentages is the same. The quantitative measurements of the rutile fractions produced at different temperatures and time of heating were done using XRD. The XRD patterns of wet-impregnated samples are given in figures 7.5 and 7.6.

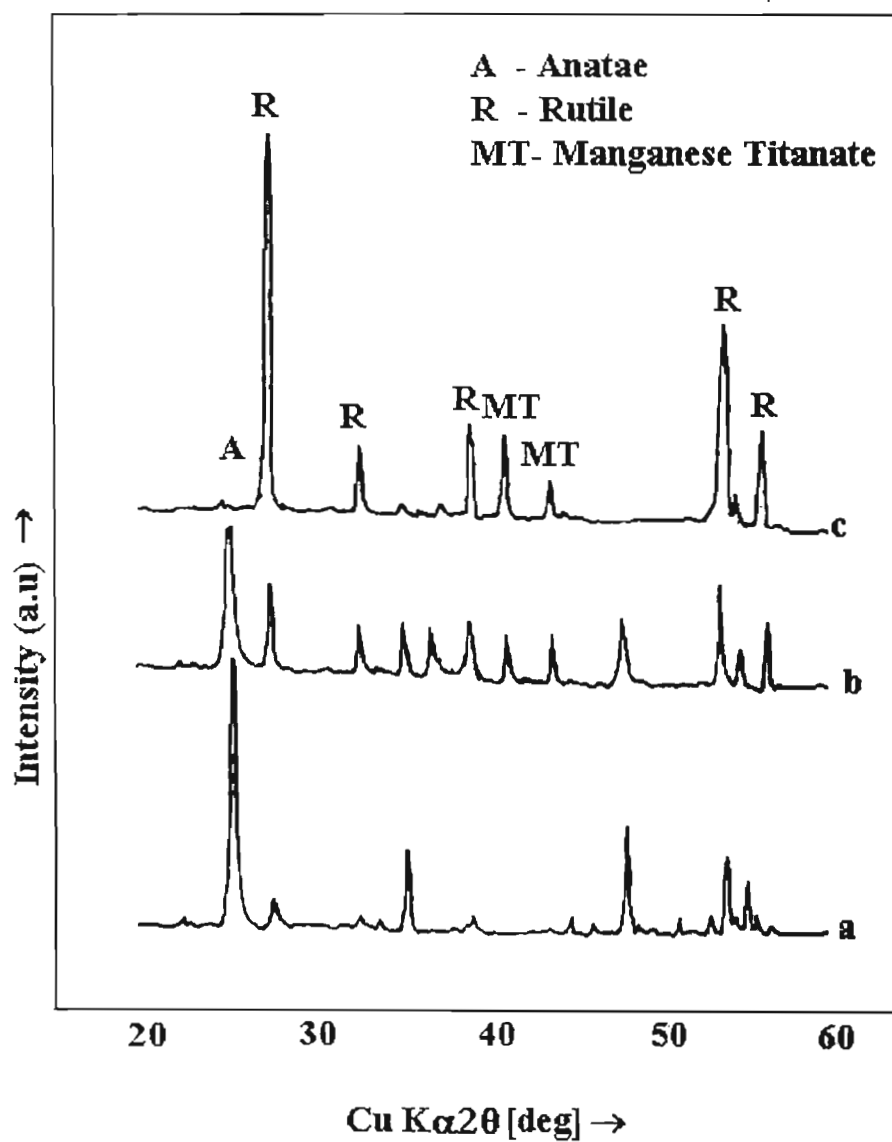
Figure 7.5: XRD Patterns of wet-impregnated 5%  $\text{MnO}_2/\text{TiO}_2$  heated at different temperatures for 6 hrs. (a)  $800^\circ\text{C}$  (b)  $825^\circ\text{C}$  (c)  $850^\circ\text{C}$



In the samples calcined at  $700^\circ\text{C}$  and above, some peaks of manganese titanate ( $\text{MnTiO}_4$ ) were also present along with peaks due to anatase and rutile. At the onset of rutilation, no peaks of  $\text{MnO}_2$  or  $\text{MnTiO}_4$  were seen, but, as the intensity of rutile peaks increased on increasing calcination temperature,

MnTiO<sub>4</sub> peaks also appeared in the pattern along with rutile peaks. On further calcination these peaks were seen to be more intense, revealing the growth of rutile during high temperature calcination. The appearance of MnTiO<sub>4</sub> peaks mirrored the fact that titania reacted with MnO<sub>2</sub> to form the titanate.

Figure 7.6: XRD Patterns of wet-impregnated 15% MnO<sub>2</sub>/TiO<sub>2</sub> heated at different temperatures. (a) 800°C (b) 850°C (c) 900°C



Different Percentages of rutile formed in wet-impregnated 5 and 15% MnO<sub>2</sub> doped TiO<sub>2</sub> samples are given in tables 7.4 and 7.5. It is found that at any time of heating at a particular temperature, wet-impregnated samples produced lower rutile compared to co-precipitated ones.

**Table.7.4: % of rutile formed during heating of wet-impregnated 5% MnO<sub>2</sub>/TiO<sub>2</sub> at different temperatures and time.**

Time of heating (hrs)	Rutile formed (%)		
	800 <sup>0</sup> C	825 <sup>0</sup> C	850 <sup>0</sup> C
1	0	9.4	41.2
2	0	17.2	65.5
3	0	24.7	79.4
4	5.1	31.5	88.1
5	6.3	37.7	93.2
6	7.6	43.4	95.9
7	8.8	48.5	97.5
8	10.3	53.2	100
9	11.6	57.4	100
10	12.8	61.2	100

In both 5 and 15% MnO<sub>2</sub> doped TiO<sub>2</sub> samples onset of rutilation was found at 800<sup>0</sup>C, 7.6% rutile was formed in 5% doped sample for 6 hrs heating and 15% doped sample got 10.1% rutile at the same time. 15% doped Sample

got rutiled completely at 850<sup>0</sup>C in 6 hrs, where as in the 5% loaded system, the rutilation was completed at 850<sup>0</sup>C for 8 hrs heating.

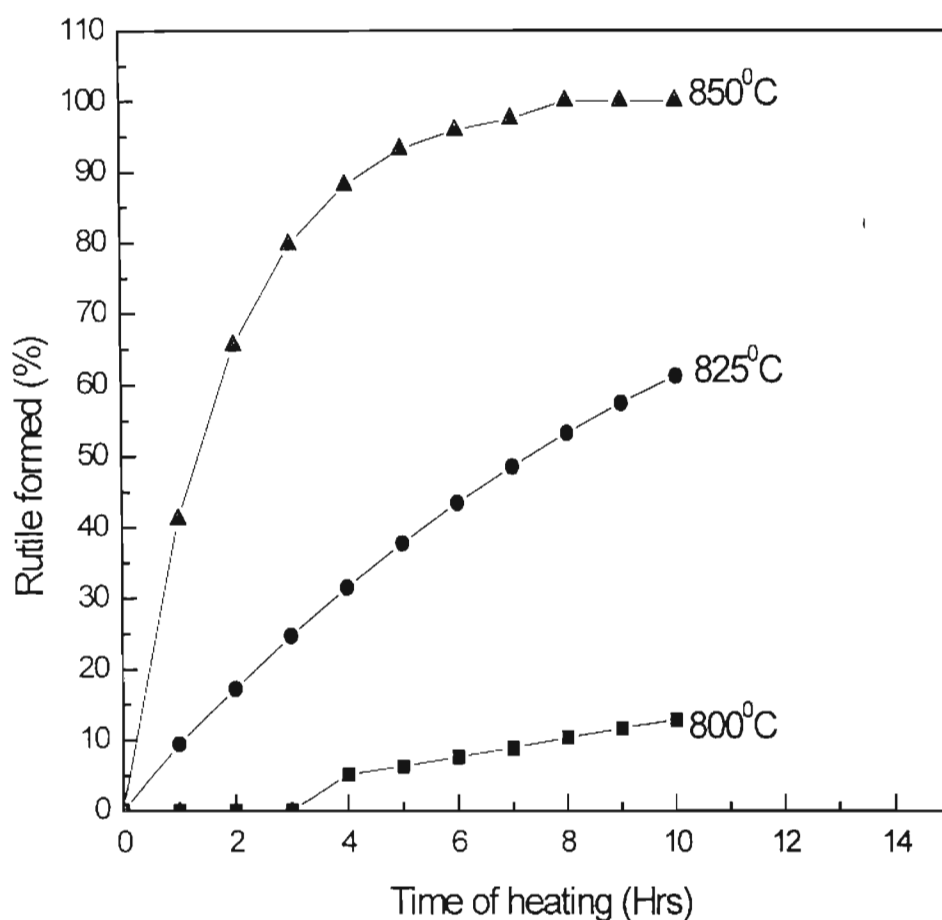
**Table.7.5: % of rutile formed during heating of wet-impregnated 15% MnO<sub>2</sub>/TiO<sub>2</sub> at different temperatures and time**

Time of heating (hrs)	Rutile formed (%)		
	800 <sup>0</sup> C	825 <sup>0</sup> C	850 <sup>0</sup> C
1	0	16.2	53.5
2	3.4	29.5	78.4
3	5.3	40.9	89.9
4	6.8	50.6	95.3
5	8.4	58.4	97.8
6	10.1	65.1	100
7	11.6	70.7	100
8	13.2	75.4	100
9	14.7	79.3	100
10	16.2	82.7	100

The variations in rutilation with time of heating at diferent temperatures are shown in figures 7.7 and 7.8. It is found that rutilation increases with increase in temperature and time of heating. Variations of rutilation in 15% doped sample are different from that of 5% doped ones. Also the variation in rutilation is lower in wet-impregnated samples compared to co-precipitated ones.

The difference in rutilation may be due to the difference in distribution of  $\text{MnO}_2$  over  $\text{TiO}_2$ . In co-precipitated samples there is uniform distribution of  $\text{MnO}_2$  since both are precipitated from a homogeneous solution.

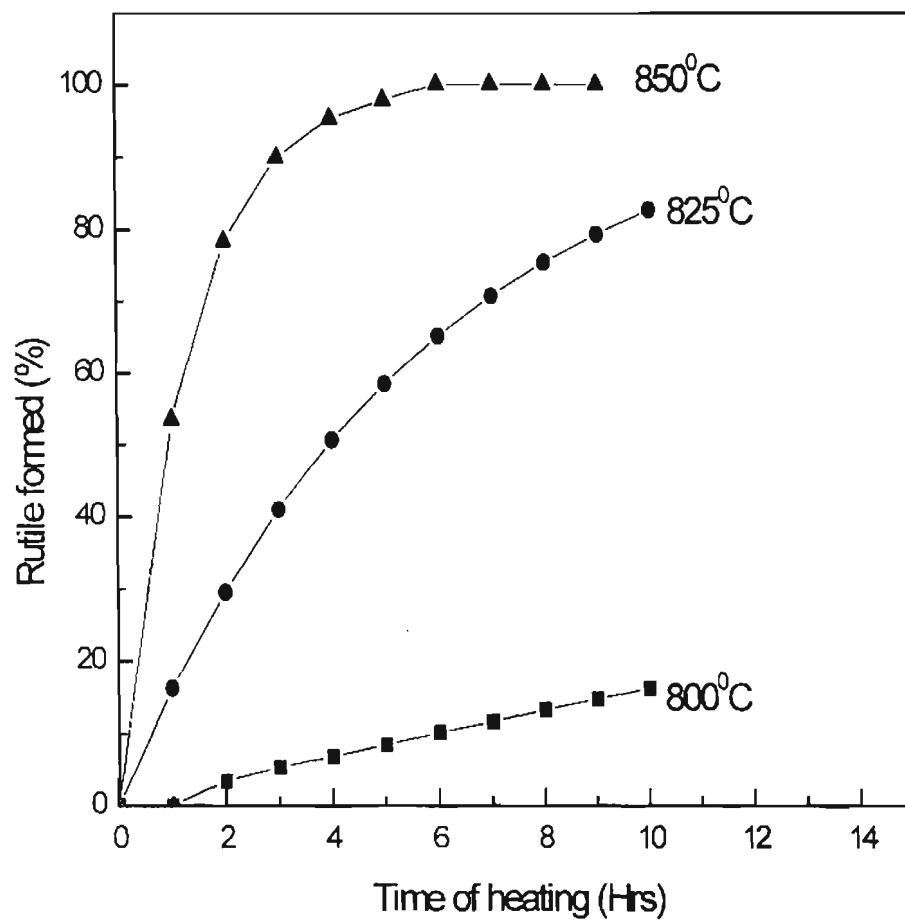
**Figure 7.7: Variation of rutile % with time at different temperatures in wet-impregnated 5%  $\text{MnO}_2/\text{TiO}_2$ .**



Therefore it is proved that rutilation strongly depends on the amount of dopant in addition to method of preparation and calcination temperature. It reflects clearly that, the co-precipitated one has higher rutile percentage at any temperature and the wet-impregnated one has the lower rutile percentage.

$\text{MnO}_2$  has created some oxygen vacancies on  $\text{TiO}_2$  surface, when calcined. This might be the reason, for the easy rutilation of these samples. This is in accordance with the literature reports, which state that, the formation of oxygen vacancies are the basic reason for rutilation since it enhances the rupture of Ti — O bonds of anatase.

**Figure 7.8: Variation of rutile % with time at different temperatures in wet-impregnated 15%  $\text{MnO}_2/\text{TiO}_2$ .**



The activation energy for the anatase-rutile transformation was calculated using the method explained in chapter 2 and is given in table 7.6. It is found that the activation energy for the transformation in co-precipitated



samples in presence of 5%  $\text{MnO}_2$  is found to be 30.59 kcal/mol while in presence of 15%  $\text{MnO}_2$  it is 26.05 kcal/mol. In case of wet-impregnated samples the activation energy for the transformation was found to be 63.33 kcal/mol in presence of 5%  $\text{MnO}_2$  while in presence of 15% it is 55.44 kcal/mol. For undoped  $\text{TiO}_2$ , activation energy for anatase-rutile transformation was reported to be  $\sim 90$  K cal/mol. Hence among 5 & 15%  $\text{MnO}_2$  15% has more lowering of activation energy and hence it is more accelerating.

Table 7.6: Activation energies for the anatase-rutile transformation in  $\text{MnO}_2$  doped  $\text{TiO}_2$ .

Method of Preparation	$\text{MnO}_2$ (%)	Activation energy K cal/mol
Co-precipitation	5	30.59
	15	26.05
Wet-Impregnation	5	63.33
	15	55.44

It is clear that the lowering of activation energy is different in wet-impregnated system as compared to co-precipitated ones. So an analysis of the activation energy values determined is useful in understanding the relative accelerating effect of  $\text{MnO}_2$  doping. It is clear that in presence of  $\text{MnO}_2$ , the activation energy is lowered much as compared to undoped.

The crystallite size of anatase after calcinations of these samples at temperatures when drastic changes in physical properties took place was calculated. The results are given in Table 7.7.

Here the anatase crystallites were seen to grow during the phase transformation from anatase to rutile. In co-precipitated 5%  $\text{MnO}_2/\text{TiO}_2$  at  $700^\circ\text{C}/8\text{hrs}$  the anatase crystallites had grown to a size of 12.4 nm (in this

sample 67.0 % of anatase was irreversibly converted to rutile). In case of 15% MnO<sub>2</sub>/TiO<sub>2</sub>, anatase crystallite size was found to be 13.6 nm at the same condition. This trend is same for wetimpregnated samples also.

**Table 7.7: Crystallite size and surface area values of un doped and MnO<sub>2</sub> doped TiO<sub>2</sub> Samples heated at different temperatures for 8 hrs**

Sample	Heating Temperature (°C)	Surface area (m <sup>2</sup> /g)	Crystallite size of anatase (nm)
Undoped TiO <sub>2</sub>	110	162.58	a*
	300	109.59	a*
	700	27.2	4.8
	900	9.13	14.2
	1000	2.54	b*
Co-precipitated 5% MnO <sub>2</sub> /TiO <sub>2</sub>	110	95.87	a*
	700	7.07	12.4
	750	1.16	22.8
Co-precipitated 15% MnO <sub>2</sub> /TiO <sub>2</sub>	110	124.36	a*
	700	6.4	13.6
	750	0.98	23.9
Wet-impregnated 5% MnO <sub>2</sub> /TiO <sub>2</sub>	110	90.76	a*
	800	10.37	12.7
	850	2.26	20.6
Wet-impregnated 15% MnO <sub>2</sub> /TiO <sub>2</sub>	110	103.81	a*
	800	7.79	11.3
	850	1.97	21.4

\* a- Amorphous TiO<sub>2</sub> \* b- Anatase phase absent

It is noteworthy that, in  $\text{MnO}_2/\text{TiO}_2$  like  $\text{Fe}_2\text{O}_3/\text{TiO}_2$ ,  $\text{Cr}_2\text{O}_3/\text{TiO}_2$ ,  $\text{NiO}/\text{TiO}_2$ , and  $\text{CuO}/\text{TiO}_2$ , as the rutile percentage increased, the anatase crystallite size also increased, but to different extents, depending on the method of preparation and nature of the metal oxide doped on  $\text{TiO}_2$ .

### 7.3 Surface area studies

The surface area decreased drastically with rutilation and this decrease was more noticeable in co-precipitated as compared to wet-impregnated ones and also with  $\text{MnO}_2$  percentage. For co-precipitated 5%  $\text{MnO}_2$  doped  $\text{TiO}_2$  the values are  $95.87 \text{ m}^2/\text{g}$ ,  $124.36 \text{ m}^2/\text{g}$  for 5 and 15% doped samples respectively before calcination. In the case of wet-impregnated samples, the surface area values are  $90.76 \text{ m}^2/\text{g}$  and  $103.81 \text{ m}^2/\text{g}$  respectively in 5 and 15% doped samples. The co-precipitated ones have larger surface area and on increasing the  $\text{MnO}_2$  percentage, better surface area is obtained before heating. On increasing the calcination temperature to  $700^\circ\text{C}$ , the surface area decreased very much and it became  $7.07 \text{ m}^2/\text{g}$  and  $6.4 \text{ m}^2/\text{g}$  in co-precipitated 5 and 15% doped ones and at  $800^\circ\text{C}$ , wet-impregnated 5% doped sample gave surface area  $10.37 \text{ m}^2/\text{g}$  and in 15% doped system it is  $7.79 \text{ m}^2/\text{g}$ . At the completion of rutilation, surface area of samples decreased very much. These changes clearly indicate the crystallographic rearrangement in  $\text{TiO}_2$ . Also the size of particles had grown during the phase transformation, which is supported by the Scanning Electron Micrographs of these samples.

In all these samples, even though, no direct relation between crystallite size and surface area could be made, a marked decrease in surface area could be seen along with a significant increase in crystallite size. At the onset of rutilation surface area was decreased and severe decrease occurred when

rutilation was completed, which may be due to growth in particle size and sintering. This is consistent with XRD data.

On comparing with the surface area of pure  $\text{TiO}_2$ , the surface area decreased on loading  $\text{MnO}_2$ . It is very clear from all these observations that the surface area decreased noticeably during rutilation, which in turn is dependent on preparation method and calcination temperature. The decrease was greater compared to pure  $\text{TiO}_2$ . So,  $\text{MnO}_2$  enhances the reduction in surface area during calcination.

#### **7.4 Scanning Electron Microscopic studies.**

In order to understand the changes in particle shape and size upon rutilation, the SEM analysis of  $\text{MnO}_2$  doped  $\text{TiO}_2$  samples before and after rutilation was carried out. Particles with sharp octahedral and needle like structures were present in the micrograph shown in Figures 7.9 and 7.10. Scanning Electron Micrographs of undoped anatase and rutile are shown in chapter 3.

The distribution of  $\text{MnO}_2$  over  $\text{TiO}_2$  is clearly found in the micrographs before rutilation, which is identified by EDAX analysis. After rutilation the individual particle size increased, which resulted in the decrease in surface area of the rutilated samples. All the particles were more or less similar in shape in co-precipitated sample. But the surface of wet-impregnated samples was found to be much aggregated even after rutilation. In these samples, the formation of manganese titanate is not completed and also dopent distribution is there on the surface, which is observed in EDAX analysis. Therefore it is believed that the formation of manganese titanate is independent of rutilation and it depends only on the temperature. For different titanates the temperatures are different

since the free energy of formation depends on the nature of metaloxide doped on  $\text{TiO}_2$ .

Figure: 7.9. Scanning Electron Micrographs of co-precipitated  $\text{MnO}_2/\text{TiO}_2$   
(a) Before rutilation (b) After rutilation.

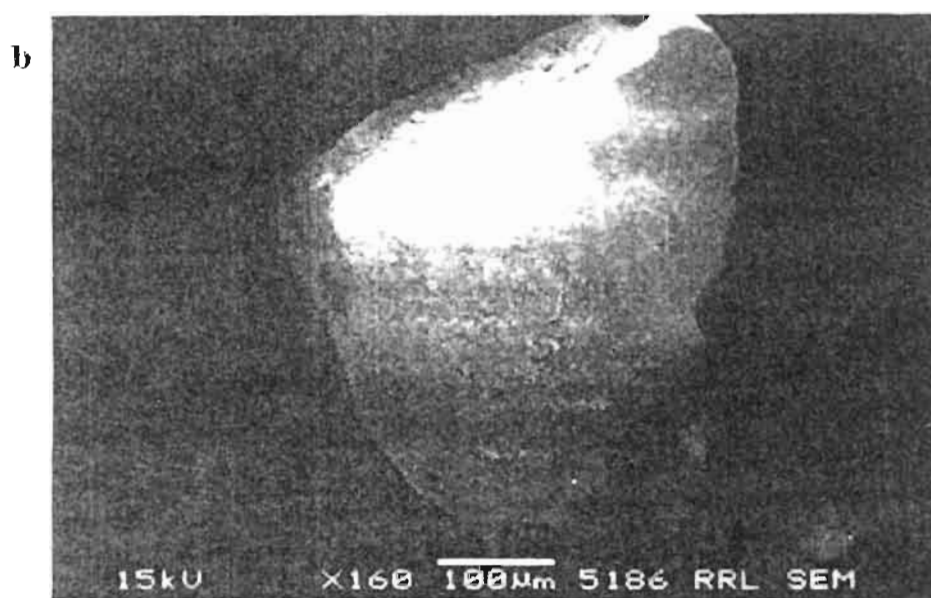
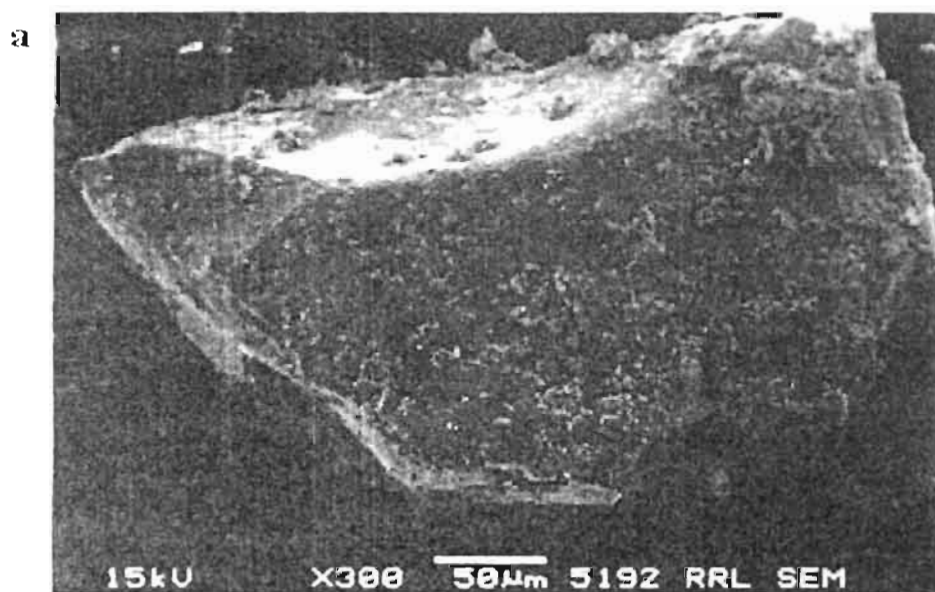
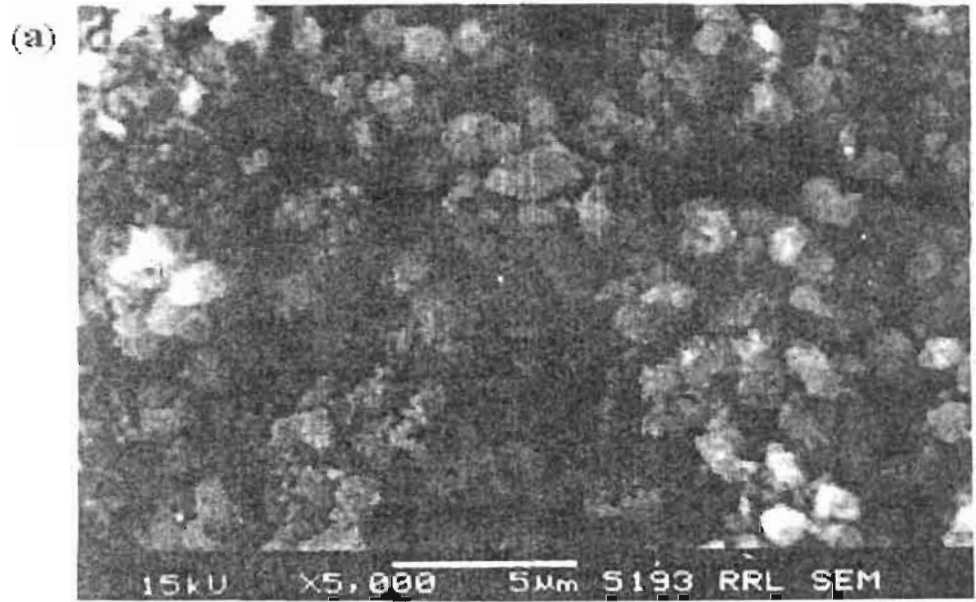


Figure: 7.10. Scanning Electron Micrographs of wet-impregnated  $\text{MnO}_2/\text{TiO}_2$   
(a) Before rutilation (b) After rutilation.



### 7.5 Transformation in Argon and Hydrogen atmospheres.

The anatase rutile transformations in Argon (inert) and hydrogen (reducing) atmospheres are investigated to understand the influence of environment on the transformation.

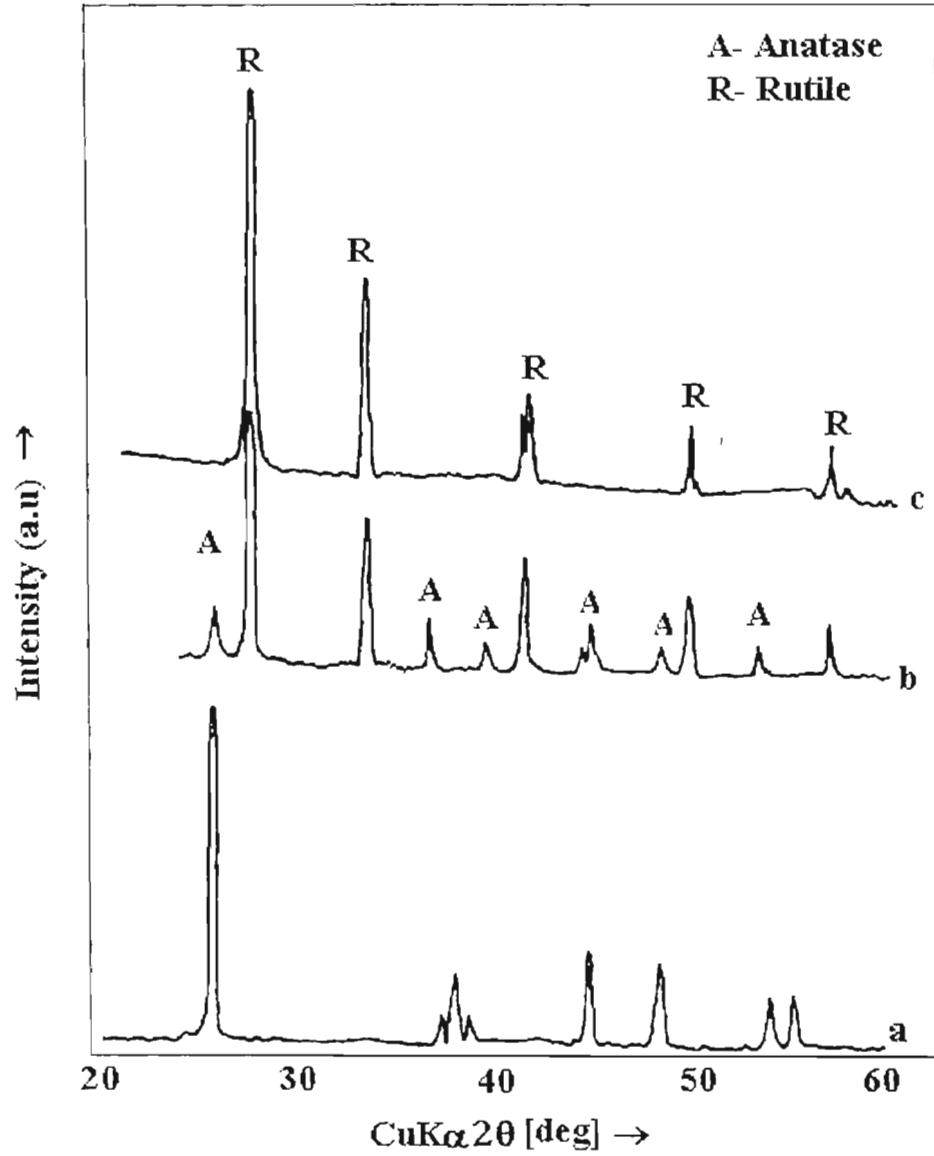
Figure.7.8. represents the XRD patterns of  $\text{MnO}_2/\text{TiO}_2$  heated in argon atmosphere. The anatase-rutile transformation was found to be more rapid in argon than in air.

In presence of argon atmosphere, the onset of rutilation was lowered to  $600^\circ\text{C}$  in co-precipitated samples. In 5%  $\text{MnO}_2/\text{TiO}_2$  the fraction of rutile formed is 12.3% and 42.9% rutile is converted from anatase phase in 15%  $\text{MnO}_2/\text{TiO}_2$  in argon atmosphere for 0.5 hrs heating at  $600^\circ\text{C}$ . This is much different from that in air. At  $650^\circ\text{C}$ , the rutilation was found to be 88.7% in 5% doped sample while in 15% doped sample, rutilation was complete at the same conditions. The fraction of rutile formed in co-precipitated 5 and 15%  $\text{MnO}_2/\text{TiO}_2$  at different temperatures are tabulated in table 7.8.

**Table.7.8:** Fraction of rutile formed in co-precipitated  $\text{MnO}_2$  doped  $\text{TiO}_2$  samples heated in argon atmosphere at different temperatures for 0.5 hrs heating.

Temperature ( $^\circ\text{C}$ )	Rutile formed	
	5% $\text{MnO}_2/\text{TiO}_2$	15% $\text{MnO}_2/\text{TiO}_2$
600	12.3	42.9
625	68.9	81.6
650	88.7	100

Figure.7.11: XRD Patterns of co-precipitated  $\text{MnO}_2$  doped  $\text{TiO}_2$  samples heated in argon atmosphere at  $650^\circ\text{C}$  for 0.5 hrs.  
 (a) Undoped  $\text{TiO}_2$  (b) 5%  $\text{MnO}_2/\text{TiO}_2$  (c) 15%  $\text{MnO}_2/\text{TiO}_2$

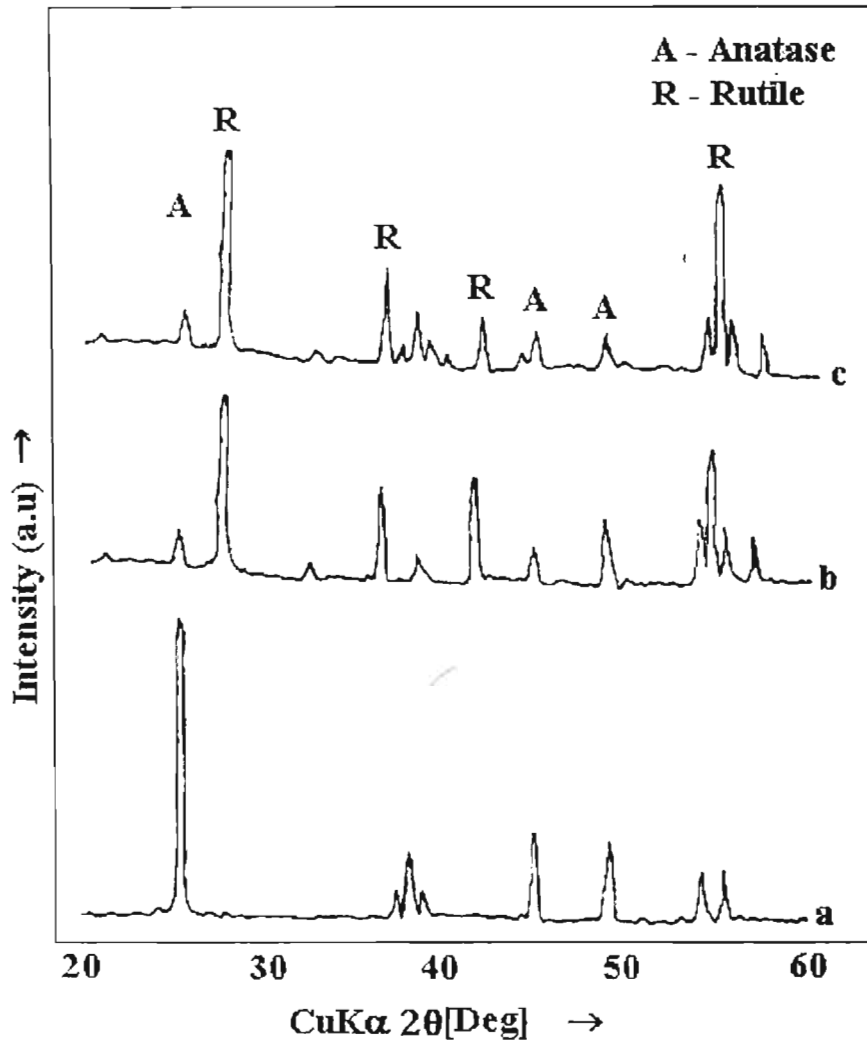


The amount of rutile formed is higher at each temperature and time of heating in 15% doped sample as compared to 5% as evident from the table. In air atmosphere, the onset of rutilation was  $650^\circ\text{C}$  (vide tables 7.2 and 7.3). At this temperature rutilation is completed in argon atmosphere.



In wet-impregnated samples at  $600^{\circ}\text{C}$ , there is no rutilation. The onset of rutilation is observed at  $625^{\circ}\text{C}$ . The XRD patterns of samples heated at  $700^{\circ}\text{C}$  are shown in figure 7.12.

Figure.7.12: XRD Patterns of wet-impregnated  $\text{MnO}_2$  doped  $\text{TiO}_2$  samples heated in argon atmosphere at  $700^{\circ}$  for 0.5 hrs.  
(a) Undoped  $\text{TiO}_2$  (b) 5%  $\text{MnO}_2/\text{TiO}_2$  (c) 15%  $\text{MnO}_2/\text{TiO}_2$



Further effect of temperature and time is same as that in co-precipitated one. Here also 15% doped samples gave more rutile than 5% doped  $\text{MnO}_2/\text{TiO}_2$ . The different amounts of rutile formed in wet-impregnated samples are summarized in table 7.9.

**Table.7.9: % of rutile formed in wet-impregnated MnO<sub>2</sub> doped TiO<sub>2</sub> samples heated in argon atmosphere at different temperatures for 0.5 hrs heating.**

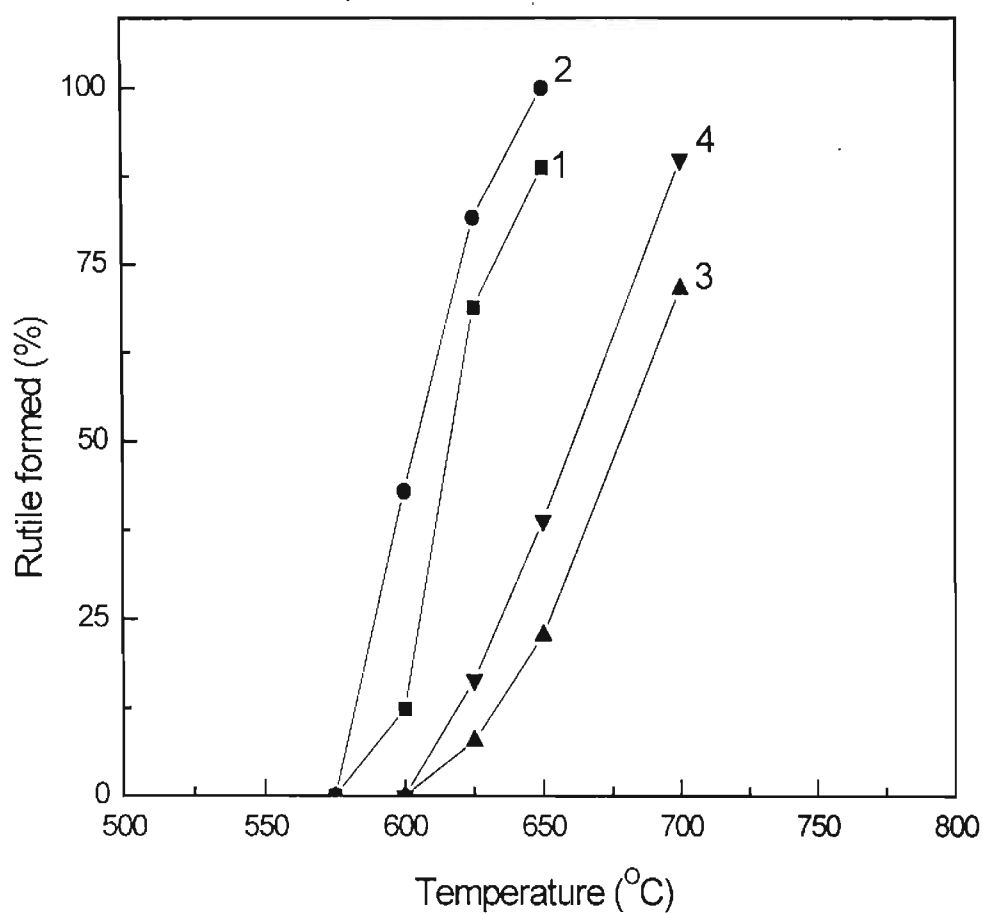
Temperature (°C)	Rutile formed	
	5% MnO <sub>2</sub> /TiO <sub>2</sub>	15% MnO <sub>2</sub> /TiO <sub>2</sub>
600	0	0
625	7.8	16.4
650	22.7	38.8
700	71.5	89.8

At 700°C, the anatase-rutile transformation was found to be 71.5 and 89.8% in 5 and 15% doped samples respectively. The formation of manganese titanate is not found in any of the patterns, which confirms that the temperature is not sufficient for the formation of it and the formation is independent of rutilation.

The variation in rutilation during heating in argon atmosphere in MnO<sub>2</sub>/TiO<sub>2</sub> samples is shown in figure 7.13. Here the transformation is accelerated but the extent of acceleration strongly depends on the method of preparation. The non-uniform distribution in wet-impregnated samples may be the cause for the deviation in transformation. Co-precipitated samples are precipitated from a homogeneous solution containing titanium and manganese ions.

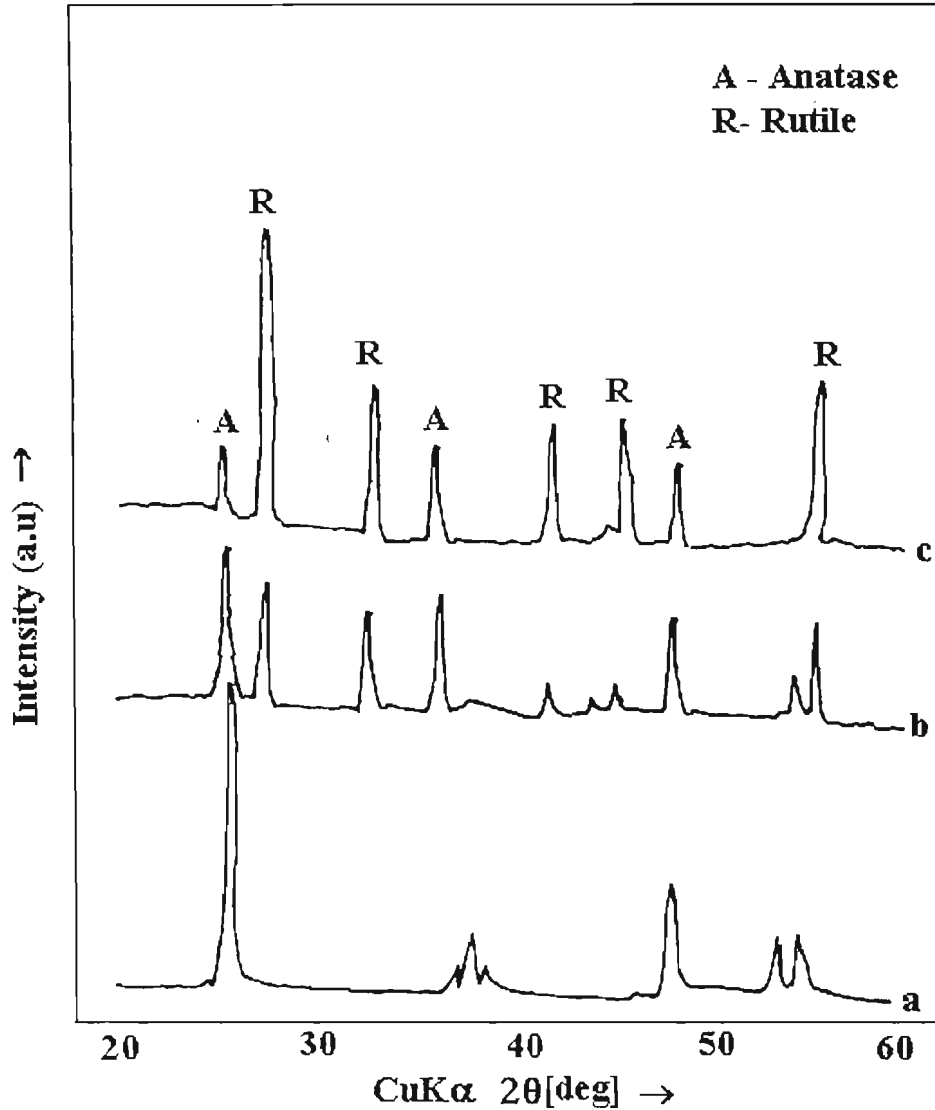
The importance of oxygen vacancies on the phase transition rate of TiO<sub>2</sub> in the presence of MnO<sub>2</sub> seems to be also confirmed by a more rapid transformation in argon than in air. Hence it can be concluded that argon atmosphere increases oxygen vacancies concentration and thus it favours the anatase-rutile transformation.

Figure.7.13: Variation of rutilation in  $\text{MnO}_2/\text{TiO}_2$  samples heated in argon atmosphere for 0.5 hrs at different temperatures.  
1- 5%  $\text{MnO}_2/\text{TiO}_2$ . 2- 15%  $\text{MnO}_2/\text{TiO}_2$ . (Co-precipitated)  
3- 5%  $\text{MnO}_2/\text{TiO}_2$ . 4- 15%  $\text{MnO}_2/\text{TiO}_2$ . (Wet-impregnated)



In hydrogen atmosphere, the anatase-rutile transformation was found to be low as compared to that in inert atmosphere and more than that in air. The XRD patterns of co-precipitated and wet-impregnated samples in different compositions are given in figures 7.14 and 7.15.

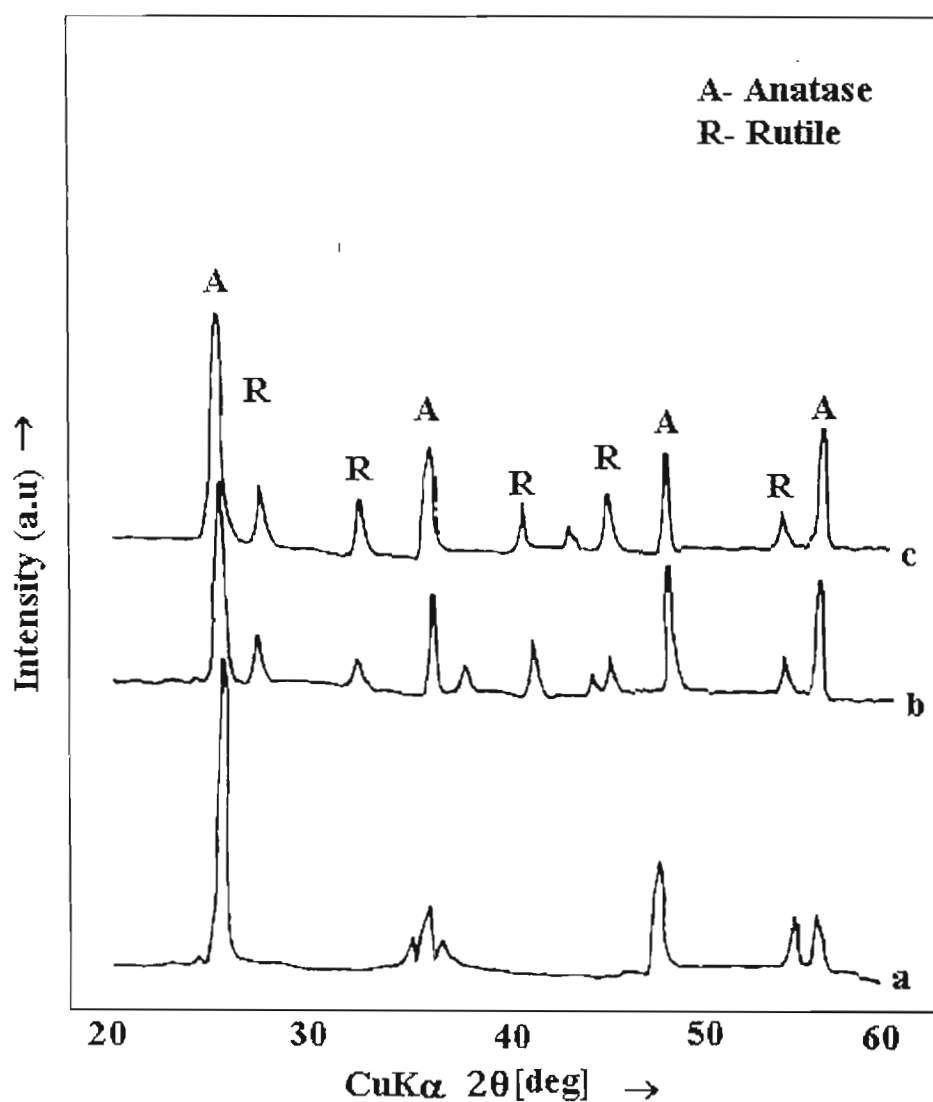
Figure.7.14: XRD Patterns of co-precipitated  $\text{MnO}_2/\text{TiO}_2$  samples heated in hydrogen atmosphere at  $750^\circ\text{C}/2\text{hrs}$ .  
 (a) Undoped  $\text{TiO}_2$  (b) 5%  $\text{MnO}_2/\text{TiO}_2$  (c) 15%  $\text{MnO}_2/\text{TiO}_2$



It is observed that on set of rutilation is different for co-precipitated and wet-impregnated samples. In case of co-precipitated, rutilation started at  $675^\circ\text{C}$  for 2 hrs heating, while in wet-impregnated ones it occurred at  $700^\circ\text{C}$ , which is different from that in argon atmosphere. The co-precipitated 5% doped samples gave 4.3 % rutile and 11.7 % rutilation was observed in 15% doped sample for 2 hrs heating at  $675^\circ\text{C}$ . When the temperature was increased to  $750^\circ\text{C}$ ,

rutilation also increased and it became 32.6 and 58.3% in 5 and 15% doped samples.

Figure.7.15: XRD Patterns of wet-impregnated  $\text{MnO}_2/\text{TiO}_2$  samples heated in hydrogen atmosphere at  $750^\circ/2\text{hrs}$ .  
(a) Undoped  $\text{TiO}_2$  (b) 5%  $\text{MnO}_2/\text{TiO}_2$  (c) 15%  $\text{MnO}_2/\text{TiO}_2$



Tables 7.10 and 7.11 represent the different fractions of rutile formed in co-precipitated and wet-impregnated samples during the calcinations at different temperatures and time.

**Table.7.10: % of rutile formed in co-precipitated MnO<sub>2</sub> doped TiO<sub>2</sub> system during heating in hydrogen atmosphere for 2 hrs.**

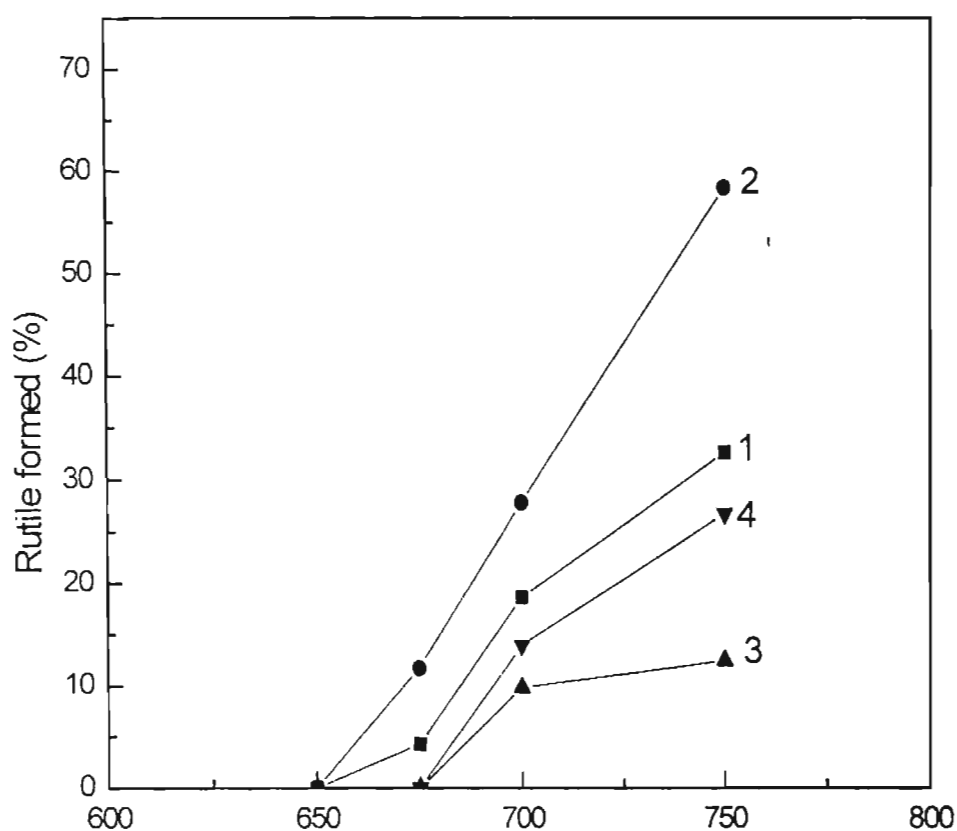
Temperature °C	Rutile formed (%)	
	5% MnO <sub>2</sub> /TiO <sub>2</sub>	15% MnO <sub>2</sub> /TiO <sub>2</sub>
650	0	0
675	4.3	11.7
700	18.6	27.8
750	32.6	58.3

**Table.7.11: % of rutile formed in wet-impregnated MnO<sub>2</sub> doped TiO<sub>2</sub> system during heating in hydrogen atmosphere for 2 hrs.**

Temperature °C	Rutile formed.	
	5% MnO <sub>2</sub> /TiO <sub>2</sub>	15% MnO <sub>2</sub> /TiO <sub>2</sub>
675	0	0
700	9.8	13.9
750	12.4	26.7

In wet-impregnated samples rutilation started slowly as compared to co-precipitated and also the formation of rutile is different at different temperatures, which again confirm that the transformation highly depends on the dopant concentration irrespective of the atmosphere of calcination. The variation in rutilation with temperature in MnO<sub>2</sub> doped TiO<sub>2</sub> samples heated in hydrogen atmosphere is shown in figure.7.16.

Figure.7.16: Variation of rutilation in  $\text{MnO}_2/\text{TiO}_2$  samples heated in hydrogen atmosphere for 2 hrs at different temperatures.  
 1- 5%  $\text{MnO}_2/\text{TiO}_2$ . 2 - 15% $\text{MnO}_2/\text{TiO}_2$  (Co-precipitated)  
 3 - 5% $\text{MnO}_2/\text{TiO}_2$ . 4 - 15% $\text{MnO}_2/\text{TiO}_2$  (Wet-impregnated)



Wet-impregnated 5% doped sample for 2 hrs heating at  $700^{\circ}\text{C}$  produced 9.8 % rutile while 15% has given 13.9% rutile at the same conditions. The fraction of rutile converted increased to 12.4 and 26.7 % respectively in 5 and 15% doped samples when temperature is increased to  $750^{\circ}\text{C}$ . There occurs some lattice defects in the sample during the heat treatment in reducing atmospheres. This results in the crystallographic rearrangements to form rutile,

a more stable phase of titania. This clearly indicates the effect of  $\text{MnO}_2$  is more important in the phase transformation and amount of  $\text{MnO}_2$  also has some important role in the phase transformations. This trend was observed in air and argon atmospheres also.

Hence it can be concluded that the anatase –rutile transformation in  $\text{MnO}_2$  doped  $\text{TiO}_2$  strongly depends on the concentration of dopants, method of preparation and the atmosphere of calcinations.

## 7.6 Conclusions

From all the above observations the following conclusions can be made.

- ☐ On loading  $\text{TiO}_2$  with  $\text{MnO}_2$  phase transformation occurs on heating at higher temperatures.
- ☐ The onset and completion temperatures of rutilation were much lower compared to all other metal oxide doped systems studied.
- ☐ Method of preparation as well as the quantity of  $\text{MnO}_2$  play major role in deciding rutile formation.
- ☐  $\text{MnTiO}_4$  phase was formed above  $700^\circ\text{C}$
- ☐ Crystallite size enlargement of anatase takes place during rutilation and  $\text{MnO}_2$  doping.
- ☐ Surface area decreases sharply with rutilation
- ☐ Surface morphology of  $\text{TiO}_2$  changes on doping  $\text{MnO}_2$ .
- ☐ The anatase-rutile transformation is more rapid in argon atmosphere than that in air and hydrogen.
- ☐ The order of enhancing rutilation by different atmospheres is in the order Argon > hydrogen > air.



## CHAPTER 8

### STUDIES ON LIQUID PHASE PHOTO OXIDATION OF TOLUENE

The first change in benzoic acid preparation came in 1850s when hippuric acid ( $C_6H_5CONHCH_2COOH$ ), from the urine of horses and cattle, replaced gum benzoin as the starting material. Hippuric acid was used extensively until 1870, when coal tar raw materials were utilized for the first time. [229,230] Phthalic acid was also used as the raw material until 1890, when the hydrolysis of benzo trichloride took over the bulk production. This route and the route employing chlorination of toluene to benzyl chloride and subsequent oxidation with  $HNO_3$  to benzoic acid remained as the major production route until after World War I. After World War II, started another change in manufacturing technique of benzoic acid, as the air oxidation of toluene was started in Germany and after the war, this method was carried over to US. The air oxidation in liquid phase using cobalt catalysts has now become the main manufacturing method in US. Considering the present and future petrochemical economic factors, it is difficult to fore see any commercial raw material other than toluene for benzoic acid production. [229,230] Benzoic acid has got many industrial applications such as, in medicines, veterinary medicines, food and industrial preservatives, dye stuffs, synthetic fiber, etc. [229].

$TiO_2$  is the most used and popular photo catalyst for various reasons, but unfortunately, although a large shift of light absorption in the visible region has been observed in almost all cases, the presence of dopant metal species has not been reported beneficial when photo oxidation reactions of organic substrates in aqueous systems were carried out. [231-234]. Some authors have reported

that the recombination rate of the electron-hole pairs increases for chromium doped  $\text{TiO}_2$  with respect to undoped  $\text{TiO}_2$ . The photo catalytic oxidation of acetic acid over  $\text{TiO}_2$  was markedly enhanced by dissolved copper ions [235]. Several authors have studied the  $\text{TiO}_2$  photo catalytic oxidation of benzene and toluene in air or oxygen. Formation of  $\text{CO}_2$  was reported in all these studies. [236-248] Analysis of the products recovered from used  $\text{TiO}_2$  by various solvents showed the formation of benzyl alcohol, benzaldehyde [241] and also benzoic acid [238,239] in the case of toluene oxidation. Similarly it was reported that the photo catalytic decomposition of toluene in aqueous  $\text{TiO}_2$  suspension was significantly promoted in the presence of copper, ferrous and manganese ions [249]. However there is no promoting effect on the photo catalytic decomposition of phenol in the presence of silver ion. [250] Moreover many other dopents are available on metal doped  $\text{TiO}_2$  preparations to efficiently decompose toxic compounds.

Air oxidation of toluene using transition metal oxides doped  $\text{TiO}_2$  in liquid phase in photochemical pathway is yet to be reported. The reaction was carried out using photo reactor described in chapter 2 by taking aqueous suspension of toluene containing a little hydrogen peroxide in presence of  $\text{TiO}_2$  doped with 15% transition metal oxides  $\text{Fe}_2\text{O}_3$ ,  $\text{Cr}_2\text{O}_3$ ,  $\text{NiO}$ ,  $\text{MnO}_2$  and  $\text{CuO}$  prepared by co-precipitation method containing anatase, rutile and mixture of anatase and rutile phases (50% each anatase and rutile phases). Irradiations were done for different hours and the samples collected after particular duration were analysed for the benzoic acid content. The activity studies were done after calcination of the samples at temperatures, when required alteration in properties occurred. The colour of the catalyst used was turned brown after irradiation and settled at the bottom of the photo reactor.

### 8.1. Studies on undoped TiO<sub>2</sub>.

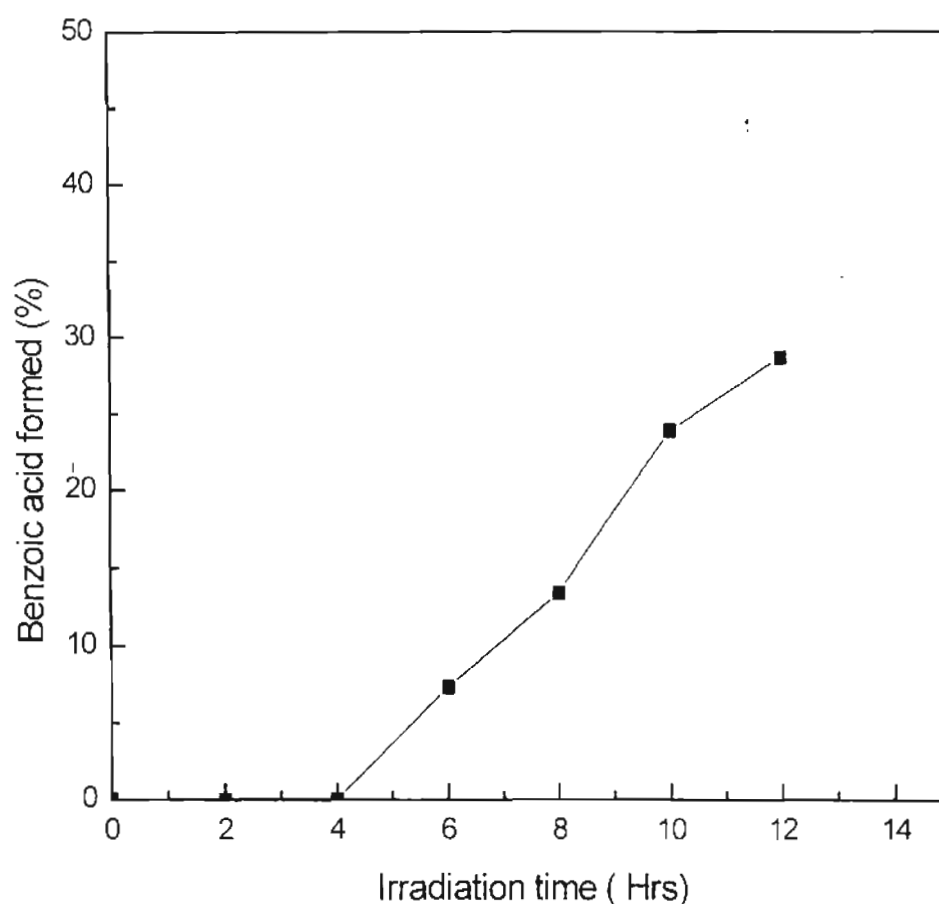
To compare the photo oxidation of aqueous suspension of toluene in presence of undoped TiO<sub>2</sub> with transition metal oxides doped TiO<sub>2</sub>, experiments were carried out using the all of them. It was seen that sample collected after irradiation for 6 hrs contained 7.3% benzoic acid. Various amounts of benzoic acid formed in presence of undoped TiO<sub>2</sub> is tabulated in table 8.1.

**Table: 8.1. The percentage conversion to benzoic acid during oxidation of toluene with undoped TiO<sub>2</sub> containing anatase phase.**

Irradiation time ( Hrs)	Benzoic acid formed (%)
0	0
2	0
4	0
6	7.3
8	13.4
10	23.9
12	28.7

The conversion obtained with undoped anatase TiO<sub>2</sub> for 12hrs irradiation was 28.7%. Figure 8.1 represent the variation in benzoic acid formation in presence of undoped TiO<sub>2</sub>. It was observed that the benzoic acid formation increases with irradiation time. Benzoic acid formation in presence of transition metal oxide doped TiO<sub>2</sub> is compared with that using undoped TiO<sub>2</sub>.

Figure 8.1. Variation in benzoic acid formation in presence of undoped TiO<sub>2</sub>. (anatase)



## 8.2. Studies on Fe<sub>2</sub>O<sub>3</sub>/TiO<sub>2</sub>.

Studies on the photo oxidation of toluene over 15% Fe<sub>2</sub>O<sub>3</sub> doped TiO<sub>2</sub> find that toluene oxidation is considerably affected by the phase transformation in TiO<sub>2</sub>. The conversion obtained with Fe<sub>2</sub>O<sub>3</sub> on anatase TiO<sub>2</sub> was 92.4% for 10hrs irradiation. But the conversion obtained was 36.4% when anatase phase was replaced with rutile. The benzoic acid formation with different phase composition of TiO<sub>2</sub> is given in table 8.2. The oxidation was found to be lowered by the phase transformation in TiO<sub>2</sub> support. Rutilation reduced the oxidation process and also percentage conversion was low with Fe<sub>2</sub>O<sub>3</sub> doped

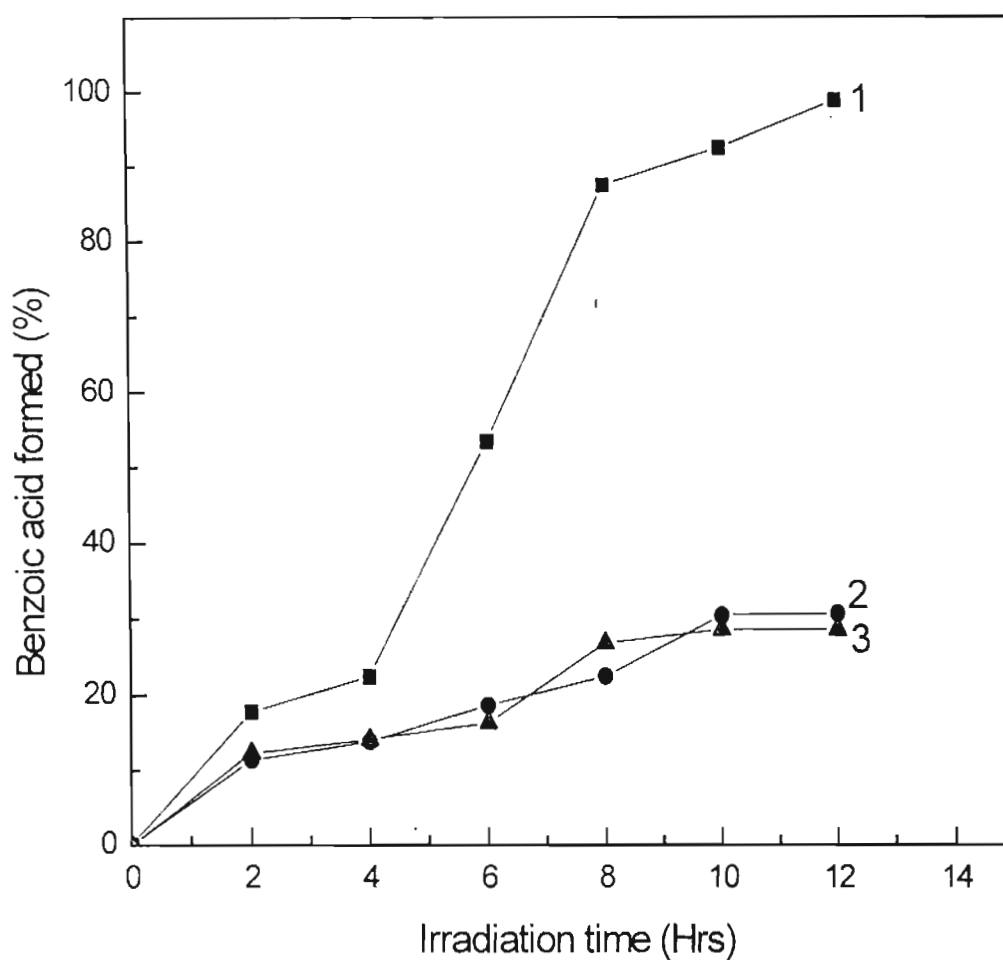
TiO<sub>2</sub> containing both anatase and rutile phase (53% rutile and 47% anatase) as compared to one containing anatase phase alone.

**Table: 8.2. The percentage conversion to benzoic acid during oxidation of toluene with 15% Fe<sub>2</sub>O<sub>3</sub> doped TiO<sub>2</sub> containing anatase, rutile and 47% anatase and 53% rutile phases.**

Irradiation time ( Hrs)	Benzoic acid formed (%)		
	With Anatase	With Rutile	With 47% anatase & 53% rutile mixture
0	0	0	0
2	17.8	11.4	12.3
4	22.4	13.8	14.1
6	53.4	18.6	16.3
8	87.4	22.4	26.8
10	92.4	30.4	28.6
12	98.8	30.7	28.6

The lowering of activity can be ascribed to the decrease in surface area of these samples during the phase transformation. Anatase has got better activity, as expected, due to their enhanced properties compared to rutile. The presence of rutile along with anatase also reduces the catalytic activity of Fe<sub>2</sub>O<sub>3</sub> doped TiO<sub>2</sub>. Figure 8.2 represents the variation in photochemical oxidation activity of Fe<sub>2</sub>O<sub>3</sub> doped TiO<sub>2</sub>.

Figure 8.2. Variation in benzoic acid formation with phase composition of 15% Fe<sub>2</sub>O<sub>3</sub> doped TiO<sub>2</sub> systems.  
1. Containing anatase 2. Containing rutile  
3. Containing 53% rutile and 47% anatase



The toluene oxidation activity is increased on doping Fe<sub>2</sub>O<sub>3</sub>. 12 hrs irradiation produced 98.8% benzoic acid in presence of Fe<sub>2</sub>O<sub>3</sub> doped TiO<sub>2</sub> while in presence of undoped TiO<sub>2</sub> only 28.7% benzoic acid was formed at the same conditions. Hence it is clear that Fe<sub>2</sub>O<sub>3</sub> doping has some enhancing effect on photo oxidation of toluene and hence Fe<sub>2</sub>O<sub>3</sub> doped TiO<sub>2</sub> can be used as a catalyst for the reaction than pure TiO<sub>2</sub> (in anatase phase). Decrease in the

catalytic activity of the system with rutilation may also be due to the changes in distribution of metal oxide on the surface of  $\text{TiO}_2$  with the crystal transformation as well as metal titanate formation at higher temperature where rutilation occurs. So, the reaction is influenced by the phase changes occurring in the support material.

### 8.3. Studies on $\text{Cr}_2\text{O}_3/\text{TiO}_2$ .

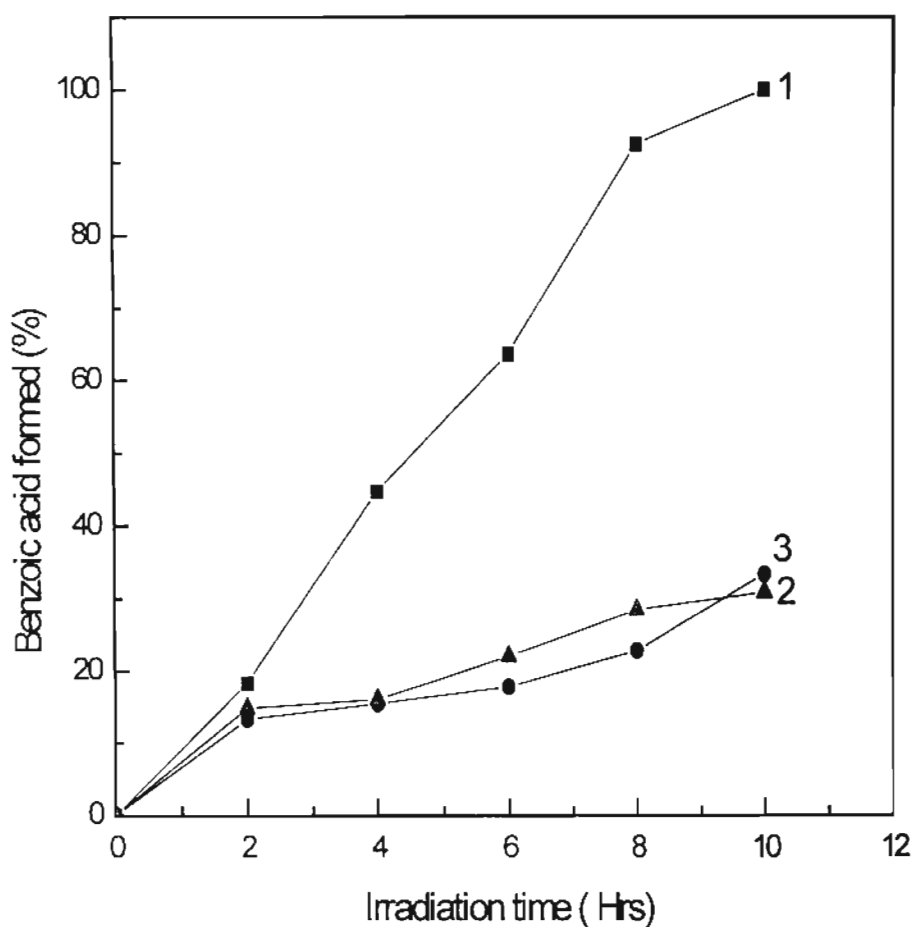
Toluene oxidation in liquid phase in photochemical pathway was carried out using 15%  $\text{Cr}_2\text{O}_3$  doped  $\text{TiO}_2$  with anatase, rutile and mixture of anatase and rutile phases (72% rutile and 28% anatase). The activity studies were done after the desired phase transformation occurred. The photo oxidation activity of  $\text{Cr}_2\text{O}_3$  doped  $\text{TiO}_2$  is affected by the rutilation in  $\text{TiO}_2$ . The conversion obtained with  $\text{Cr}_2\text{O}_3$  doped with anatase  $\text{TiO}_2$  was 100% for 10hrs irradiation. But the conversion obtained was 33.3% when anatase phase was replaced with rutile. The benzoic acid formation with different phase compositions of  $\text{TiO}_2$  is given in table 8.3. Benzoic acid formation was 30.8% with  $\text{Cr}_2\text{O}_3/\text{TiO}_2$  containing both anatase and rutile phases.

**Table: 8.3. The percentage conversion to benzoic acid during oxidation of toluene with 15%  $\text{Cr}_2\text{O}_3$  doped  $\text{TiO}_2$  containing anatase, rutile and 28% anatase and 72% rutile phases.**

Irradiation time (Hrs)	Benzoic acid formed (%)		
	With Anatase	With Rutile	With 28% anatase & 72 % rutile mixture
0	0	0	0
2	18.3	13.3	14.8
4	44.7	15.4	16.0
6	63.6	17.8	22.0
8	92.5	22.8	28.4
10	100	33.3	30.8

Thus change in the phase composition of  $\text{TiO}_2$  affects the photo oxidation of toluene using  $\text{Cr}_2\text{O}_3$  supported on  $\text{TiO}_2$ . Figure 8.3 represent the variation in photochemical oxidation activity of  $\text{Cr}_2\text{O}_3$  doped  $\text{TiO}_2$  with phase transformation of  $\text{TiO}_2$ .

**Figure 8.3. Variation in benzoic acid formation with phase composition of 15%  $\text{Cr}_2\text{O}_3$  doped  $\text{TiO}_2$  systems.**  
 1. Containing anatase 2. Containing rutile  
 3. Containing 72%rutile and 28%anatase



$\text{Cr}_2\text{O}_3$  doped  $\text{TiO}_2$  is also a good catalyst for the reaction compared to undoped  $\text{TiO}_2$  since 10 hrs irradiation produced 100% conversion of toluene to benzoic acid and this system is better than  $\text{Fe}_2\text{O}_3$  doped  $\text{TiO}_2$ . Anatase is the



best as expected, due to its better properties compared to rutile. Also there is a drastic decrease in surface area at the completion of rutilation. Decrease in the catalytic activity may also be due to the difference in distribution of metal oxide on the surface of  $\text{TiO}_2$  with the crystal transformation and also metal titanate formation may affect the distribution. This reaction is also influenced by the phase changes in the support material on which  $\text{Cr}_2\text{O}_3$  is present.

#### **8.4. Studies on NiO/TiO<sub>2</sub>.**

The photochemical toluene oxidation activity of 15% NiO doped  $\text{TiO}_2$  was studied and was found that the conversion to benzoic acid is very low as compared to other catalyst systems under investigation. On irradiation for 8 hrs with NiO supported on anatase  $\text{TiO}_2$ , only 6.5% benzoic acid was formed. Different percentages of benzoic acid formed during irradiation of aqueous suspension of toluene containing NiO doped  $\text{TiO}_2$  with different phases are tabulated in table 8.4.

NiO supported on rutile  $\text{TiO}_2$  for 8 hrs irradiation gave only 1.6% benzoic acid formation while NiO supported on mixture of 54% anatase and 46% rutile form converted almost the same amount at same conditions. It is clear that doping NiO with  $\text{TiO}_2$ , reduces significantly the photo oxidation activity of undoped  $\text{TiO}_2$ .

Another important observation found here is the formation of benzaldehyde during the reaction detected qualitatively (not quantitatively) by the Tollen's reaction. Hence it can be a selective catalyst system for converting toluene to benzaldehyde. However this reaction was not further followed up.

**Table: 8.4. The percentage conversion to benzoic acid during oxidation of toluene with 15%NiO doped TiO<sub>2</sub> containing anatase, rutile and 54% anatase and 46% rutile phases.**

Irradiation time (Hrs)	Benzoic acid formed (%)		
	With Anatase	With Rutile	With 54% anatase & 46% rutile mixture
0	0	Nil	Nil
2	0	Nil	Nil
4	2.3	Nil	Nil
6	4.8	Nil	Nil
8	6.5	Nil	Nil
10	6.5	1.6	1.8

Thus NiO doped TiO<sub>2</sub> is not a catalyst for the photochemical oxidation of toluene to benzoic acid even with anatase phase. The nominal conversion to benzoic acid may be due to the photo catalytic activity of TiO<sub>2</sub>.

#### **8.5. Studies on CuO/TiO<sub>2</sub>.**

Using 15% CuO doped TiO<sub>2</sub> containing anatase phase of titania, toluene conversion to benzoic acid reached 49.6% for 8 hrs irradiation. Table 8.5 gives the different percentages of benzoic acid formed during irradiation of aqueous suspension of toluene containing CuO doped TiO<sub>2</sub> with different phases.

**Table: 8.5. The percentage conversion to benzoic acid during oxidation of toluene with CuO/TiO<sub>2</sub> containing anatase, rutile and 50% anatase and rutile phases.**

Irradiation time (Hrs)	Benzoic acid formed (%)		
	With Anatase	With Rutile	With 50% anatase & rutile mixture
0	0	0	0
2	13.0	0	0
4	32.3	2.8	2.4
6	48.9	13.4	12.4
8	49.6	23.4	23.6
10	49.8	24.1	23.8

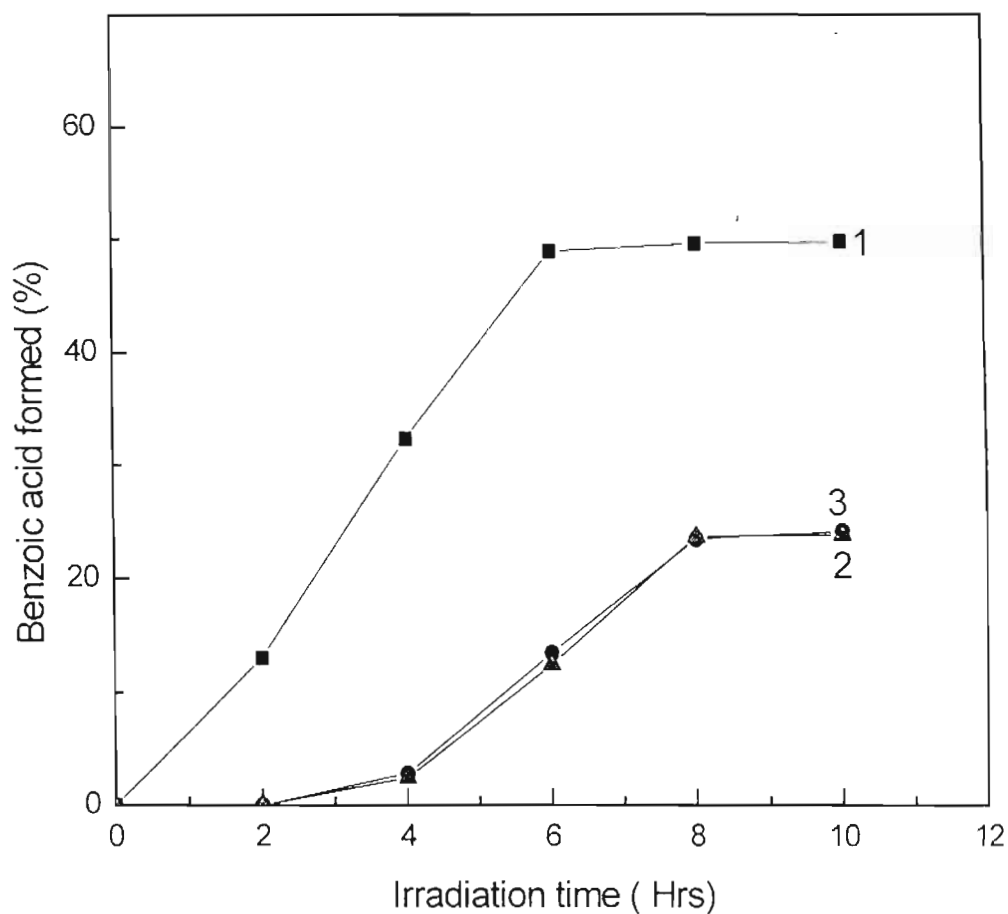
Here also the photochemical oxidation of toluene is affected by rutilation. The percentage conversion dropped to 24.1% when CuO is supported on rutile phase for 10 hrs irradiation. 49.8% benzoic acid was formed with anatase supported CuO for the same irradiation time. Figure 8.4 gives the variation in benzoic acid formation with irradiation time using different phases of TiO<sub>2</sub> support.

Here also the oxidation activity of the catalyst is decreased by the presence of rutile. The required properties of TiO<sub>2</sub> to act as a good catalyst support decreases on rutilation. The surface area of CuO doped TiO<sub>2</sub> decreased drastically on rutilation. Decrease in the catalytic activity of the system with rutilation may also due to the changes in distribution of metal oxide on the surface of titania, which may decrease with the crystal transformation and metal titanate formation at higher temperature where rutilation occurs. These

may be the reason for the decrease in photo oxidation activity. So, this reaction also is influenced by the phase changes occurring in the support material.

**Figure 8.4. Variation in benzoic acid formation with different phase composition of CuO/TiO<sub>2</sub> systems.**

1. Containing anatase
2. Containing rutile
3. Containing 50% anatase and rutile



### 8.6. Studies on MnO<sub>2</sub>/TiO<sub>2</sub>.

Very interesting result is obtained for the photooxidation of toluene using MnO<sub>2</sub> doped TiO<sub>2</sub>. Here the anatase phase TiO<sub>2</sub> supported MnO<sub>2</sub> formed 45.5% benzoic acid from toluene for 2hrs irradiation. At 4hrs irradiation, 50.3% benzoic acid was formed. Table 8.6 gives the different percentages of

benzoic acid formed during the irradiation of  $\text{MnO}_2$  doped  $\text{TiO}_2$  with different phases.

**Table: 8.6. The percentage conversion of benzoic acid during oxidation of toluene with  $\text{MnO}_2/\text{TiO}_2$  containing anatase, rutile and 52% anatase and 48% rutile phases.**

Irradiation time (Hrs)	Benzoic acid formed (%)		
	With Anatase	With Rutile	With 52% anatase & 48% rutile mixture
0	0	0	0
2	45.5	0	12.1
4	50.3	11.9	12.3
6	17.3	17.1	16.8
8	15.2	16.2	15.9
10	13.2	12.4	11.6

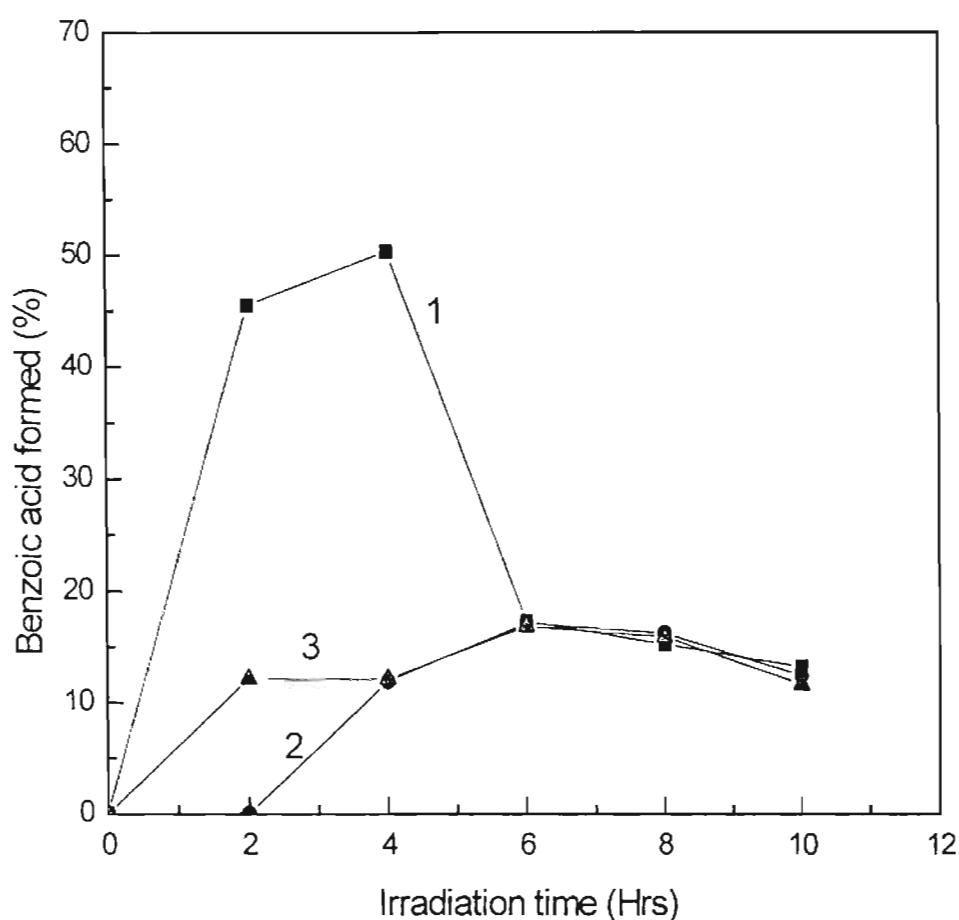
On further increase of irradiation, the percentage of benzoic acid dropped slowly reaching 13.2% at 10 hrs. It may be due to decomposition of benzoic acid to carbon dioxide and water. Figure 8.5 gives the variation in benzoic acid percentage with time of irradiation using  $\text{MnO}_2$  supported on different phases of  $\text{TiO}_2$ .

Like  $\text{Fe}_2\text{O}_3/\text{TiO}_2$ ,  $\text{Cr}_2\text{O}_3/\text{TiO}_2$  and  $\text{CuO}/\text{TiO}_2$  systems, in this system also, rutilation lowered the oxidation activity as expected but the extent of lowering is higher as compared to others. Thus the photo oxidation of toluene is affected by the phase modification in the  $\text{TiO}_2$  support. In the case of  $\text{MnO}_2$  doped  $\text{TiO}_2$ , prolonged irradiation resulted in the degradation since toluene layer disappeared showing the conversion of toluene but benzoic acid quantity decreased, which shows that benzoic acid is getting decomposed. The optimum time of irradiation is found to be 4 hrs where around 50% benzoic acid

conversion is obtained. Thus it is clear that the  $\text{MnO}_2$  doped  $\text{TiO}_2$  can act as a catalyst for the decomposition of benzoic acid and it may decompose organic pollutants.

**Figure 8.5. Variation in benzoic acid formation with different phase composition of  $\text{MnO}_2/\text{TiO}_2$  systems.**

1. Containing anatase
2. Containing rutile
3. Containing both anatase and rutile



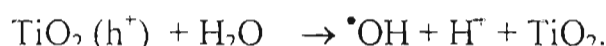
Hence it can be concluded that  $\text{Cr}_2\text{O}_3$  and  $\text{Fe}_2\text{O}_3$  doped  $\text{TiO}_2$  can give 100% conversion in photo oxidation of toluene to benzoic acid as compared to undoped  $\text{TiO}_2$  and with  $\text{CuO}$  and  $\text{MnO}_2$  doped  $\text{TiO}_2$  the yield of benzoic acid is less.  $\text{MnO}_2$  doped  $\text{TiO}_2$  on higher irradiation time makes degradation of

benzoic acid formed. NiO doped TiO<sub>2</sub> is not a catalyst for photo oxidation of toluene to benzoic acid. Undoped TiO<sub>2</sub> gives more yield of benzoic acid than NiO doped TiO<sub>2</sub>. Selective oxidation to benzaldehyde is detected with this system.

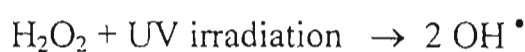
### 8.7. Mechanism of Photochemical oxidation of Toluene.

The mechanism of degradation of toluene during irradiation with transition metal oxides supported on TiO<sub>2</sub> is believed to be as follows.

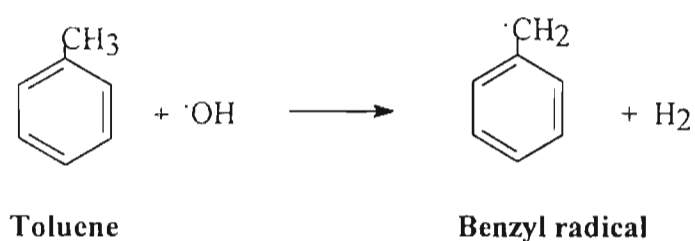
The photo catalytic reaction starts with the exposure of aqueous suspension of toluene in presence of metaloxide supported on TiO<sub>2</sub> to UV light. After exposure to light two reaction starters are generated; one is electron (e<sup>-</sup>) and the other is positive electron holes (h<sup>+</sup>). One of the notable characteristics of TiO<sub>2</sub> is that the oxidising power of the holes is greater than the reducing power of the excited electrons. Now TiO<sub>2</sub> absorb H<sub>2</sub>O on to its surface and generates hydroxyl radicals, which have strong oxidation capacity. In this reaction TiO<sub>2</sub> is regenerated to original form.



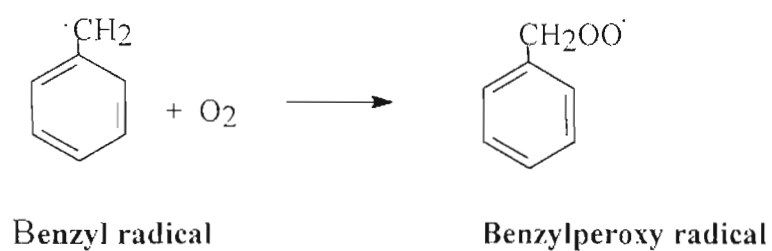
The decomposition of hydrogen peroxide added also produces hydroxyl radicals.



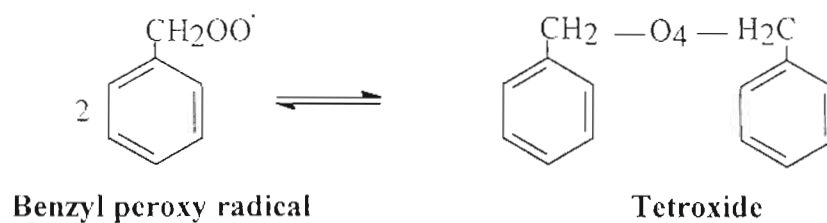
The hydroxyl radical can abstract the hydrogen from the methyl group leading to a benzyl radical.



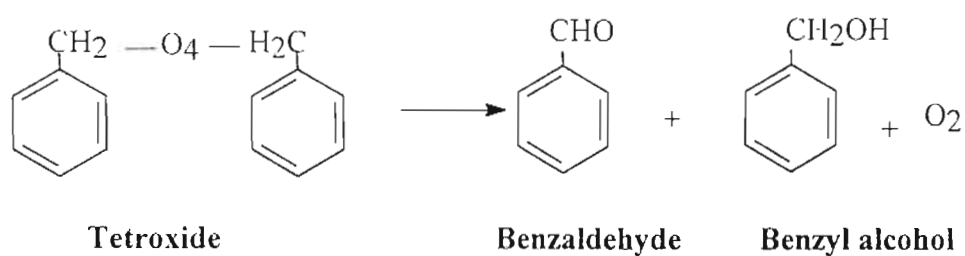
The benzyl radical can then react with  $O_2$  to form a benzylperoxy radical.



The benzyl peroxy radical can couple to form a tetroxide proposed by Von Sonntag and Schuchmann for oxidation in aqueous phase [251] and applied in photocatalysis by Heller et al. [252,253]

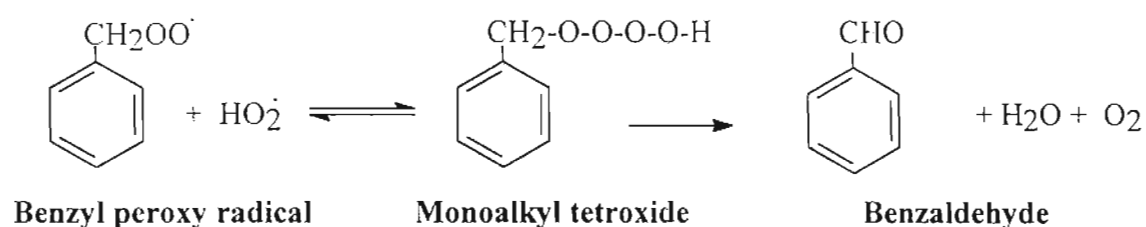


The tetroxide decomposes to benzaldehyde, benzyl alcohol and molecular oxygen (the Russel reaction) [254]

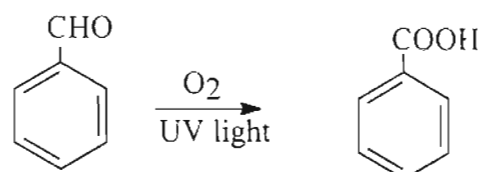




The benzyl peroxy radical can also react with a hydroperoxy radical (formed in the reaction system) to form a monoalkyl tetroxide that decomposes to benzaldehyde, molecular oxygen and water ( the 'Russell-like' reaction [255] )



Benzaldehyde gets oxidized easily in to benzoic acid, especially in the presence of  $\text{O}_2$  and UV irradiation.



The brown colour of the catalyst after irradiation may be due to the adsorption of some intermediate products formed during the photo catalytic oxidation of toluene.

The difference in photo catalytic activity between  $\text{TiO}_2$  and doped  $\text{TiO}_2$  can be attributed to the characteristics such as the larger particle size or the lower anatase/rutile ratio of pure  $\text{TiO}_2$ . Powders with more rutile could be less active due to the de hydroxylation caused by the anatase to rutile phase transformation since hydroxylation reduces hole trapping by surface hydroxyls, enhancing recombination and oxygen or organic species adsorption. A decrease in specific surface area can also affect the photo activity.

Dopents can affect the photo activity of  $\text{TiO}_2$  by changing the number of active sites, surface groups and the acid-base properties. The different behaviour of the various samples is also related to the solubility of the transition metal oxide in the  $\text{TiO}_2$  support, which depends strongly on the radius and the charge of the corresponding ion.[256] Sha Jin et al. have reported that photo catalytic activities enhanced for decompositions of organic compounds over metal-photo deposited titanium dioxide and that the photo catalytic activities of the metal-deposited  $\text{TiO}_2$  were superior to that of the  $\text{TiO}_2$  film and were highly stable.[257] The present study also confirms that metal oxide dispersed  $\text{TiO}_2$  is better catalyst than pure  $\text{TiO}_2$ . The reasons for the enhanced activity and efficiency may be due to various factors like change in the number of active sites, surface groups, acid base properties, solubility of metal oxide in  $\text{TiO}_2$  etc.

### 8.8. Conclusions

The following conclusions can be made from the studies on the photo oxidation of toluene with metal oxides supported on  $\text{TiO}_2$ .

- >  $\text{Fe}_2\text{O}_3$  and  $\text{Cr}_2\text{O}_3$  supported on  $\text{TiO}_2$  produced more yield of benzoic acid from toluene during irradiation.
- > The yield of benzoic acid is less with  $\text{CuO}$  doped  $\text{TiO}_2$ .
- >  $\text{MnO}_2$  doped  $\text{TiO}_2$  is acting as a catalyst for the decomposition of benzoic acid at higher irradiation time.
- >  $\text{NiO}$  supported on  $\text{TiO}_2$  is not a catalyst for photooxidation of toluene.
- > Selective oxidation of toluene to benzaldehyde is observed in  $\text{NiO}$  supported on  $\text{TiO}_2$ .

- Severe decrease in photo oxidation activity was observed with rutilation.
- Order of photo oxidation activity for toluene: anatase > rutile  $\cong$  mixture of anatase & rutile.
- The photo catalytic activity decreases in the order  
Cr<sub>2</sub>O<sub>3</sub> doped TiO<sub>2</sub> > Fe<sub>2</sub>O<sub>3</sub> doped TiO<sub>2</sub> > CuO doped TiO<sub>2</sub> >  
Undoped TiO<sub>2</sub> > MnO<sub>2</sub> doped TiO<sub>2</sub> > NiO doped TiO<sub>2</sub>.

---

---

*SUMMARY AND CONCLUSIONS*

---

---

## CHAPTER 9

### SUMMARY AND CONCLUSION

TiO<sub>2</sub> supported catalysis is an emerging field and the development of new and better methods for their preparation is the need of the hour. As the stable dioxide, TiO<sub>2</sub> exists in three polymorphs, corresponding to the naturally occurring mineral anatase, rutile and brookite. Titania exhibits transformation from one crystal structure to another as the temperature or pressure is varied. This phenomenon is known as polymorphism. The structural differences between anatase and rutile make the transformation irreversible.

The phase in which TiO<sub>2</sub> exists in the selected conditions is important for selecting TiO<sub>2</sub> as a catalyst or catalyst support. Also the properties of the titania are determined by the phase composition and the particle size of each phase. The phase composition and the particle size evolve as functions of time and temperature during heat treatment. The anatase to rutile transformation involves an overall contraction of the structure and a movement of ions, so that a co-operative rearrangement of Ti<sup>4+</sup> and O<sup>2-</sup> ions occurs. To say more specifically, two of the six Ti – O bonds of anatase break and re-unite in a slightly distorted manner, to form rutile structure. It has been proposed that [54-56] the removal of oxygen ions, which generates lattice vacancies, accelerates the transformation and hence, the cations, having the valency less than four, which correspondingly increase the oxygen vacancy, would enhance the transformation [54]. Because of its irreversible nature, there is no phase equilibria involved in this transformation and hence, does not have any specific transition temperature [51]. Hence it becomes necessary to find out the exact temperature at which phase transformation takes place in presence of various

transition metal oxides for its application as catalysts in safe temperature ranges.

The present investigations were done using the uncalcined hydrated titanium hydroxide (titania pulp-amorphous material) containing 82%  $\text{TiO}_2$  produced by the Travancore Titanium Products Ltd., Trivandrum, Kerala, India.

Quantitative analysis of the transformation kinetics of anatase to rutile was studied in presence of 5 and 15%  $\text{Fe}_2\text{O}_3$ ,  $\text{NiO}$ ,  $\text{Cr}_2\text{O}_3$ ,  $\text{CuO}$  and  $\text{MnO}_2$  which were prepared through two different methods and heated in air, inert (argon) and reducing atmosphere (hydrogen). Photo catalytic oxidation of toluene to benzoic acid was also carried out using all the five systems with different phase contents of titania.

Crystallization temperature of anatase from amorphous titania pulp decreased in presence of  $\text{Fe}_2\text{O}_3$ ,  $\text{Cr}_2\text{O}_3$ ,  $\text{NiO}$ ,  $\text{CuO}$  and  $\text{MnO}_2$ . Hence these metal oxides have a strong influence on the crystallization temperature. Rutilation started at different temperatures depending on the metal oxide and the method of preparation. Co-precipitated ones got rutilated at lower temperatures compared to wet-impregnated samples. In most of the cases, the onset temperatures of rutilation were lower in presence of the metal oxides used in this study, compared to pure  $\text{TiO}_2$ . Table 9.1 represents the onset temperature of rutilation in presence of different transition metal oxides in presence of air. Pure  $\text{TiO}_2$  prepared from titania pulp has an anatase to rutile transition temperature of 900 – 1000°C.

All these metal oxides were present in a very fine nature at lower temperatures and during heating metal oxides reacted with  $\text{TiO}_2$  to form

corresponding titanates as seen in XRD patterns. The temperature of formation is a characteristic of the particular titanate.

**Table 9.1. Onset temperature of rutilation in presence of different transition metal oxides doped TiO<sub>2</sub> prepared through different methods.**

Method of preparation	Nature and amount of metal oxide doped	On set temperature of rutilation (°C)
Co-precipitation	5% Fe <sub>2</sub> O <sub>3</sub>	700
	15% Fe <sub>2</sub> O <sub>3</sub>	700
	5% NiO	700
	15% NiO	700
	5% Cr <sub>2</sub> O <sub>3</sub>	800
	15% Cr <sub>2</sub> O <sub>3</sub>	600
	5% CuO	750
	15% CuO	700
	5% MnO <sub>2</sub>	650
	15% MnO <sub>2</sub>	650
Wet-impregnation	5% Fe <sub>2</sub> O <sub>3</sub>	800
	15% Fe <sub>2</sub> O <sub>3</sub>	800
	5% NiO	850
	15% NiO	850
	5% Cr <sub>2</sub> O <sub>3</sub>	900
	15% Cr <sub>2</sub> O <sub>3</sub>	900
	5% CuO	750
	15% CuO	750
	5% MnO <sub>2</sub>	800
	15% MnO <sub>2</sub>	800

Out of all these samples, the onset temperature of rutilation was very low for MnO<sub>2</sub> loaded and 15% Cr<sub>2</sub>O<sub>3</sub> doped TiO<sub>2</sub> sample prepared by co-

precipitation. The activation energy for the transformation was found to be lowered much on doping  $\text{TiO}_2$  with metal oxides in comparison with pure  $\text{TiO}_2$  where the activation energy is 90 kcal/mol.

In argon atmosphere the anatase to rutile transformation temperature was decreased more than that in air and in hydrogen atmosphere, the transformation takes place more rapidly than that in air. In all these cases more rutilation was found in co-precipitated samples compared to wet-impregnated. Also the amount of metal oxide is more important in deciding rutilation.

Better surface area, was obtained with co-precipitated samples compared to wet-impregnated ones. On loading metal oxides like  $\text{Fe}_2\text{O}_3$ ,  $\text{NiO}$ ,  $\text{Cr}_2\text{O}_3$ ,  $\text{CuO}$  and  $\text{MnO}_2$ , the surface area decreased in all the samples. Method of preparation and percentage of the loaded metal oxides have greater influence on surface area. Drastic decrease in surface area was observed upon rutilation.

The surface morphology of  $\text{TiO}_2$  changes on heating in presence of metal oxides and also the nature of metal oxides is very important in deciding the morphology. As expected, because of better properties, the anatase form of metal oxide doped  $\text{TiO}_2$  showed higher activity for photo oxidation of toluene. All these catalysts are yet to be reported for this reaction. The percentage conversion of toluene to benzoic acid decreased drastically upon rutilation. In  $\text{NiO/TiO}_2$  samples, the activity is low for anatase form it self and only partial oxidation to benzaldehyde was observed.

With all these findings, it can be concluded that,  $\text{TiO}_2$  as a support should be characterized with high surface area, phase purity and high onset temperature of rutilation, which should be well above the optimum temperature of a designated reaction in which it is employed as a catalyst. Variation in



physical properties, depending upon the method of preparation is greater in TiO<sub>2</sub> supported catalysts. Hence, a detailed investigation of properties of the samples prepared through each method is necessary and appropriate. A thorough awareness about the rutilation temperature of the catalyst is also a must, before exploiting titania supported catalysts industrially.

#### Suggestions for future work

The anatase to rutile transformation in presence of lower percentages (< 1) is also to be studied. The toluene oxidation through photochemical path using these metal oxides doped TiO<sub>2</sub> are also equally important, from an industrial point of view. It can be done by setting up a continuous process. However the investigations made here are necessary for developing the catalysts for industrial purpose. Various other industrially important reactions can also be tried over these catalysts after knowing the effect of rutilation on those reactions.

---

---

*REFERENCES*

---

---

## REFERENCES

1. *Annals of Philosophy*, 11, **1818**, 112.
2. Crell, *Chemische Annalen*, 40, **1791**, 103.
3. C. Thenard *J. de Mat, Brussels*, 1, **1829**, 119.
4. Berzelius Letters, Almquist and Wiksell, upsale, **1912-1914**. (Letters to Thomson.)
5. M.H. Klaproth, *Analytical Essays towards promoting the chemical knowledge of mineral substances (English translation)*, Cadell and Davies, London, **1801**, 200.
6. Jelks Barksdale, *Titanium, its occurrence, chemistry and Technology*, second edition, the Ronald press company. New york, **1966**.
7. Roskill, '*The Economics of Titanium 1991*', Roskill Information services Ltd., London, 7<sup>th</sup> Edition, **1991**.
8. "*Technology in Indian titaniumdioxide industry*" DSIR, Ministry of Sci& Tech., New Delhi. **1993**, 15
9. E.A. Barringer and H.K. Boowen. *J. Am. Ceram. Soc.*, 65, **1982**, 199.
10. C.J. Barbe and M. Gretzel. *Mat. Res. Soc. Symp. Proc.*, 73, **1996**, 43.
11. B.O. Regan and M. Gretzel. *Nature* 353, **1991**, 737.
12. J.H. Wohlgementz; D.B. Warfield and G.A. Johnson. *IEEE*, **1982**, 809.
13. F. Cao; G. Oskam and P.C. Searson. *J. Phys. Chem.B*, 99, **1995**, 17071.
14. A. Gutarra; A. Azens; B. Stjerna and C.G. Gransqvist. *Appl. Phys. Lett.* 64, **1994**, 28.
15. Janet M. Kesselman, Amit Kumar and Nathan S. Lewis. Elsevier, **1993**, 193.

16. S.Y Huang; L. Kavan; I. Exner and M. Gratzel. *J. Electrochem. Soc.* L142, **1995**, 142.
17. W.J. Macklin and R. Neat. *J. Solid State Ionics.* 53, **1992**, 694.
18. F. Bonino; L. Busani; M. Manstretta; B. Rovitto and B. Scrosti. *J. Power Sources* 6, **1981**, 261.
19. T. Ohzuku; Z. Takehara and S. Yoshizawa. *ElectrochimActa* , 24, **1979**, 219
20. T. Ohzuku; T. Kodama and T. Hirai. *J. Power Sources* 14, **1985**, 153.
21. R.V. de Krol; A. Goossens and J. Schoonman. *J. Phys. Chem. B*, 103, **1999**, 7151.
22. H. Cheng; J. Ma; Z. Zhao and L. Qi. *Chem. Mater.* 7, **1995**, 663.
23. T. Fuyuki and H. Matsunami. *Jpn. J. Appl. Phys.* 25, **1986**, 1288.
24. A. Bally; K. Prasad; R. Sanjines; P.E. Schmid; F. Levy; J. Benoit; C. Barthou and P. Benalloul. *Mat. Res. Soc. Symp. Proc.* 424, **1997**, 471.
25. R.U. Flood and S. Fitzmaurice. *J. Phys. Chem. B.* 99, **1995**, 8954.
26. H. Lindstrom; S. Sodergren; A. Solbrand; H. Rensmo; J. Hjelm; A. Hgfeldt and S.E. Lindquist. *J. Phys. Chem. B*, 101B, **1997**, 7710.
27. L. Koran; B.O. Regan; A. Ray and M. Gratzel. *J. Electrochem. Soc.* 346, **1993**, 291.
28. P.V. Kamat in “*Semiconductor Nanoparticles - Physical, Chemical and Catalytic aspects.*” Eds. P.V. Kamat and D. Maisel, Elsevier, Amsterdam, **1997**.
29. K. Chiba and K. Nakatani. *Thin Solid Films.* 112, **1984**, 359.
30. M. Ferroni; V. Guidi and G. Martinelli. *Nano str. Mat* 7, **1996**, 709.

31. Y.C. Yeh; T.Y. Tseng and D.A. Chang. *J. Am. Ceram. Soc.*, 73, 1990, 1992.
32. K.L. Sieferting and G.L. Griffin. *J. Electrochem. Soc.*, 137, 1990, 814.
33. H. Tang; K. Prasad; R. Sanjines and F. Levy. *Sensors Actuators B*. 26-27, 1995, 71.
34. A.J. Burggraaf; K. Kiezer and B.A. Van Hassel. *Solid State Ionics*. 32 & 33, 1989, 444.
35. Q. Xu and M.A. Anderson. *J. Am. Ceram. Soc.*, 77, 1994, 1939.
36. V.T. Zaspalis; K.Kiezer and A.J. Burggraaf. *Appl. Catal.* 74, 1991, 249.
37. A. Lambort; J.P. Fabre; C. Guizard and L. Cot. *J. Am.Ceram.Soc.*, 72, 1989, 257.
38. S. Anderson and A.D. Wadsley. *Acta. Crystallograph.*, 15, 1962. 194.
39. Y. Ionue and M. Tsuji. *J. Nucl. Sci. Technol.* 13, 1976, 85.
40. Y. Ionue and M. Tsuji. *Bull. Chem. Soc. Jpn.*, 51, 1978, 794.
41. G.R. Dhoshi and V.N. Sastry. *Indian J. Chem.*, 1977, 904.
42. A.M. Adrianov. *J. Appl. Chem. USSR*, 51, 1978, 1789.
43. R.T. Lidd and Coat jr in “*Hand book of gem identification.*” Gemological Institute of America. Los Angeles. 1966.
44. D. Mac Innes in “*Synthetic gems and allied crystal manufacture.*” Noyes data Corp., Park Ridge, N.J, 1973.
45. G.H. Haerlling. *J. Am. Ceram. Soc.*, 82, 1999, 797.
46. M.Z.C.Hu, G.A. Miller, E.A. Payzant and C.J. Rown. *J. Mat. Sci.*, 35, 2000, 2927.
47. H. Nishizava and M. Katsube. *J. Solid State Chem.*, 131, 1997, 43.
48. Kirk-Othmer ‘*Encyclopedia of chemical Technology*’.  
Wiley-Inter Science publication, John Wiley and Sons, 3<sup>rd</sup> edition, 1983.

49. A. Navrotsky and O.J. Kleppa, *J. Am. Ceram. Soc.*, 50, **1980**, 112.
50. S.N. Vaidya, *Bull., Mater. Sci.*, 22, 3, **1999**, 287
51. C.N.R. Rao; S.R. Yoganarasimhan and P.A. Faeth. *Trans. Faraday Soc.*, 57, **1961**, 504.
52. Y.Inoue, S.Yin, S.Uchida, Y.Fujishiro, M.Ishitsuka, E.Min, and T.Sato, *Br. ceram. Trans.* 97, **1998**, 222.
53. Hengzhong Zhang and Jillian.F. Banfield. *Chem.Mater*, 14, **2002**, 4145.
54. R.D. Shannon and J.A. Pask. *J. Am. Ceram. Soc.*, 48, **1965**, 391.
55. K.J.D. Mackenzie. *J. Br. Ceram. Soc.*, 74, **1975**, 121.
56. J.A. Gambao and D.M. Pasquevich. *J. Am. Ceram. Soc.*, 75, **1992**, 2934.
57. D. Shannon. *J. Appl. Phys.*, 35, **1964**, 3414.
58. A.F. Wells "Structural Inorganic Chemistry." 3<sup>rd</sup> Edn., Oxford University Press, Oxford, UK, **1962**, 76.
59. S.R. Yoganarasimhan and C.N.R. Rao. *Trans. Farad. Soc.*, 58, **1962**, 1579.
60. K.J.D. Mackenzie. *J. Br. Ceram. Soc.*, 74, **1975**, 29.
61. F.C. Gennari and D.M. Pasquevich. *J. Mat. Sci.*, 33, **1998**, 1571.
62. F.C. Gennari and D.M. Pasquevich. *J. Am. Ceram.Soc.*, 82, **1999**, 1915.
63. S. Vemury and S.E. Pratsinis. *J. Am. Ceram. Soc.*, 78, **1995**, 2984.
64. J.Soria, J.C. Conesa, V. Augugliaro, L. Palmisano, M. Schiavello and A. Sclafani. *J. Phys. Chem.*, 95, **1991**, 274.
65. Y. Lida and S. Ozaki. *J. Am. Ceram. Soc.*, 44, **1961**, 120.
66. X.Z. Ding; Z.Z. Qi and Y.Z. He. *Nano str. Mat.*, 4, **1994**, 663.
67. K.J.D. Mackenzie. *J. Br. Ceram. Soc.*, 74, **1975**, 77.
68. Z. Yuan and L. Zhang. *Nano str. Mat.*, 10, **1998**, 1127.
69. S.Riyas, V.Ahmedyasir and P.N.MohanDas, *Bull. Mater. Sci*, 25, 4,

2002, 267

70. K.J.D. MacKenzie, *J. Br. Ceram. Soc.*, 77, 1976, 107.
71. Robert D Shannon and Joseph A. Pask, *J. Am. Ceram. Soc.* 48, 1965, 188.
72. Julio A Gamboa and Daniel M. Pasquevich *J. Am. Ceram. Soc.* 75, 1992, 38.
73. A. Nobile jr and M.W. Davis jr. *J. Catal.*, 116, 1989, 383.
74. K.J.D. Mackenzie and P.J. Melling. *J. Br. Ceram. Soc.*, 73, 1974, 179.
75. J.H. Sinfelt "*Materials science in energy technology.*" Academic Press Inc., 1979, 6.
76. K. Tanabe and H. Hattori. *Energy Shigen (Resources)*, 2, 1981, 570.
77. K.I. Aika; H. Hattori and A. Ozaki. *J. Catal.*, 27, 1972, 424.
78. C.N.R. Rao. *Acc. of Chem. Res.*, 17, 1984, 83.
79. M.J. Reddy and D.W. Reddy. *J. Am. Ceram. Soc.*, 70, 1987, 358.
80. Wilska, Seppo, *Acta Chemica Scandinavica* 8, 1954, 223
81. Gribb, A. Amy and F. Banfield Jillian *American Mineralogist.* 2, 1997, 443
82. Kumar, Krishnankutty Nair, *Scripta Metallurgica et Materialia.* 32, 1995, 667
83. W.R. Moser, *J. Mat. Res.* 10, 1995, 857
84. S.C. Emerson *Stud. Surf. Sci. Cata.* 118, 1998, 489
85. Suslick, Kenneth, "*Sonochemistry,*" *Science* 247, 1990, 982
86. F.E. Massoth "*Advances in catalysis.*" Academic Press, New York. 27, 1978, 265,
87. G. Muralidhar; F.E. Massoth and J. Shabtai. *J. Catal.*, 85, 1984, 44.
88. H. Shimada; T. Sato; Y. Yoshimura; J. Hiraishi and A. Nishijima. *J. Catal.*, 110, 1988, 275.
89. R.B. Quincy; M. Hondlla and D.M. Hercules. *J. Catal.*, 106, 1987, 85.

90. M. Takeuchi; S. Matsuda; F. Nakajima and H. Okada. *Proc. National meeting of AMC Soc.*, Atlanta, Georgia, **1981**.112
91. M. Takeuchi. US patent No: 4, 206, 036. **1980**.
92. S. Matsuda; T. Kano; J. Imahashi and F. Nakajima. *Ind. Engg. Chem. Fundamental*, 21, **1982**, 18.
93. K. Nagakawa; T. Suzuki; T. Kobayashi and M. Haruta. *Chem. Lett.*, **1996**, 1029.
94. K. Mori; A. Miyamoto and Y. Murakami. *J. Catal.*,95,**1985**, 482.
95. G.C. Bond; A.J. Sarkani and G.D. Parfitt. *J. Catal.*, 57, **1979**, 476.
96. I.E. Wachs; R.Y. Saleh; S.S. Chan and C.C. Chersich. *Appl. Catal.*, 15, **1985**, 339.
97. R.Y. Saleh; I.E. Wachs; S.S. Chan and C.C. Chersich. *J. Catal.*, 98, **1986**, 102.
98. G.C. Bond. *J. Catal.*, 116, **1989**, 531.
99. R. Haase; U. Illgen; J. Schere and I.W. Schulz. *Appl. Catal.*,19, **1985**, 13.
100. E.I. Andreikov. *React. Kinet. Catal. Lett.*, 22, **1983**, 351.
101. Y. Murakami; M. Inomata; A. Miyamoto and K. Mori. *Proc. 7<sup>th</sup> Inter. Cong. Catal.*,Tokyo,**1980**, B **1981**, 1344.
102. M. Inomata; A. Miyamoto and Y. Murakami. *J. Chem. Soc. Chem. Commun.*, **1980**, 223.
103. A.J. Hengstum; J.G. Van Ommen; H. Bosch and P.J. Gellings. *Appl. Catal.*, 8, **1983**, 369.
104. F. Cavari; F. Parrinello and F. Trifirp. *J.Mol. Catal.*, 43,**1987**, 117.
105. M. Santi and A. Anderson. *J. Mol. Catal.*, 59, **1990**, 233.
106. B.M.Reddy; I.Ganesh and E.P.Reddy. *J. Phys. Chem.B*, 101, **1997**, 1769.



107. Vejux and P. Courtine. *J. Solid State Chem.*, 29, **1978**, 93.
108. Gasior and T. Machej. *J. Catal.*, 83, **1983**, 472.
109. G.C. Bond; J.P. Zurita; S. Flamerz; P.J. Gellings; H. Bosch; J. Van Ommen and B.J. Kip. *Appl. Catal.*, 22, **1986**, 361.
110. C. Cristini; P. Forzatti and G. Busca. *J. Catal.*, 116, **1989**, 586.
111. G.T. Went S.T. Oyama and A.J. Bell. *J. Phys. Chem. B*, 94, **1990**, 4240.
112. H. Eckert and I.E. Wachs. *J. Phys. Chem. B*, 93, **1989**, 6796.
113. T. Machej; J. Haber; A.M. Turek and I.E. Wachs. *Appl. Catal.*, 70, **1991**, 115.
114. G.T. Went; L.-J. Leu and A.T. Bell. *J. Catal.*, 134, **1992**, 479.
115. A. Baiker; P. Dollenmeier; M. Gliusk and A. Reller. *Appl. Catal.*, 35, **1989**, 351.
116. B.M. Reddy; E.P. Reddy and S.T. Srinivas. *J. Phys. Chem. B*, 96, **1992**, 7076.
117. Christmann "Introduction to surface physical chemistry." Steinkopff Verlag, Darm Stadt., **1991**, 332.
118. M. Ichikawa. *J. Catal.*, 56, **1979**, 127.
119. L.M. Tau and C.O. Bennett. *J. Catal.*, 89, **1984**, 285.
120. T.K. Kundu; M. Mukherjee and D. Chakravorthy. *J. Mat. Sci.*, 33, **1998**, 1759.
121. L.M. Tau and C.O. Bennett. *J. Catal.*, 89, **1984**, 327.
122. B. Sen and J.L. Falconer. *J. Catal.*, 125, **1990**, 35.
123. M.A. Vannice and R.L. Garten. *J. Catal.*, 63, **1980**, 255.
124. J.S. Smith; P.A. Thrower and M.A. Vannice. *J. Catal.*, 68, **1981**, 270.
125. G.B. Raupp and J.A. Dumesic. *J. Phys. Chem. B*, 88, **1984**, 660.
126. E.L. Kugler and R.L. Garten. US pat., No: 4, 273, 724. June 16, **1981**.

127. G.B. Raupp and J.A. Dumesic. *J. Catal.*, 95, **1985**, 601.
128. J.A. Rabo; A.P. Risch and M.L. Poutsma. *J.Catal.*, 53, **1978**, 295.
129. H. Arai; K. Mitsuishi and T. Seiyama. *Chem Lett.*, **1984**, 1291.
130. T. Ishihara; K. Eguchi and H. Arai. *Appl. Catal.*, 30, **1987**, 225.
131. T. Ishihara; K. Eguchi and H. Arai. *Appl. Catal.*, 40, **1988**, 87.
132. N. Horiuchi; T. Ishihara; K. Eguchi & H. Arai. *Chem.Lett.*, **1988**, 499.
133. S. Matsuda and A. Kato. *Appl. Catal.*, 8, **1983**, 149.
134. F. Nakajima. Japan patent No: 52, 6953, **1977**, No: 52, 6954, **1977**, No: 52, 35342, **1977**.
135. K. Matsushida. Japan patent No: 52, 2919, **1977**.
136. F. Nakajima. US patent No: 4,085, 193, **1978**.
137. M. Kancheva; V. Bushev and D. Klissuski. *J. Catal.*, 145, **1994**, 96.
138. M. Inomata; A. Myamoto and Y. Murakami. *J.Catal.*, 62, **1980**, 140.
139. A. Myamoto; K. Kobayashi; M. Inomata and Y. Murakami. *J. Phys. Chem. B*, 86, **1982**, 2945.
140. M. Inomata; A. Myamoto and Y. Murakami. *J. Phys. Chem. B*, 85, **1981**, 2372.
141. M. Inomata; K. Mori; A. Myamoto; T. Ui and Y. Murakami. *J. Phys. Chem. B*, 87, **1983**, 754.
142. F. Jansen; F. Vanden Kerkhof; H. Bosh and J. Ross. *J. Phys. Chem. B*, 91, **1987**, 5921.
143. Idem. *Ibid*, 6633.
144. M. Gasior; J. Haber; T. Machej and T.C. Zeppe. *J. Mol. Catal.*, 43, **1988**, 359.
145. N.Y. Topsoe. *J. Catal.*, 128, **1991**, 499.
146. Z.C. Kang and Q.X. Bao. *Appl. Catal.*, 26, **1986**, 251.

147. Y. Nagakawa; T. Ouo; H. Miyata and Y. Kubokawa. *J. Chem. Soc. Faraday Trans. 79*, **1983**, 2929.
148. A. Khodakov; B. Olthof; A.T. Bell and E. Ighesia. *J.Catal.*, 181, **1999**, 205.
149. I.E. Wachs and B.M. Weckhuysen. *Appl. Catal. A*,157,**1997**, 67.
150. E.Payen; M.Gueltonm and J.Gimbolt. *J. Phys. Chem.B*, 92, **1988**, 1230.
151. G. Centi; D. Pinelli; F.Trifiro; D. Ghossoub; M. Guelton and L. Gengembre. *J.Catal.*, 130, **1991**, 238.
152. H. Bosch and F. Janssen. *Catal. Today*, 2, **1988**, 369.
153. J.E. Sueiras; N. Homs; P. Ramirez de la Piscina; M. Gracia and J.L.G.Fierro. *J. Catal.*, 98, **1986**, 264.
154. J.Santos; J. Philipos and J.A. Dumesic. *J. Catal.*, 81, **1983**, 147.
155. A. Nobile jr; V. Van Brunt and M.W. Davis. *J. Catal.* 127, **1991**, 227.
156. H. Hattori; M. Itoh and K. Tanabe. *J. Catal.*, 38, **1975**, 172.
157. H. Hattori; M. Itoh and K. Tanabe. *J. Catal.*, 41, **1976**, 46.
158. M. Itoh; H. Hattori and K. Tanabe. *J. Catal.*, 35, **1974**, 225.
159. P. Iengo; G. Apride; M.D. Serio; D. Gazzoli and E. Santacesaria. *Appl. Catal. A*, 178, **1999**, 97.
160. N.E. Quaranta; J. Soria; W.C. Corberan and J.L.G. Fierro. *J. Catal.*, 171, **1997**, 1.
161. J.R. Sohn; Y. Il Pae; H. Jang and M.Y. Park. *J. Catal.*, 127, **1991**, 449.
162. J.R. Sohn and H.J. Kim. *J. catal.*, 101, **1986**, 428.
163. K. Tanaka and J.M. White. *J. Phys. Chem. B*, 86, **1982**, 3977.
164. Idem,*Ibid*, 4708.
165. K. Tanaka and J.M. White. *J. Catal.*, 79, **1983**, 81.
166. E. Akubuiro and X.E. Verykios. *Appl. Catal.*, 14, **1985**, 215.

167. G.S. Lane and E.E. Wolf. *J. Catal.*, 105, **1987**, 386.
168. Y.Takita; H.Yamada; M.Hashida and T.Ishihara. *Chem.Lett.*, **1990**, 715.
169. Y. Nitta; Y. Ueda and T. Imanaka. *Chem. Lett.*, **1994**, 1095.
170. Y. Nitta and K. Kobiro. *Chem. Lett.*, **1995**, 165.
171. Y. Nitta; K.Kobiro and Y.Okamoto. *Proc. 70<sup>th</sup> Ann. Meeting. Chem. Soc. Jpn. I*, **1996**, 573.
172. Y. Nitta and K. Kobiro. *Chem. Lett.*, **1996**, 897.
173. K. Foger and H. Jaeger. *J. Catal.*, 120, **1989**, 465.
174. W. Choi and M.R. Hoffmann. *Environ. Sci. Technol.*, 25, **1995**, 1646.
175. P. Murugavel and H.W. Roesky. *Angew. Chem.*, 36, **1997**, 477.
176. M.A. Cambour; M. Constantini; A. Corma; L. Gilbert; P. Estev; A. Martinez and S. Valencia. *J. Chem. Soc. Chem. Commun.***1996**, 1339.
177. A.L.Pruden and D.F. Ollis, *Environ.Sci. Technol.*, 17, **1983**, 628
178. A.L.Pruden and D.F. Ollis, *J.Catal.*, 82, **1983**, 404
179. C.V. Hsiao, C.L. Lee and D.F.Ollis, *J.Catal.*, 82, **1983**, 418
180. T. Nguyen and D.F.Ollis, *J. Phys.Chem.*, 88,**1984**, 3386.
181. S.Ahmed and D.F.Ollis, *solar energy*,32, **1984**, 597
182. D.F.Ollis,C.Y.Hsiao, L. Budiman and C.L. Lee. *J.Catal.* 88, **1984**, 89.
183. A. Fujishima and K. Honda, *Nature*, 238, **1972**, 37.
184. D.F.Ollis,E.Pelizzetti and N.Serpone, in *photocatalysis: Fundamentals and applications*,N.Serpone and E. Pelizzetti(eds), John Wiley & sons, New York, **1989**,603.
185. M.A.Fox, *Acc. Chem.Res.*, 16,**1983**, 3114.
186. D.F.Ollis *Environ. Sci.Technol.*48, **1985**, 194.
187. R.W. Matthews *J.Chem.Soc. Faraday Trans I*, 457,**1984**, 80,
188. R.W. Matthews *Wat.Res.* 20, **1986**, 569.

189. M.R. Hoffmann; S.J. Martin; W.Y. Choi and D.W. Bahnemann.  
*Chem. Rev.* 95, **1995**, 69.
190. G. Dagan and M. Tomkiewicz. *J. Phys. Chem. B*, 97, **1993**, 12651.
191. C.C. Wang; Z. Zhang and J.Y. Ying. *Nano str. Mat.*, 9, **1997**; 583.
192. S. Weaver and G. Mills. *J. Phys. Chem. B*, 101, **1997**, 3769.
193. W. Choi and M.R. Hoffmann. *Environ. Sci. Technol.*, 25, **1995**, 1646.
194. W. Choi and M.R. Hoffmann. *J. Phys. Chem. B*, 100, **1996**, 216.
195. T.R.N. Kutty and S. Ahuja. *Mat. Res. Bull.*, 30, **1995**, 233.
196. H. Kominami; T. Matsura; K. Iwai; B. Ohtani; S. Nishimoto and Y. Kera. *Chem. Lett.*, **1995**, 693.
197. H. Kominami; J. Kato; M. Kohno; Y. Kera and B. Ohtani. *Chem. Lett.*, **1996**, 1051.
198. S. Kagaya; Y. Bitoh and K. Hasegawa. *Chem. Lett.*, **1997**, 155.
199. P. Kopf; E. Gilbert and S.H. Eberle. *J. Photochem. Photobiol., A*, 136, **2000**, 163.
200. Y. Lee; Y.M. Gao; K. Dwight and A. Wold. *Mat. Res. Bull.*, 27, **1992**, 685.
201. I. Sopyan; M. Watanabe; S. Murasawa; K. Hashimoto and A. Fujishima. *Chem. Lett.*, 32, **1996**, 69.
202. Janet M. Kesselman, Amit Kumar and Nathan S. Lewis. *Photo catalytic purification and treatment of water and air*. Elsevier, **1993**, 26
203. M. Muneer; R. Philip and S. Das. *Res. Chem. Intermed.*, 23, **1997**, 233.
204. K. Ionnis; K. Theophanics; M. Shakellarides; Vasilis; A. Sakkas and A. Albinis. *Environ. Sci. Technol.*, 35, **2001**, 398.
205. K. Tennakone and I.R.N. Kottegoda. *J. Photochem. Photobiol., A*, 93, **1996**, 79.

206. G.N. Schranzer; T.D. Guth; J. Salehi; N. S trampach; Liu Nam Hui and M.R. Palmer. *Chem. Phys. Lett.*, 102, **1983**, 509.
207. D.W. Bahnemann. *Israel. J. Chem.*, 33, **1993**, 115.
208. C. Anderson and A.J. Bard. *J. Phys. Chem. B*, 101, **1997**, 2611:
209. M. Anpo; H.Yamashita; Y.Ichihashi; Y. Fuji& M. Honda. *Ibid*, 2632.
210. S.G. Zhang; Y. Fuji; H. Yamashita; K. Koyano; T. Tatsumi and M. Anpo. *Chem. Lett.*, **1997**, 659.
211. S.G. Zhang; Y. Ichihashi; H. Yamashita; T. Tatsumi and M. Anpo. *Chem. Lett.*, **1996**, 895.
212. Y. Xu and C.H. Langford. *J. Phys. Chem. B*, 101, **1997**, 3115.
213. J.E. Tanguay; S.C. Suib and R.W.Coughlin. *J.Catal.*, 117, **1989**, 335.
214. M.V.Rao, K.Rajeshwar, V.R.Paivermeker. J.Dubow. *J.Phys. Chem.* 84,**1980**, 1987.
215. K.Tanaka,T.Hisanaga,K. Harada. *J. Chem.*, 13,**1989**, 5
216. K.Tanaka, T.Hisanaga, K.Harada. *J. photochem .Photobiol. A: Chem.* 48, **1989**, 155
217. F.D. Snell and C.L. Hilton "Encyclopedia of industrial chemical analysis." Inter Sci.Publ., John Wiley& Sons, New York. 7, **1968**, 65.
218. J.A. Longford. *J. Appl. Cryst.*, 11, **1978**, 102.
219. Wauthoz; M.Ruwet; T.Machej and P.Gränge. *Appl.Catal.*, 69,**1991**, 149.
220. I.M. Kolthoff; P.J.Elving and E.B. Sandell "Treatise on analytical chemistry." 5, **1961**, 49.
221. N.H. Furman "Standard methods of chemical analysis." 1, **1966**, 539.
222. I.M. Kolthoff; P.J. Elving and E.B. Sandell. "Treatise on analytical chemistry." 2, **1962**, 404.
223. I.M.Kolthoff; P.J. Elving and E.B. Sandell "Ibid", 8,**1961**, 61.,

224. A.O.Thomas,*Practicalchemistry*, **1992**, 206.
225. G.H. Jeffery, J. Bassett,J.Mendham and R.C. Denney, *Text book of quantitative Chemical analysis*, 5, **1989**, 455.
226. J.Arbiol, J. Cerda, G. Dezanneau, A. Cirera, F. Peiro, A. Cosnet and J.R. Morante, *J. Appl.Phy*, 2, **2002**, 857.
227. M.K.Akhtar and S.E. Pratsinis, *J. Am. Ceram.Soc*, 75, **1992**, 3408.
- 228 S. Hishita, I. Mutoh, K. Koumoto and H. Yanagida, *Ceram.Int*, 9, **1983**, 61.
228. M.C. Carotta, M. Ferroni, D. Gnani, V. Guidi, M. Merli, G. Martinelli, M.C. Casale and M. Notarosens, *Actuators B*, 58, **1999**, 310.
229. F.D. Snell and C.L. Hilton in "*Encyclopedia of industrial chemical analysis*." 7,**1968**, 65. Inter Sci. Publ., John Wiley& Sons, New York.
230. H.F. Mark; D.F. Othmer; C.G. Over berger and G.T. Seaborg in "*Encyclopedia of chemical technology*." Inter Sci. Publ. John Wiley and Sons. New York. 3, 3<sup>rd</sup> Edn., **1978**, 781.
231. L. Palmisano, V. Augugliaro, A. Sclafani, M. Schiavello, *J. Phys. Chem*, 92, **1998**, 6710.
232. L. Palmisano, M. Schiavello, A. Sclafani, C. Martin, I. Martin, V.Rives, *Catal. Lett.* 24, **1994**, 303
233. C. Martin, I. Martin, V.Rives, L. Palmisano, M. Schiavello, *J. Catal*, 134, **1992**, 434.
234. I. Litter, J.A. Navio, *J. Photochem. Photobiol. A: Chem*, 98, **1996**, 171.
235. S.A. Larson, J.L. Falconer, *Catal.Lett.* 44, **1997**, 57.
236. O. d'Hennezel, D.F. Ollis, *J. Catal.* 167, **1997**, 118.
237. O. d'Hennezel, *Ph.D. thesis*, North Carolina State University/Ecole Centrale de Lyon, **1998**.

238. Y. Luo, D.F. Ollis, *J. Catal.* 163, **1996**, 1.
239. M.L. Sauer, M.A. Hale, D.F. Ollis, *J. Photochem. Photobiol. A:Chem.* 88, **1995**, 169.
240. T. Ibusuki, K. Takeuchi, *Atmos. Environ.* 20, **1986**, 1711.
241. S.A. Larson, J.L. Falconer, *Catal. Lett.* 44, **1997**, 57.
242. J. Blanco, P. Avila, A. Bahamonde, E. Alvarez, B. Sanchez, M. Romero, *Catal. Today* 29, **1996**, 437.
243. R. Atkinson, S.M. Aschmann, *Int. J. Chem. Kinetics* 21, **1989**, 355.
244. R. Seuwen, P. Warneck, *Physico-Chemical Behavior of Atmospheric Pollutants*, 1, **1994**, 137.
245. O. d'Hennezel, D.F. Ollis, in: J.W. Hightower, W.N. Delgass, E. Iglesia, A.T. Bell (Eds.), *Studies in Surf. Sci. Catal.* 101, Part A, Elsevier, Amsterdam, **1996**, 435.
246. W.A. Jacoby, D.M. Blake, J.A. Fennell, J.E. Boulter, L.M. Vargo, M.C. George, S.K. Dolberg, *J. Air and Waste Manage. Assoc.* 46, **1996**, 891.
247. X. Fu, W.A. Zeltner, M.A. Anderson, *Appl. Catal.* B6, **1995**, 209.
248. S. Sitkiewitz, A. Heller, *New J. Chem.* 20, **1996**, 233.
249. J. Blanco, P. Avila, A. Bahamonde, E. Alvarez, B. Sanchez, M. Romero, *Catal. Today*, 29, **1996**, 437.
250. R. Atkinson, S.M. Aschmann, *Int. J. Chem. Kinetics*, 21, **1989**, 355.
251. C. Von Sonntag, H.P. Schuchmann, *Angew. Chem. Int. Ed. Engl.* 30, **1991**, 1229.
252. S. Sitkiewitz, A. Heller, *New J. Chem*, 20, **1996**, 233.
253. J. Schwitzgebel, J.G. Ekerdt, H. Gerischer, A. Heller, *J. Phys. Chem*, 99, **1995**, 5633.



254. G.A.Russel, *J. Am. Chem. Soc.*, 79, **1957**, 3871.
255. C. Von Sonntag, in: *Taylor and Francis (Eds.). The Chemical Basis of Radiation Biology*, London, **1987**.
256. A.Dipaola, G. Marci, L. Palmisano, M. Schiavello, K. Uosaki, S. Ikeda and B. Ohtani, *J. Phys.Chem. B*, 106, **2002**, 637.
257. Sha Jin, Fumihide Shiraishi, *Chem. Engg. Journal*, 97, **2004**, 203.